



The
University
Of
Sheffield.

Controlled Radical Polymerization in Surfactant-Free Emulsion Polymerization

Dominic Matthew Gray

**The University of Sheffield
Department of Chemistry**

**A thesis submitted in partial fulfilment of the requirements for the degree
of Doctor of Philosophy**

April 2019

Declaration

The work described in this thesis was carried out at the University of Sheffield under the supervision of Dr Sebastian Spain between October 2014 to April 2019 and has not been submitted, either wholly or in part, for this or any other degree. All the work is the original work of the author, except where acknowledged.

Signature: _____

Dominic Matthew Gray

April 2019

Abstract

This Thesis describes the polymerization of methyl methacrylate (MMA) in the presence or absence of 1,1-diphenylethylene (DPE) in surfactant-free emulsion polymerization (SFEP), with subsequent polymerizations of either styrene (St) or benzyl methacrylate (BzMA) in the presence of the latex formed. The effect of varying amphiphilicity of several RAFT agents in reversible addition-fragmentation chain-transfer (RAFT) SFEP was also investigated.

Firstly, the precursor polymer is synthesised by SFEP of methyl methacrylate in the presence of varying concentrations of DPE. The molecular weight and (dispersity) \bar{D} of the resulting PMMA can be reduced by increasing the DPE concentration in the polymerization, with varying initiator concentration having little effect. Increasing the DPE content also reduced the rate of polymerization. Mass spectroscopy (MS) indicated the presence of only 1 DPE unit per polymer chain, contrary to other emulsion polymerization studies, with diffusion-ordered nuclear magnetic resonance (DOSY NMR) spectroscopy showing the presence of free DPE and DPE bound to the polymer chains. Utilizing DPE in SFEP yielded a bimodal particle distribution as judged by transmission electron microscopy (TEM), with a secondary particle distribution forming over the first hour of the polymerization.

Secondly, St and BzMA are polymerized in the presence of PMMA latex synthesised in the presence or absence of DPE. The rate of polymerization of each of these two monomers is increased by the presence of DPE in the precursor, indicating that the precursor is a source of radicals by either thermal cleavage of the polymer chains or the uncapping of the polymer by DPE. Only very low BzMA conversion is achieved when the precursor did not contain DPE. Polymerizations of St contained a considerable amount of precursor after the attempted extension, whereas the polymerization of BzMA contained very little precursor, as judged by SEC. PSDs analysed by TEM show an increase in particle diameter, broadening of the size distribution, and the formation of a secondary particle size distribution during the polymerization of St or BzMA.

Finally, the polymerization of methyl methacrylate is conducted in the presence of several RAFT agents. Solution polymerizations confirmed that these RAFT agents enabled good control over the molecular weight and \bar{D} , but their success in SFEP depended on the amphiphilicity of the RAFT agent. For two RAFT agents, this could be altered by changing the pH, with the anionic or cationic derivatives giving considerably better control. Size exclusion chromatography (SEC), incorporating a UV detector at $\lambda = 260$ nm, showed the presence of the amphiphilic RAFT agents throughout the MWD and the absence of RAFT end-groups when using hydrophobic RAFT agents. However, control over molecular weight

and \bar{D} is achieved at the cost of reduced control over the particle size distribution (PSD) of the latex.

Overall, the information given in this Thesis brings us closer to the controlled SFEP synthesis of diblock copolymers. With the DPE method being used to form diblock copolymers of PMMA-*b*-PBzMA, despite the hydrophobicity of DPE. While the success of the use of RAFT agents to form precursor polymers for later extension is dependent on the amphiphilicity of the RAFT agent. These methods can be used in the SFEP synthesis of diblock copolymers for coatings where the use of diblock copolymers helps to prevent polymer phase separation and the presence of a surfactant can have negative effects on the quality of the final product.

Conferences

January 2015	9 th Annual RSC conference: Biomaterials Chemistry Group, London, UK
April 2016	Macro Group UK Young Researchers Meeting, Liverpool, UK
July 2016	Warwick 2016 Polymer conference, Warwick, UK
April 2017	Colloid Young Researchers Meeting, Sheffield, UK
June 2017	Macro Group UK Young Researchers Meeting, Edinburgh, UK
July 2018	Macro Group UK Young Researchers Meeting, Dublin, Ireland
September 2018	Early Career Colloid Meeting, Sheffield, UK

Acknowledgements

Firstly, I would like to thank my supervisor Dr Seb Spain for adopting me when my original supervisor was offered a job elsewhere. All your guidance, support and encouragement are greatly appreciated. Apart from the one time you tried to help me in the lab.

I would also like to thank the Spain Group, past and present, for being understanding and motivational throughout my PhD. Kat, Laila, Simon, Sarah, Laura, Rheanna, Emma, Tom, Jasmine, Marissa, Anna, Ellen, Josh and Sam, you are the reasons I came into the office every day.

To my independent advisor Prof. Steve Armes thank you for all your ideas and letting me be a part of your CDT, together with Joe Gaunt, who always nudged me in the right direction and was always there with help. Also, I would like to acknowledge the Armes group for the use of all their equipment, their instruction on how best to use it, their company in the office and occasionally their RAFT agents.

It has been a privilege to undertake this work at the University of Sheffield. I would like to acknowledge the staff in stores, accounts, DDSS, and all other chemistry Staff who helped me over the years. As well as Dr Svet Svokov and Dr Chris Hill for their help with TEM and Dr Sandra van Meurs for her help with the NMR facilities and running my DOSY NMR samples in Sheffield.

Thanks to the EPSRC and BASF for funding this work and my supervisors at BASF Dr Sebastian Enck and Dr Alex Schenzel. My time on placement as BASF was enlightening and gave me an opportunity to live in Germany, which I am grateful for.

Thank you to my Mum and Dad for being the pushiest of parents but for giving me all the opportunities to succeed, the Jelly School (Tom, Dan, Oli and Caitlin) for reminding me to be silly occasionally, and Sheffield Mavericks and Sheffield Bears Ice hockey teams for putting to good use the time my PhD kept me up at night.

Leanne, thank you for being my PhD wife. You have sat through many tantrums, tears and outbursts over the years and I am beyond grateful for every second that you have put up with me during this hard time.

Nomenclature

AIBN	-	2,2'-azobisisobutyronitrile
APS	-	Ammonium persulfate
ATRP	-	Atom transfer radical polymerization
BzMA	-	Benzyl methacrylate
CLRP	-	Controlled / living radical polymerization
CPB	-	2-cyano-2-propyl benzodithioate
CTA	-	Chain transfer agent
\bar{D}	-	Dispersity
D_h	-	Hydrodynamic radius
DLS	-	Dynamic light scattering
DMF	-	Dimethylformamide
DOSY	-	Diffusion ordered spectroscopy
DPE	-	1,1-diphenylethylene
HDC	-	Hydrodynamic chromatography
logD	-	Log(diffusion coefficient)
M_n	-	Number-average molecular weight
M_w	-	Weight-average molecular weight
mCTA	-	Macromolecular chain transfer agent
MMA	-	Methyl methacrylate
MPETTC	-	Morpholine-functionalised trithiocarbonate based PETTC derivative
MWD	-	Molecular weight distribution
NMP	-	Nitroxide mediated polymerization
NMR	-	Nuclear magnetic resonance
PBzMA	-	Poly(benzyl methacrylate)
PETTC	-	4-cyano-4-(2-phenylethane sulfanyl thiocarbonyl) sulfanylpentanoic acid
PMMA	-	Poly(methyl methacrylate)
PMMA-DPE	-	Poly(methyl methacrylate) polymerized in the presence of 1,1-diphenylethylene
PSD	-	Particle size distribution
PSt	-	Poly(styrene)
RAFT	-	Reversible addition-fragmentation chain-transfer
RBF	-	Round bottom flask
RDRP	-	Reversible-deactivation radical polymerization

RI	-	Refractive index
SEC	-	Size exclusion chromatography
SFEP	-	Surfactant-free emulsion polymerization
St	-	Styrene
T _g	-	Glass transition temperature
TEM	-	Transmission electron microscopy
TGA	-	Thermogravimetric analysis
THF	-	Tetrahydrofuran

Chapter One

1. Introduction

1.1. Polymer Science

Polymers are made up of single repeat units known as monomers. Naturally occurring (DNA, proteins and rubber) and synthetic polymers are everywhere around us in coatings, packaging, currency, medical delivery systems and many more. These cover many areas due to the wide array of possible monomers and the ability of polymers to have linear, branched, cross-linked and several other architectures allowing further alteration of their properties.

1.1.1. Step and chain growth polymerizations

Flory divided polymerizations into two categories; condensation or step-growth polymerizations and addition or chain growth polymerizations.¹ Step-growth reactions usually involve the loss of a small molecule during polymerization. One example of this is the formation of polyesters. Chain growth polymerization requires the monomer to contain an active species where polymerization occurs.

Step growth polymerization forms dimers and trimers which then react to give longer chain lengths over time. This leads to slow evolution in molecular weight early in the reaction followed by relatively rapid growth of the molecular weight later in the reaction. In contrast, the molecular weight of polymers produced by chain growth increases rapidly at the start of the reaction and then can often decrease at higher conversions due to the lack of monomer and possibly other side reactions.

1.1.2. Molecular weight of polymers

Polymers do not have a specific molecular weight but instead are produced with a range of chain lengths. Parameters are used to describe the molecular weight of a polymer such as M_n , M_w and dispersity (\mathfrak{D}). The equations defining each of these parameters are given below.

$$M_n = \frac{\sum n_i M_i}{\sum n_i} \quad (1.1)$$

$$M_w = \frac{\sum n_i M_i^2}{\sum n_i M_i} \quad (1.2)$$

$$\mathfrak{D} = \frac{M_w}{M_n} \quad (1.3)$$

Where n is the number of chains and M is the molar mass of these chains with i units.

The molecular weight of a polymer product can be a number-average (M_n) or a weight-averaged (M_w). \mathfrak{D} is used to describe the width of the molecular weight distribution. For a monomer, M_n would be equal to M_w and therefore have a dispersity of 1. Typical \mathfrak{D} values for

conventional free radical polymerizations range from 1.5 to 5.0 but can sometimes be greater than 10. Controlled methods of polymerisation are used to reach a targeted M_n and also reduce D . These will be discussed later.

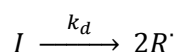
1.1.3. Mechanism of chain growth polymerization

Chain growth polymerizations will be the focus of this thesis. The mechanism of chain growth polymerization in the case of free-radical polymerization can be seen in Figure 1.1.

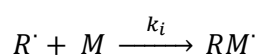
Free radicals to initiate the polymerization are commonly formed by the thermal decomposition of an azo- or peroxide initiator. This is an example of homolytic fission. However, these radicals can also be formed via redox reactions, as well as UV and ionising radiation. The rate constant for thermal decomposition (k_d) varies considerably depending on the type of initiator and the reaction temperature.

The radicals formed by decomposition then attack the vinyl group of a monomer to give $RM\cdot$. This process is known as initiation. These radical centres then add more monomer units by propagation. The rate constant of propagation (k_p) must be considerably higher than other rate constants for the polymer to reach a significant molecular weight: k_p typically ranges from $10^2 - 10^4 \text{ M}^{-1} \text{ s}^{-1}$ depending on the type of vinyl monomer.²

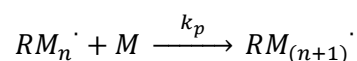
(A) Decomposition



(B) Initiation



(C) Propagation



(D) Termination

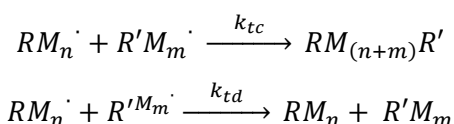


Figure 1.1. The mechanism of free radical polymerisation: (A) decomposition of the initiator, (B) initiation of the polymer chain, (C) propagation of the growing polymer chain and (D) termination by combination or disproportionation.

Termination of a radical can occur in a multitude of ways. The two most common can be seen in Figure 1.1D. Combination occurs when two polymer chain ends possessing a radical couple together to form a dead polymer chain. Disproportionation is the process of hydrogen atom abstraction by one active chain end from another, yielding a saturated and unsaturated chain end. Often one form of termination dominates over the other. Examples of this are styrene terminating mainly by combination and methyl methacrylate largely terminating by disproportionation.³

The rate of polymerization can be determined by the rate of the consumption of monomer. Monomer is consumed only during the initiation and propagation steps of a free-radical polymerization. However, such a small amount is consumed during initiation that this can be ignored in the rate equation. This means that the rate of polymerization R_p can be expressed as:

$$\frac{-d[M]}{dt} \approx R_p = k_p[RM_n^{\cdot}][M] \quad (1.4)$$

Where $[M]$ is the concentration of monomer, k_p is the rate constant of propagation and $[RM_n^{\cdot}]$ is the concentration of polymer radicals. If we assume that the rate of initiation (R_i) is equal to the rate of termination (R_t) (the so-called steady-state approximation), then the concentration of polymer radicals remains constant throughout the polymerization:

$$\frac{d[RM_n^{\cdot}]}{dt} = R_i - R_t = 0 \quad (1.5)$$

Termination is composed of two main pathways, combination and disproportionation, as mentioned above. The amount of termination by either pathway varies considerably with the monomer type but these rates can be expressed as:

$$R_{tcom} = -k_{tc}[P_n^{\cdot}][P_m^{\cdot}] \quad (1.6)$$

$$R_{tdis} = -k_{td}[P_n^{\cdot}][P_m^{\cdot}] \quad (1.7)$$

The rate of termination (R_t) can be expressed as the rate of loss of polymer radicals and combined with equation (1.5):

$$R_t = -\frac{d[RM_n^{\cdot}]}{dt} = 2k_t[RM_n^{\cdot}]^2 = R_i \quad (1.8)$$

This equation can then be combined with equation (1.4):

$$R_p = k_p[M] \left(\frac{R_i}{2k_t} \right)^{\frac{1}{2}} \quad (1.9)$$

This expression can be refined by the replacement of R_i . As specified earlier, thermal initiators decompose to produce a pair of radicals. This is the decomposition step and the rate of

decomposition (R_d) is considerably slower than the rate of addition to monomer. This makes the decomposition step rate-limiting, allowing the rate of initiation to be expressed as:

$$R_i = R_d = 2fk_d[I] \quad (1.10)$$

Where k_d is the decomposition rate constant and f is the initiator efficiency, which is defined as the fraction of radicals that initiate polymer chains. This can then be substituted into equation (1.9):

$$R_p = k_p[M] \left(\frac{fk_d[I]}{k_t} \right)^{\frac{1}{2}} \quad (1.11)$$

From this equation, it is clear that the rate of propagation is first order with respect to monomer concentration and varies with the square root of the initiator concentration. This means that when the polymerization is nearing complete conversion that the polymer chains will be considerably shorter and therefore dispersity (\bar{M}_w/\bar{M}_n) increases.

1.2. Emulsion polymerization

Polymerizations can be carried out as bulk, solution or heterogeneous polymerizations. Heterogeneous polymerizations are particle-forming polymerizations where one or more reagent or product is insoluble in the continuous phase. Examples include precipitation, dispersion, suspension and emulsion polymerization. A common continuous phase for such heterogeneous polymerizations is water as it is readily available, environmentally-friendly, cheap, non-toxic and has a high heat capacity.

In precipitation polymerization all reagents are soluble in the reaction medium. However, the polymer that is formed is insoluble and therefore precipitates during the reaction. Dispersion polymerization is a form of precipitation polymerization. Dispersion polymerizations usually contain a suitable stabilizer to ensure the particles remain dispersed in the reaction medium. This means that further polymerization can occur within these particles. This results in relatively narrow size distributions with mean particle diameters of 0.1-15 μm .⁴

Suspension polymerization occurs when the monomer is insoluble in the continuous phase of a polymerization, but due to agitation and stabilizer (emulsifier) the monomer remains dispersed as droplets. Initiators are monomer-soluble and therefore the locus of the polymerization is inside the monomer droplets. The particles are usually considerably larger than dispersion methods, e.g. up to 2 mm diameter.⁴

Emulsion polymerizations consist of water-immiscible monomer and polymer but the initiator is soluble in the continuous phase. Due to the insolubility of the monomer and polymer, a stabiliser is often used. This leads to the formation of particles of typically 0.01 – 1 μm .⁵ There

are also other sub-types of emulsion polymerization, for example miniemulsion polymerization,⁶ which involves high shear using a homogeniser or ultrasound.

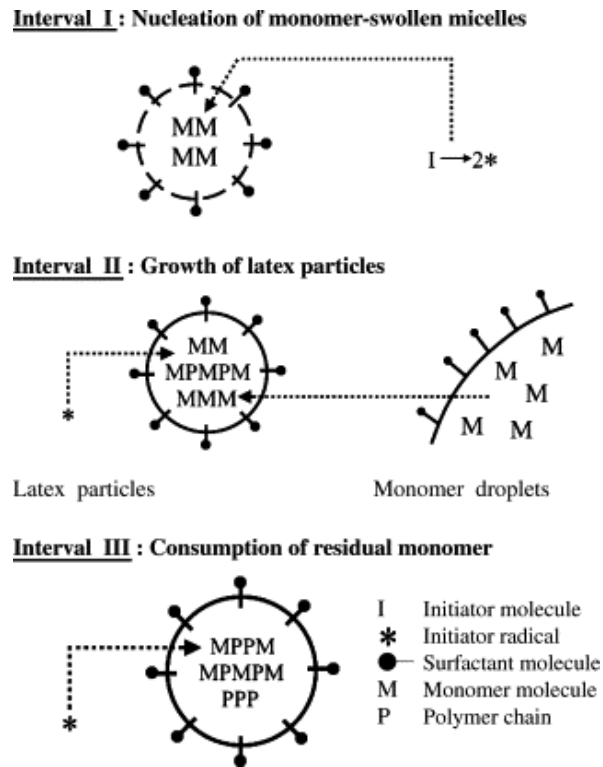


Figure 1.2. A schematic representation of the mechanism of micellar nucleation.⁷ Reprinted (adapted) with permission from Elsevier (License number: 4550300944820).

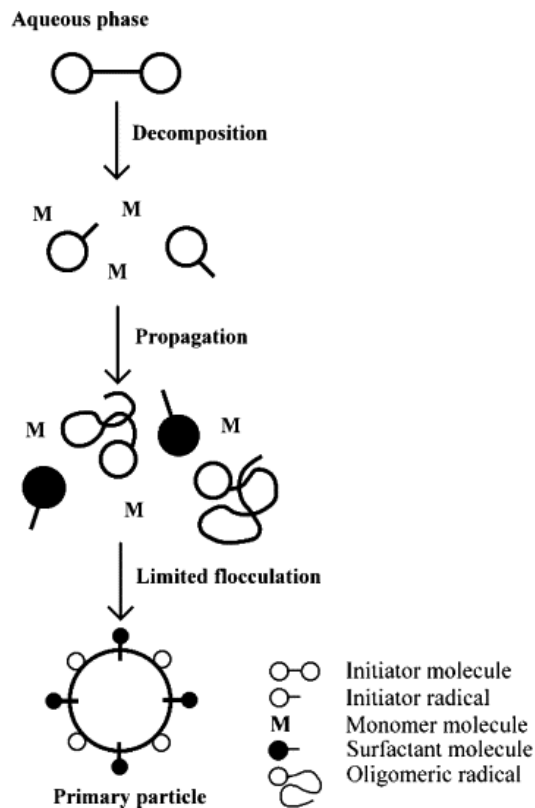


Figure 1.3. A schematic representation of the mechanism of homogeneous nucleation.⁷ Reprinted (adapted) with permission from Elsevier (License number: 4550300944820).

Stabilisation of the monomer droplets and latex in emulsion polymerization can be achieved electrostatically or sterically.⁸⁻¹⁰ Electrostatic repulsion can be conferred by cationic (e.g. cetyltrimethylammonium bromide (CTAB)),¹¹ or anionic (e.g. sodium dodecyl sulfate)¹² surfactants. Steric stabilisation is usually imparted by the inclusion of polymer chains that adhere to the outside of the particle (e.g. poly(ethylene oxide)-*b*-poly(styrene)).¹³ Steric stabilizers are often used when the latex is required to be stable at high electrolyte concentrations.⁴ Stabilization can also be provided by solid particles (for example silica particles).¹⁴

Emulsion polymerizations can be carried out without any stabilizer or surfactant.¹⁵ This is advantageous as surfactant can affect film formation and migrate to the polymer surface over time when applied as coatings leading to poor film opacity and visual appearance, as well as foaming and poor adhesion.¹⁶ The transport of surfactant forms hydrophilic channels in the coating, causing water ingress, decreasing the water and corrosion resistance of the coating. Efforts to avoid this phenomenon have been taken: one example is the inclusion of the reactive surfactant, sodium dodecyl allyl sulfosuccinate.¹⁷ Polymeric surfactants can also be used due to their decreased mobility within the film compared to conventional surfactants.¹⁸ This would require the formation of an amphiphilic block copolymer in an aqueous continuous phase using one of the controlled radical polymerizations discussed later in this Introduction. These amphiphilic polymers can also be used as a coating binder. The added advantage here being the lack of polymer phase separation, giving better film properties.

In the absence of stabiliser, ionic initiators, such as persulfates, can be used to introduce charge to the outside of the polymer particles. This helps to prevent flocculation, coagulation and sedimentation of the particles during and post-reaction. Due to the lower surface area that the initiator can stabilise, the particle number is lowered by two orders of magnitude to 10^{12} L^{-1} .¹⁰ To help stabilise the particle, a secondary hydrophilic monomer or a secondary solvent can also be added.^{19, 20}

Emulsion polymerizations takes place in 3 stages, as proposed by Harkins,²¹⁻²³ as well as Smith and Ewart.^{24, 25} A schematic representation of this process can be seen in Figure 1.2. The first stage is nucleation, which can occur via either homogeneous or heterogeneous nucleation pathways.

Heterogeneous or micellar nucleation occurs when initiator reacts with solubilised monomer, which propagates to form a z-mer.²⁶ At this critical chain length, the z-mer will become suitably hydrophobic and enter a micelle before propagating to form a particle. Monomer can be contained within micelles (when stabiliser is included above the critical micelle concentration (CMC)), monomer droplets and in the continuous phase. A z-mer is much more

likely to enter a micelle than a monomer droplet due to the much higher total surface area of the micelles compared to droplets (micelle concentration = 10^{19} - 10^{21} L⁻¹, diameter of micelles = 5-10 nm, monomer droplet concentration = 10^{12} - 10^{14} L⁻¹, diameter of monomer droplets = 1-10 μ m) For St and MMA, 99 % of particle nucleation occurs via this method when the surfactant concentration is above the CMC.^{27, 28}

In the absence of any micelles, the z-mer will precipitate and form particles. This is homogeneous nucleation as proposed by Priest,²⁹ Roe,³⁰ Fitch and Tsai.⁵ Such particles then swell with monomer from the aqueous phase and become a polymerization locus. A schematic representation of this can be seen in Figure 1.3. This is the primary mechanism for particle formation in surfactant-free formulations but can also occur when stabiliser is present below or around its CMC.³¹ It has been suggested that these oligomers could also aggregate to form micelles in solution.³² However, this theory is still being debated.⁷

As the number of particles increases over stage one, so does the polymerization rate. Micelles that do not contain a growing radical toward the end of stage one supply further monomer and stabiliser to growing particles as their diameter increases. This occurs as the concentration of surfactant drops below the CMC. Once the number of particles reaches a constant value this is the end of stage one. This can be attained between 2 and 25 % monomer conversion and is reached faster with more hydrophilic monomers.³ Reasons for this include the presence of both methods of nucleation and a higher concentration of monomer dissolved in the aqueous phase. Stage one controls the particle size distribution of the product latex. A shorter stage one produces a narrower particle size distribution. Stage one can be shortened by using a low surfactant concentration but larger particles will be produced.³³

Diffusion of monomer from droplets ensures that the monomer concentration in the continuous phase remains constant throughout stage two, therefore keeping the rate of polymerization constant. The number of particles usually remains constant during this period but some can coalesce over the course of reaction. The steady state will continue until the monomer droplets are fully consumed. At this point, the polymerization enters stage 3 with a slower reaction rate due to the lack of remaining monomer. This is represented graphically in Figure 1.4. This point is again reached earlier with monomers of greater aqueous solubility as well as the swelling ability of polymer particles.³⁴ The polymerization rate will continue to decrease unless the gel effect contributes to an increase in rate due to the presence of multiple active radicals within the same particle. This can occur if the growing particle is sufficiently viscous.³⁵

The kinetics of emulsion polymerization in stage 2 are determined by the average number of active radicals per particle. This is divided into cases one, two and three where the average

number of radicals per particle is less than 0.5, equal to 0.5 and greater than 0.5, respectively. Case two is the most common of these scenarios and is referred to as zero-one kinetics. In case two, there is no desorption of radicals and rapid termination occurs when a radical enters a particle that already contains a radical. For case one to occur, radical desorption and termination in the aqueous phase must be significant. This is likely to arise for a more hydrophilic monomer because chain transfer to monomer could lead to desorption and termination. For case three to occur, the particles must be sufficiently large to contain more than one active radical coupled with a slow rate of termination.³

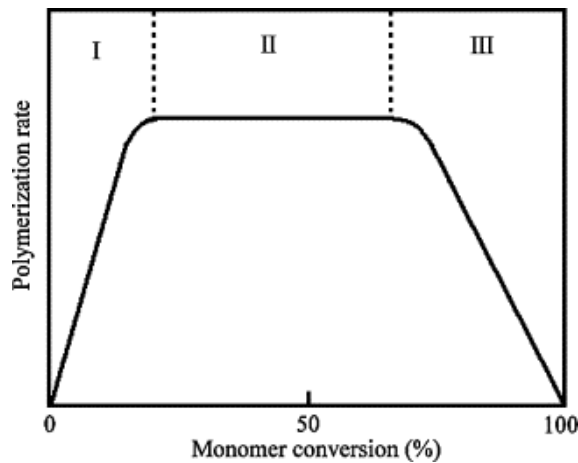


Figure 1.4. The effect of monomer conversion on the polymerization rate over the three stages of emulsion polymerization. Reprinted (adapted) with permission from Elsevier (License number: 4550300944820).

Smith and Ewart produced the following equation (1.13) by the substitution of equation (1.12) into equation (1.4) to calculate the rate of polymerization (R_p) assuming zero-one kinetics:

$$[P\cdot] = \frac{N'\bar{n}}{N_A} \quad (1.12)$$

$$R_p = k_p[M]_p \left(\frac{\bar{n}N'}{N_A} \right) \quad (1.13)$$

Where N' is the concentration of micelles and particles, k_p the propagation rate constant, $[M]_p$ the concentration of monomer in the particles, \bar{n} the average number of free radicals per particle, N_p the number of particles per unit volume and N_A is Avogadro's constant. This equation also assumes all the characteristics of case two kinetics. Increasing the temperature of the reaction increases the rate by increasing k_p and the particle concentration due to the greater rate of radical generation.

An increase in molecular weight in bulk and solution free-radical polymerizations occurs at the expense of polymerization rate. This is not the case in emulsion polymerization due to the polymerization being contained within the particles. This compartmentalization effect means

that extra initiator can be added, thus increasing the polymerization rate without affecting the molecular weight.⁷ This can also be seen from equation (1.13) as the rate of polymerization has no dependence on the concentration of initiator.

The dispersity of the polymerization is affected by the use of emulsion polymerization methods. Termination by transfer to monomer is the same for both homogeneous and heterogeneous polymerizations with $\bar{D} = 2$. Homogeneous polymerizations are more likely to undergo termination by disproportionation or combination of short chains with long chains. However, case two behaviour for emulsion polymerization dictates that the combination of two polymers is likely to be between a longer propagating polymer chain and a radical containing oligomer entering the particle. This gives a \bar{D} value of 2, compared to $\bar{D} = 1.5$ for homogeneous systems. The greatest difference comes from termination by disproportionation where $\bar{D} = 4$ for heterogeneous and $\bar{D} = 2$ for homogeneous polymerizations. This is due to disproportionation, with micelle-entering oligomers being considerably smaller than the propagating radicals and increasing \bar{D} considerably. This effect is reduced in case three kinetics as any two radicals are more likely to be a greater length. While polymers in stage three and stage one may be considerably different to those in stage two, the overall dispersity is usually lower than that for homogeneous polymerizations.³

This research was CASE sponsored by BASF SE, specifically their coatings department. Emulsion polymerization forms latexes which are used as binders in coatings. The other two main components of a coating are pigments and dispersants.³⁶ The latex particles form a polymer film on drying and the strength and durability of the resulting film are dependent on the polymer properties.³⁷ For example, methyl methacrylate, used as the main monomer of this volume of work, is used in coatings due to its increased resistance to UV-induced degradation.³⁸

Coherent films are easy to form using low glass transition temperature (T_g) polymers, the resistance of films consisting of these polymers is poor. However, higher T_g polymers, such as styrene (another monomer used in this Thesis), provide better barrier properties in coatings.³⁹ The easiest way to produce films at room temperature with improved resistance properties is to blend the polymer.⁴⁰ However, this can lead to polymer separation and poor film appearance and adhesion. One way to avoid this is to chemically link the two polymers together, forming a diblock copolymer, using living / controlled radical polymerization.

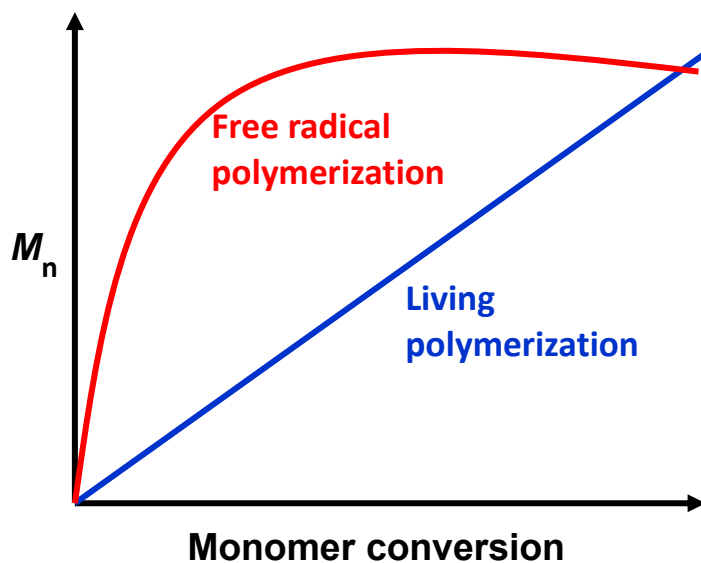


Figure 1.5. Molecular weight (M_n) vs monomer conversion plots for conventional free radical polymerization and living polymerization.

1.4. Nitroxide-mediated polymerization (NMP)

Nitroxide-mediated polymerization (NMP) was developed by CSIRO in the 1980s⁴⁴ and requires the use of nitroxides or alkoxyamines as reversible capping agents that are incorporated into the polymer chain. The NMP mechanism is shown in Figure 1.6. The NMP equilibrium can be achieved with either a bicomponent (free-radical initiator and nitroxide) or monocomponent (where these are the same molecule) alkoxyamine system. The most common nitroxide is 2,2,6,6-tetramethyl-1-piperidinyloxy (TEMPO).^{45, 46} Disadvantages of these NMP reactions are the high temperature and expensive control reagents that can be difficult to remove.⁴⁷ NMP can be used with various vinyl monomers but is incompatible with methacrylates. However, use of specific nitroxides,⁴⁸ or the statistical copolymerization of methacrylates with St,⁴⁹ suggests that this restriction can be minimized.

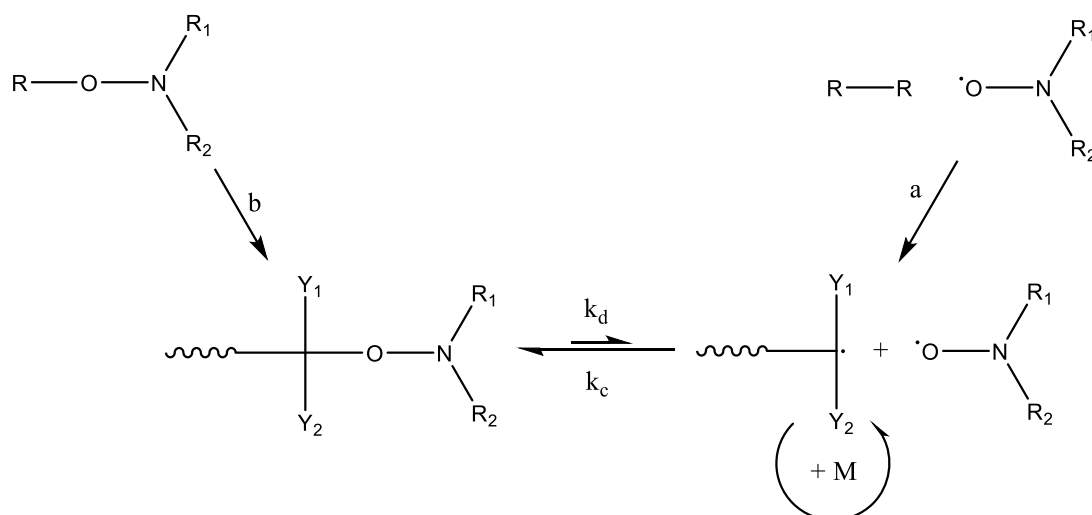


Figure 1.6. Nitroxide-mediated polymerization equilibrium from bicomponent initiating system (a) and monocomponent initiating system (b).⁴⁷

NMP can be used in heterogeneous polymerizations for suspension,⁴⁵ dispersion,⁵⁰ and emulsion polymerizations.⁵¹ Initially NMP in emulsion polymerization suffered problems with nitroxide partitioning and monomer droplet nucleation.⁵² These issues could be overcome by the use of a pair of nitroxides e.g. TEMPO and 4-stearoyl-TEMPO.⁵³ However, due to the high temperatures required for homolytic cleavage of TEMPO, pressurised reactors were needed. This could be avoided with the use of SG1-based alkoxyamines, which allowed acrylic polymerizations to take place at around 90 °C.⁵⁴ These reactions have been carried out under seeded emulsion,⁵⁵ mini-emulsion⁵⁶ and under ab-initio conditions.⁵⁴

Surfactant-free emulsion polymerization (SFEP) has also been utilised with NMP. To achieve this, some publications specify the need to use a co-solvent,⁵⁷ an additional hydrophilic monomer,⁵⁸ and / or the formation of a macromolecular chain transfer agent (mCTA) in bulk or solution to be extended in aqueous conditions.^{59, 60} For example, Thomson *et al.*⁶¹ reported the formation of a mCTA in a one-pot system under SFEP conditions utilising the more hydrophilic methyl acrylate with butyl methacrylate and styrene. This was achieved by adding a small amount of all three monomers initially and then the majority of the BMA and St to be polymerized thereafter.

1.5. Atom Transfer Radical Polymerization (ATRP)

ATRP was developed independently by Sawamoto⁶² and Matyjaszewski⁶³ in 1995. This method involves the use of an alkyl halide (R-X) and a transition metal catalyst (M-L_n), which is usually copper-based. This system can be used for a wide range of monomers but removal of the metal catalyst post-polymerization represents a problem for the industrial application

of this technique. This type of RDRP has also been used for suspension,⁶⁴ dispersion,⁶⁵ and emulsion polymerizations.⁶⁶

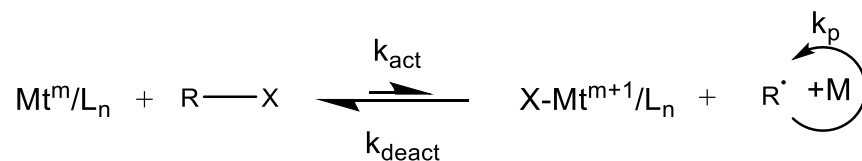


Figure 1.7. Mechanism of ATRP. Mt = transition metal, L_n = complexing ligand, R = polymer chain, X = Br or Cl.

In emulsion polymerization, the partitioning of the metal catalyst is crucial for achieving a controlled radical polymerization. If the complex is too hydrophilic the reaction will be uncontrolled because the majority of the catalyst will be located within the aqueous phase.⁶⁷ Anionic surfactants are incompatible with ATRP,⁶⁸ so the use of cationic and non-ionic surfactant is necessary.^{67, 69, 70} However, using conventional ATRP led to poor colloidal stability.⁷¹ This led to the use of reverse ATRP using water-soluble initiators and the catalyst in a higher oxidation state.⁷² In addition, the use of mini-emulsion⁷³ and Pickering emulsion⁷⁴ systems has been explored.

Some examples of SFEP ATRP feature a macro-initiator. One category of these reactions is the use of simple polymer chain macro-initiators.^{75, 76} Wu *et al.*⁷⁷ used this method by producing a poly(ethylene glycol) monomethyl ether methacrylate (PEGMA) macro-initiator and stabiliser before extending with MMA or St.

In principle, comparable reactions to conventional ab initio SFEP can be carried out with small molecule ATRP initiators specifically synthesised for these reactions in miniemulsion,^{78, 79} as well as reverse ATRP in miniemulsion using conventional APS and K-50 initiators.⁸⁰

1.6. Reversible addition-fragmentation chain-transfer (RAFT) polymerization

Reversible addition-fragmentation chain-transfer (RAFT) polymerization was first reported by Chiefari *et al.*⁸¹ and patented by Moad *et al.*⁸² in 1998. RAFT polymerization can often yield $\bar{D} < 1.3$ and a simple equation can be used to predict the degree of polymerization (below).⁸³

$$DP = \frac{[M]}{[CTA]} \quad (1.14)$$

Where [M] is the concentration of monomer and [CTA] is the concentration of RAFT agent. Unlike ATRP, RAFT does not require a metal catalyst and can be used under mild conditions

with a wide range of monomers. However, selection of the RAFT agent does play an important role in the degree of control over the polymerization.⁸⁴ The generic structures of several groups of RAFT agent can be seen in Figure 1.8. The Z group activates the C=S bond toward radical addition and stabilises the transition state after free-radical addition. The R group should be a good radical leaving group and should then be able to re-initiate polymerization of the chosen monomer quickly to avoid retardation.^{81, 85} The varying Z group defines these different RAFT agents: dithiobenzoates (Z = alky or aryl), trithiocarbonates (Z = SR'), dithiocarbamates (Z = NR'R'') and xanthates (Z = OR'). The use of xanthates has been described as macromolecular design by interchange of xanthate (MADIX) polymerization.⁸⁶

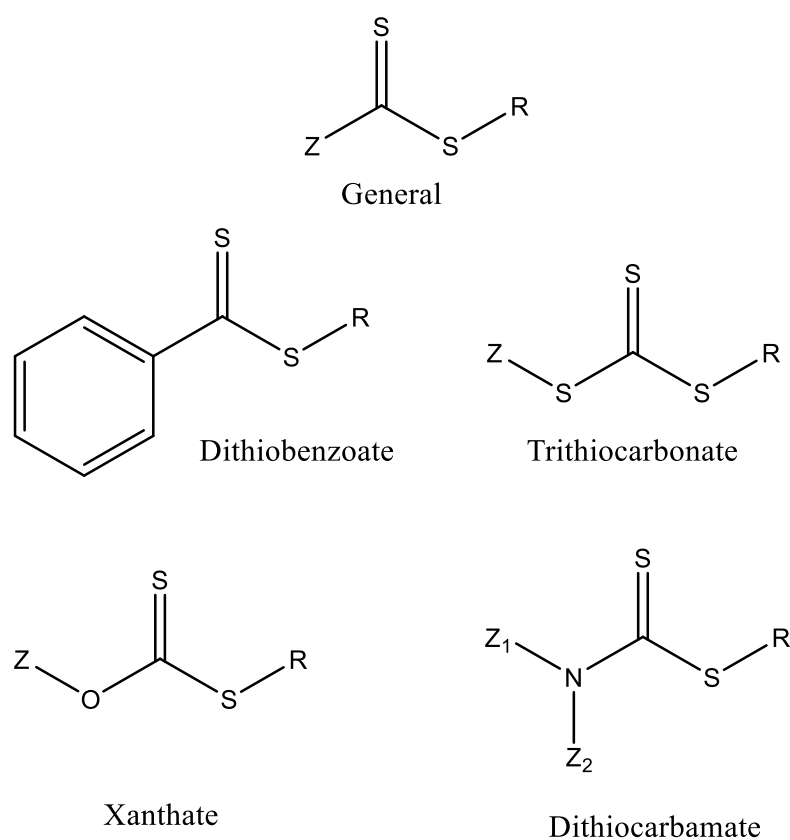


Figure 1.8. Generic chemical structures of RAFT agents.

The R and Z group must each be carefully selected for a given monomer. Moad *et al.*⁸⁷ published a guide to the selection of these substituents in 2005 which can be seen in Figure 1.9. Solid lines indicate good control and dashed lines indicate reduced control. The more reactive RAFT agents have carbon or sulfur atoms connected to the C=S double bond (e.g. trithiocarbonate). In contrast, C=S bonds with adjacent oxygen or nitrogen atoms (xanthates and dithiocarbamates) are less reactive towards radical addition. More reactive RAFT agents give best results with more activated monomers (MAMs). Less reactive RAFT agents exhibit better control with less active monomers (LAMs) due to the poor

leaving group ability of the monomer. The use of a more activated RAFT agent will therefore retard the polymerization. MAMs contain a vinyl group adjacent to an aromatic ring (e.g. styrene, St), carbonyl (e.g. methyl methacrylate, MMA) or nitrile group (e.g. acrylonitrile, AN). LAMs contain a vinyl group adjacent to an oxygen or nitrogen lone pair (e.g. vinyl acetate, VAc) or the heteroatom of a heteroaromatic ring (e.g. *N*-vinylpyrrolidone, NVP).⁸⁸

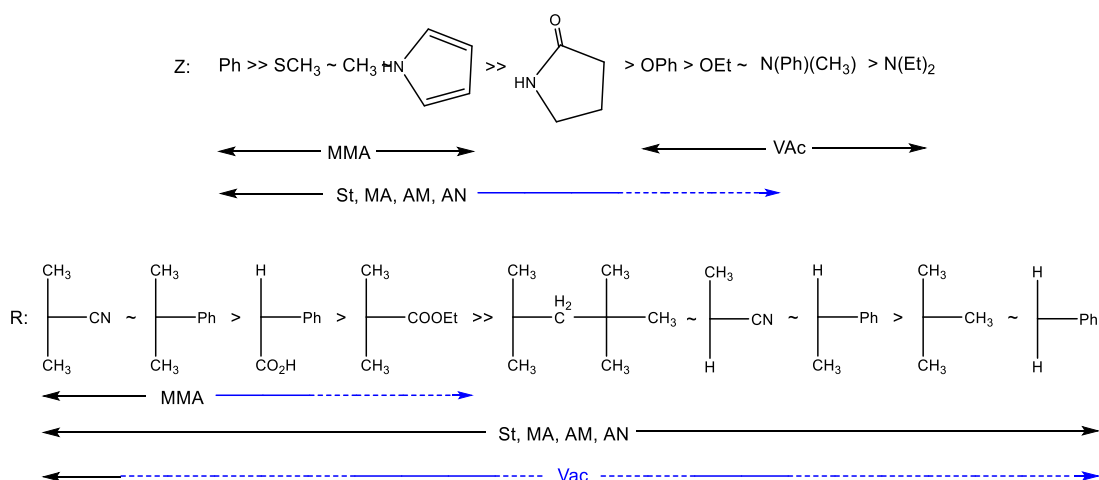


Figure 1.9. Guidelines for the selection of R and Z groups of RAFT agents. Z groups addition rates decreased and fragmentation rates increase from left to right. R groups fragmentation rates decrease from left to right.⁸⁷ Reproduced from Moad (2005) with permission from CSIRO Publishing.

So-called switchable RAFT agents can be used to polymerize both LAMs and MAMs successively, on the addition of acid or base.^{85, 89} A representation of this switch can be seen in Figure 1.10. When polymerizing diblock copolymers it is best to synthesise the poly(MAMs) block first as poly(LAMs) are poor leaving groups, but reinitiation can be slow. An alternative answer to this problem is the use of fluorinated RAFT agents.^{90, 91} These “F-RAFT agents” were presented as possible “universal” RAFT agents but have yet to be fully explored due to the difficulty of their synthesis.

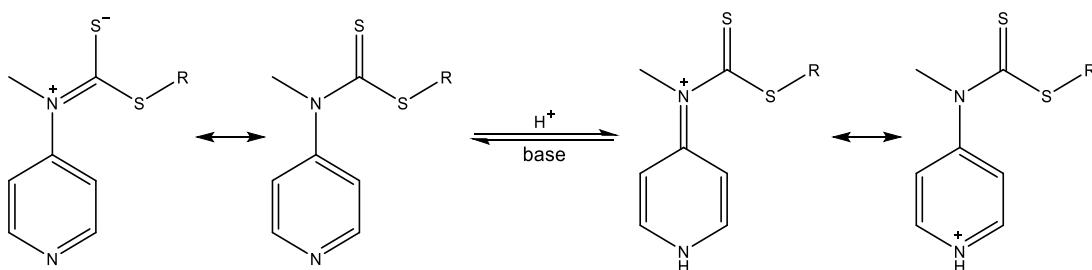


Figure 1.10. *N*-(4-pyridinyl)-*N*-methyldithiocarbamate switchable RAFT agents.

The synthesis of RAFT agents is often challenging, making their purchase on synthesis expensive, which has perhaps impeded commercialisation of this technique. However, the original RAFT patent filed by CSIRO has recently expired which may lead to further

commercialisation of RAFT agents, such as those developed by Lubrizol.⁹² Synthesis of RAFT agents is covered in detail in a review by Keddie *et al.*⁹³ and an overview can be seen in Figure 1.11.

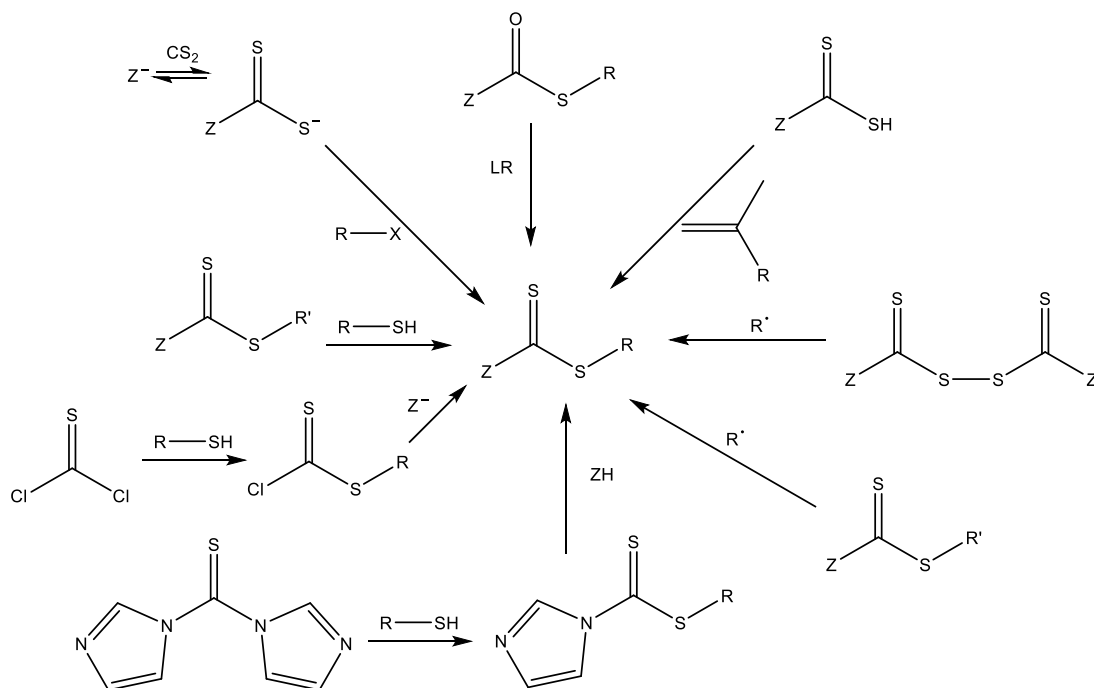
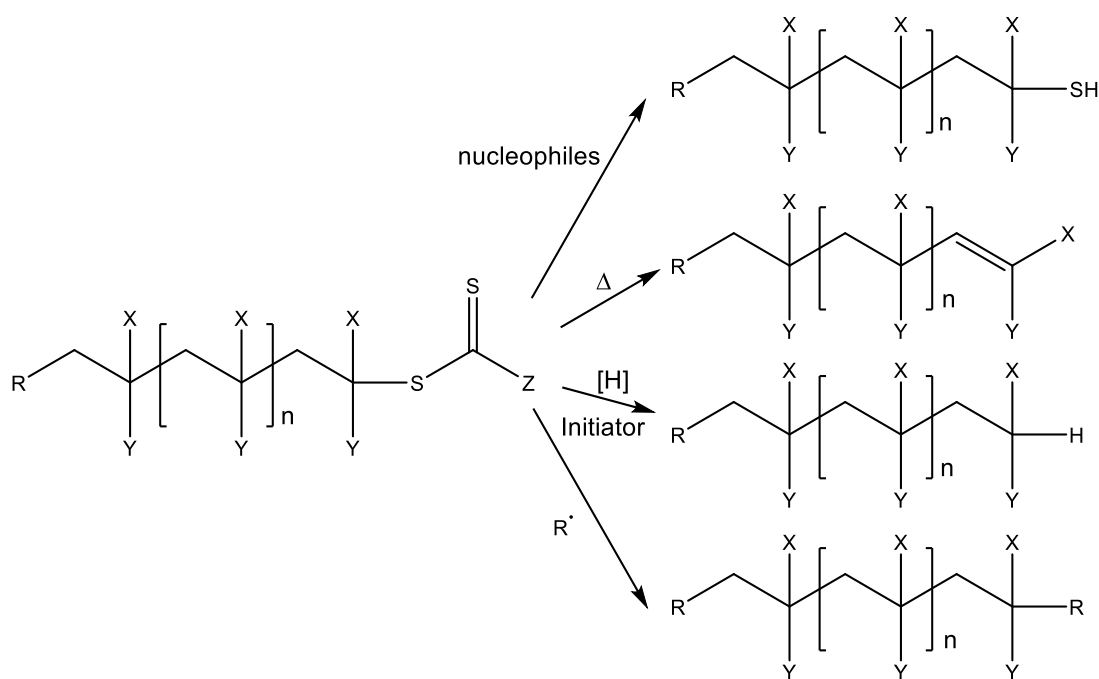


Figure 1.11. Overview of RAFT agent synthesis. Reprinted (adapted) with permission from (Keddie, D. J.; Moad, G.; Rizzardo, E.; Thang, S. H., RAFT Agent Design and Synthesis. *Macromolecules* **2012**, 45 (13), 5321-5342). Copyright (2012) American Chemical Society.⁹³

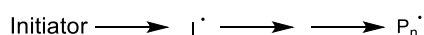
Due to the sulfur-based nature of RAFT agents there are certain disadvantages to using RAFT polymerization, such as the colour and unpleasant odour of the final polymers. These disadvantages can be overcome by removal of the RAFT end group after the polymerization.⁸⁴ Chong *et al.*⁹⁴ discussed possible reactions to remove the RAFT end group, as shown in Scheme 1.2. Reaction of the polymer product with nucleophiles and reducing agents yields thiols. Thermolysis and reaction with radicals, here represented as reduction and termination, are other well understood routes to end-group removal.



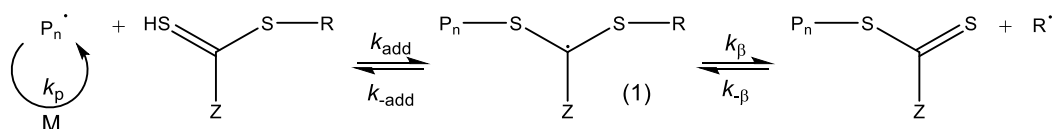
Scheme 1.2. Four possible routes for RAFT agent end group removal ([H] = H atom donor).⁹⁴

A schematic representation of the mechanism of RAFT polymerization can be seen in Scheme 1.3.⁸⁷ The initiation step is the same as free-radical polymerizations (FRPs) indeed, the initiator used in RAFT polymerizations is the same (e.g. azo compounds). This can also be said of the termination step to produce dead polymer which is here represented by a combination reaction between two polymer chains. $P_n \cdot$ enters the first equilibrium by addition to the C=S double bond of the RAFT agent. This step is referred to here as the reversible chain transfer step. This involves formation of intermediate (1) before eliminating $R \cdot$ from the RAFT agent. If this step is slow then it is likely that species (1), could undergo side reactions or retard the polymerization if reinitiation by $R \cdot$ is slow. This can also be said for species (2) in a later step, if $P \cdot$ is not a sufficiently good leaving group. $R \cdot$ will then propagate to form another polymer chain in the reinitiation step or $P \cdot$ being further chain extended. At this point, chain equilibration is attained whereby there is rapid exchange of the active polymer chains between $P_m \cdot$ and $P_n \cdot$. As discussed earlier in this introduction, the initiation step is the rate determining step of free-radical polymerizations and therefore the rate of polymerization should be the same in both free-radical and RAFT polymerizations. That is if the optimal RAFT agent for the polymerization of a given monomer is used, the reversible chain transfer step should not retard the polymerization. If none of the steps of RAFT polymerization are retarded this should allow the chains to grow at essentially the same rate and keep \bar{D} low. Early RAFT polymerizations had long inhibition periods and retardation of the rate of polymerization due to the reasons discussed above.⁹⁵

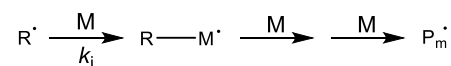
Initiation



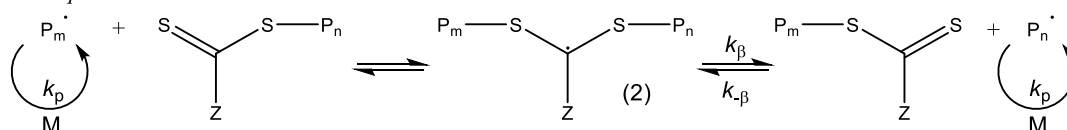
Reversible chain transfer



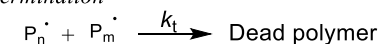
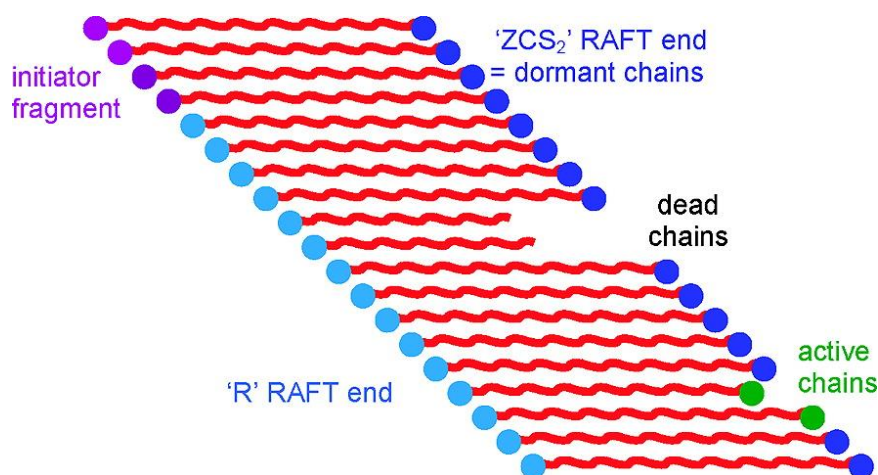
Reinitiation



Chain equilibration



Termination

Scheme 1.3. Mechanism of RAFT polymerization.⁸⁷Scheme 1.4. A representation of end-groups during a RAFT polymerization according to Moad et al.⁹⁶ Reprinted (adapted) with permission from (Moad, G.; Rizzardo, E.; Thang, S. H., Toward living radical polymerization. Accounts of Chemical Research **2008**, 41 (9), 1133-1142). Copyright (2008) American Chemical Society.

A schematic representation of the possible end-groups of a RAFT polymerization was presented by Moad et al.⁹⁶ and can be seen in Scheme 1.4. The irreversible termination of polymer chains is suppressed in RAFT polymerization but is still present. This is likely to occur under monomer-starved conditions and, as a result, polymerizations are often stopped prior to full conversion being reached. This means that a greater number of chains contain the RAFT agent as a chain end capper, which can then be reinitiated at a later time to produce diblock copolymers and other architectures. It is worth noting at this point that the RAFT polymerization mechanism requires the use of additional radicals to reinitiate the polymerization.

RAFT polymerization can be carried out in a range of solvents such as benzene,⁸¹ alcohols,⁹⁷ and supercritical CO₂.⁹⁸ However, the focus of this Thesis is the use of controlled techniques in aqueous media, namely emulsion polymerizations. As a result, solution and bulk RAFT polymerizations will not be discussed further.

1.6.1. Heterogeneous RAFT polymerization

Although RAFT polymerization has been carried out under suspension polymerization conditions,^{99, 100} this Thesis, and therefore this Introduction, will focus on emulsion polymerization (and dispersion polymerization when necessary).

RAFT emulsion polymerization originally suffered from poor colloidal stability, incomplete conversion, high dispersity and independence of molecular weight on RAFT agent concentration.¹⁰¹⁻¹⁰³ It was determined that these side effects were the result of inadequate transportation of RAFT agent through the aqueous phase and the high rate of radical exit from micelles. These effects can lead to a long inhibition period at the start of the polymerization.¹⁰¹ This leads to the polymerization taking place in the monomer droplets or the polymerization taking part in the absence of RAFT agent due to poor partitioning, leading to reduced control.¹⁰⁴ When oligomers enter monomer droplets they are much less likely to exit than if they enter micelles, due to the much larger droplet volume. This negates the considerable surface area difference between these two species which drives the micellar nucleation of particles in conventional emulsion polymerization discussed earlier.¹⁰⁵ It is also worth noting that RAFT emulsion polymerization may not follow zero-one kinetics, as suggested by Monteiro *et al.*¹⁰² This is because transfer of activity to longer chains from an oligomer entering a micelle is likely and the probability of two longer chain radicals terminating instantaneously being lower than for an oligomer and long chain active radical.

Despite these disadvantages, small molecule RAFT agents can be used in *ab initio* polymerizations. It was reported by Charmot *et al.*⁸⁶ that MADIX polymerization of St and butyl acrylate (BA) proceeded without rate retardation and the molecular weights were consistent with the theoretical molecular weights. However, the dispersities of these polymerizations were higher than expected ($\mathcal{D} = 2.1$ and 1.4 , for St and BA, respectively). These polymers were extended to form block copolymers by Monteiro *et al.*¹⁰², who found the semi-batch approach with a monomer-starved feed gave less irreversible termination and less polystyrene homopolymer.

It has been reported by various groups^{101, 106} that the RAFT agent concentration can be higher at the surface of particles formed in heterogeneous polymerization. This partitioning can be useful for polymer growth from the surface but with the complication that the RAFT agent or oligomers at the surface typically have higher dispersities ($3 < \mathcal{D} < 5$).

When using a conventional RAFT agent, the use of a secondary monomer in an emulsion polymerization can often be beneficial. A review by Lubnin *et al.*¹⁰⁴ states that the polymerization of acrylic monomers gave good control of molecular weight. However, when methacrylates were used, fewer than the theoretical number of chains were produced. When 10% acrylic monomer was added to these polymerizations, the rate was lowered enough to produce predicted molecular weights. This review also stated that amphiphilic RAFT agents often afforded better control than those which were deemed more hydrophilic or hydrophobic. This was attributed to hydrophilic RAFT agents residing mostly in the water phase and hydrophobic RAFT agents, or those with too high an affinity for the monomer droplets, being unable to reach the micelles. Nozari and Tauer¹⁰⁷ also showed that the balance of hydrophilicity between RAFT agent and initiator can be an important factor in the overall control of the polymerization.

Surfactant-free emulsion polymerization (SFEP) was also conducted using these small RAFT agents. This is usually carried out with a surface-active RAFT agent or surfmer. Stoffelbach *et al.*¹⁶ reported the use of 2-(dodecylthiocarbonothioylthio)-2-methylpropanoic acid, sodium salt (TTCA, Figure 1.12). When polymerizing n-butyl methacrylate (nBMA), the polymerization was fast and yielded small, stable particles. However, there was no control over the molecular weight and the RAFT agent was proven to be inappropriate for methacrylates under bulk polymerization conditions. Additionally, when TTCA was used for the polymerization of St the reaction was completely inhibited. This was attributed to the hydrophilicity of the leaving group allowing it to exit the micelles. As mentioned previously, the addition of a secondary monomer can be beneficial for RAFT emulsion polymerization. When a small amount of St or n-butyl acrylate (nBA) was added to the SFEP of nBMA, under bulk or heterogeneous conditions, considerably more control was conferred on the polymerization. Also, colloiddally stable particles were produced with diameters of less than 150 nm.

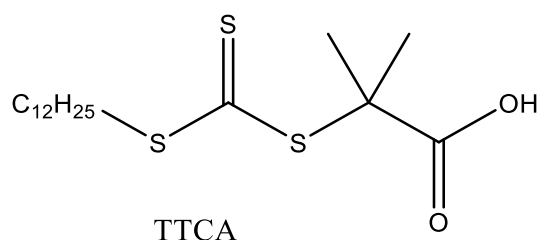


Figure 1.12. Structure of 2-(dodecylthiocarbonothioylthio)-2-methylpropanoic acid (TTCA).

Building on the use of surfmers, Kwak *et al.*¹⁰⁸ reported a RAFT agent with the attributes of a surfactant, photo-initiator and terminator (suriniferter). More specifically, 4-diethylthiocarbamoylsulfanylmethyl benzoic acid (DTBA, Figure 1.13) was employed for the

SFEP of MMA. Linear evolution of molecular weight with conversion was observed up to 60%. However, at this point the molecular weight decreased dramatically and M_n values obtained were considerably higher than theoretical values. Attempts to include an additional traditional surfactant led to less controlled polymerizations. Kim *et al.*¹⁰⁹ built on this work by polymerizing MMA and monitoring the change in particle size with DTBA concentration. Below a critical value the particles could not be stabilised, demonstrating the surface activity of DTBA. A related study also examined the polymerization of St in the presence of DTBA.¹¹⁰ Other surfactants have been used and each contain both hydrophilic and hydrophobic moieties.¹¹⁰⁻¹¹² Unfortunately none gave useful control over the polymerization with molar mass not being dependent on the RAFT agent concentration.¹¹¹ Zhou *et al.*¹¹³ attributed this to insufficient hydrophilicity of the RAFT agents, despite the R group of DTBA being sufficiently hydrophilic to exit micelles.

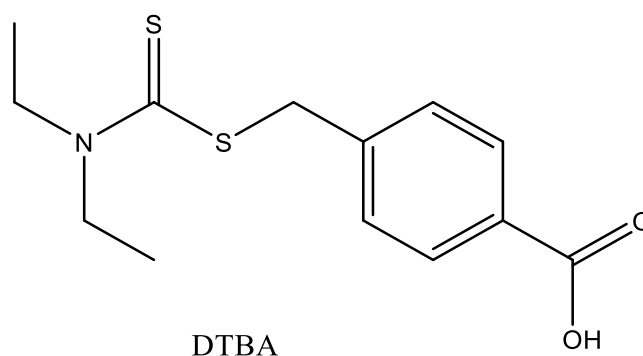


Figure 1.13. Structure of 4-diethylthiocarbamoylsulfanylmethyl benzoic acid (DTBA).

Monteiro *et al.*¹⁰¹ reported the use of a seed latex for RAFT emulsion polymerization. A PMMA seed was formed by conventional emulsion polymerization and the RAFT agent and additional St were added in a second step. Although this formulation still showed retardation of the polymerization due to RAFT group exit. Gilbert *et al.*¹¹⁴ continued this work using a PSt seed and then transported the RAFT agent to the seed particles using acetone. The acetone was later removed and the successful RAFT polymerization of additional St carried out. Additional SDS surfactant was also required for this second step in both the above publications. Future work was also carried out with xanthates and included the formation of diblock PSt-*b*-PnBA core-shell particles.^{115, 116}

This approach was extended by Ferguson *et al.*¹¹⁷ who pioneered the use of a macromolecular chain transfer agent (mCTA). Thus, poly(acrylic acid) (PAA) was prepared in aqueous solution to form the mCTA. Extension with BA was then carried out to produce oligomeric diblocks that formed micelles in solution. Both reactions were completed successfully in the absence of any surfactant. The RAFT agent in these polymerizations was initially attached to a polymer, this means that the rate of radical exit is lessened and therefore reduces

polymerization in the monomer droplets. This also inhibits the formation of an oily-layer and coagulation. As a result, this method addresses several problems encountered with heterogeneous RAFT polymerizations.

Manguian *et al.*¹¹⁸ later synthesised a hydrophilic mCTA composed of poly(2-(diethylamino)ethyl methacrylate). However, this was accomplished by solution polymerization in ethanol. After precipitation in acetone, the mCTA was extended with St in an aqueous emulsion polymerization. Synthesis of the mCTA can also be conducted under bulk conditions using a hydrophobic mCTA. However, using PSt mCTA required surfactant and a secondary co-solvent to carry out the extension polymerization in aqueous conditions.¹¹⁹ For this polymerization to be carried out under surfactant-free conditions, sodium acrylate was incorporated as a co-monomer in the mCTA synthesis.¹²⁰

Ferguson *et al.*¹²¹ used these hydrophilic mCTAs in a process later named polymerization-induced self-assembly (PISA). Which has become a major area of interest for RAFT polymerization in recent years. Canning *et al.*¹²² presented a thorough review recently about this process and the limitations of PISA. Including the use of this technique to synthesise morphologies in aqueous media such as jellyfish and framboidal vesicles.

1.7. The DPE method

1.7.1. General background

1,1-Diphenylethylene (DPE) is a colourless, odourless, inexpensive, commercially available molecule. At the time of starting this research project it was believed that DPE was non-toxic. However, recently it has been determined that DPE is toxic to aquatic life with long lasting effects. The structure of DPE can be seen in Figure 1.14. Due to steric hindrance, and the stabilisation of radicals by conjugation with the two phenyl rings, DPE is unable to homopolymerize by free radical polymerization, with attempts to polymerize DPE forming only dimers.¹²³

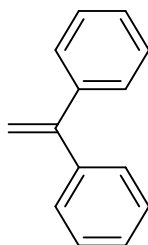


Figure 1.14. Structure of 1,1-diphenylethylene.

DPE has been reported to copolymerize using anionic polymerization. “Super polystyrene”, a BASF product,¹²⁴ is an example of this formed by the anionic co-

polymerization of St with DPE. Yuki *et al.*¹²⁵ reported that incorporating DPE into PSt increased the T_g .^{125, 126} It was also found that the yield decreased significantly with increasing DPE content. It is thought that the product is an alternating copolymer, as the stabilising effect of the two phenyl rings of DPE means addition to DPE is favoured by anions.¹²⁷

There are also a number of publications involving the use of DPE in cationic polymerization.^{128, 129} One example involves ρ -substituted styrenes; ρ -methyl-, ρ -butyl-, ρ -acetoxy- and ρ -*tert*-butoxystyrene.¹³⁰ Copolymerization occurs to give narrow dispersity and a molecular weight of more than 10,000. ^1H NMR spectroscopy showed that these copolymers contained less than 10% DPE, despite additional DPE being present in the monomer feed. There was no evidence for DPE-DPE units within the copolymer chains in this study.

The reactivity ratios of DPE in free radical polymerization have been reported to be almost zero.¹³¹ This has led to the use of DPE as a retarder and polymer chain-end capper. Kice *et al.*¹³² published the first use of DPE with free radicals and methyl methacrylate in 1959. However, controlled radical polymerization mediated by DPE was not patented until 2000 by Bremser at BASF.¹³³ A subsequent research paper was published in 2001 by Wieland *et al.*¹³⁴, with Bremser as a co-author. The use of DPE in free-radical polymerizations was then dubbed “the DPE method”.

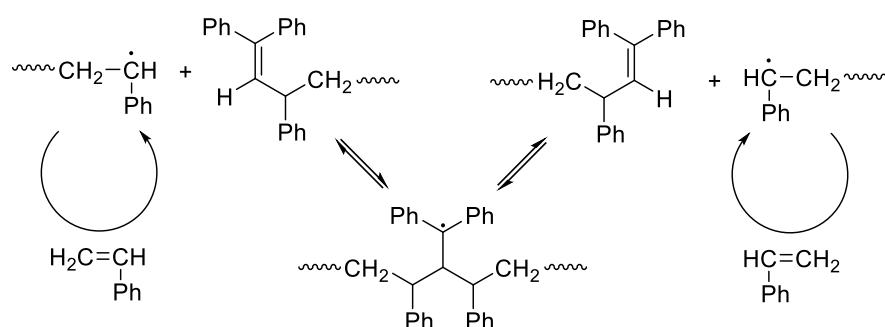
All the RDRP techniques discussed above each have their own disadvantages. It is hoped that the DPE method can combine the best aspects of conventional emulsion polymerization i.e. environmentally friendly aqueous conditions and cost efficiency, with those of RDRP i.e. control of polymer architecture, molecular weight, and Đ. This method has been used for a wide range of monomers such as styrenics,^{135, 136} acrylates,^{137, 138} acrylic acid,^{139, 140} maleic anhydride,¹⁴¹ and *N*-vinyl compounds.¹²⁶ Use of this molecule is therefore hoped to be applicable to every major monomer group without the need to tailor its properties, as seen with RAFT agents. The use of DPE was also anticipated to yield better product properties, (e.g. colourless products) when included in polymerizations, without the need to remove metals or end-groups post-polymerization. The low cost and commercial availability of this capper also lends to its use on an industrial scale without greatly affecting the final product price.

1.7.2. Mechanism of the DPE method

1.7.2.1. Mechanism of precursor formation

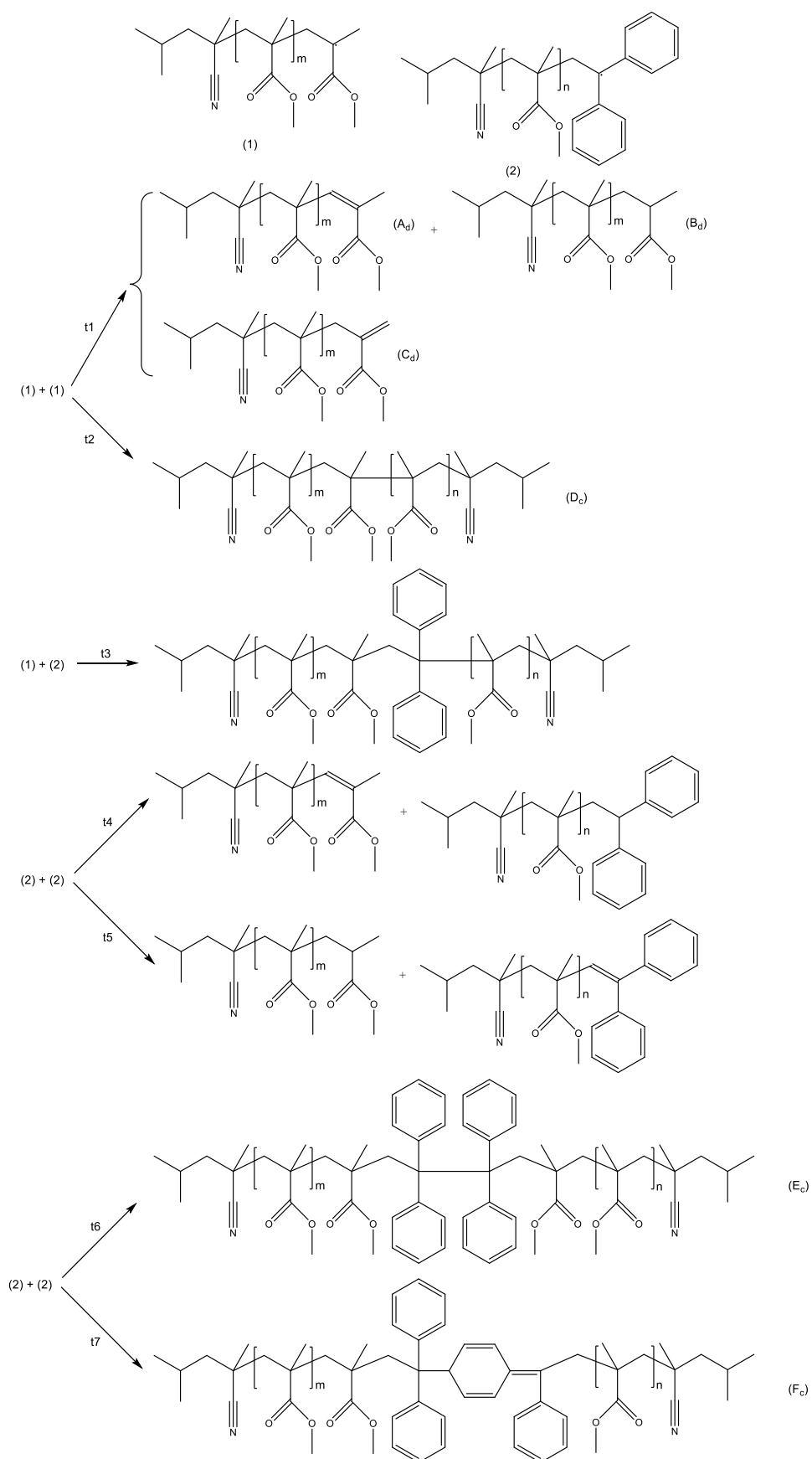
The mechanism of the DPE method is still being debated and will be discussed here in the context of both stage one (precursor formation) and stage two (extension of the precursor).

For stage one polymerizations, one early hypothesis was that the DPE method could have an analogous mechanism to that of RAFT polymerization. This idea was mentioned briefly in the original DPE publication by Wieland *et al.*¹³⁴ and can be seen in Scheme 1.5. However, no data was given to support this claim. As a result, this mechanism can most likely be discounted.



Scheme 1.5. Possible DPE mechanism analogous to the RAFT polymerization mechanism.¹³⁴ Reprinted (adapted) with permission from John Wiley and Sons (License number: 4577031400552).

Perhaps the most elegant summary of the possible mechanisms was reported by Zhao *et al.*¹³¹ (Scheme 1.6). In this scheme, the reactions of DPE capped (2) and uncapped (1) PMMA can be seen. Zhao *et al.* methodically work through the possible mechanisms discounting them using different techniques.¹³¹ Both t1 and t2 are discounted early in the discussion. Such termination pathways involve conventional disproportionation and recombination and so cannot be responsible for control otherwise the free radical polymerization of MMA would be controlled. However, there is evidence from ¹H and ¹³C NMR spectroscopy that the t1 product is present in the final polymer. Zhao *et al.* also suggest that t4 and t5 should be negligible reaction pathways. This is because of the lack of disproportionation products in the polymerizations of St, where the primary termination route is combination. This leaves t3, t6 and t7 as possible termination pathways that contain one or more DPE units.



Scheme 1.6. PMMA termination pathways of the DPE method.¹³¹ Reprinted (adapted) with permission from John Wiley and Sons (License number: 4550310475411).

In contrast, Zhao *et al.*¹³¹ concluded that t3 was the primary termination pathway using MS data. Also, ¹H NMR spectra of the polymers contained none of the resonances between 5 and 6 ppm observed by Viala. These results were obtained from a solution polymerization compared to Viala's emulsion polymerization study. It is possible that this affects the termination pathway. A full breakdown of reaction conditions can be seen in Table 1.1. However, the M:I:DPE ratio was varied by Zhao *et al.* who used ratios both above and below that reported by Viala publication. Varying the temperature and using different initiators also yielded data supporting the same t3 termination pathway. It should be noted that Zhao *et al.* quenched their polymerizations at low molecular weights (1000 – 3000 Da), which may have led to fewer DPE-capped chains. This would make it less likely for a t6 or t7 termination pathway to occur. Overall, the main difference between the two publications is the homogeneous solution polymerization compared to the heterogeneous emulsion polymerization. It is also worth noting that, despite a lack of investigation into this mechanism, only the publications by Zhao and co-workers reported the t3 pathway as the primary one.^{147,}

148

Table 1.1. Comparison table of publications by Viala *et al.*¹⁴³ and Zhao *et al.*¹³¹ M and I denote monomer and initiator, respectively.

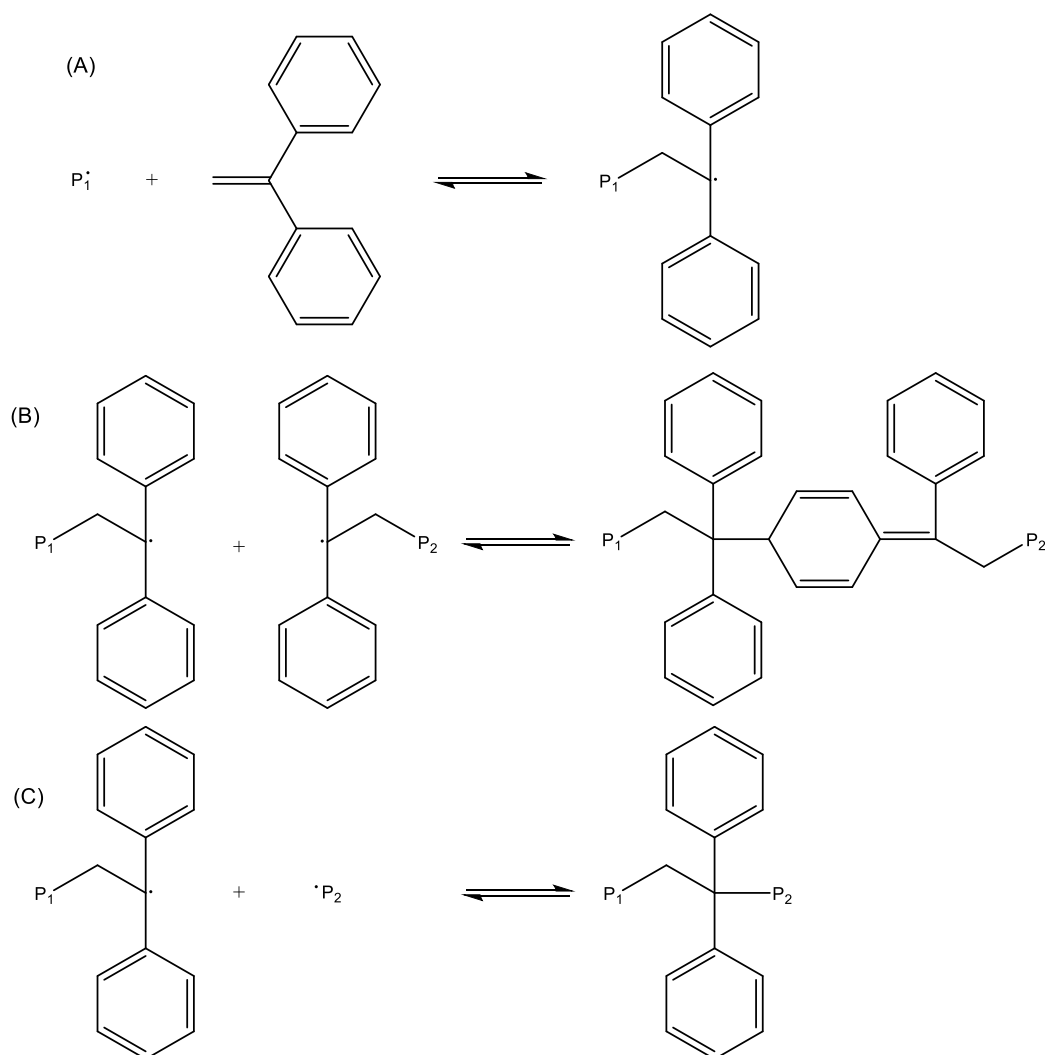
Author	M:I:DPE	Initiator	Temperature (°C)	Polymerization
Viala	34:1.17:1	APS	70	Emulsion
Zhao	40:2:1	ABVN	60	Solution
Zhao	20:1:3	ABVN	60	Solution
Zhao	20:1:3	AIBN	80	Solution

It is also unclear whether the capping of DPE is reversible. No meaningful data has been presented to support or refute this. Never the less, several publications refer to it and represent it as an equilibrium.^{131, 134, 143, 147, 149} This would play a large role in the mechanism and the characteristics of the polymers that would be formed with DPE as an end capper. As a result, stage two mechanisms remain ambiguous.

1.7.2.2. Mechanism of diblock copolymer formation

The formation of diblock copolymers using the DPE method is widely accepted despite often unsatisfactory data, which will be discussed later. One possible mechanism could involve the combination of a polymer radical capped with DPE with another DPE capped or uncapped polymer radical ((B) or (C), Scheme 1.7). This would then be followed by the uncapping of P₁[·] (A). P₁[·] could then consume a secondary monomer until termination or again being capped by DPE. Viala *et al.*¹⁵⁰ investigated this using thiophenol as a radical scavenger. The precursor was heated to 60 °C for 20 hours in the presence of thiophenol. ¹H NMR spectroscopy was used to monitor the S-H resonance over time. If radicals were formed, thiophenol should be consumed so this signal should decrease. This was not observed, indicating that the capping

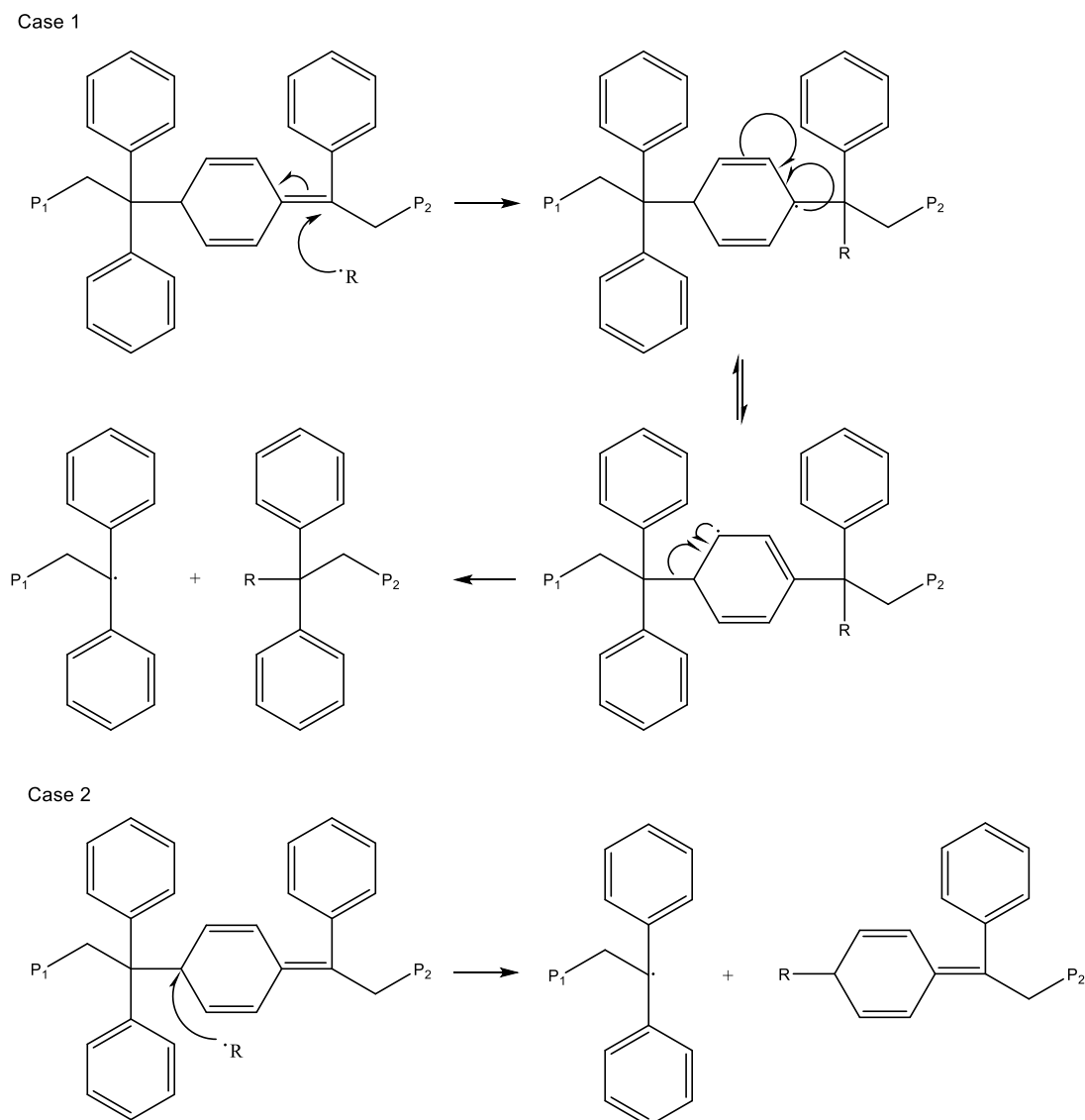
is not reversible. On the other hand, Zhao *et al.*¹³¹ heated a precursor in the presence of TEMPO at 120 °C for 8 h and used SEC to show an approximate halving of the molecular weight. Therefore, the higher temperature may be required to remove the DPE molecule. When this reaction was performed at 60 °C, there was little change in the ¹H NMR spectrum. However, at 120 °C, an unsaturated methylene and sharp aromatic proton resonances could be seen. This was attributed to the depolymerization / uncapping of the DPE molecule and this molecule was compared to the depolymerization of α -methyl styrene. However, the latter depolymerization occurred at over 200 °C.¹⁵¹ It is worth noting that the ceiling temperature of α -methyl styrene is just above 60 °C so the possibility of DPE uncapping is not unreasonable.¹⁵² The uncapping of the DPE molecule at 120 °C may represent a problem in emulsion polymerization as a pressurised reactor would be needed. Another point to consider is that the Viala¹⁴³ and Zhao¹³¹ publications, discussed in the context of the stage one mechanism, involve different termination pathways and were carried out under different polymerization conditions.



Scheme 1.7. Possible reactivation pathways for DPE containing precursor polymer.

If the capping of DPE is not reversible, then the extension of the precursor requires a new influx of radicals. Little work has considered the possible mechanism of this attack except a single publication, again by Viala *et al.*¹⁴³ As discussed above, this paper uses thiophenol to disprove the reversible capping of DPE. Scheme 1.8 outlines two possible pathways to produce diblock copolymers by attack of radicals at the semiquinoid moiety. However, it is unclear which of these mechanisms occurs. Viala *et al.* does report that the lack of a thermally self-initiating monomer for stage 2 (such as St) led to no polymerization taking place in stage two. However, no analysis is presented in Viala's Thesis to corroborate this finding. When PSt was used to extend a PnBA precursor, the final conversion varied considerably but an increase in conversion was observed (37%,¹⁴⁶ and 87%¹³⁶). Whether this is due to the capping equilibria of DPE or the self-initiation of St remains unclear.

There are also conflicting reports as to whether the DPE capper is still contained within the polymer chain after the formation of the diblock. If DPE is removed from the polymer chain it is not clear how this would occur if the capping of DPE is not reversible. For a reaction to require additional initiator for stage 2 but not contain the DPE capper suggests that the semiquinoid structure is not formed via a reversible reaction at the reaction temperature but the capping of the polymer chain by DPE is. This could also lead to the formation of more homopolymer.



Scheme 1.8. Possible mechanisms for the radical attack at the semiquinoid unit of a DPE containing polymer.¹⁴³
Reprinted (adapted) with permission from Elsevier (License number: 4576501059173).

1.7.3. DPE method characteristics

The DPE method has been reported in bulk,¹³⁴ solution,¹⁵³ and heterogeneous polymerizations.¹⁵⁰ The vast majority of these reactions are emulsion polymerizations and therefore much of the discussion below is based around heterogeneous polymerization using the DPE method. Whenever a polymerization is not heterogeneous this will be indicated.

Viala *et al.*¹⁵⁴ reported the emulsion polymerization of MMA in both the presence and absence of DPE. These are referred to as the copolymer and reference PMMA, respectively. The copolymer had a considerably lower molecular weight by SEC.

Many of the DPE method publications involve the polymerization of MMA as a precursor.^{134, 153} Viala *et al.*¹⁵⁰ examined the formation of precursor particles by the emulsion polymerization of St. However, these reactions only reached 50% conversion in 24 h whereas MMA

polymerizations reached 80% in 15 h. Additionally, when agitation was stopped phase separation was observed. No explanation was given for these observations.

Zhao *et al.*¹⁴⁷ showed that in the emulsion polymerization of MMA, the rate of polymerization decreased significantly in the presence of DPE. This phenomenon was also observed in bulk and solution polymerizations.¹⁵⁵ Zhao *et al.* adjusted the MMA:DPE ratio from 400:1 to 100:1. Moreover, higher DPE contents led to slower reaction rates.

Wieland *et al.*¹³⁴ showed that for a bulk polymerization, the overall conversion and the molecular weight decreased as the DPE:initiator ratio was increased. The initiator concentration was kept constant. There was no clear effect on dispersity (\bar{D}), but all polymerizations afforded $\bar{D} < 1.75$.

As mentioned previously for a RAFT polymerization, the evolution of conversion against molecular weight should be linear. This was not observed by Zhao *et al.*¹⁴⁷ when using the DPE method. The molecular weight increased linearly at low conversion but began to decrease in the later stages of the reaction. This occurred at lower conversion with increasing DPE concentration. Linear evolution of molecular weight at low conversion before decreasing molecular weight was also observed in bulk and solution.¹³⁸

Interestingly, when the DPE:APS ratio is kept constant the rate of emulsion polymerization increases on increasing the DPE and APS concentration.¹⁴⁹ This would be expected for an increase in initiator concentration but suggests that an equal increase in DPE content is not enough to slow the reaction. No comparison to a reaction in the absence of DPE was provided.

In stage two of the DPE method, the molecular weight increases over the secondary reaction in bulk, solution and heterogeneous polymerizations.^{144, 147, 155} Size exclusion chromatography (SEC) data does show an increase in molecular weight but does not show whether the newly formed polymer is a block copolymer or simply a higher molecular weight homopolymer. Many of the MWDs for the precursor and diblock copolymer overlap.¹⁵⁵ This could be the result of secondary monomer homopolymerization and could be higher molecular weight compared to the precursors due to the decreased concentration of DPE.. This can also be said for ¹H NMR data;¹⁴⁴ the resonance increase for a second polymer can be monitored but again does not prove block copolymer formation.

Viala *et al.*¹⁴³ published the extension of PMMA-DPE precursor with an additional amount of MMA in solution polymerization. The conversion over time in the stage two polymerization is decreased by the addition of PMMA-DPE. It is unlikely that there is any free DPE to retard the polymerization because the precursor was purified by multiple reprecipitation steps. It is noted that thermal polymerization of MMA became significant after 8 h and increased the

overall conversion. Moreover, the molecular weight of the polymer is reduced by the presence of precursor, of which there is still a significant amount in the final product. Both findings suggest that the precursor is involved in the second step polymerization in some way.

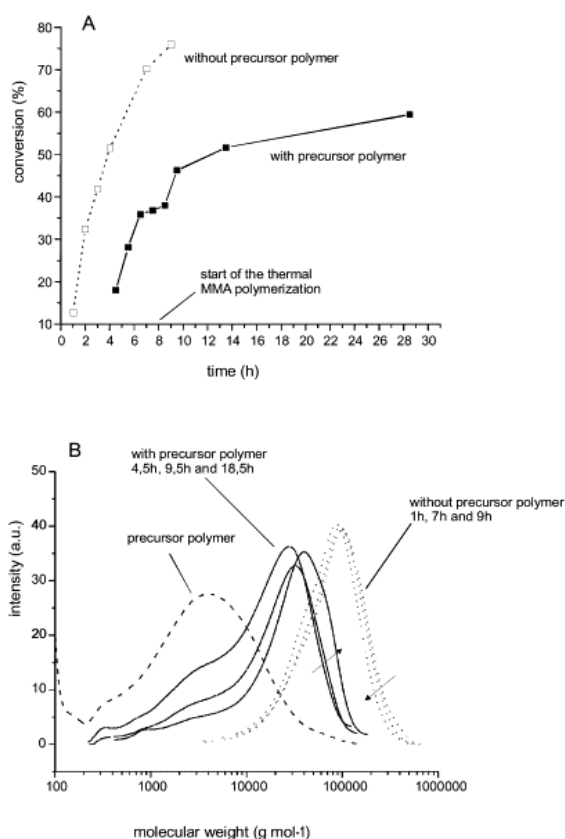


Figure 1.15. Polymerization kinetics in the presence and absence of PMMA-DPE. A) Monitoring conversion with time B) molecular weight distribution change with time.¹⁴³ Reprinted (adapted) with permission from Elsevier (License number: 4550320198601).

Raether *et al.*¹²⁶ used IR spectroscopy to attempt to show block formation. PMMA-DPE precursor was extended with St and then extracted with hot cyclohexane to remove St homopolymer. IR bands for PSt were still present after the extraction and the same process with a homopolymer mixture of PMMA and PSt removed most of the PSt. Moreover, scanning electron microscopy (SEM) was used to show that phase separation occurred on a shorter length scale for the diblock copolymer compared to a homopolymer mixture. This was also observed in other publications but homopolymer was not removed in these cases.^{144, 149}

When the DPE:APS ratio was kept constant during the precursor formation, the resulting diblock copolymer was also different. SEC data reported by Wang *et al.*¹⁴⁹ show cleaner extension with a less pronounced tail when using precursors prepared with higher DPE and APS concentrations. An increase in the rate of polymerization of stage two monomer St was also observed. This could be due to an increased proportion of DPE capped precursor that could be extended.

Stage two heterogenous polymerizations have also been shown to produce bimodal particle distribution when n-butyl acrylate (nBA) was polymerized in the presence of PMMA-DPE precursor latex.¹⁴⁴ Additional surfactant added at stage 2 could not prevent secondary nucleation and it is likely that these latex particles contain PnBA homopolymer. It was also noted that coagulation occurred when the synthesis of PMMA-b-PSt was attempted.¹⁴⁹ This was attributed to insufficient surfactant added in stage 2 to stabilise the growing particles. However, Zhao *et al.*¹⁴⁷ did not report considerable coagulation but did note an increase in average particle diameter when St was polymerized in the presence of precursor without additional surfactant.

Viala and coworkers^{143, 150} published some of the more compelling evidence for the formation of diblocks in stage 2 of the DPE method. AA-MMA-DPE was synthesised as a precursor in emulsion polymerization and was extended with St. This polymer was then precipitated into excess acetone to remove homo-PSt and then into water to remove residual precursor. The amount of polymer remaining was determined as the block copolymer yield (BCY) and was plotted against the mass ratio of precursor:monomer (St) in Figure 1.16.¹⁵⁰ Both concentrations of ACPA initiator used in stage two gave a maximum BCY of 95% whereas when no initiator was added the maximum BCY was 77%. Thus, it was inferred that too high a concentration of precursor led to the recoupling of precursor polymer rather than the extension with St. If the precipitation cycles removed residual precursor and homo-PSt it is likely that the remainder is P(AA-*stat*-MMA)-*b*-PSt terpolymer. However, the only additional analysis undertaken was the corresponding particle size distributions.

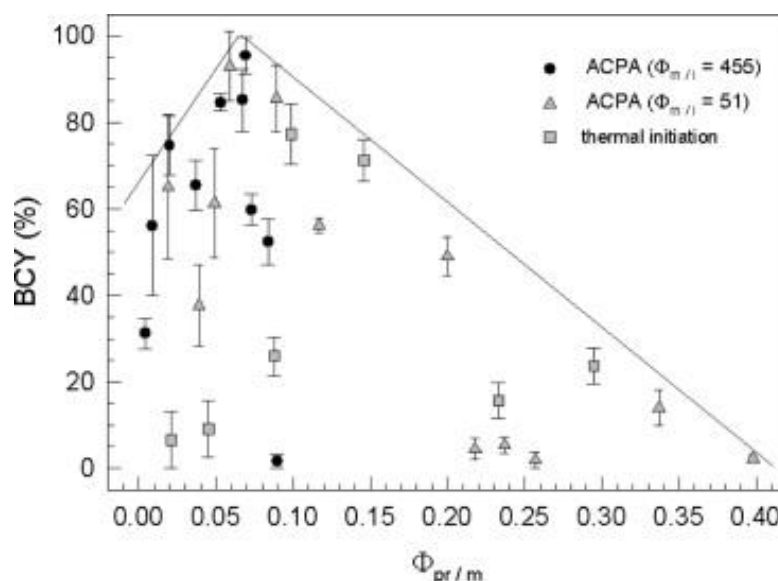


Figure 1.16. Block copolymer yield against the mass ratio of AA-*stat*-MMA-DPE:St. Data sets are the ratio of St:ACPA initiator including thermal initiation without additional ACPA in step two.¹⁵⁰ Reprinted (adapted) with permission from Elsevier (License number: 4550320456140).

1.7.4. Surfactant-free emulsion polymerization using the DPE method

The DPE method has been used only sparsely in SFEP. Viala et al.¹⁵⁴ polymerized MMA in the presence of DPE in aqueous media without surfactant. However, this reaction was only used to monitor the reaction via calorimetry. Findings were consistent with those of conventional emulsion polymerizations: the rate of polymerization was retarded by the presence of DPE. This was the only analysis undertaken of this system.

Multiple SFEP publications have been published by Fan and coworkers.¹⁵⁶⁻¹⁵⁸ The synthesis of PSt-DPE precursors is perhaps the most interesting in the context of this Thesis. The MWDs of the resulting polymers are broad, often with multiple peaks and low molecular weight tails. The dispersity and molecular weight of the precursor could be reduced by increasing the amount of St fed into the reactor over the course of the polymerization. The rate of polymerization and the particle size were also reduced by addition of DPE to the SFEP. Similar polymerizations were also conducted with glycidyl methacrylate (GMA) as the major monomer. However, this reaction did not proceed by emulsion polymerization and TEM and SEM only showed film formation rather than particles. This work was extended to produce flower-like and raspberry-like particles for drug delivery applications consisting of mixtures of PSt, PGMA and PAA with DPE and crosslinker divinyl benzene. Particle size distributions and appearance are the main focus of this study and little information is provided for the polymers.

This SFEP method has been used to encapsulate various particles including iron oxide, carbon black and zinc oxide.^{139, 145, 159}

1.8. Thesis aims

The aim of this Thesis was to investigate controlled radical polymerization via surfactant-free aqueous emulsion polymerization. It is hoped the use of surfactant-free emulsion polymerization can be used to produce latexes of diblock copolymers for coatings combined with the DPE method to do this in an industrially relevant, scalable, and cost-effective way.

This was initially investigated using the DPE method. The synthesis of precursor and the effect of concentration of DPE and APS initiator in the surfactant-free emulsion polymerization of methyl methacrylate is examined. The mechanism of the DPE method is investigated by determining the number of DPE units per polymer chain and the location of DPE within the latex is also examined. The effect of the presence of DPE is also examined on the PSD of the PMMA latex.

Chapter 2 examines the extension of PMMA precursor, synthesised in the absence and presence of DPE, by polymerizing styrene or benzyl methacrylate. The aim in this Chapter is to determine if the DPE method can be used to form diblock copolymers and to investigate the feasibility and mechanism of reactivation of the precursor. This is done by completing stage 2 DPE method polymerizations in the presence and absence of additional initiator. This chapter contains is the first available data of the use of benzyl methacrylate with the DPE method.

Finally, the use of RAFT polymerization in surfactant free aqueous systems is reported. This is the first reported instance of using small molecular RAFT agents that are not “suriniferters” and without further additions e.g. secondary solvent. RAFT agents are first assessed in solution polymerization to determine their effectiveness with the chosen monomer (MMA) under the selected conditions. Before being used in surfactant-free emulsion polymerizations at varying pH to control the amphiphilicity of the RAFT agents used. AIBN initiator is also utilised in control experiments to examine the effect of RAFT end-group charge stabilisation in surfactant-free systems.

1.9. References

1. Flory, P. J., *Principles of Polymer Chemistry*. Cornell University Press: Ithaca and London, 1953; Vol. 1.
2. Braunecker, W. A.; Matyjaszewski, K., Controlled/living radical polymerization: Features, developments and perspectives. *Progress in Polymer Science* **2007**, 32 (1), 93-146.
3. Odian, G., *Principles of polymerisation*. 4th ed.; Wiley: New York, 2004.
4. Lovell, P. A.; El-Aasser, M. S., *Emulsion polymerization and emulsion polymers*. J. Wiley: Chichester, 1997.
5. Fitch, R. M., *Polymer colloids: a comprehensive introduction*. Academic Press: London, 1997.
6. Asua, J. M., Miniemulsion polymerization. *Progress in Polymer Science* **2002**, 27 (7), 1283-1346.
7. Chern, C. S., Emulsion polymerization mechanisms and kinetics. *Progress in Polymer Science* **2006**, 31 (5), 443-486.
8. Gallego, L. J.; Grimson, M. J.; Rey, C.; Silbert, M., Temperature-dependence of the steric interaction in colloidal dispersions stabilized by grafted chains. *Colloid and Polymer Science* **1992**, 270 (11), 1091-1093.
9. Romero-Cano, M. S.; Martin-Rodriguez, A.; Chauveteau, G.; de las Nieves, F. J., Colloidal stabilization of polystyrene particles by adsorption of nonionic surfactant - II. Electrosteric stability studies. *Journal of Colloid and Interface Science* **1998**, 198 (2), 273-281.
10. Verwey, E. J. W.; Overbeek, J. T. G., *Theory of the Stability of Lyophobic Colloids*. Elsevier: New York, 1948.
11. Naves, A. F.; Palombo, R. R.; Carrasco, L. D. M.; Carmona-Ribeiro, A. M., Antimicrobial Particles from Emulsion Polymerization of Methyl Methacrylate in the Presence of Quaternary Ammonium Surfactants. *Langmuir* **2013**, 29 (31), 9677-9684.
12. Cunningham, M. F.; Geramita, K.; Ma, J. W., Measuring the effects of dissolved oxygen in styrene emulsion polymerization. *Polymer* **2000**, 41 (14), 5385-5392.

13. Jialanella, G. L.; Firer, E. M.; Piirma, I., Synthesis of polystyrene-block-polyoxyethylene for use as a stabilizer in the emulsion polymerization of styrene. *Journal of Polymer Science Part A-Polymer Chemistry* **1992**, *30* (9), 1925-1933.
14. Zhang, K.; Wu, W.; Meng, H.; Guo, K.; Chen, J. F., Pickering emulsion polymerization: Preparation of polystyrene/nano-SiO₂ composite microspheres with core-shell structure. *Powder Technology* **2009**, *190* (3), 393-400.
15. Gilbert, R. G., *Emulsion Polymerization: A Mechanistic Approach*. Academic Press: London, 1995.
16. Stoffelbach, F.; Tibiletti, L.; Rieger, J.; Charleux, B., Surfactant-Free, Controlled/Living Radical Emulsion Polymerization in Batch Conditions Using a Low Molar Mass, Surface-Active Reversible Addition-Fragmentation Chain-Transfer (RAFT) Agent. *Macromolecules* **2008**, *41* (21), 7850-7856.
17. Wang, X.; Sudol, E. D.; El-Aasser, M. S., Emulsion polymerization of styrene using a reactive surfactant and its polymeric counterpart: Kinetic studies. *Macromolecules* **2001**, *34* (22), 7715-7723.
18. Bückmann, A. J. P.; Overbeek, G. C.; Nabuurs, T., Self-crosslinking surfactant-free acrylic dispersions for high-performance coatings applications. *Paint and Coatings Industry*: **2001**; Vol. 17, pp 40-53.
19. Yan, C.; Cheng, S. Y.; Feng, L. X., Kinetics and mechanism of emulsifier-free emulsion copolymerization: Styrene-methyl methacrylate-acrylic acid system. *Journal of Polymer Science Part A-Polymer Chemistry* **1999**, *37* (14), 2649-2656.
20. Camli, S. T.; Buyukserin, F.; Balci, O.; Budak, G. G., Size controlled synthesis of sub-100 nm monodisperse poly(methylmethacrylate) nanoparticles using surfactant-free emulsion polymerization. *Journal of Colloid and Interface Science* **2010**, *344* (2), 528-532.
21. Harkins, W. D., A general theory of the reaction loci in emulsion polymerization. *Journal of Chemical Physics* **1945**, *13* (9), 381-382.
22. Harkins, W. D., A general theory of the reaction loci in emulsion polymerization 2. *Journal of Chemical Physics* **1946**, *14* (1), 47-48.
23. Harkins, W. D., A general theory of the mechanism of emulsion polymerization. *Journal of the American Chemical Society* **1947**, *69* (6), 1428-44.
24. Smith, W. V.; Ewart, R. H., Kinetics of Emulsion Polymerization. *Journal of Chemical Physics* **1948**, *16* (6), 592-599.
25. Smith, W. V., The Kinetics of Styrene Emulsion Polymerization. *Journal of the American Chemical Society* **1948**, *70* (11), 3695-3702.
26. Smith, W. V., Chain Initiation in Styrene Emulsion Polymerization. *Journal of the American Chemical Society* **1949**, *71* (12), 4077-4082.
27. Herrera-Ordóñez, J.; Olayo, R., On the kinetics of styrene emulsion polymerization above CMC. II. Comparison with experimental results. *Journal of Polymer Science Part A-Polymer Chemistry* **2000**, *38* (12), 2219-2231.
28. Herrera-Ordóñez, J.; Olayo, R., Methyl methacrylate emulsion polymerization at low monomer concentration: Kinetic modeling of nucleation, particle size distribution, and rate of polymerization. *Journal of Polymer Science Part A-Polymer Chemistry* **2001**, *39* (14), 2547-2556.
29. Priest, W. J., Particle Growth in the Aqueous Polymerization of Vinyl Acetate. *Journal of Physical Chemistry* **1952**, *56* (9), 1077-1082.
30. Roe, C. P., Surface Chemistry Aspects of Emulsion Polymerization. *Industrial and Engineering Chemistry* **1968**, *60* (9), 20-&.
31. Tauer, K.; Deckwer, R.; Kuhn, I.; Schellenberg, C., A comprehensive experimental study of surfactant-free emulsion polymerization of styrene. *Colloid and Polymer Science* **1999**, *277* (7), 607-626.
32. Wang, Y. M.; Pan, C. Y., Study of the mechanism of the emulsifier-free emulsion polymerization of the styrene/4-vinylpyridine system. *Colloid and Polymer Science* **1999**, *277* (7), 658-665.
33. He, Y. P.; Sun, Y. L.; Zhu, L. H.; Xiao, X. Q.; Xu, B. W.; Si, T.; Wang, H., A study on the nucleation mechanisms under critical micelle concentration (CMC) in emulsion

polymerization of methyl methacrylate (MMA). *Iranian Polymer Journal* **2015**, *24* (11), 935-944.

34. Zollars, R. L., Kinetics of the Emulsion Polymerization of Vinyl-acetate. *Journal of Applied Polymer Science* **1979**, *24* (5), 1353-1370.

35. Vanderhoff, B. M. E., The Gel Effect at Low Conversions in Emulsion Polymerization. *Journal of Polymer Science* **1958**, *33* (126), 487-490.

36. Tiarks, F.; Frechen, T.; Kirsch, S.; Leuninger, J.; Melan, M.; Pfau, A.; Richter, F.; Schuler, B.; Zhao, C. L., Formulation effects on the distribution of pigment particles in paints. *Progress in Organic Coatings* **2003**, *48* (2-4), 140-152.

37. Ayoub, M., *Emulsion copolymerization latices for interior and exterior coatings. Pigment and Resin Technology* **1997**, *26*, 6-11.

38. Darowicki, K.; Szocinski, M.; Schaefer, K.; Mills, D. J., Investigation of morphological and electrical properties of the PMMA coating upon exposure to UV irradiation based on AFM studies. *Progress in Organic Coatings* **2011**, *71* (1), 65-71.

39. Fream, A. J.; Magnet, S. E., *Low VOC, high performance coating formulation using surfactant-free latex blends*. Surface Coatings International: 2000; Vol. **83**, pp 447-454.

40. Eckersley, S. T.; Helmer, B. J., Mechanistic considerations of particle size effects on film properties of hard/soft latex blends. *Journal of Coatings Technology* **1997**, *69* (864), 97-107.

41. Szwarc, M., Living Polymers. *Nature* **1956**, *178* (4543), 1168-1169.

42. Szwarc, M.; Levy, M.; Milkovich, R., Polymerization Initiated by Electron Transfer to Monomer - A New Method of Formation of Block Polymers. *Journal of the American Chemical Society* **1956**, *78* (11), 2656-2657.

43. Jenkins, A. D.; Jones, R. G.; Moad, G., Terminology for reversible-deactivation radical polymerization previously called "controlled" radical or "living" radical polymerization (IUPAC Recommendations 2010). *Pure and Applied Chemistry* **2010**, *82* (2), 483-491.

44. Solomon, D. H.; Rizzardo, E.; Cacioli, P. Free radical polymerization and the produced polymers. 1985.

45. Georges, M. K.; Veregin, R. P. N.; Kazmaier, P. M.; Hamer, G. K., Narrow Molecular-Weight Resins by a Free-Radical Polymerization Process. *Macromolecules* **1993**, *26* (11), 2987-2988.

46. Gonzalez-Blanco, R.; Saldivar-Guerra, E.; Herrera-Ordonez, J.; Cano-Valdez, A., TEMPO Mediated Radical Emulsion Polymerization of Styrene by Stepwise and Semibatch Processes. *Macromolecular Symposia* **2013**, *325* (1), 89-95.

47. Nicolas, J.; Guillauneuf, Y.; Lefay, C.; Bertin, D.; Gignes, D.; Charleux, B., Nitroxide-mediated polymerization. *Progress in Polymer Science* **2013**, *38* (1), 63-235.

48. Detrembleur, C.; Jerome, C.; De Winter, J.; Gerbaux, P.; Clement, J. L.; Guillauneuf, Y.; Gignes, D., Nitroxide mediated polymerization of methacrylates at moderate temperature. *Polymer Chemistry* **2014**, *5* (2), 335-340.

49. Fierens, S. K.; Van Steenberge, P. H. M.; Vermeire, F.; Reyniers, M. F.; Marin, G. B.; D'Hooge, D. R., An evaluation of the impact of SG1 disproportionation and the addition of styrene in NMP of methyl methacrylate. *Aiche Journal* **2018**, *64* (7), 2545-2559.

50. Zetterlund, P. B.; Kagawa, Y.; Okubo, M., Controlled/living radical polymerization in dispersed systems. *Chemical Reviews* **2008**, *108* (9), 3747-3794.

51. Marestin, C.; Noel, C.; Guyot, A.; Claverie, J., Nitroxide mediated living radical polymerization of styrene in emulsion. *Macromolecules* **1998**, *31* (12), 4041-4044.

52. Qiu, J.; Charleux, B.; Matyjaszewski, K., Controlled/living radical polymerization in aqueous media: homogeneous and heterogeneous systems. *Progress in Polymer Science* **2001**, *26* (10), 2083-2134.

53. Maehata, H.; Liu, X. Z.; Cunningham, M.; Keoshkerian, B., TEMPO-Mediated emulsion polymerization. *Macromolecular Rapid Communications* **2008**, *29* (6), 479-484.

54. Charleux, B.; Nicolas, J., Water-soluble SG1-based alkoxyamines: A breakthrough in controlled/living free-radical polymerization in aqueous dispersed media. *Polymer* **2007**, *48* (20), 5813-5833.

55. Bon, S. A. F.; Bosveld, M.; Klumperman, B.; German, A. L., Controlled radical polymerization in emulsion. *Macromolecules* **1997**, *30* (2), 324-326.
56. Farcet, C.; Lansalot, M.; Charleux, B.; Pirri, R.; Vairon, J. P., Mechanistic aspects of nitroxide-mediated controlled radical polymerization of styrene in miniemulsion, using a water-soluble radical initiator. *Macromolecules* **2000**, *33* (23), 8559-8570.
57. Wang, C.; Li, X. R.; Li, P. Z., Effect of cosolvent NMP on properties of cationic fluorocarbon emulsifier-free emulsion. *Colloid and Polymer Science* **2013**, *291* (5), 1271-1278.
58. Darabi, A.; Jessop, P. G.; Cunningham, M. F., One-Pot Synthesis of Poly((diethylamino)ethyl methacrylate-co-styrene)-b-poly(methyl methacrylate-co-styrene) Nanoparticles via Nitroxide-Mediated Polymerization. *Macromolecules* **2015**, *48* (7), 1952-1958.
59. Darabi, A.; Shirin-Abadi, A. R.; Pinaud, J.; Jessop, P. G.; Cunningham, M. F., Nitroxide-mediated surfactant-free emulsion copolymerization of methyl methacrylate and styrene using poly(2-(diethylamino)ethyl methacrylate-co-styrene) as a stimuli-responsive macroalkoxyamine. *Polymer Chemistry* **2014**, *5* (21), 6163-6170.
60. Delaittre, G.; Nicolas, J.; Lefay, C.; Save, M.; Charleux, B., Surfactant-free synthesis of amphiphilic diblock copolymer nanoparticles via nitroxide-mediated emulsion polymerization. *Chemical Communications* **2005**, (5), 614-616.
61. Thomson, M. E.; Manley, A. M.; Ness, J. S.; Schmidt, S. C.; Cunningham, M. F., Nitroxide-Mediated Surfactant-Free Emulsion Polymerization of n-Butyl Methacrylate with a Small Amount of Styrene. *Macromolecules* **2010**, *43* (19), 7958-7963.
62. Kato, M.; Kamigaito, M.; Sawamoto, M.; Higashimura, T., Polymerization of methyl-methacrylate with the carbon-tetrachloride dichlorotris(triphenylphosphine)ruthenium(II) methylaluminum bis(2,6-di-tert-butylphenoxide) initiating system - possibility of living radical polymerization. *Macromolecules* **1995**, *28* (5), 1721-1723.
63. Wang, J. S.; Matyjaszewski, K., Controlled Living Radical Polymerization - Atom-Transfer Radical Polymerization in the Presence of Transition-Metal Complexes. *Journal of the American Chemical Society* **1995**, *117* (20), 5614-5615.
64. Cao, J.; Zhang, L. F.; Jiang, X. W.; Tian, C.; Zhao, X. N.; Ke, Q.; Pan, X. Q.; Cheng, Z. P.; Zhu, X. L., Facile Iron-Mediated Dispersant-Free Suspension Polymerization of Methyl Methacrylate via Reverse ATRP in Water. *Macromolecular Rapid Communications* **2013**, *34* (22), 1747-1754.
65. Wang, K.; Wang, Y. X.; Zhang, W. Q., Synthesis of diblock copolymer nano-assemblies by PISA under dispersion polymerization: comparison between ATRP and RAFT. *Polymer Chemistry* **2017**, *8* (41), 6407-6415.
66. Haloi, D. J.; Mandal, P.; Singha, N. K., Atom Transfer Radical Polymerization of Glycidyl Methacrylate (GMA) in Emulsion. *Journal of Macromolecular Science Part A-Pure and Applied Chemistry* **2013**, *50* (1), 121-127.
67. Gaynor, S. G.; Qiu, J.; Matyjaszewski, K., Controlled/"living" radical polymerization applied to water-borne systems. *Macromolecules* **1998**, *31* (17), 5951-5954.
68. Peng, H.; Cheng, S. Y.; Feng, L. X., Properties of poly(n-butyl methacrylate) prepared by reverse atom transfer radical polymerization in an aqueous dispersed system. *Journal of Applied Polymer Science* **2003**, *89* (6), 1542-1547.
69. Xue, Z. G.; Wang, Z.; He, D.; Zhou, X. P.; Xie, X. L., Synthesis of poly(n-butyl acrylate) homopolymer and poly(styrene-b-n-butyl acrylate-b-styrene) triblock copolymer via AGET emulsion ATRP using a cationic surfactant. *Journal of Polymer Science Part A-Polymer Chemistry* **2016**, *54* (5), 611-620.
70. Jousset, S.; Qiu, J.; Matyjaszewski, K., Atom transfer radical polymerization of methyl methacrylate in water-borne system. *Macromolecules* **2001**, *34* (19), 6641-6648.
71. Eslami, H.; Zhu, S. P., Emulsion atom transfer radical polymerization of 2-ethylhexyl methacrylate. *Polymer* **2005**, *46* (15), 5484-5493.

72. Qiu, J.; Gaynor, S. G.; Matyjaszewski, K., Emulsion polymerization of n-butyl methacrylate by reverse atom transfer radical polymerization. *Macromolecules* **1999**, *32* (9), 2872-2875.
73. Matyjaszewski, K.; Qiu, J.; Tsarevsky, N. V.; Charleux, B., Atom transfer radical polymerization of n-butyl methacrylate in an aqueous dispersed system: A miniemulsion approach. *Journal of Polymer Science Part A-Polymer Chemistry* **2000**, *38*, 4724-4734.
74. Li, J.; Hitchcock, A. P.; Stover, H. D. H., Pickering Emulsion Templated Interfacial Atom Transfer Radical Polymerization for Microencapsulation. *Langmuir* **2010**, *26* (23), 17926-17935.
75. Cheng, C. J.; Fu, Q. L.; Liu, Z. B.; Shen, L.; Qiao, Y. L.; Fu, C. Q., Emulsifier-free synthesis of crosslinkable ABA triblock copolymer nanoparticles via AGET ATRP. *Macromolecular Research* **2011**, *19* (10), 1048-1055.
76. Rusen, E.; Diacon, A.; Mocanu, A.; Culita, D. C.; Dinescu, A.; Zecheru, T., "A real" emulsion polymerization using simple ATRP reaction in the presence of an oligo-initiator with a dual activity of emulsifier and initiator. *Colloids and Surfaces a-Physicochemical and Engineering Aspects* **2018**, *555*, 1-7.
77. Wu, J. J.; Jiang, H. J.; Zhang, L. F.; Cheng, Z. P.; Zhu, X. L., Synthesis of amphiphilic nanoparticles and multi-block hydrophilic copolymers by a facile and effective "living" radical polymerization in water. *Polymer Chemistry* **2016**, *7* (14), 2486-2491.
78. Stoffelbach, F.; Griffete, N.; Bui, C.; Charleux, B., Use of a simple surface-active initiator in controlled/living free-radical miniemulsion polymerization under AGET and ARGET ATRP conditions. *Chemical Communications* **2008**, (39), 4807-4809.
79. Cheng, C. J.; Fu, Q. L.; Bai, X. X.; Liu, S. J.; Shen, L.; Fan, W. Q.; Li, H. X., Facile synthesis of gemini surface-active ATRP initiator and its use in soap-free AGET ATRP mini-emulsion polymerisation. *Chemical Papers* **2013**, *67* (3), 336-341.
80. Zhu, G. H.; Zhang, L. F.; Pan, X. Q.; Zhang, W.; Cheng, Z. P.; Zhu, X. L., Facile Soap-Free Miniemulsion Polymerization of Methyl Methacrylate via Reverse Atom Transfer Radical Polymerization. *Macromolecular Rapid Communications* **2012**, *33* (24), 2121-2126.
81. Chiefari, J.; Chong, Y. K.; Ercole, F.; Krstina, J.; Jeffery, J.; Le, T. P. T.; Mayadunne, R. T. A.; Meijs, G. F.; Moad, C. L.; Moad, G.; Rizzardo, E.; Thang, S. H., Living free-radical polymerization by reversible addition-fragmentation chain transfer: The RAFT process. *Macromolecules* **1998**, *31* (16), 5559-5562.
82. Le, T. P.; Moad, G.; Rizzardo, E.; Thang, S. H. Polymerization with living characteristics with controlled dispersity, polymers prepared thereby, and chain-transfer agents used in the same. 1998.
83. Chong, Y. K.; Le, T. P. T.; Moad, G.; Rizzardo, E.; Thang, S. H., A more versatile route to block copolymers and other polymers of complex architecture by living radical polymerization: The RAFT process. *Macromolecules* **1999**, *32* (6), 2071-2074.
84. Willcock, H.; O'Reilly, R. K., End group removal and modification of RAFT polymers. *Polymer Chemistry* **2010**, *1* (2), 149-157.
85. Benaglia, M.; Chen, M.; Chong, Y. K.; Moad, G.; Rizzardo, E.; Thang, S. H., Polystyrene-block-poly(vinyl acetate) through the Use of a Switchable RAFT Agent. *Macromolecules* **2009**, *42* (24), 9384-9386.
86. Charmot, D.; Corpart, P.; Adam, H.; Zard, S. Z.; Biadatti, T.; Bouhadir, G., Controlled radical polymerization in dispersed media. *Macromolecular Symposia* **2000**, *150*, 23-32.
87. Moad, G.; Rizzardo, E.; Thang, S. H., Living radical polymerization by the RAFT process. *Australian Journal of Chemistry* **2005**, *58* (6), 379-410.
88. Moad, G.; Rizzardo, E.; Thang, S. H., Living Radical Polymerization by the RAFT Process - A Third Update. *Australian Journal of Chemistry* **2012**, *65* (8), 985-1076.
89. Benaglia, M.; Chiefari, J.; Chong, Y. K.; Moad, G.; Rizzardo, E.; Thang, S. H., Universal (Switchable) RAFT Agents. *Journal of the American Chemical Society* **2009**, *131* (20), 6914-6915.
90. Coote, M. L.; Izgorodina, E. I.; Cavigliasso, G. E.; Roth, M.; Busch, M.; Barner-Kowollik, C., Addition-fragmentation kinetics of fluorodithioformates (F-RAFT) in styrene,

vinyl acetate, and ethylene polymerization: An ab initio investigation. *Macromolecules* **2006**, *39* (13), 4585-4591.

91. Theis, A.; Stenzel, M. H.; Davis, T. P.; Coote, M. L.; Barner-Kowollik, C., A synthetic approach to a novel class of fluorine-bearing reversible addition-fragmentation chain transfer (RAFT) agents: F-RAFT. *Australian Journal of Chemistry* **2005**, *58* (6), 437-441.

92. <https://www.lubrizol.com/-/media/Lubrizol/Lubricant-and-Fuel-Additives/Viscosity-Modifiers/Documents/Scaled-Production-of-RAFT-CTA.pdf>.

93. Keddie, D. J.; Moad, G.; Rizzardo, E.; Thang, S. H., RAFT Agent Design and Synthesis. *Macromolecules* **2012**, *45* (13), 5321-5342.

94. Chong, Y. K.; Moad, G.; Rizzardo, E.; Thang, S. H., Thiocarbonylthio end group removal from RAFT-synthesized polymers by radical-induced reduction. *Macromolecules* **2007**, *40* (13), 4446-4455.

95. Moad, G.; Chiefari, J.; Chong, Y. K.; Krstina, J.; Mayadunne, R. T. A.; Postma, A.; Rizzardo, E.; Thang, S. H., Living free radical polymerization with reversible addition-fragmentation chain transfer (the life of RAFT). *Polymer International* **2000**, *49* (9), 993-1001.

96. Moad, G.; Rizzardo, E.; Thang, S. H., Toward living radical polymerization. *Accounts of Chemical Research* **2008**, *41* (9), 1133-1142.

97. Zhao, W.; Gody, G.; Dong, S. M.; Zetterlund, P. B.; Perrier, S., Optimization of the RAFT polymerization conditions for the in situ formation of nano-objects via dispersion polymerization in alcoholic medium. *Polymer Chemistry* **2014**, *5* (24), 6990-7003.

98. Gregory, A. M.; Thurecht, K. J.; Howdle, S. M., Controlled dispersion polymerization of methyl methacrylate in supercritical carbon dioxide via RAFT. *Macromolecules* **2008**, *41* (4), 1215-1222.

99. Biasutti, J. D.; Davis, T. P.; Lucien, F. P.; Heuts, J. P. A., Reversible addition-fragmentation chain transfer polymerization of methyl methacrylate in suspension. *Journal of Polymer Science Part A-Polymer Chemistry* **2005**, *43* (10), 2001-2012.

100. Cunningham, M. F., Controlled/living radical polymerization in aqueous dispersed systems. *Progress in Polymer Science* **2008**, *33* (4), 365-398.

101. Monteiro, M. J.; Hodgson, M.; De Brouwer, H., The influence of RAFT on the rates and molecular weight distributions of styrene in seeded emulsion polymerizations. *Journal of Polymer Science Part A-Polymer Chemistry* **2000**, *38* (21), 3864-3874.

102. Monteiro, M. J.; Sjoberg, M.; van der Vlist, J.; Gottgens, C. M., Synthesis of butyl acrylate-styrene block copolymers in emulsion by reversible addition-fragmentation chain transfer: Effect of surfactant migration upon film formation. *Journal of Polymer Science Part A-Polymer Chemistry* **2000**, *38* (23), 4206-4217.

103. Monteiro, M. J.; de Brouwer, H., Intermediate radical termination as the mechanism for retardation in reversible addition-fragmentation chain transfer polymerization. *Macromolecules* **2001**, *34* (3), 349-352.

104. Lubnin, A.; Lenhard, S.; Lai, J., RAFT emulsions, microemulsions and dispersions. *Surface Coatings International Part B-Coatings Transactions* **2006**, *89* (4), 293-304.

105. McLeary, J. B.; Klumperman, B., RAFT mediated polymerisation in heterogeneous media. *Soft Matter* **2006**, *2* (1), 45-53.

106. Uzulina, I.; Kanagasabapathy, S.; Claverie, J., Reversible addition fragmentation transfer (RAFT) polymerization in emulsion. *Macromolecular Symposia* **2000**, *150*, 33-38.

107. Nozari, S.; Tauer, K., Calorimetric study on the influence of the nature of the RAFT agent and the initiator in ab initio aqueous heterophase polymerization. *Polymer* **2005**, *46* (4), 1033-1043.

108. Kwak, J.; Lacroix-Desmazes, P.; Robin, J. J.; Boutevin, B.; Torres, N., Synthesis of mono functional carboxylic acid poly(methyl methacrylate) in aqueous medium using surfactant. Application to the synthesis of graft copolymers polyethylene-g-poly(methyl methacrylate) and the compatibilization of LDPE/PVDF blends. *Polymer* **2003**, *44* (18), 5119-5130.

109. Kim, J.; Kwak, J.; Kim, D., Particle growth Behavior of poly(methyl methacrylate) nanoparticles synthesized by the reversible addition fragmentation transfer living radical polymerization reaction. *Journal of Applied Polymer Science* **2007**, *106* (6), 3816-3822.
110. Kim, J.; Kwak, J.; Kim, Y. C.; Kim, D., Preparation and size control of monodispersed surface charged polystyrene nanoparticles by reversible addition fragmentation transfer reaction. *Colloid and Polymer Science* **2006**, *284* (7), 771-779.
111. Shim, S. E.; Shin, Y.; Lee, H.; Choe, S., Emulsion polymerization of methyl methacrylate using a surface-active RAFT agent: The role of surfactant. *Polymer Bulletin* **2003**, *51* (3), 209-216.
112. Shim, S. E.; Shin, Y.; Jun, J. W.; Lee, K.; Jung, H.; Choe, S., Living-free-radical emulsion photopolymerization of methyl methacrylate by a surface active iniferter (suriniferter). *Macromolecules* **2003**, *36* (21), 7994-8000.
113. Zhou, J. H.; Yao, H. T.; Ma, J. Z., Recent advances in RAFT-mediated surfactant-free emulsion polymerization. *Polymer Chemistry* **2018**, *9* (19), 2532-2561.
114. Prescott, S. W.; Ballard, M. J.; Rizzardo, E.; Gilbert, R. G., Successful use of RAFT techniques in seeded emulsion polymerization of styrene: Living character, RAFT agent transport, and rate of polymerization. *Macromolecules* **2002**, *35* (14), 5417-5425.
115. Smulders, W.; Monteiro, M. J., Seeded emulsion polymerization of block copolymer core-shell nanoparticles with controlled particle size and molecular weight distribution using xanthate-based RAFT polymerization. *Macromolecules* **2004**, *37* (12), 4474-4483.
116. Smulders, W.; Gilbert, R. G.; Monteiro, M. J., A kinetic investigation of seeded emulsion polymerization of styrene using reversible addition-fragmentation chain transfer (RAFT) agents with a low transfer constant. *Macromolecules* **2003**, *36* (12), 4309-4318.
117. Ferguson, C. J.; Hughes, R. J.; Pham, B. T. T.; Hawke, B. S.; Gilbert, R. G.; Serelis, A. K.; Such, C. H., Effective ab initio emulsion polymerization under RAFT control. *Macromolecules* **2002**, *35* (25), 9243-9245.
118. Manguian, M.; Save, M.; Charleux, B., Batch emulsion polymerization of styrene stabilized by a hydrophilic Macro-RAFT agent. *Macromolecular Rapid Communications* **2006**, *27* (6), 399-404.
119. Vosloo, J. J.; De Wet-Roos, D.; Tonge, M. P.; Sanderson, R. D., Controlled free radical polymerization in water-borne dispersion using reversible addition-fragmentation chain transfer. *Macromolecules* **2002**, *35* (13), 4894-4902.
120. Freal-Saison, S.; Save, M.; Bui, C.; Charleux, B.; Magnet, S., Emulsifier-free controlled free-radical emulsion polymerization of styrene via RAFT using dibenzyltrithiocarbonate as a chain transfer agent and acrylic acid as an ionogenic comonomer: Batch and spontaneous phase inversion processes. *Macromolecules* **2006**, *39* (25), 8632-8638.
121. Ferguson, C. J.; Hughes, R. J.; Nguyen, D.; Pham, B. T. T.; Gilbert, R. G.; Serelis, A. K.; Such, C. H.; Hawke, B. S., Ab initio emulsion polymerization by RAFT-controlled self-assembly. *Macromolecules* **2005**, *38* (6), 2191-2204.
122. Canning, S. L.; Smith, G. N.; Armes, S. P., A Critical Appraisal of RAFT-Mediated Polymerization-Induced Self Assembly. *Macromolecules* **2016**, *49* (6), 1985-2001.
123. Hinton, C. V.; Spencer, H. G., Copolymerization of Methyl Acrylate with 1,1-Diphenylethylene - Effect of Concentration on Composition. *Macromolecules* **1976**, *9* (5), 864-866.
124. Perkins, H. L.; Wilson, R. W. High impact resistant, high gloss polystyrene composition used for forming articles, such as refrigerator components. US6011117-A, US6011117-A 04 Jan 2000 C08L-053/02 200013 Pages: 5.
125. Yuki, H.; Hotta, J.; Okamoto, Y.; Murahash, S., Anionic copolymerization of styrene and 1,1-diphenylethylene. *Bulletin of the Chemical Society of Japan* **1967**, *40* (11), 2659-2663.
126. Raether, B.; Nuyken, O.; Wieland, P.; Bremser, W., Free-radical synthesis of block copolymers on an industrial scale. *Macromolecular Symposia* **2002**, *177*, 25-41.

127. Evans, A. G.; George, D. B., Catalytic action of anionic catalysts. Part I. Interaction of butyl-lithium with 1,1-diphenylethylene. *Journal of the Chemical Society* **1961**, (0), 4653-4659.
128. Feng, D. S.; Higashihara, T.; Faust, R., Facile synthesis of diphenylethylene end-functional polyisobutylene and its applications for the synthesis of block copolymers containing poly(methacrylate)s. *Polymer* **2008**, *49* (2), 386-393.
129. Li, D. W.; Faust, R., Living carbocationic sequential block copolymerization of isobutylene with alpha-methylstyrene. *Macromolecules* **1995**, *28* (5), 1383-1389.
130. Yasuoka, K.; Kanaoka, S.; Aoshima, S., Cationic copolymerization of 1,1-diphenylethylene with p-substituted styrenes. *Journal of Polymer Science Part A-Polymer Chemistry* **2012**, *50* (14), 2758-2761.
131. Zhao, M. J.; Chen, D.; Shi, Y.; Yang, W. T.; Fu, Z. F., Polymerization Mechanism of MMA in the Presence of 1,1-Diphenylethylene. *Macromolecular Chemistry and Physics* **2013**, *214* (15), 1688-1698.
132. Kice, J. L.; Taymoorian, F., The reactivity of diphenylethylene and related olefins toward free radicals - evidence for anomalous reactions of radicals from diphenylethylene. *Journal of the American Chemical Society* **1959**, *81* (13), 3405-3409.
133. Bremser, W.; Strickmann, F.; Bendix, M.; Paulus, W.; Raether, R. B.; Christie, D. I. Preparation of polymeric reaction products comprises reacting, in aqueous phase, radical convertible monomer in presence of a radical initiator and a monoethylenically unsaturated aromatic hydrocarbon compound. 2000.
134. Wieland, P. C.; Raether, B.; Nuyken, O., A new additive for controlled radical polymerization. *Macromolecular Rapid Communications* **2001**, *22* (9), 700-703.
135. Tasdelen, M. A.; Degirmenci, M.; Yagci, Y.; Nuyken, O., Block copolymers by using combined controlled radical and radical promoted cationic polymerization methods. *Polymer Bulletin* **2003**, *50* (3), 131-138.
136. Wang, W. W.; Zhang, Q. Y., Synthesis of block copolymer poly (n-butyl acrylate)-b-polystyrene by DPE seeded emulsion polymerization with monodisperse latex particles and morphology of self-assembly film surface. *Journal of Colloid and Interface Science* **2012**, *374*, 54-60.
137. Zhang, H. P.; Zhang, Q. Y.; Zhang, B. L.; Guo, F. G., Preparation of magnetic composite microspheres by surfactant free controlled radical polymerization: Preparation and characteristics. *Journal of Magnetism and Magnetic Materials* **2009**, *321* (23), 3921-3925.
138. Luo, Y. D.; Chou, I. C.; Chiu, W. Y.; Lee, C. F., Synthesis of PMMA-b-PBA Block Copolymer in Homogeneous and Miniemulsion Systems by DPE Controlled Radical Polymerization. *Journal of Polymer Science Part A-Polymer Chemistry* **2009**, *47* (17), 4435-4445.
139. Zhou, Y. Y.; Zhang, Q. Y.; Liu, Y. L.; Wang, W. W., Encapsulation and dispersion of carbon black by an in situ controlling radical polymerization of AA/BA/St with DPE as a control agent. *Colloid and Polymer Science* **2013**, *291* (10), 2399-2408.
140. Guo, F. G.; Zhang, Q. Y.; Zhang, B. L.; Zhang, H. P.; Zhang, L., Preparation and characterization of magnetic composite microspheres using a free radical polymerization system consisting of DPE. *Polymer* **2009**, *50* (8), 1887-1894.
141. Guo, F. G.; Zhang, Q. Y.; Zhang, H. P.; Zhang, B. L.; Gu, J. W., Controlled preparation of Fe₃O₄/P (St-MA) magnetic composite microspheres by DPE method. *Journal of Polymer Research* **2011**, *18* (4), 745-751.
142. Beckhaus, H. D.; Schaetzer, J.; Ruchardt, C., Thermolabile hydrocarbons .23. The dimer of 2-methyl-1,1-diphenylpropyl radicals and its reactivity. *Tetrahedron Letters* **1983**, *24* (32), 3307-3310.
143. Viala, S.; Antonietti, M.; Tauer, K.; Bremser, W., Structural control in radical polymerization with 1,1 diphenylethylene: 2. Behavior of MMA-DPE copolymer in radical polymerization. *Polymer* **2003**, *44* (5), 1339-1351.
144. Wang, W. W.; Liu, M. J.; Gu, J. W.; Zhang, Q. Y.; Mays, J. W., Convenient synthesis and morphology of latex particles composed of poly (methyl methacrylate)-b-poly

(n-butyl acrylate) by 1, 1-diphenylethylene (DPE) seeded emulsion polymerization. *Journal of Polymer Research* **2014**, *21* (8), 8.

145. Yuan, D.; Zhang, H., Nanosized palladium supported on diethylenetriamine modified superparamagnetic polymer composite microspheres: Synthesis, characterization and application as catalysts for the Suzuki reactions. *Applied Catalysis A-General* **2014**, *475*, 249-255.

146. Wang, W. W.; Zhang, Q. Y.; Guo, F. F.; Gu, J. W.; Yin, C. J., Preparation of diblock copolymer PBA-b-PSt by DPE method in emulsion. *Journal of Polymer Research* **2011**, *18* (5), 1229-1235.

147. Zhao, M. J.; Shi, Y.; Fu, Z. F.; Yang, W. T., Preparation of PMMA-b-PSt Block Copolymer via Seeded Emulsion Polymerization in the Presence of 1,1-Diphenylethylene. *Macromolecular Reaction Engineering* **2014**, *8* (8), 555-563.

148. Zhao, M. J.; Fu, Z. F.; Shi, Y.; Yang, W. T., Polymerization Mechanism in the Presence of 1,1-Diphenylethylene Part 2: Synthesis and Characterization of PMA and PSt. *Macromolecular Chemistry and Physics* **2015**, *216* (22), 2202-2210.

149. Wang, W. W.; Zhang, H. P.; Geng, W. C.; Gu, J. W.; Zhou, Y. Y.; Zhang, J. P.; Zhang, Q. Y., Synthesis of poly (methyl methacrylate)-b-polystyrene with high molecular weight by DPE seeded emulsion polymerization and its application in proton exchange membrane. *Journal of Colloid and Interface Science* **2013**, *406*, 154-164.

150. Viala, S.; Tauer, K.; Antonietti, M.; Lacik, I.; Bremser, W., Structural control in radical polymerization with 1, 1-diphenylethylene. Part 3. Aqueous heterophase polymerization. *Polymer* **2005**, *46* (19), 7843-7854.

151. Cowie, J. M.; Bywater, S., Molecular weight distribution changes during thermal breakdown of poly-alpha-methylstyrene. *Journal of Polymer Science* **1961**, *54* (159), 221-&.

152. McCormick, H. W., Ceiling temperature of alpha-methylstyrene. *Journal of Polymer Science* **1957**, *25* (111), 488-490.

153. Chen, D.; Fu, Z. F.; Shi, Y., Synthesis of amphiphilic diblock copolymers by DPE method. *Polymer Bulletin* **2008**, *60* (2-3), 259-269.

154. Viala, S.; Tauer, K.; Antonietti, M.; Kruger, R. P.; Bremser, W., Structural control in radical polymerization with 1,1-diphenylethylene. 1. Copolymerization of 1,1-diphenylethylene with methyl methacrylate. *Polymer* **2002**, *43* (26), 7231-7241.

155. Luo, Y. D.; Chiu, W. Y., Synthesis and Kinetic Analysis of DPE Controlled Radical Polymerization of MMA. *Journal of Polymer Science Part A-Polymer Chemistry* **2009**, *47* (24), 6789-6800.

156. Fan, X.; Jia, X.; Liu, J.; Liu, Y.; Zhang, H.; Zhang, B.; Zhang, Q., Morphology evolution of poly(glycidyl methacrylate) colloids in the 1,1-diphenylethene controlled soap-free emulsion polymerization. *European Polymer Journal* **2017**, *92*, 220-232.

157. Fan, X. L.; Liu, J.; Jia, X. K.; Liu, Y.; Zhang, H.; Wang, S. Q.; Zhang, B. L.; Zhang, H. P.; Zhang, Q. Y., A series of nanoparticles with phase-separated structures by 1,1-diphenylethene controlled one-step soap-free emulsion copolymerization and their application in drug release. *Nano Research* **2017**, *10* (9), 2905-2922.

158. Fan, X. L.; Liu, Y.; Jia, X. K.; Wang, S. Q.; Li, C. M.; Zhang, B. L.; Zhang, H. P.; Zhang, Q. Y., Regulating the size and molecular weight of polymeric particles by 1,1-diphenylethene controlled soap-free emulsion polymerization. *RSC Advances* **2015**, *5* (115), 95183-95190.

159. Chou, I. C.; Lee, C. F.; Chiu, W. Y., Preparation of Novel Suspensions of ZnO/Living Block Copolymer Latex Nanoparticles via Pickering Emulsion Polymerization and Their Long Term Stability. *Journal of Polymer Science Part A-Polymer Chemistry* **2011**, *49* (16), 3524-3535.

Chapter Two

2. Surfactant-free emulsion polymerization of methyl methacrylate incorporating 1,1-diphenylethylene

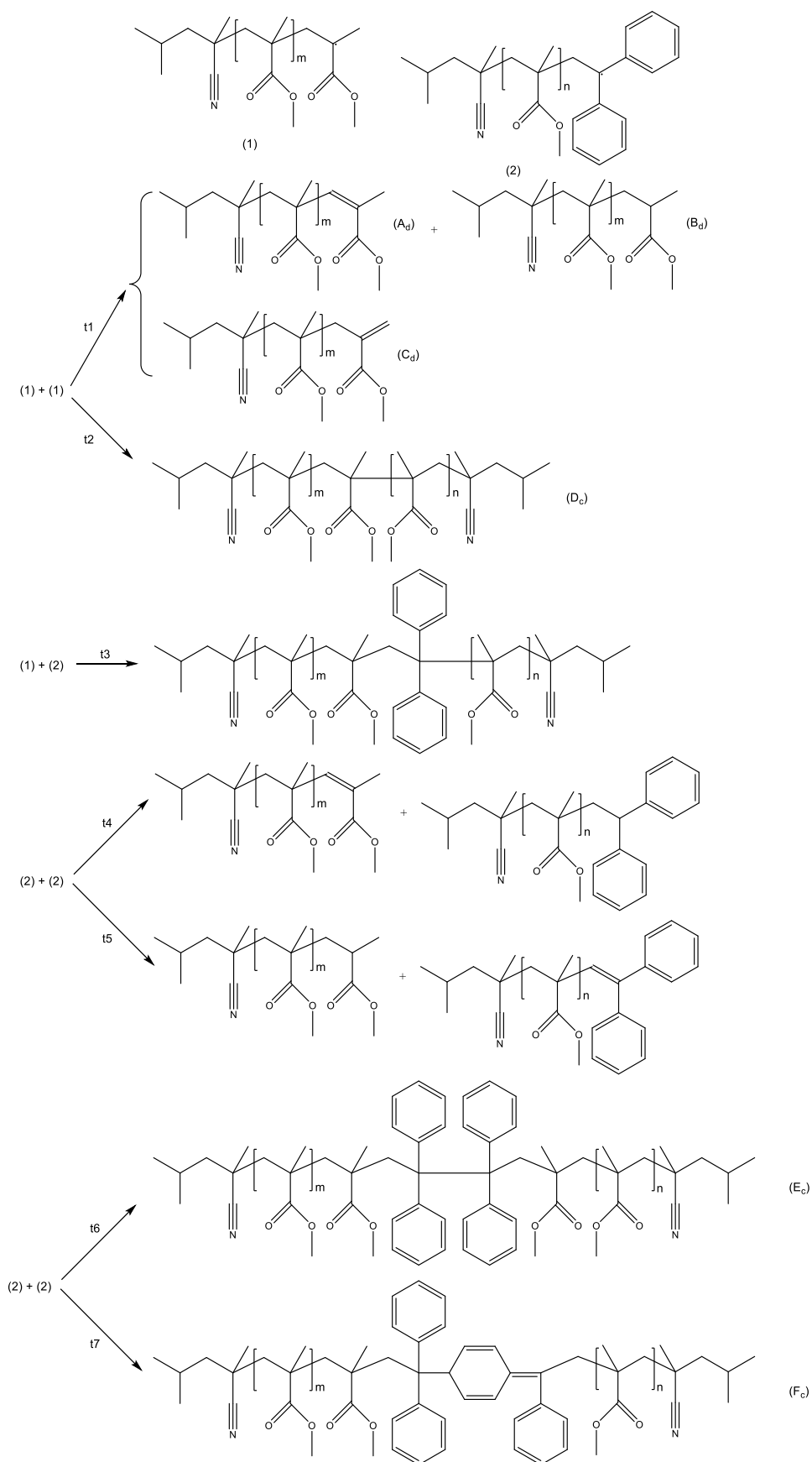
2.1. Introduction

Surfactant-free emulsion polymerization (SFEP) offers potential advantages over conventional emulsion polymerization such as ease of purification and improved qualities of the resultant films. This has led to SFEP being utilised to produce polymers for applications such as polymer opals,¹ coatings² and drug delivery vehicles.³ However, SFEP is not yet as fully understood as conventional emulsion polymerization. To expand the scope of SFEP, this technique has been combined with reversible deactivation radical polymerization (RDRP).^{4, 5} This enables the synthesis of diblock copolymers, which leads to microphase separation rather than full separation seen with polymer mixtures and better film properties as a result of this.

The incorporation of 1,1-diphenylethylene (DPE) into polymerizations, known as the DPE method, is a possible strategy for synthesising diblock copolymers but this is not a class of controlled living radical polymerization (CLRP) or reversible-deactivation radical polymerization (RDRP). The DPE method has been used in the bulk,⁶ solution⁷ and heterogeneous polymerizations⁸ using 1,1-diphenylethylene as an end-capper/polymerization retarder. In previous publications, DPE was found to reduce polymer molecular weight and \bar{M}_w , as well as the rate of polymerization of styrenics,⁹ methacrylates¹⁰ and acrylates¹¹. DPE has also been used to form diblock copolymers.¹² The following Chapter focuses on stage 1 of the DPE method, the formation of a precursor to be later extended by secondary monomer addition.

It is still unclear which mechanism is correct for DPE polymerizations, with a schematic overview published by Zhao *et al.*¹⁰ (Scheme 2-1). This scheme outlines the likely termination pathways of (1) poly(methyl methacrylate) (PMMA) and (2) PMMA capped with DPE. Use of the DPE method in solution polymerization indicates that t_3 is the dominant termination pathway. However, Viala *et al.*¹³ used the DPE method for emulsion polymerization and found t_7 to be the dominant pathway. Little evidence has been published supporting either pathway in subsequent publications on DPE polymerizations.

Some previous work has been carried out combining SFEP with DPE. One example of this is the work on encapsulants. Zang and co-workers have published several papers describing the encapsulation of magnetic iron oxide particles using PMMA-*stat*-PAA in the presence of DPE.¹⁴⁻¹⁶ These polymers were subsequently extended with glycidyl methacrylate (GMA), St or 2-(dimethylamino)ethyl methacrylate (DMA). The DPE method has also been used in SFEP to encapsulate carbon black particles with PAA-co-PBA-DPE and later extend these copolymer chains with PSt.¹⁷



Scheme 2-1. PMMA termination pathways for the DPE method.¹⁰ Reprinted (adapted) with permission from John Wiley and Sons (License number: 4550310475411).

Other works involve the addition of a hydrophilic comonomer to the reaction. Fan *et al.*¹⁸ synthesised PSt-co-AA/GMA with DVB crosslinker to form raspberry-like, flower-like, core-shell nanoparticles and nanocapsules and examined their possible application as drug delivery systems. Bremser *et al.*¹⁹ as well as Viala *et al.*^{13, 20} copolymerized AA with MMA in the presence of DPE to form hydrophilic precursors via SFEP. However, these copolymers were not extensively analysed and the emphasis of these studies was the analysis of the extension of these precursors with a mixture of methacrylates and styrene.

SFEP of a single monomer in the presence of DPE has not been extensively researched. Fan *et al.*²¹ investigated the polymerization of GMA in the presence of DPE. However, TEM and SEM images show film formation rather than polymer particles when DPE is added to the reaction. This was adjusted by Fan *et al.*²² for use with St. The rate of polymerization was retarded by the addition of DPE and the molecular weight distributions of the copolymers were said to be broad but no dispersity values were given. Interestingly, the inclusion of DPE in the polymerization reduced the particle size compared to PSt particles prepared without DPE. Finally, Viala *et al.*²³ reported the polymerization of MMA with DPE. This system was only used for calorimetry studies, which showed a slower rate of polymerization of MMA when DPE was introduced. All other reactions used to generate further data contained surfactant. No other analysis of the SFEP system was carried out in this prior study.

This Chapter describes the surfactant-free emulsion polymerization of MMA in the presence and absence of DPE with varying concentrations of both DPE and APS. The initial focus of this work was to optimise the use of DPE in surfactant-free emulsion polymerization and validate the effect of DPE for this particular system. This was examined using gravimetric analysis, NMR spectroscopy, MS and SEC. An interesting effect of excluding surfactant from these emulsion polymerizations is a bimodal particle distribution. This was observed by TEM, with DLS unable to distinguish between the two particle populations. These two types of particles were separated by centrifugation and examined further.

Due to the number of polymers produced in this Chapter with similar formulae a shorthand system has been used. D0A1; D and A referring to DPE and APS content, respectively, and the following number referring to the parts per hundred monomer content of DPE to the nearest whole number and the relevant initial APS content with respect to the original 2% DPE system.

2.2. Experimental Details

2.2.1. Materials

1,1-Diphenylethylene (DPE; 97 %) was purchased from Sigma-Aldrich and distilled under reduced pressure before use. Methyl methacrylate (MMA; 99 %, ≤ 30 ppm MEHQ), ammonium persulfate (APS, ≥ 98 %) and ammonium hydroxide solution (~ 25 % NH_3) were all purchased from Sigma-Aldrich (UK). MMA inhibitor was removed using a basic aluminium oxide column. NMR solvents CDCl_3 (99.80 % D) and acetone- d_6 (≥ 99.9 atom % D) were purchased from VWR Chemicals (UK) and Aldrich (UK), respectively. Deionised water was obtained from an Elgastat Option 3 water purifier.

2.2.2. Polymerization of methyl methacrylate in the presence and absence of DPE at varying DPE and APS concentrations

Refer to Table 2-1 for reaction quantities. A 500 mL flanged reactor fitted with overhead stirrer, condenser, nitrogen inlet and septa seal was charged with H_2O (86 g). This H_2O and an aliquot of MMA were separately deoxygenated for 30 minutes. The reactor was then placed into a water bath and heated to 90 °C under nitrogen with stirring. Deoxygenated MMA was weighed into a vial containing DPE and slowly injected into the reaction vessel (see quantities below). After 5 minutes a 25 % w/v APS solution in H_2O was added. 2 mL sample aliquots were taken at predetermined time points and the reaction was allowed to continue until complete or for up to 6 h. Reactions were quenched by opening the reactor to air and cooling to room temperature. The resulting latex was adjusted to pH 8 after the reaction using 25 % w/v ammonium hydroxide solution. Solid samples were obtained using a Lablyo mini-lyophilizer.

Table 2-1. DPE and APS content required for each reaction.

Sample name	MMA (g)	DPE (g)	APS (g)
D0A1	14.86 (0.148 mol)	0	0.276 (1.21 mmol)
D0A2	14.86 (0.148 mol)	0	0.553 (2.42 mmol)
D0A3	14.86 (0.148 mol)	0	0.829 (3.63 mmol)
D1A1	14.70 (0.147 mol)	0.16 (0.888 mmol)	0.276 (1.21 mmol)
D1A2	14.70 (0.147 mol)	0.16 (0.888 mmol)	0.553 (2.42 mmol)

D1A3	14.70 (0.147 mol)	0.16 (0.888 mmol)	0.829 (3.63 mmol)
D2A1	14.54 (0.145 mol)	0.32 (1.78 mmol)	0.276 (1.21 mmol)
D2A2	14.54 (0.145 mol)	0.32 (1.78 mmol)	0.553 (2.42 mmol)
D2A3	14.54 (0.145 mol)	0.32 (1.78 mmol)	0.829 (3.63 mmol)
D3A1	14.38 (0.144 mol)	0.48 (2.66 mmol)	0.276 (1.21 mmol)
D3A2	14.38 (0.144 mol)	0.48 (2.66 mmol)	0.553 (2.42 mmol)
D3A3	14.38 (0.144 mol)	0.48 (2.66 mmol)	0.829 (3.63 mmol)

2.2.3. ¹H nuclear magnetic resonance (NMR) spectroscopy

All NMR spectra were recorded using a 400 MHz Bruker AV3-HD spectrometer using either CDCl₃ or acetone-d₆ as solvent. Spectra were analysed using Bruker TopSpin software.

Diffusion ordered spectroscopy (DOSY) NMR spectra were obtained by Dr Sandra van Meurs at the University of Sheffield using 95 % and 5 % gradient strengths with 8 free induction decays (FIDs) between these values. Number of scans per spectrum = 16, with other values such as d20 and p30 being optimized for each sample.

2.2.4. Gravimetric analysis

Solids contents for each timepoint and final products were measured using a Kern DAB 100-3 moisture analyzer. A minimum of 1 g of latex was heated in an aluminium pan to 150 °C until a constant mass was attained.

2.2.5. Size exclusion chromatography (SEC)

The SEC set-up consisted of an Agilent Technologies 1260 Infinity system with a refractive index (RI) detector. HPLC-grade *N,N*-dimethylformamide (DMF) containing 0.1 % lithium bromide (LiBr) was used as eluent. Operating parameters were 50 °C, with a flow rate of 1.0 mL min⁻¹ and an injection volume of 100 µL. Samples were prepared as 1 mg mL⁻¹ solutions with toluene (0.1 %) as a flow rate marker. The instrument was calibrated using Agilent EasiVial PMMA standards consisting of *M_p* values between 960 and 1,568,000 g mol⁻¹. Data were analyzed using Agilent GPC/SEC software.

2.2.6. *Dynamic light scattering (DLS)*

Particle hydrodynamic diameters were measured using a Malvern Zetasizer Nano-ZS instrument with a scattering angle of 173 °. Samples were diluted to 0.005 wt% using DI water and measurements obtained in disposable cuvettes over 4 runs with at least 3 being used to create an average result.

2.2.7. *Transmission electron microscopy (TEM)*

Copper/palladium grids were carbon-coated in-house before being glow discharged for a minimum of 30 s dependent on grid age. 0.5 % w/w PMMA latex was then pipetted onto the surface of the grid and left to adhere for 60 s. Filter paper was used to remove excess sample before staining using uranyl formate (0.75 % w/v). After 20 seconds excess stain was removed with filter paper and dried using a vacuum hose. Images were obtained using a FEI Tecnai Spirit microscope operating at 80 kV and equipped with a Gatan 1 K CCD camera. Particles were manually sized using ImageJ software.²⁴

2.3. Results and Discussion

2.3.1. *Polymerization retardation by DPE*

Solids contents of the PMMA latexes was used to monitor monomer conversion. For all the following reactions, around 14.9 wt% solids was expected at 100 % conversion. When DPE was not added to the reaction, the concentration of APS had very little effect on the kinetics of the reaction with all reactions reaching 100 % conversion within 30 minutes (Figure 2.1). A sharp reduction in the solids content at 180 mins for the 1 % APS sample is attributed to coagulation due to a lower amount of charge stabilizing persulfate end-groups in comparison to the other reactions. Once the latex had been removed from the reactor and the aggregate dispersed, the solids contents were close to the theoretical limit of 14.9 %.

In agreement with the calorimetry studies carried out by Viala *et al.*²³ the polymerization rate of MMA can be reduced by addition of DPE (Figure 2.2). This indicates that, when used in conjunction with SFEP, DPE acts as a polymerization retarder. Also, as observed for conventional emulsion polymerization, an increase in the DPE content leads to a further reduction in the rate of polymerization.⁸ The final solids content also decreases with increasing DPE content. There are several reasons why this occurred, including greater coagulation and the capping of initiator leading to some unreacted monomer. There are 2 final points for every run as once the reaction had been cooled and removed from the reactor some of the coagulum dispersed and increased the solids content.

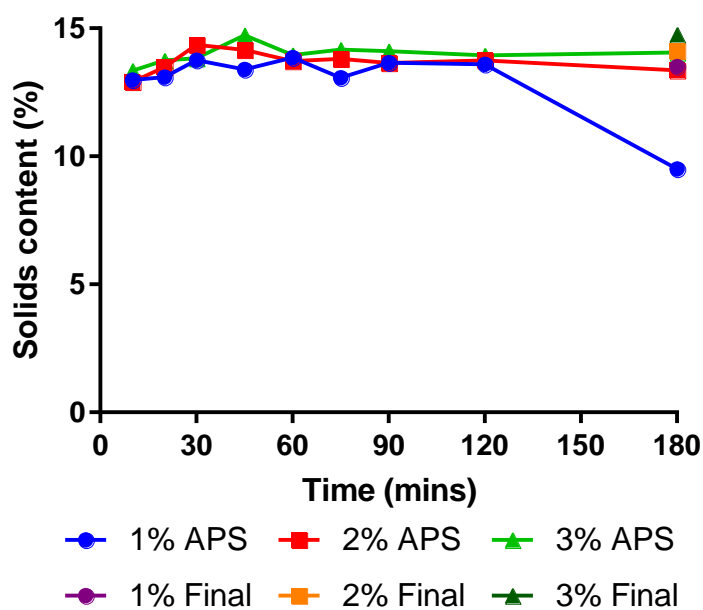


Figure 2.1. Solids contents kinetics, obtained by gravimetric analysis, of emulsion polymerizations of MMA without DPE.

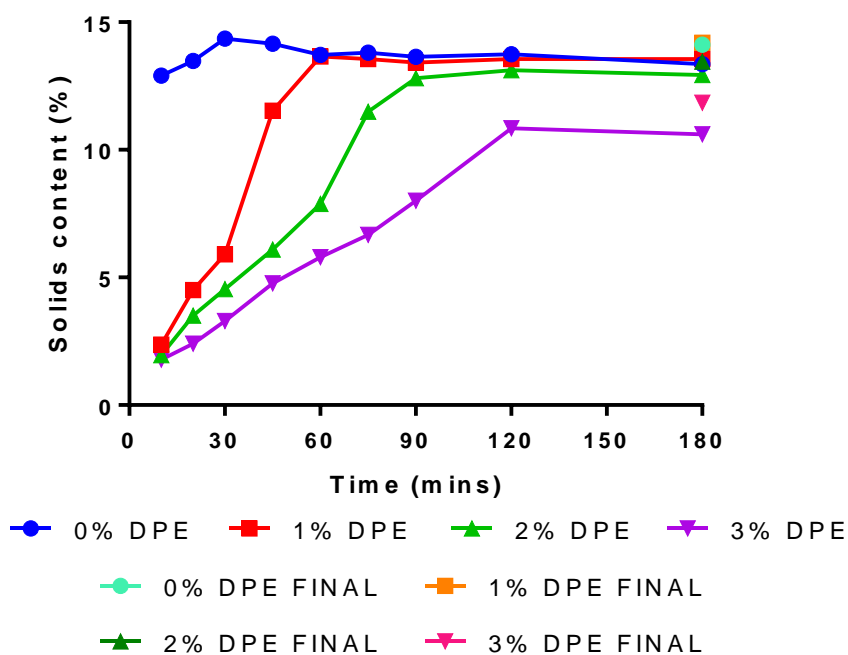


Figure 2.2. Solids content against time, obtained by gravimetric analysis, of the emulsion polymerization of MMA with increasing DPE content.

The solids content over time for reactions containing 3 % DPE with differing APS content is shown in Figure 2.3. As the APS content of the reaction is increased the polymerization rate increases also. This is expected when increasing the initiator concentration in emulsion polymerization and the same trend can also be seen for 1% and 2% DPE systems (Figure 2.4

and Figure 2.5). Reactions containing 3 % DPE and 3 % APS were quenched at 3 h as conversion had reached a maximum and the solids content had begun to decrease, whereas reactions containing 1 and 2 % APS were run for 6 h, as it was unclear with 2 % APS (and obvious with 1 % APS) that the reaction was not complete. However, after 6 h, the reaction had ceased and when reactions were run for 24 h there was no further increase in solids content. This was attributed to the high temperature (90 °C) for the reaction with most, if not all, APS being consumed after 6 hours. The half-life of KPS should be similar to that of APS, which was calculated to be 33 mins with similar conditions.²⁵ Conversions decrease over time after reaching their maximum. This was attributed to coagulation of the latexes due to the lack of a suitable surfactant or stabilizer. The APS initiator fragment at the start of a majority of chains provides the only colloidal stabilisation. This appears to be insufficient to prevent coagulation during the reaction. A reduction in the final conversion and rate of polymerization was also seen in the SFEP of St but the amount of coagulation was not reported.²²

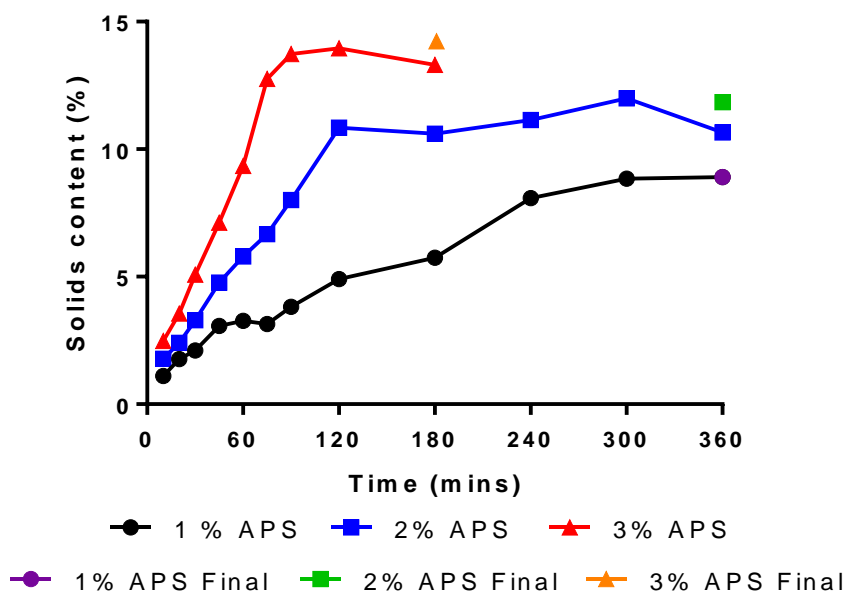


Figure 2.3. Solids contents over time, obtained by gravimetric analysis, for emulsion polymerizations of MMA at 90 °C, containing 3 % DPE with varying APS concentration.

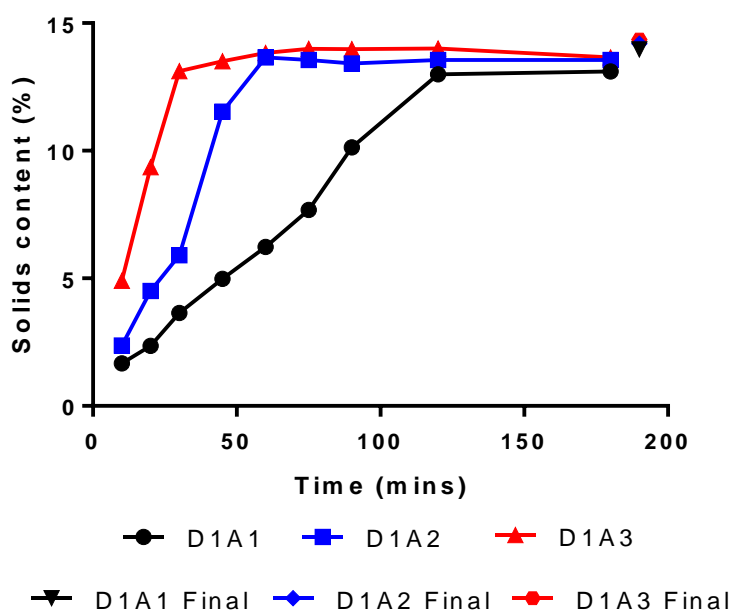


Figure 2.4. Solids contents over time, obtained by gravimetric analysis, for emulsion polymerizations of MMA at 90 °C, containing 1 % DPE with varying APS concentration.

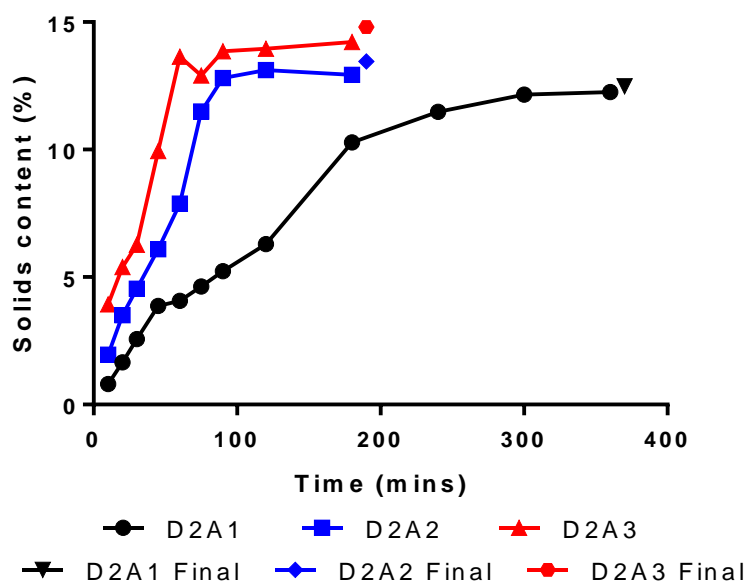


Figure 2.5. Solids contents over time, obtained by gravimetric analysis, for emulsion polymerizations of MMA at 90 °C, containing 2 % DPE with varying APS concentration.

2.3.2. Molecular weight and \bar{D} reduction by DPE

SEC in DMF containing 0.1 % LiBr was used to determine molecular weight distributions for all polymers formed with and without DPE. Molecular weight distributions (MWDs) (relative to PMMA standards) for reactions containing no DPE and varying APS content can be seen in Figure 2.6. The M_n values calculated are 99.9 kDa, 50.6 kDa and 47.9 kDa for 1, 2 and 3 % APS content, respectively. The higher M_n for the 1 % APS system was attributed to the lower

initiator concentration creating fewer chains, allowing PMMA radicals to propagate for longer within the latex particles before other active radicals could terminate the polymerization.

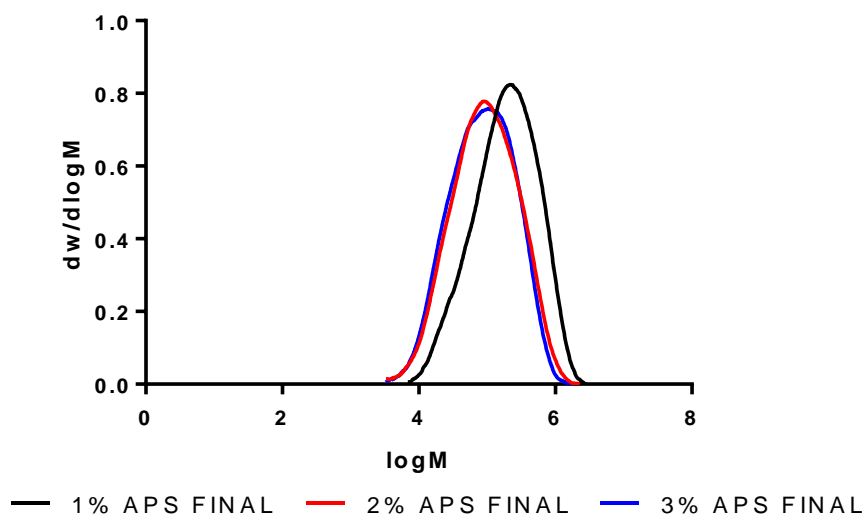


Figure 2.6. MWDs for PMMA formed in the absence of DPE with varying APS content. M_n was determined by SEC in DMF (0.1 % LiBr) against PMMA standards.

Final molecular weight distributions for increasing DPE content with 2% APS can be seen in Figure 2.7. The peaks shift to lower molecular weights with increasing DPE content. The dispersity and M_n of the final products of the varying APS and DPE concentrations is shown in Table 2-2. The M_n of the samples decrease with increasing DPE content and remain comparable for various concentrations of initiator at the same DPE content. This again indicates that DPE acts as a chain-capper, enabling some control over the molecular weight and dispersity. Increasing APS concentration reduces the dispersity slightly but not below the upper limit values that are expected for a well-controlled RDRP (e.g. $\bar{D} = 1.3$).²⁶

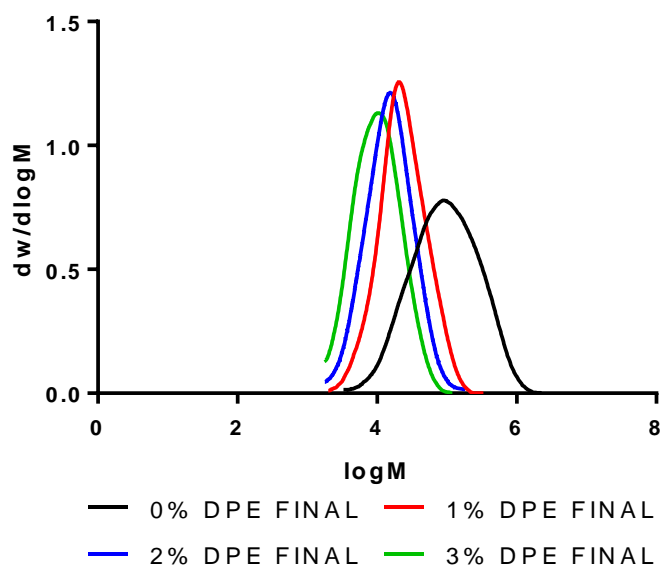


Figure 2.7. MWDs for 2 % APS content emulsion polymerizations of MMA with varying DPE content. M_n was determined by SEC in DMF (0.1 % LiBr) against PMMA standards.

In other RDRP techniques, e.g. ATRP and RAFT polymerization, the DP can be predicted from the $[M]/[Initiator]$ and $[M]/[CTA]$ molar ratios, respectively. Inspecting, Table 2-2 the M_n , and therefore DP, of these polymers is not dependent on the concentration of initiator which shows that the $[M]/[Initiator]$ molar ratio used for ATRP is not applicable for this system. However, $[M]/[CTA]$ yields the same M_n for each percentage DPE content irrespective of the APS concentration. Which is true for the values given in Table 2-2. Using the equation $DP = [M]/[DPE]$ for these reactions predicts decreasing DP values as the DPE content is increased and at lower conversions. Lower conversions are obtained for 2 % and 3 % DPE when increasing the APS content. This is not true for 1 % DPE as 95 % conversion was attained for all reactions, but the M_n does decrease with increasing APS concentration. However, it does not match the expected values. Increasing the DPE content does reduce the M_n but the lower conversion has no effect on these values, so we cannot use these methods to predict the DP of DPE-mediated reactions. If DPE is acting as a polymer chain capper that terminates the chain then, assuming no other reactions, the kinetic chain length should be related to the relative rates of addition to MMA or DPE.

Table 2-2. Summary of M_n and \mathcal{D} data obtained from SEC data for all DPE and APS concentrations in the synthesis of PMMA latexes. M_n was determined by SEC in DMF (0.1 % LiBr) against PMMA standards.

		APS content		
		1 %	2 %	3 %
DPE content	0 %	$M_n = 99,900$ $\mathcal{D} = 3.01$	$M_n = 50,600$ $\mathcal{D} = 3.20$	$M_n = 47,900$ $\mathcal{D} = 2.99$
	1 %	$M_n = 15,850$ $\mathcal{D} = 2.30$	$M_n = 17,100$ $\mathcal{D} = 1.81$	$M_n = 19,250$ $\mathcal{D} = 1.79$
	2 %	$M_n = 13,000$ $\mathcal{D} = 1.93$	$M_n = 11,150$ $\mathcal{D} = 1.80$	$M_n = 11,150$ $\mathcal{D} = 1.65$
	3 %	$M_n = 7,950$ $\mathcal{D} = 1.82$	$M_n = 7,700$ $\mathcal{D} = 1.73$	$M_n = 7,950$ $\mathcal{D} = 1.57$

Figure 2.8 shows the molecular weight distributions obtained at various time points throughout the D2A2 reactions. The highest molecular weight polymer peak in such data increases slightly in both molecular weight and dispersity over the course of the reaction. However, the two lower molecular weight peaks decrease during the course of the reaction. These could be shorter DPE-capped PMMA chains that are consumed during the reaction, or the proportion of longer polymer chains may be increasing while the products responsible for the smaller molecular weight peaks remain at a constant concentration. This supports the hypothesis that DPE is acting as a polymer end-capper, as the molecular weight of the polymer produced remains relatively constant throughout the polymerization.

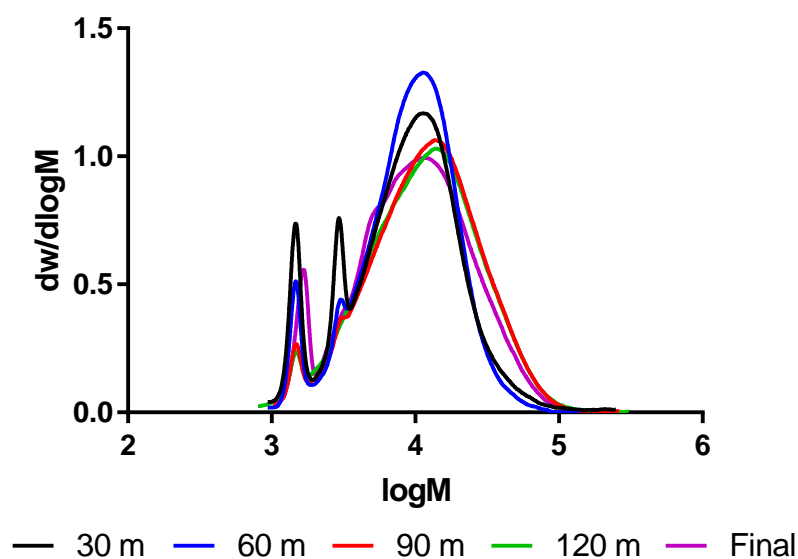


Figure 2.8. MWDs of kinetic samples obtained during reaction D2A2. M_n was determined by SEC in DMF (0.1 % LiBr) against PMMA standards.

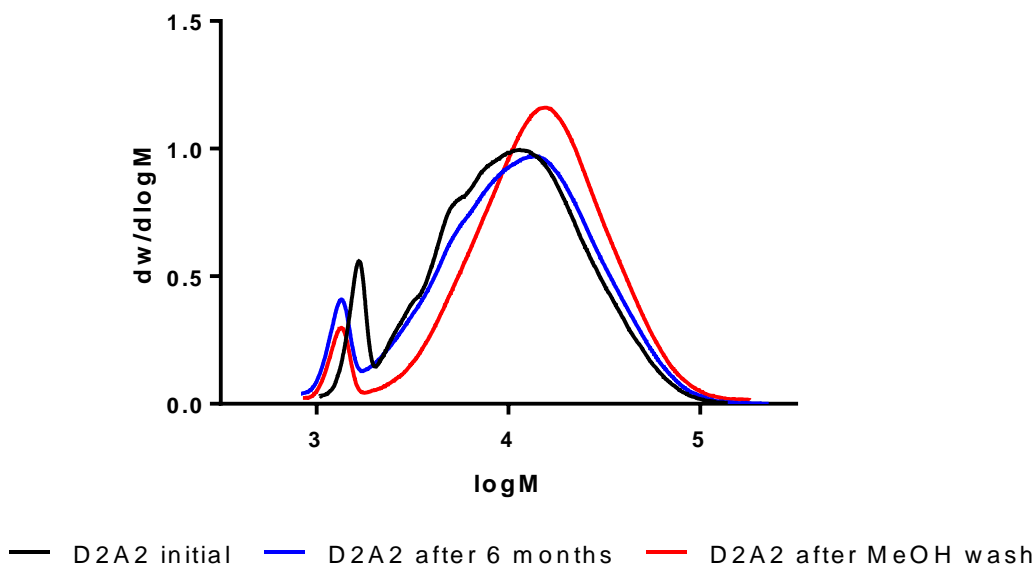


Figure 2.9. MWDs obtained for the PMMA formed in reaction D2A2. M_n was determined by SEC in DMF (0.1 % LiBr) against PMMA standards.

When samples were reanalysed six months later, it was found that the MWDs had changed. The lower molecular weight signals ($\log M < 4$) are less prominent. If such signals correspond to monomer or oligomers then they might be lost via evaporation but this seems unlikely. It is possible that these species are short polymer chains with reactive end-groups that could have reacted during storage at ambient temperature.

These low molecular weight species could be partially removed via a methanol wash. The MWD of the methanol-washed product is shown in Figure 2.9. Methanol is commonly used

to precipitate PMMA but it is a solvent for low molecular weight PMMA chains.^{8, 27} The final products of all reactions were reanalysed by SEC after washing with methanol and these data were used in the discussion above.

Previous data of the DPE method has been shown in bulk and solution to obtain dispersity of those obtainable by other RDRP methods ($\mathcal{D} < 1.3$).^{9, 10} However, when DPE was incorporated into emulsion polymerization dispersity values > 2 were observed.⁸ The data shown in this Chapter obtains values less than this but it is clear emulsion polymerizations and SFEPs require more research to reach a similar standard to other RDRP methods.

2.3.3. Analysis of polymer chain composition by ^1H NMR spectroscopy

^1H NMR spectroscopy was used to examine the amount of free DPE in the reaction solution and also the amount of DPE that is attached to the polymer chain. In principle, if DPE is attached to the polymer chain, then peaks corresponding to the semiquinoid structure mentioned previously should be present (t7, Scheme 2-1).¹⁰

The ^1H NMR spectrum of the 0% DPE 2% APS (D0A2) system is shown in Figure 2.10. All peaks can be assigned to either PMMA or solvents. Figure 2.11 shows the stacked ^1H NMR spectra recorded for D0A2 and D2A2. These spectra are similar except for the aromatic resonances of DPE at 7.3-7.5 ppm. Owing to relatively small amounts of DPE present in the reaction solution, its resonances are considerably weaker than those of PMMA. The ^1H NMR spectrum of PMMA depends on the polymer tacticity.²⁸ As the peaks between 0.5 and 2.5 ppm do not change, this indicates that the presence of DPE in such polymerizations does not affect the tacticity of the PMMA product.

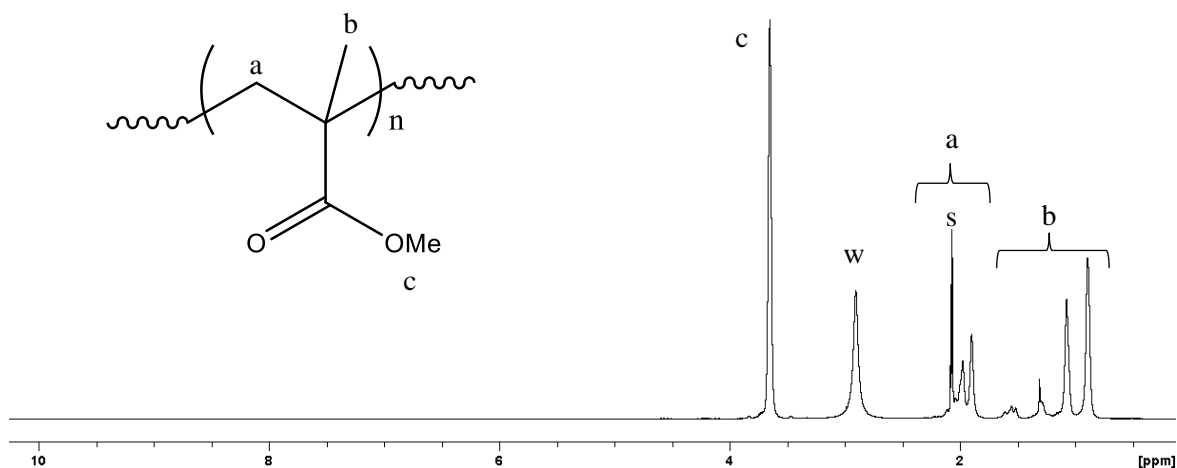


Figure 2.10. ^1H NMR spectrum obtained for D0A2 polymerizations of MMA. Peaks labelled w and s correspond to water and acetone, respectively. Spectrum obtained using sample dissolved in d_6 -acetone.

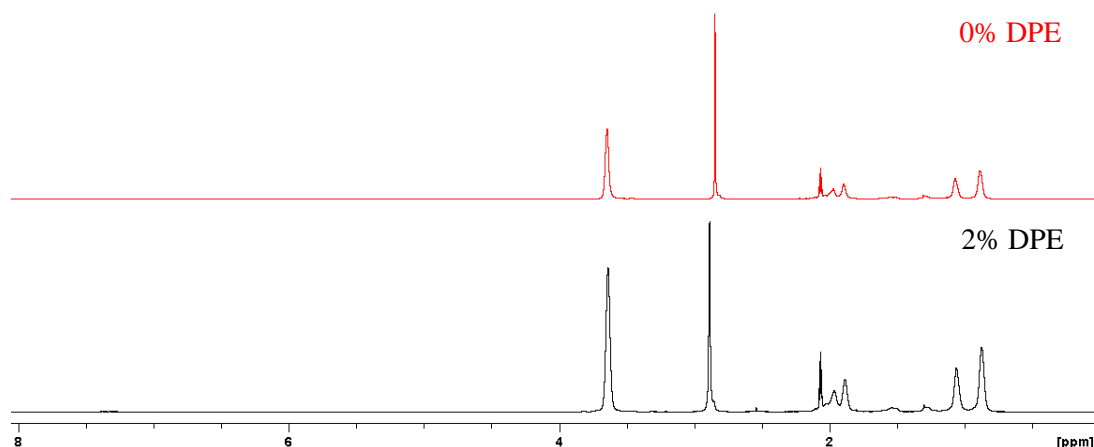


Figure 2.11. ^1H NMR spectra obtained for D0A2 and D2A2 in d_6 -acetone.

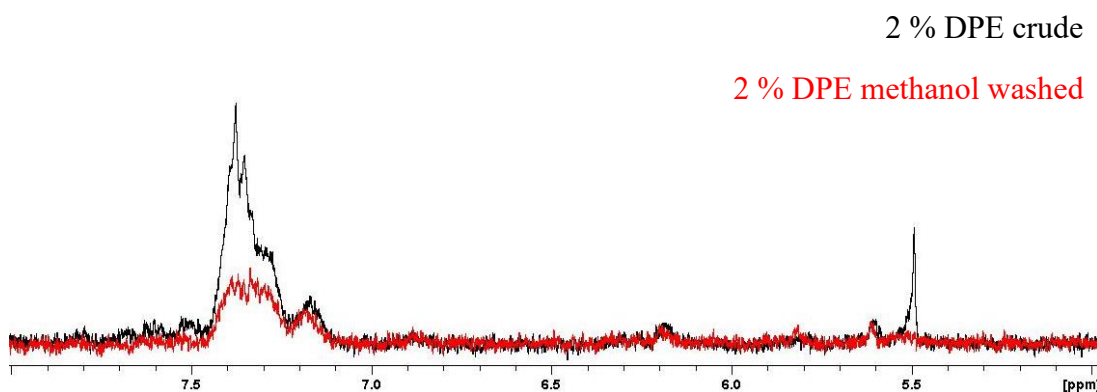


Figure 2.12. ^1H NMR spectra obtained for D2A2 before and after washing with methanol. Samples dissolved in d_6 -acetone.

Figure 2.12 shows ^1H NMR spectra recorded for D2A2 final samples before and after washing with methanol. These spectra indicate that the methanol wash removes most, if not all, free DPE in the reaction solution. This free DPE would not be removed by the freeze drying owing to the relatively high boiling point of DPE (270 °C). Nevertheless, some DPE remains after methanol washing. This DPE is either conjugated to the PMMA chains or present in its small molecule form.

Figure 2.13 shows partial ^1H NMR spectra of D0A2 and D2A2 after being washed with methanol. These signals are rather weak and barely resolved against noise. Viala *et al.*²³ published a ^1H NMR spectrum that contains several signals in the 5 – 8 ppm region. Several signals were attributed to signals of the semiquinoid structure, b and c in Figure 2.13, while other peaks at 5.9 and 6.65 ppm were not assigned. Such semiquinoid signals are not observed in the spectra presented in this Thesis but these peaks lie in the same region as the H_d and H_e signals of MMA monomer. In principle, residual MMA and free DPE should be removed with methanol, but peaks attributed to these species still remain after washing. It is possible that the termination products differ, with the semiquinoid structure not being present in these

polymer products. This hypothesis will be discussed when analysing more detail in mass spectroscopy data presented later in this Chapter.

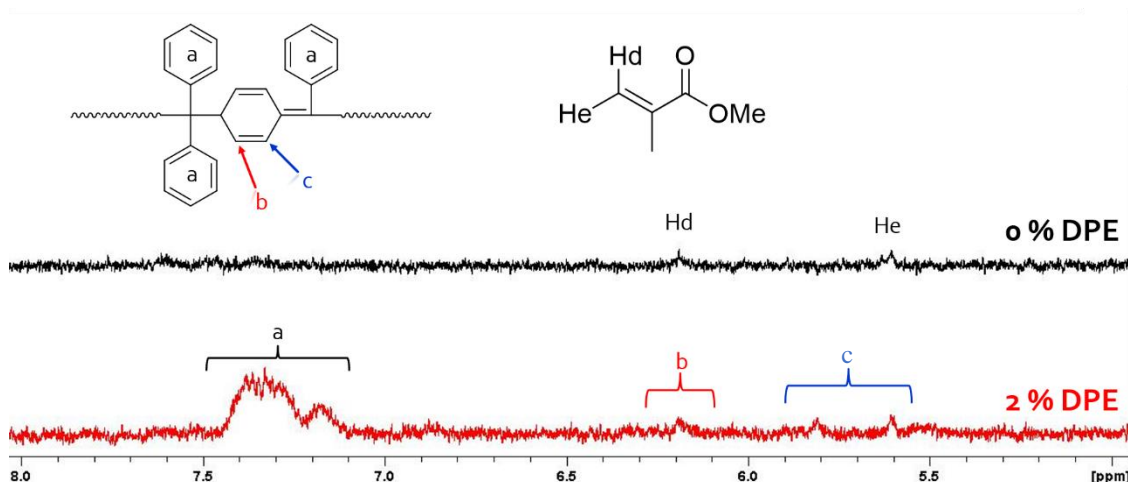


Figure 2.13. Partial ^1H NMR spectra obtained for D0A2 and D2A2 PMMA between 5 and 8 ppm. Samples dissolved in d_6 -acetone.

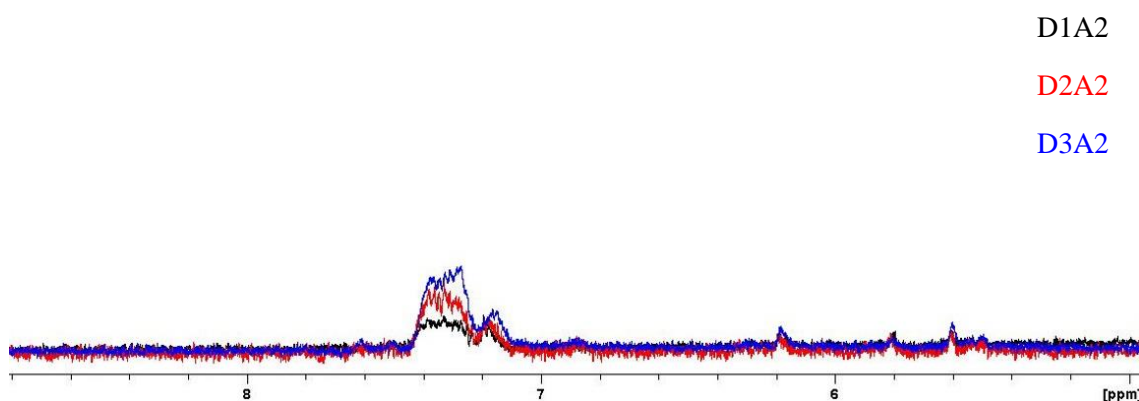


Figure 2.14. Overlaid ^1H NMR spectra of D1A2, D2A2, and D3A2 PMMA between 5 and 9 ppm. Samples dissolved in d_6 -acetone.

The ^1H NMR spectra recorded for D1A2, D2A2 and D3A2 after washing with methanol are shown in Figure 2.14. These spectra indicate that more DPE is conjugated to the polymer chains when higher DPE concentrations are used. This could be because to more polymer chains are capped with DPE or perhaps a higher amount of DPE per chain (e.g. α,α - or α,ρ -termination of DPE-capped chains). While excess DPE contained within the latex was originally thought to not be problematic, the possible danger to aquatic life discovered recently may cause this to need further thought before being applied in coatings to avoid leaching of the compound.

2.3.4. Determination of DPE capping of the polymer chain by diffusion ordered spectroscopy (DOSY) NMR

To further confirm the presence of DPE in the polymer chains, diffusion ordered spectroscopy (DOSY) NMR studies were carried out. This analytical technique discriminates between the ^1H NMR spectroscopy resonances depending on the diffusion coefficient of the corresponding species. In particular, polymers diffuse much more slowly compared to small molecules.

The DOSY NMR spectra of D2A2 can be seen in Figure 2.15. The log diffusion coefficients (logD) of signals assigned to PMMA and solvents are calculated as -8.294 and -9.534 log m²/s, respectively. The aromatic resonances of DPE are too weak to be seen in the spectrum. The spectra can be enhanced to show these peaks, but several of the lower ppm resonances begin to merge together. To examine the DPE resonances, the partial DOSY NMR spectrum of D2A2 between 6 and 9 ppm is shown in Figure 2.16. From this the logD value of the aromatic resonances is -8.865 log m²/s. This lies between the values observed for PMMA and solvent molecules and was attributed to DPE being conjugated to the polymer chains and free DPE present in the solution. This is because the DPE resonances for these two species overlap in the 1D ^1H NMR spectrum and hence could not be separated, resulting in an averaged logD value.²⁹

To further investigate this, the sample was washed with methanol to remove any residual DPE that was not attached to polymer chains. As shown previously, such methanol washing reduces the intensity of the DPE resonance in the ^1H NMR spectrum. To obtain this DOSY NMR spectrum the x axis had to be cut off between 6 and 9 ppm to effectively monitor the resonance decay between 5 and 95 % of their original values (Figure 2.17). Post-washing, the logD value of the aromatic protons became closer to that of PMMA (-9.37 log m²/s). This confirms the postulated averaged logD. However, the logD value is still lower than that of PMMA. This could be because DPE is only present within lower molecular weight chains or it may indicate that free DPE is still present within the sample. Interestingly, the signal at 6.2 ppm has a similar logD to that of the aromatic resonances. If this peak was due to residual monomer, as suggested previously, it should have a much lower logD value. This is consistent with overlapping peaks owing to a semiquinoid linkage and free MMA. To assess this possibility, the polymers were also examined by mass spectroscopy.

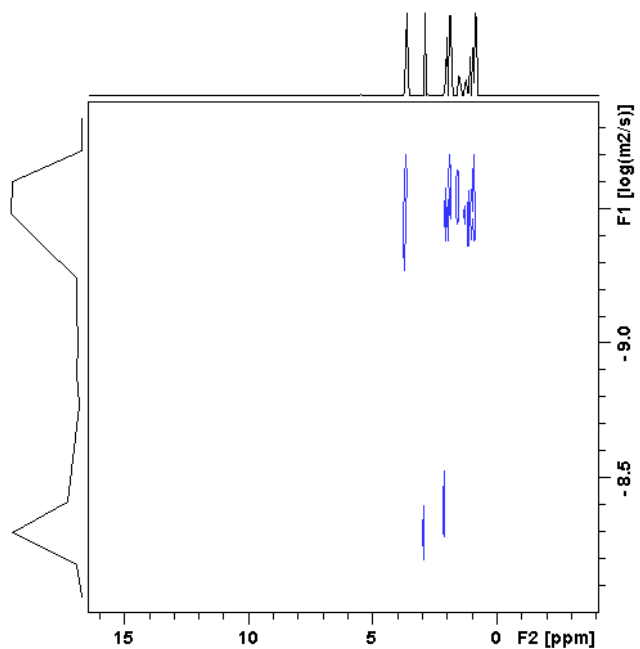


Figure 2.15. DOSY NMR spectrum of D2A2 PMMA.

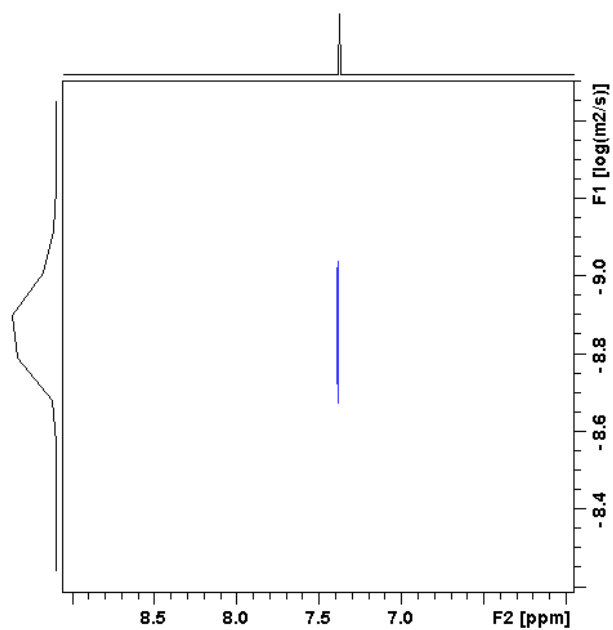


Figure 2.16. Partial DOSY NMR spectrum of D2A2 PMMA between 6 and 9 ppm.

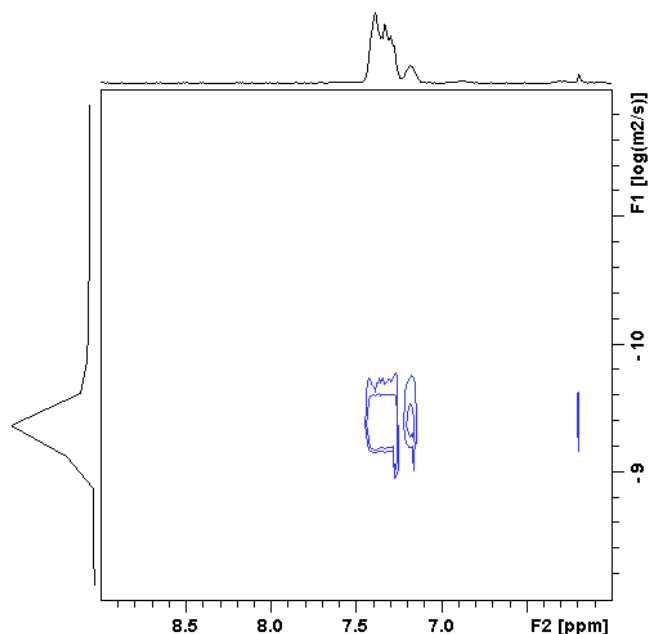


Figure 2.17. Partial DOSY NMR spectrum of D2A2 PMMA between 6 and 9 ppm, after being washed with methanol.

2.3.5. Mass Spectroscopy analysis

Electrospray ionisation (ESI) mass spectroscopy (MS) analysis of PMMA prepared in the presence and absence of DPE was conducted. The mass spectrum of D0A2 can be seen in Figure 2.18. This spectrum only contains peaks corresponding to PMMA and makes assigning the PMMA-DPE spectra considerably easier. By far the largest peak in Figure 2.18 corresponds to $-\text{SO}_4^-$ and $-\text{H}$ end groups ($296.96 + (n \times 100.05)$). This was attributed to the disproportionation termination product, with the distance between these peaks corresponding to the molecular weight of the MMA repeat unit (100.05 Da). The theoretical and experimental m/z values for this fragment are given in Table 2-3.

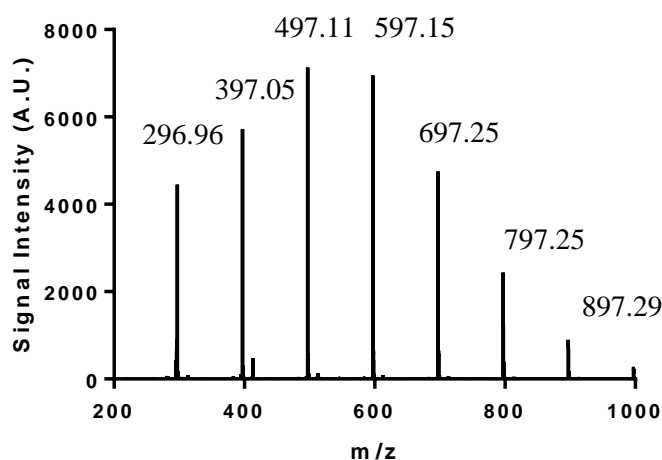


Figure 2.18. Partial ESI mass spectrum of D0A2 PMMA between 200 and 1,000 m/z .

Lower intensity peaks in this spectrum are observed at m/z ratios of $413.05 + (n \times 100.05)$ (Figure 2.19). This peak series is attributed to $-\text{SO}_4^-$ and $-\text{OH}$ end groups, with the latter being formed as a result of the use of APS initiator.³⁰ These hydroxyl radicals are formed by the reaction of sulfate radicals with water.³¹ Weaker peaks were also observed at 381 and $383 + (n \times 100.05)$. Several possible anions could correspond to these m/z values, all of which are shown in Table 2-3. As electrospray ionisation MS is a relatively gentle ionisation technique it is unlikely that the fragments caused by the loss of a methyl group are the dominant products for $m/z = 481.14$. Both fragments corresponding to the 483.15 m/z ratio are assigned to the loss of a methyl group but in different positions on the final MMA unit. Again, it seems unlikely that these fragments would occur given the use of such a soft ionisation technique but they seem to be the only possible fragments that correspond to this m/z ratio.

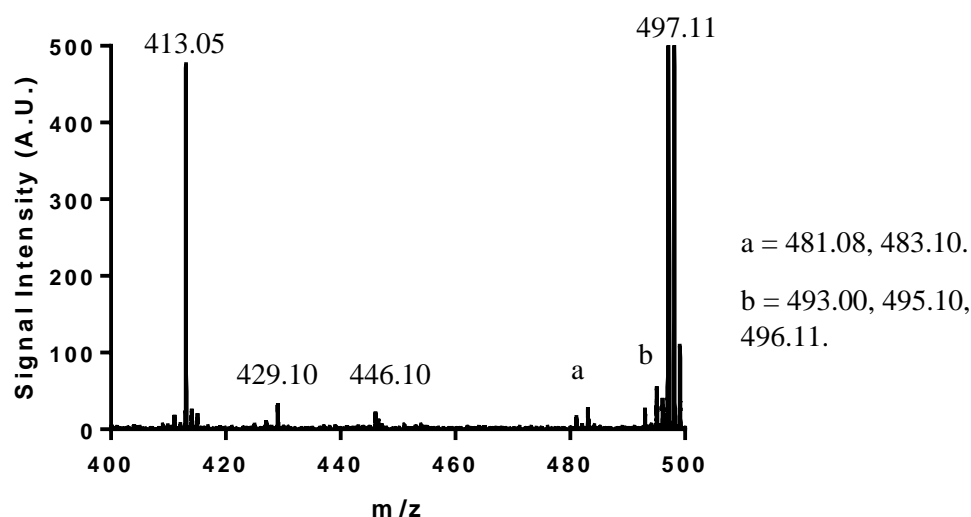


Figure 2.19. Mass spectrum of D0A2 between 400 and 500 m/z .

Table 2-3. End groups, empirical formula and theoretical and experimental m/z values for D0A2 PMMA species synthesised in the absence of DPE.

EG1	EG2	Empirical formula	Theoretical m/z	Actual m/z
$-\text{SO}_4\text{H}$	$-\text{H}$	$\text{C}_{10}\text{H}_{17}\text{O}_8\text{S}^-$	297.06 ($n = 2$)	297.00
$-\text{SO}_4\text{H}$	$-\text{OH}$	$\text{C}_{15}\text{H}_{25}\text{O}_{11}\text{S}^-$	413.11 ($n = 3$)	413.00
$-\text{OH}$	$-\text{H}$	$\text{C}_{20}\text{H}_{31}\text{O}_9^-$	415.20 ($n = 4$)	415.10
Unknown	Unknown	Unknown	Unknown	429.10
Unknown	Unknown	Unknown	Unknown	446.10
$-\text{SO}_4\text{H}$	Various	$\text{C}_{19}\text{H}_{29}\text{O}_{12}\text{S}^-$	481.14 ($n=4$)	481.08
$-\text{SO}_4\text{H}$	MAA	$\text{C}_{19}\text{H}_{31}\text{O}_{12}\text{S}^-$	483.15 ($n=4$)	483.10
$-\text{SO}_4\text{H}$	$-\text{SO}_4\text{H}$	$\text{C}_{15}\text{H}_{25}\text{O}_{14}\text{S}_2^-$	493.07 ($n=4$)	493.00
$-\text{SO}_4\text{H}$	Unsaturated	$\text{C}_{20}\text{H}_{31}\text{O}_{12}\text{S}^-$	495.15 ($n=4$)	495.10
Unknown	Unknown	Unknown	Unknown	496.11

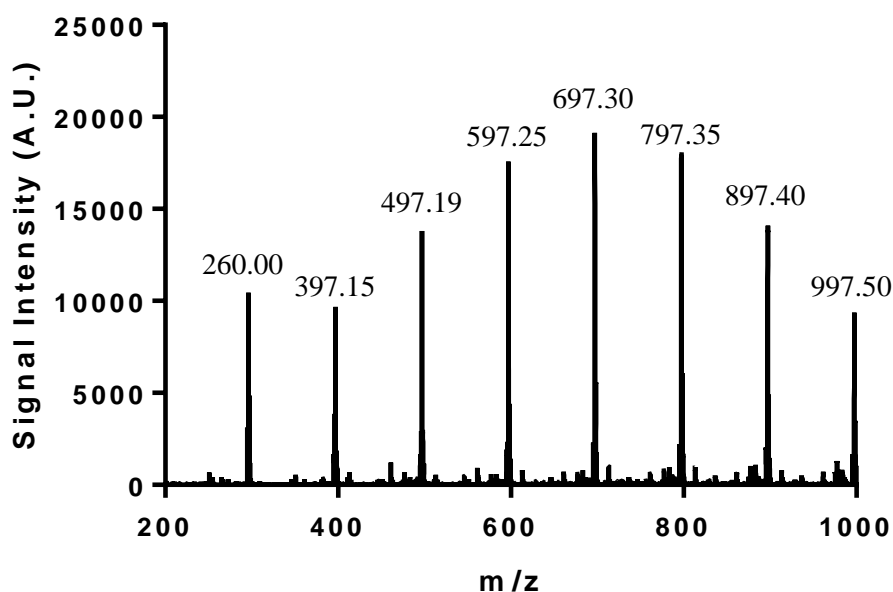


Figure 2.20. Partial mass spectrum of D2A2 PMMA between 200 and 1,000 m/z.

Figure 2.20 shows the mass spectrum obtained for D2A2. Like the spectrum for D0A2, by far the most dominant peak series in this D2A2 spectrum is at $297.00 + (n \times 100.05)$. This suggests that the disproportionation product, rather than a termination product containing DPE, is still the most common termination mechanism. The mass spectrum of D2A2 is considerably noisier than that of D0A2. This possibly indicates more side reactions, in the presence of DPE.

Figure 2.21 displays the D2A2 mass spectrum between m/z values of 400 and 500. This region was chosen as all peaks with a single anionic charge should not have 2 DPE units in the ion, with Table 2-4 listing all the peaks that are not present in the mass spectrum of D0A2. It is possible that ions may overlap with the same m/z value from fragments in D2A2 that are not in the D0A2 sample, but as they cannot be separated, they will be omitted. While two of the ions cannot be assigned, the 411.15 m/z species is attributed to a PMMA ion without any DPE in the chain. However, it is unclear why the intensity of this fragment should increase on addition of DPE.

The remaining ions given in Table 2-4 each contain a single DPE unit. This is in agreement with previous publications that suggest DPE is not a comonomer repeat unit but a chain capper.^{10, 13} Many of the end groups discussed above would require that DPE is not the terminal unit but is instead present in the chain. This suggests that the termination product given in t3 previously (Scheme 2-1) is correct, with DPE being the combination point for two polymer radicals. One exception to this hypothesis is the proton end group, which may have terminated the radical of a DPE unit at the end of the polymer chain (t4, Scheme 2-1).

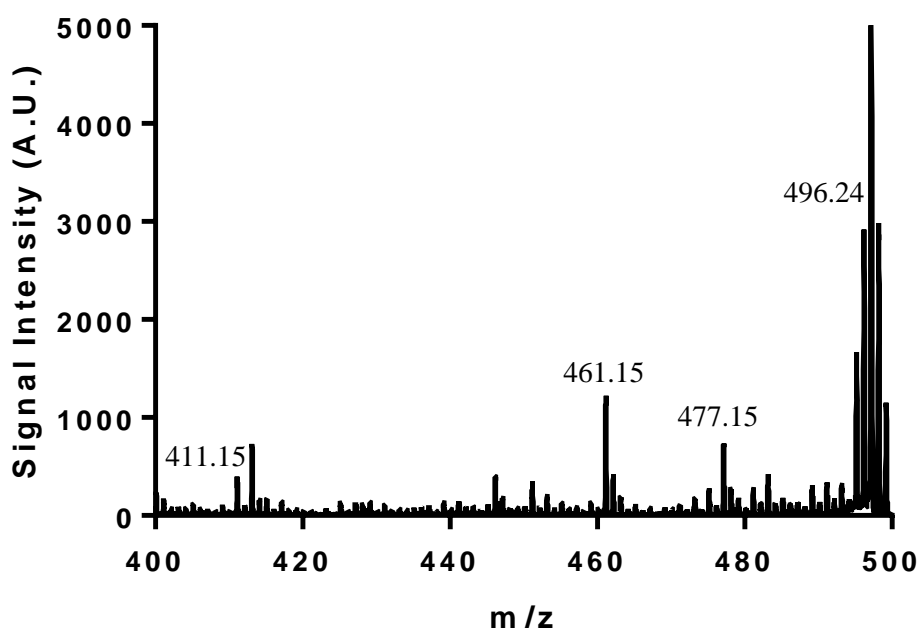


Figure 2.21. Partial mass spectrum of D2A2 PMMA between 400 and 500 m/z.

Table 2-4. Additional m/z peaks of D2A2 that were not observed in the D0A2 sample between 400 and 500 m/z.

EG1	EG2	DPE	Empirical formula	Theoretical m/z	Actual m/z
-SO ₄ H	-CH ₂ ⁻	No	C ₁₆ H ₂₇ O ₁₀ S ⁻	411.13	411.15
Unknown	Unknown	Unknown	Unknown	Unknown	451.20
-SO ₄ H	Unsaturated	1	C ₂₃ H ₂₅ O ₈ S ⁻	461.13 (n=2)	461.15
-SO ₄ H	Unsaturated	1	C ₂₄ H ₂₉ O ₈ S ⁻	475.14 (n=2)	475.15
-SO ₄ H	-H	1	C ₂₄ H ₂₉ O ₈ S ⁻	477.16 (n=2)	477.15
Unknown	Unknown	Unknown	Unknown	Unknown	489.20
-SO ₄ H	-CH ₂ ⁻	1	C ₂₅ H ₃₁ O ₈ S ⁻	491.17 (n=2)	491.15

As mentioned previously, the 400 – 500 m/z region was chosen to eliminate any polymer chains containing a semiquinoid DPE-DPE unit in the polymer chain. However, there are no additional peaks observed in the higher m/z regions that are not present in the 400 - 500 m/z region. Therefore, for an ion to contain a semiquinoid unit, its m/z value must overlap with the existing peaks discussed above. The only signals where this could be the case are at 477.15 and 475.15 m/z, which correspond to hydroxyl and proton, and hydroxyl and unsaturated end groups, respectively. It seems unlikely that these fragments would be present without the polymer chains that are initiated with sulfate instead of hydroxyl ions also being present. These are the major ions for both the PMMA synthesised in the absence of DPE and the postulated PMMA-DPE ions that contain a single DPE unit.

From the data shown above we can infer that the mechanism of the DPE method in SFEP conditions does not involve the semiquinoid structure shown in t7 (Scheme 2-1) that was shown to be the main termination pathway in emulsion polymerization of MMA in the presence of DPE.²³ Perhaps surprisingly the mechanism of SFEP of MMA is shown above to be the same as that seen in solution polymerization of MMA (t3, Scheme 2-1). While the concentration of DPE and initiator does not seem to affect the mechanism, other factors, such as temperature, could also change the mechanism.

2.3.6. Bimodal particle size distribution caused by DPE

2.3.6.1. Particle size distributions obtained by dynamic light scattering (DLS)

PMMA particles synthesised without DPE were sized using dynamic light scattering (DLS). The particle size distributions obtained (Figure 2.22) are unimodal with number-average particle diameters of 380 ± 2 nm, 400 ± 9 nm and 395 ± 6 nm for 1, 2 and 3 % APS, respectively. Varying the initiator concentration does not seem to affect the particle diameter within experimental error. Polydispersity appears to increase at higher APS concentration. Camli *et al.*³² reported that, at higher initiator concentrations, both the particle size and polydispersity increased. This was attributed to increasing ionic strength resulting in particle aggregation owing to reduced electrostatic repulsion as a result of charge shielding.

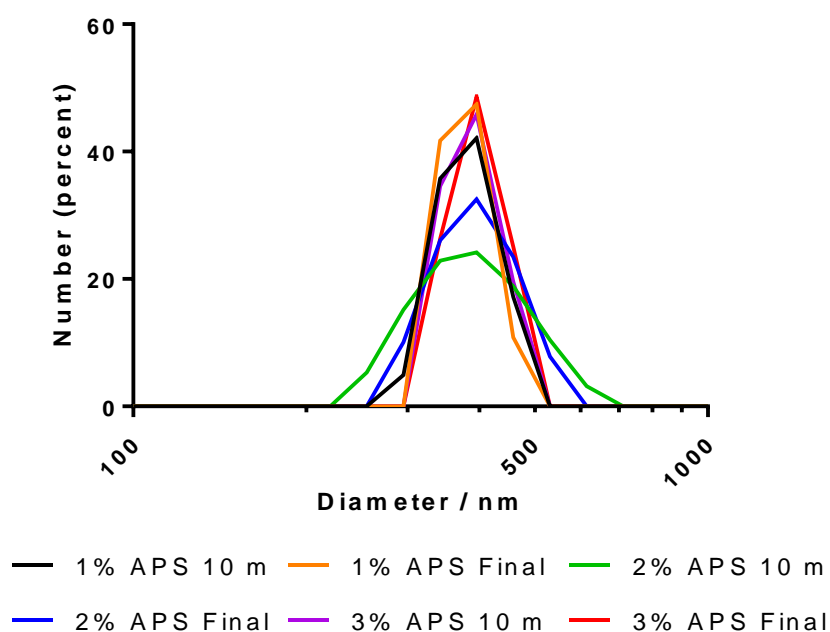


Figure 2.22. Particle size distributions determined by DLS of PMMA latexes synthesised in the absence of DPE with varying APS concentrations.

The evolution in particle size distribution over time for these MMA polymerizations was monitored using DLS. The particles reached their full size within 10 min at all APS

concentrations. However, the solids contents indicated that the polymerization was not complete before 30 min. It is expected that the particles should be swollen with monomer at 10 min and may shrink as the conversion increased due to the higher density of PMMA relative to MMA monomer.

However, when DPE is introduced into such polymerizations, particle size distributions became difficult to measure using DLS, with monomodal distributions, bimodal distributions or broad distributions being observed. Examples of each of these size distributions for the same sample can be seen in Figure 2.23. This is attributed to a bimodal particle distribution where the difference in particle diameter is too small to be fully resolved consistently by DLS. The CONTIN model was used to fit this data, as this model assumes more than one particle size, but the two populations could not be resolved.³³ To gain a more detailed understanding of the particle size distributions, transmission electron microscopy (TEM) was used.

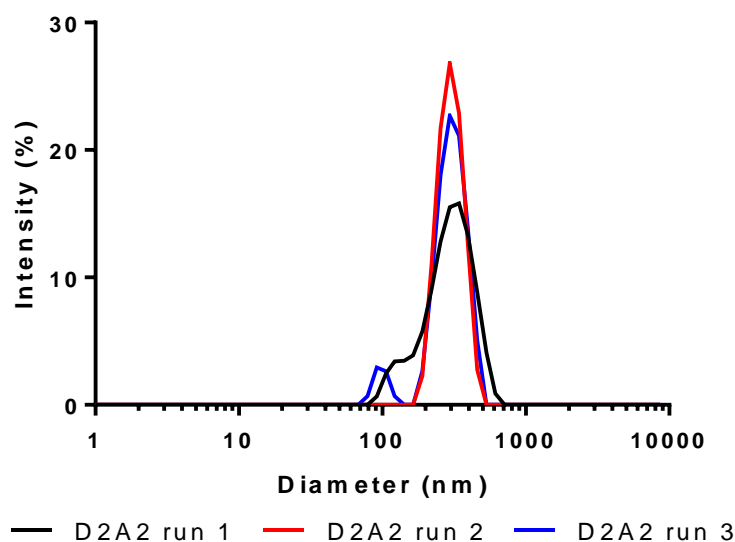


Figure 2.23. Particle size distributions determined by DLS of PMMA latexes synthesised in D2A2 reagent concentrations.

2.3.6.2. Particle size distributions obtained by transmission electron microscopy (TEM)

The particle sizes obtained by TEM for 0 % DPE syntheses are comparable to those obtained by DLS (Table 2-5 and Table 2-6). Number-average diameters were determined to be 330 ± 25 , 315 ± 30 and 330 ± 30 nm for 1, 2 and 3 % APS concentrations, respectively. The TEM diameters are smaller than those determined by DLS, owing to DLS measuring D_h . The TEM diameter is very similar for all non-DPE reactions. Samples removed from the 0 % DPE reaction mixtures after 10 and 30 min were also analyzed by TEM. The particle diameters observed after 10 min were identical to those measured for the final product. This agrees with the DLS data: the size of the latex does not change significantly after 10 min.

Latexes prepared in the presence of DPE were analysed by TEM. This technique indicated bimodal particle distributions (Table 2-5 and Table 2-7). The smaller particles in all the final products were around 50 nm in diameter with the larger particles being around 250 nm (Table 2-6 and Table 2-8). Kato *et al.*³⁴ reported that bimodal particle size distributions with a 6-fold size difference could be distinguished by DLS but a 3.3-fold difference could not be resolved. This supports the above DLS data: a 5-fold size difference is not likely to be fully resolved. The histograms of the measured particle diameters in these images show two distinct population, rather than a single broad distribution (Table 2-5).

This bimodal size distribution has not been reported in previous publications of PMMA-DPE synthesised by SFEP.²³ Fan *et al.*²² reported the SFEP of St but this phenomenon was not observed in this publication. However, broadening of the particle size distribution occurred when DPE was added to the dispersion polymerization of St in ethanol as reported by Srisopa *et al.*³⁵ To overcome this problem, DPE was dissolved in toluene and added 1 hour after the start of the reaction. The use of such a co-solvent may be worth exploring as future work.

The final latex prepared with 3 % DPE content and 3 % APS contain a trimodal particle distribution. These particles appear to be hollow, as they have collapsed under the ultra high vacuum needed for TEM, and are shown in Figure 2.24. Several similar particles are also present in D3A2 samples but are much fewer in number. However, it is not yet clear how these particles are formed.

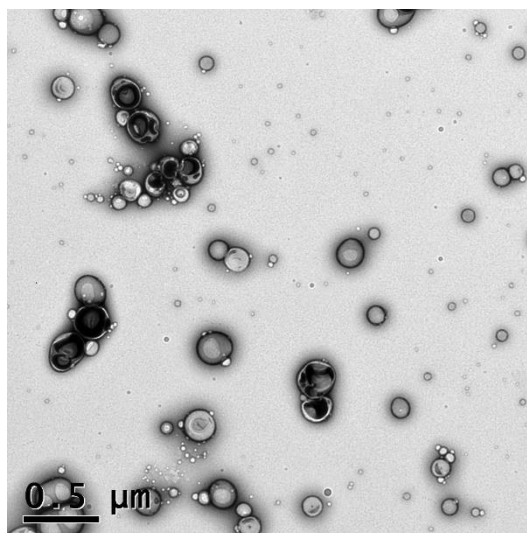
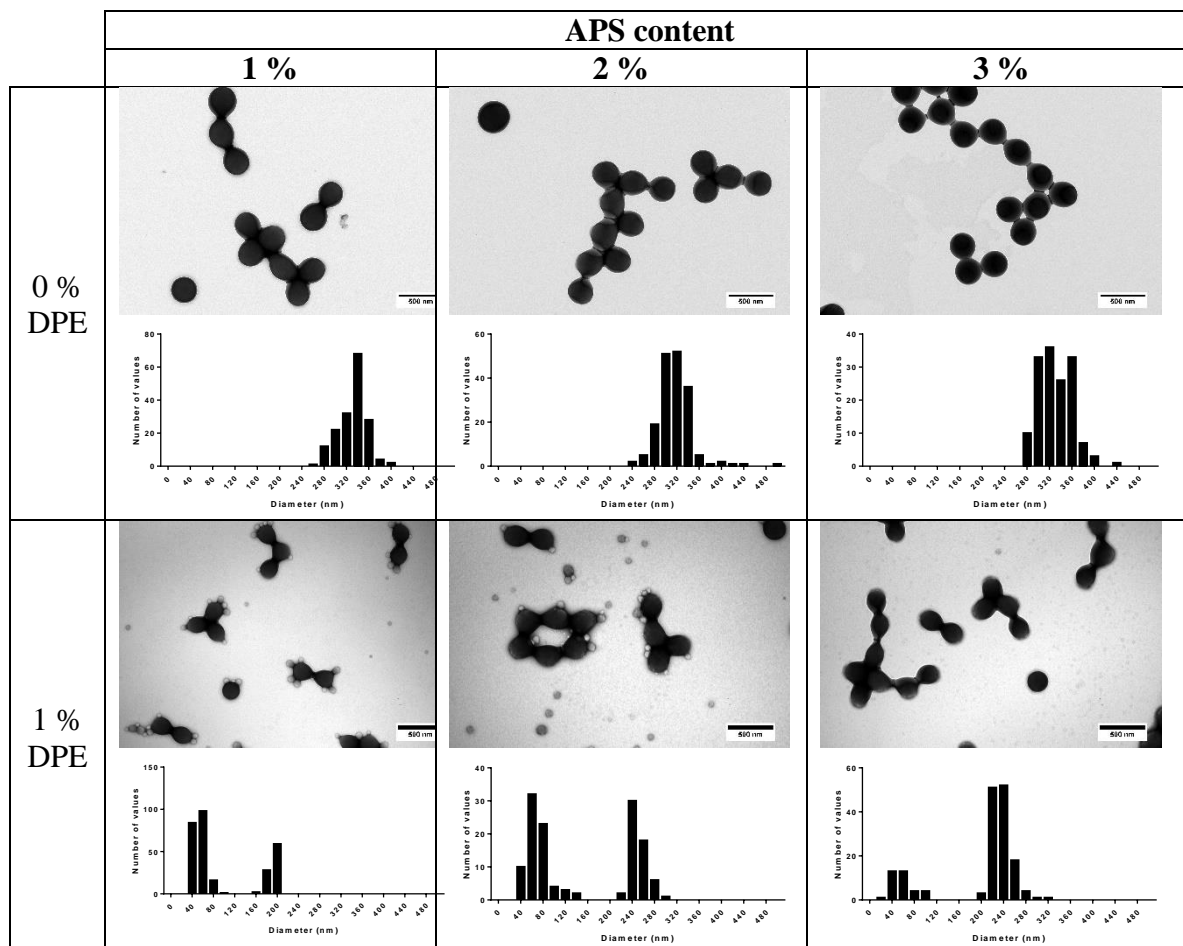


Figure 2.24. TEM image of the hollow particles present as part of a D3A3 PMMA latex final sample.

TEM was used to analyse particles synthesised in the presence and absence of DPE, i.e. D0A2 and D2A2. The presence of DPE reduces the average diameter of the large particles of D2A2 compared to the particle diameter of D0A2 (206 ± 13 nm and 286 ± 22 nm, respectively). The average particle diameter for D2A2 would be even lower if the smaller particles (49 ± 13 nm), were included in this average. Fan *et al.*²² also made this observation when St was polymerized

using SFEP in the presence of DPE. However, increasing the DPE content does not lead to a reduction in particle diameter, regardless of the APS concentration. Moreover, increasing the APS concentration in the polymerization does not have any obvious effect on the particle diameter.

Table 2-5. TEM images and particle size histograms for PMMA latexes synthesised at various APS contents and either 0 or 1 % DPE content.

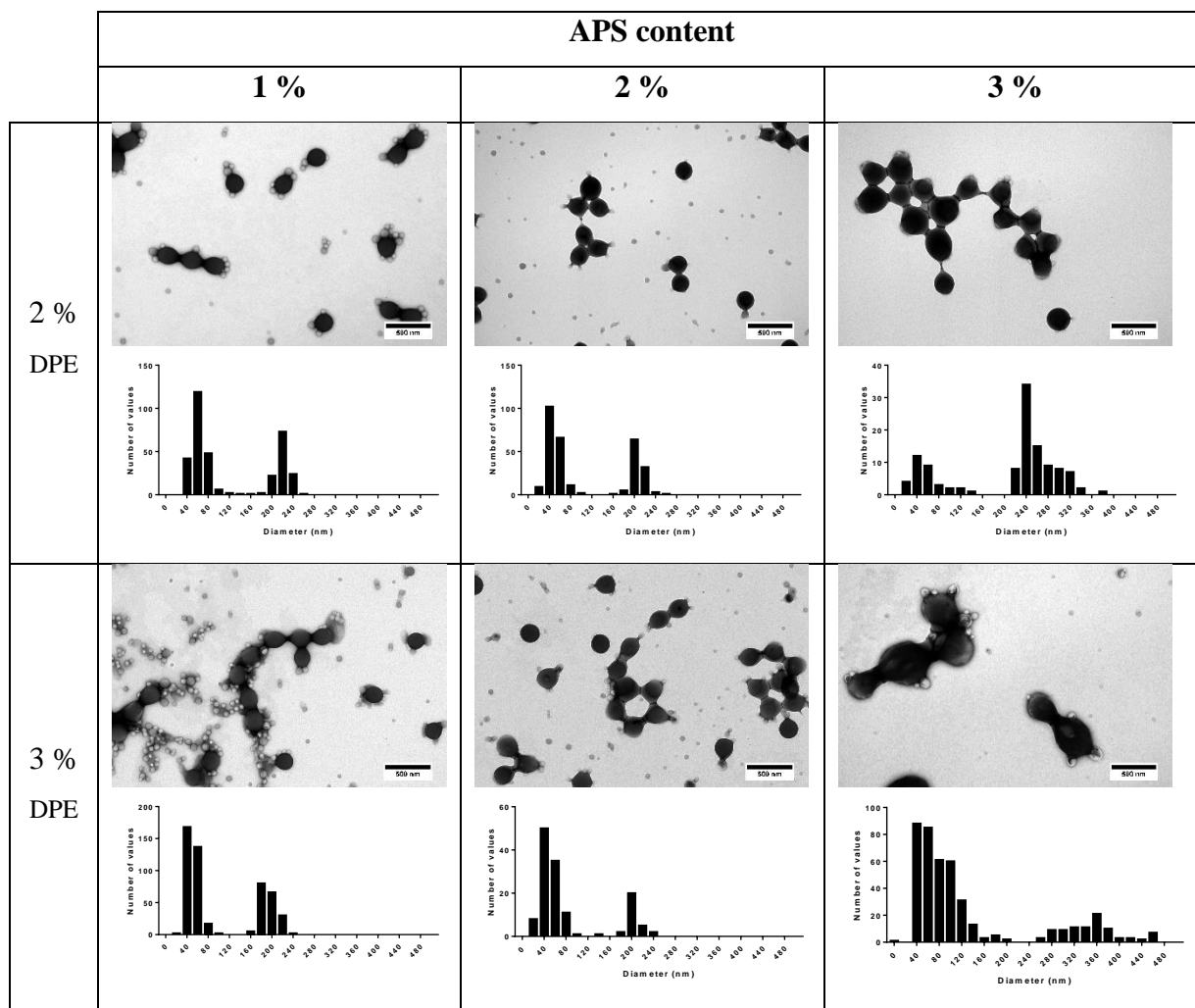


Note: Histograms of TEM images do not accurately represent the actual ratio of small to large particles and are merely used to show the two distinct populations and their approximate diameters.

Table 2-6. Average particle diameters for small and large PMMA particles synthesised with 1-3 % APS content and either 0 or 1 % DPE content.

	APS content		
	1 % APS	2 % APS	3 % APS
0 % DPE	293 ± 12 nm	286 ± 22 nm	290 ± 13 nm
1 % DPE	192 ± 8 nm	250 ± 15 nm	237 ± 17 nm
	53 ± 12 nm	70 ± 21 nm	59 ± 19 nm

Table 2-7. TEM images and particle size histograms for PMMA latexes synthesised with 1-3 % APS contents and either 2 or 3 % DPE content.

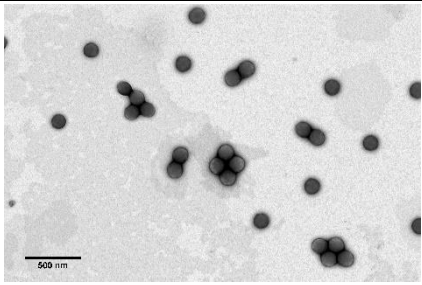
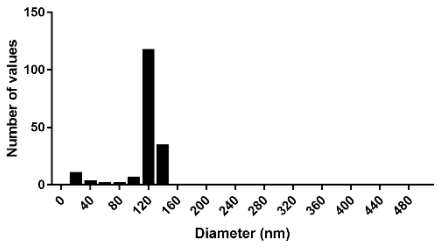
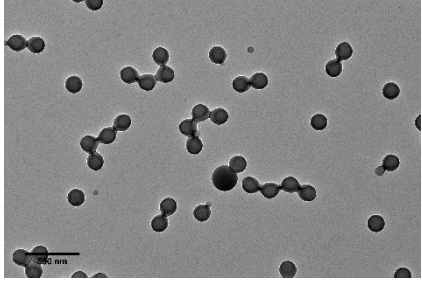
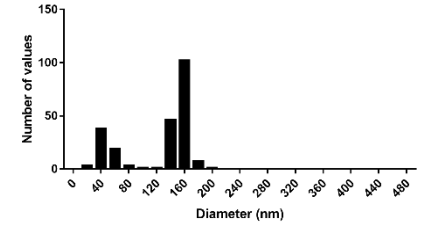
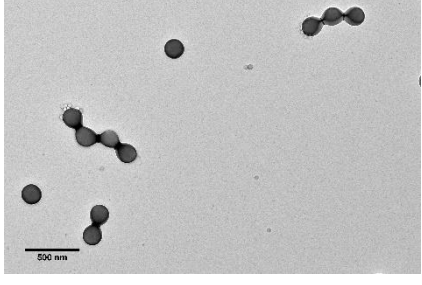
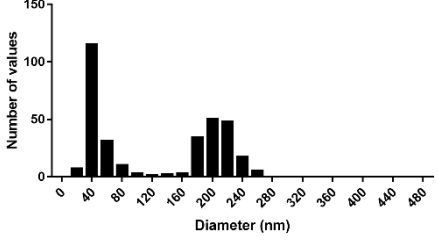
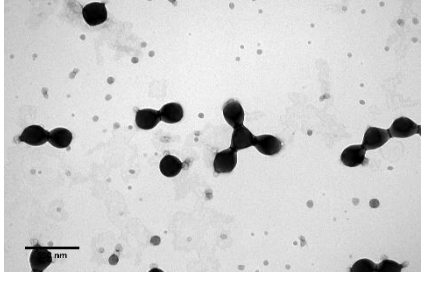
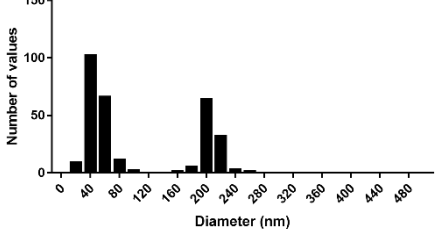


Note: histograms of TEM images do not accurately represent the actual ratio of small to large particles and are instead used to show the two distinct populations and their approximate particle diameters.

Table 2-8. Average particle diameters for small and large PMMA particles synthesised with 1-3 % APS contents and either 2 or 3 % DPE contents.

	APS content		
	1 % APS	2 % APS	3 % APS
2 % DPE	219 ± 15 nm	206 ± 13 nm	263 ± 34 nm
	62 ± 15 nm	49 ± 13 nm	57 ± 27 nm
3 % DPE	194 ± 14 nm	205 ± 17 nm	349 ± 51 nm
	51 ± 12 nm	47 ± 13 nm	52 ± 15 nm 103 ± 27 nm

Table 2-9. TEM images and particle size histograms obtained for D2A2 samples at various time points throughout the PMMA emulsion polymerization.

Time	TEM images	Histograms of PSDs
10 min		
30 min		
60 min		
Final		

A bimodal size distribution could arise via two mechanisms: (i) secondary nucleation, which results in some particles growing for a shorter time or (ii) some particles no longer growing during the polymerization. To determine which of these mechanisms was more likely, samples were taken during these MMA polymerizations and analysed by TEM. For all samples, there are either very few or no small particles formed after 10 min. The number of particles increases at 30 min and at 60 min the smaller particle population is discernible (Table 2-9), indicating that the smaller particles are the result of secondary nucleation. One possible explanation is that the DPE contained within the monomer droplets remains as a secondary nucleation point once these droplets have been almost completely depleted of MMA. This would then allow

them to start growing as particles but not allow them to reach the same diameter as those formed at the start of the polymerization.

2.3.7. Separation of bimodal particle size distributions

The separation of large and small particles was attempted for the PMMA latex synthesised with 2% DPE and 2% APS (D2A2) using 0.2 μm PTFE filters. The smaller particles should pass through this filter and can be collected. The larger particles were then redispersed, with this process being repeated several times.

DLS size distributions of the two fractions of D2A2 particles separated by filtration are shown in Figure 2.25. These show two unimodal size distributions with no significant contamination from the other population.

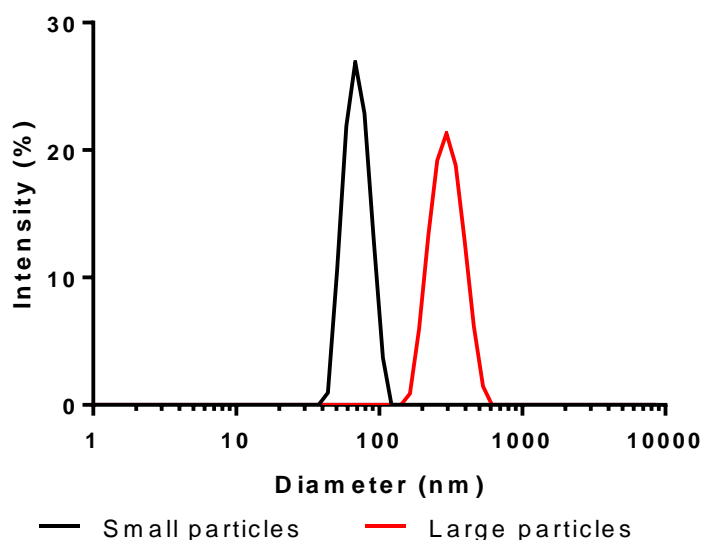


Figure 2.25. DLS particle size distributions obtained for the D2A2 fractions that pass through the filter (small particles) and those that do not (large particles).

TEM images and histograms of these two fractions are shown in Figure 2.24. The separation is shown to be effective for removing the larger particles from the sample, with no particles above 150 nm being observed by TEM. Unfortunately, the large particles remained impure. There are still some small particles contained within this sample and also some particulate matter which may originate from the filter. Therefore, the population of smaller particles can be analyzed but the large particles still contain fractions of both populations.

When ^1H NMR spectra of the small and large particle populations are overlaid they contain the same polymer signals. The major difference is a lack of aromatic signals in the spectrum recorded for the large particles. This is attributed to the presence of free DPE in the solution, as this would freely flow through the filter and be reduced in concentration with each filtration. However, it could also be due to a higher concentration of DPE within the polymer. Neither

sample could be washed with methanol as there was insufficient amounts of sample after separation.

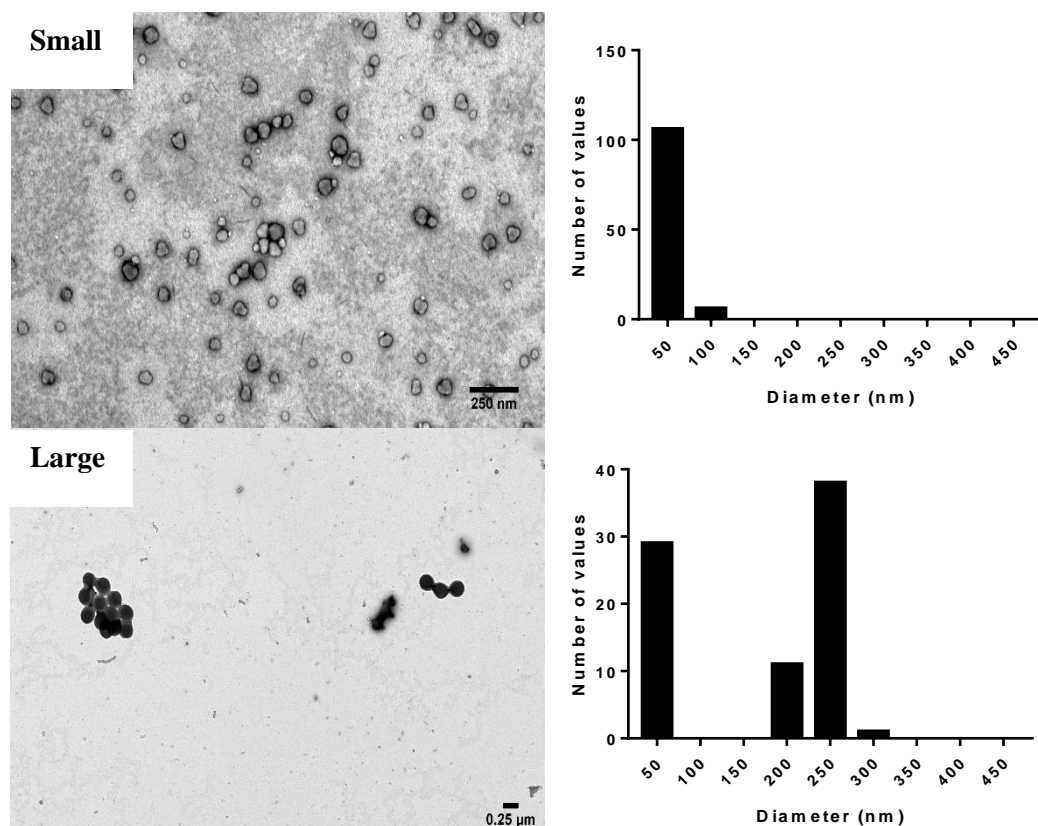


Figure 2.26. TEM images and histograms obtained for the small and large particle populations within D2A2.

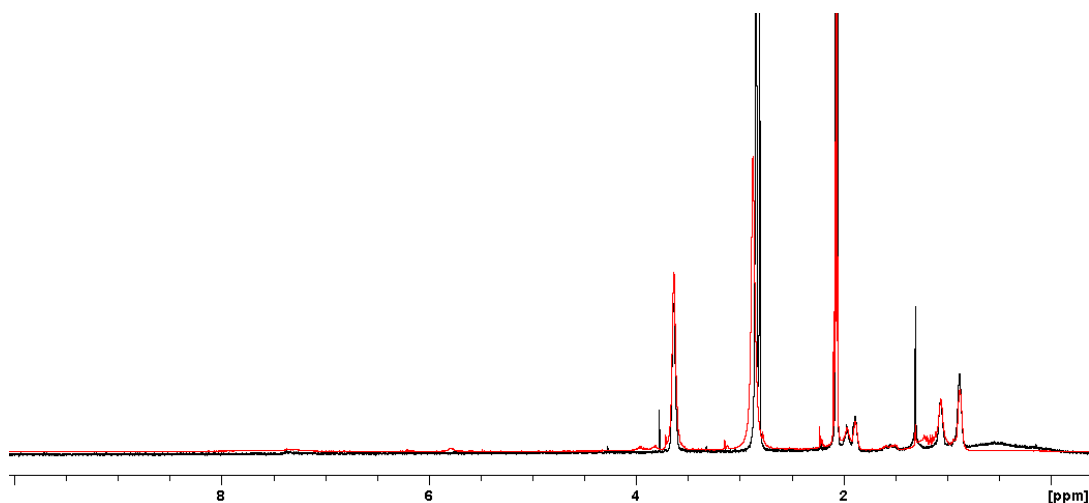


Figure 2.27. ¹H NMR spectra of the small (red) and large (black) particle populations within D2A2 latex.

Figure 2.28 shows the MWDs obtained by SEC for the two D2A2 fractions. The smaller particles that pass through the filter comprise polymer chains of lower molecular weight and dispersity compared to the larger particles. This could be caused by a higher concentration of DPE within these particles, which would be consistent with the previously discussed mechanism of formation of the bimodal particle size distribution. Thus, the smaller particles

may be formed from the consumed monomer droplets. This is also supported by the higher DPE content indicated by the ^1H NMR spectrum. However, this could merely be free DPE within the sample that is not attached to a polymer chain. The broader MWD of the polymer chains within the larger particles is likely to be because of the mixture of the two particle populations still present within this sample. Nevertheless, it suggests that the larger particles do contain the majority, if not all, of the higher molecular weight polymer chains.

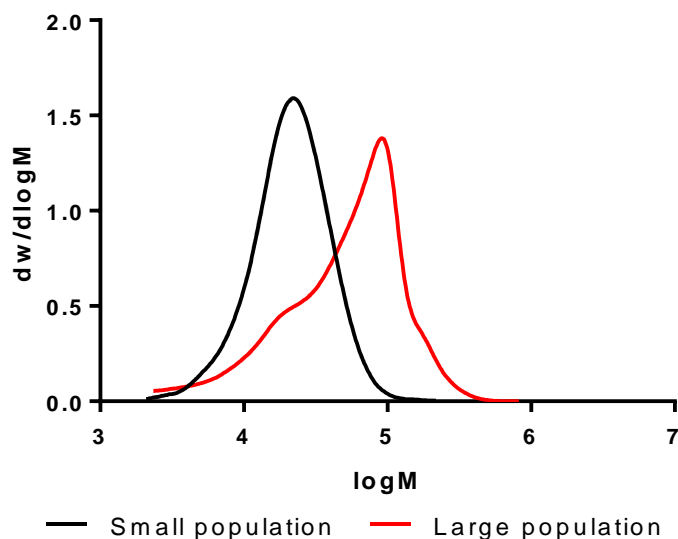


Figure 2.28. MWDs from SEC analysis of the two populations of particles within D2A2 latexes. M_n was determined by SEC in DMF (0.1 % LiBr) against PMMA standards.

2.4. Conclusions

In this Chapter, DPE has been used in conjunction with SFEP to polymerize MMA using varying concentrations of DPE and APS. As for previous studies involving DPE, the rate of polymerization can be reduced by increasing the DPE content. This capping of the growing polymer chains also has the effect of lowering the M_n and dispersity. However, this does not appear to offer the same level of control as other forms of living radical polymerization. In this work the dispersity cannot be lowered below 1.5 and the molecular weight of PMMA cannot be predicted from the MMA/DPE molar ratio. NMR spectroscopy indicates that not all DPE molecules become part of the polymer backbone as the intensity of the aromatic resonances can be reduced by washing the polymer with good solvents for DPE. DOSY NMR has been used to confirm this finding, with MS suggesting that at least one DPE unit is contained in the polymer chain and is most likely a single unit per chain mechanism.

A new observation for SFEP synthesis using the DPE method is the formation of a bimodal particle size distribution, as observed by TEM. The cause of this bimodality is still under investigation, but it has been confirmed that secondary particle nucleation takes place within

the first 30 minutes of the MMA polymerization. This bimodality could potentially be applicable in coating applications giving good quality finish, adhesion and resistance properties as a result of improved particle packing.³⁶ Particle fractionation has been achieved by ultrafiltration. This shows that the two populations contain polymers of different molecular weights by SEC, but similar compositions by ¹H NMR spectroscopy. However, the population of large particles also contains some small particles and neither fraction could be washed with methanol to remove free DPE.

2.5. References

1. Egen, M.; Zentel, R., Surfactant-free emulsion polymerization of various methacrylates: Towards monodisperse colloids for polymer opals. *Macromolecular Chemistry and Physics* **2004**, *205* (11), 1479-1488.
2. Cheng, S. J.; Zhao, Y. X.; Wu, Y. M., Surfactant-free hybrid latexes from enzymatically hydrolyzed starch and poly(butyl acrylate-methyl methacrylate) for paper coating. *Progress in Organic Coatings* **2018**, *118*, 40-47.
3. Zhou, X. J.; Yang, Q.; Li, J. Y.; Nie, J. J.; Tang, G. P.; Du, B. Y., Thermo-sensitive poly(VCL-4VP-NVP) ionic microgels: synthesis, cytotoxicity, hemocompatibility, and sustained release of anti-inflammatory drugs. *Materials Chemistry Frontiers* **2017**, *1* (2), 369-379.
4. Zhou, J. H.; Yao, H. T.; Ma, J. Z., Recent advances in RAFT-mediated surfactant-free emulsion polymerization. *Polymer Chemistry* **2018**, *9* (19), 2532-2561.
5. Kim, Y.; Kim, K.; Lee, B. H.; Choe, S., Molecular weight control of PS spheres using soap free and RITP-soap free emulsion polymerization. *Macromolecular Research* **2012**, *20* (9), 977-984.
6. Luo, Y. D.; Chiu, W. Y., Synthesis and Kinetic Analysis of DPE Controlled Radical Polymerization of MMA. *Journal of Polymer Science Part A-Polymer Chemistry* **2009**, *47* (24), 6789-6800.
7. Chen, D.; Fu, Z. F.; Shi, Y., Synthesis of amphiphilic diblock copolymers by DPE method. *Polymer Bulletin* **2008**, *60* (2-3), 259-269.
8. Zhao, M. J.; Shi, Y.; Fu, Z. F.; Yang, W. T., Preparation of PMMA-b-PSt Block Copolymer via Seeded Emulsion Polymerization in the Presence of 1,1-Diphenylethylene. *Macromolecular Reaction Engineering* **2014**, *8* (8), 555-563.
9. Wieland, P. C.; Raether, B.; Nuyken, O., A new additive for controlled radical polymerization. *Macromolecular Rapid Communications* **2001**, *22* (9), 700-703.
10. Zhao, M. J.; Chen, D.; Shi, Y.; Yang, W. T.; Fu, Z. F., Polymerization Mechanism of MMA in the Presence of 1,1-Diphenylethylene. *Macromolecular Chemistry and Physics* **2013**, *214* (15), 1688-1698.
11. Wang, W. W.; Zhang, Q. Y., Synthesis of block copolymer poly (n-butyl acrylate)-b-polystyrene by DPE seeded emulsion polymerization with monodisperse latex particles and morphology of self-assembly film surface. *Journal of Colloid and Interface Science* **2012**, *374*, 54-60.
12. Wang, W. W.; Zhang, H. P.; Geng, W. C.; Gu, J. W.; Zhou, Y. Y.; Zhang, J. P.; Zhang, Q. Y., Synthesis of poly (methyl methacrylate)-b-polystyrene with high molecular weight by DPE seeded emulsion polymerization and its application in proton exchange membrane. *Journal of Colloid and Interface Science* **2013**, *406*, 154-164.
13. Viala, S.; Antonietti, M.; Tauer, K.; Bremser, W., Structural control in radical polymerization with 1,1 diphenylethylene: 2. Behavior of MMA-DPE copolymer in radical polymerization. *Polymer* **2003**, *44* (5), 1339-1351.
14. Yuan, D.; Zhang, H., Nanosized palladium supported on diethylenetriamine modified superparamagnetic polymer composite microspheres: Synthesis, characterization and

application as catalysts for the Suzuki reactions. *Applied Catalysis A-General* **2014**, *475*, 249-255.

15. Zhang, H. P.; Zhang, Q. Y.; Zhang, B. L.; Guo, F. G., Preparation of magnetic composite microspheres by surfactant free controlled radical polymerization: Preparation and characteristics. *Journal of Magnetism and Magnetic Materials* **2009**, *321* (23), 3921-3925.

16. Guo, F. G.; Zhang, Q. Y.; Wang, W. W.; Zhang, H. P.; Sun, J. L., Preparation of pH-responsive Fe₃O₄/Poly (acrylic acid-stat-methyl methacrylate-block-(2-dimethylamino) ethyl methacrylate) magnetic composite microspheres and its application in controlled release of drug. *Materials Science & Engineering C-Materials for Biological Applications* **2011**, *31* (5), 938-944.

17. Zhou, Y. Y.; Zhang, Q. Y.; Liu, Y. L.; Wang, W. W., Encapsulation and dispersion of carbon black by an in situ controlling radical polymerization of AA/BA/St with DPE as a control agent. *Colloid and Polymer Science* **2013**, *291* (10), 2399-2408.

18. Fan, X. L.; Liu, J.; Jia, X. K.; Liu, Y.; Zhang, H.; Wang, S. Q.; Zhang, B. L.; Zhang, H. P.; Zhang, Q. Y., A series of nanoparticles with phase-separated structures by 1,1-diphenylethene controlled one-step soap-free emulsion copolymerization and their application in drug release. *Nano Research* **2017**, *10* (9), 2905-2922.

19. Bremser, W.; Raether, B., A method for controlled radical polymerization and for the synthesis of solvent free dispersions. *Progress in Organic Coatings* **2002**, *45* (2-3), 95-99.

20. Viala, S.; Tauer, K.; Antonietti, M.; Lacik, I.; Bremser, W., Structural control in radical polymerization with 1, 1-diphenylethylene. Part 3. Aqueous heterophase polymerization. *Polymer* **2005**, *46* (19), 7843-7854.

21. Fan, X.; Jia, X.; Liu, J.; Liu, Y.; Zhang, H.; Zhang, B.; Zhang, Q., Morphology evolution of poly(glycidyl methacrylate) colloids in the 1,1-diphenylethene controlled soap-free emulsion polymerization. *European Polymer Journal* **2017**, *92*, 220-232.

22. Fan, X. L.; Liu, Y.; Jia, X. K.; Wang, S. Q.; Li, C. M.; Zhang, B. L.; Zhang, H. P.; Zhang, Q. Y., Regulating the size and molecular weight of polymeric particles by 1,1-diphenylethene controlled soap-free emulsion polymerization. *RSC Advances* **2015**, *5* (115), 95183-95190.

23. Viala, S.; Tauer, K.; Antonietti, M.; Kruger, R. P.; Bremser, W., Structural control in radical polymerization with 1,1-diphenylethylene. 1. Copolymerization of 1,1-diphenylethylene with methyl methacrylate. *Polymer* **2002**, *43* (26), 7231-7241.

24. Schneider, C. A.; Rasband, W. S.; Eliceiri, K. W., NIH Image to ImageJ: 25 years of image analysis. *Nature Methods* **2012**, *9* (7), 671-675.

25. Chen, Y.; Sajjadi, S., Particle formation and growth in ab initio emulsifier-free emulsion polymerisation under monomer-starved conditions. *Polymer* **2009**, *50* (2), 357-365.

26. Chong, Y. K.; Le, T. P. T.; Moad, G.; Rizzardo, E.; Thang, S. H., A more versatile route to block copolymers and other polymers of complex architecture by living radical polymerization: The RAFT process. *Macromolecules* **1999**, *32* (6), 2071-2074.

27. Hatada, K.; Kitayama, T.; Ute, K.; Terawaki, Y.; Yanagida, T., End-group analysis of poly(methyl methacrylate) prepared with benzoyl peroxide by 750 MHz high-resolution H-1 NMR spectroscopy. *Macromolecules* **1997**, *30* (22), 6754-6759.

28. Smith, L. M.; Coote, M. L., Effect of temperature and solvent on polymer tacticity in the free-radical polymerization of styrene and methyl methacrylate. *Journal of Polymer Science Part A-Polymer Chemistry* **2013**, *51* (16), 3351-3358.

29. Antalek, B.; Hewitt, J. M.; Windig, W.; Yacobucci, P. D.; Mourey, T.; Le, K., The use of PGSE NMR and DECRA for determining polymer composition. *Magnetic Resonance in Chemistry* **2002**, *40*, S60-S71.

30. Tauer, K.; Deckwer, N., Polymer end groups in persulfate-initiated styrene emulsion polymerization. *Acta Polymerica* **1998**, *49* (8), 411-416.

31. Liang, C. J.; Su, H. W., Identification of Sulfate and Hydroxyl Radicals in Thermally Activated Persulfate. *Industrial & Engineering Chemistry Research* **2009**, *48* (11), 5558-5562.

32. Camli, S. T.; Buyukserin, F.; Balci, O.; Budak, G. G., Size controlled synthesis of sub-100 nm monodisperse poly(methylmethacrylate) nanoparticles using surfactant-free emulsion polymerization. *Journal of Colloid and Interface Science* **2010**, *344* (2), 528-532.
33. Rasteiro, M. G.; Lemos, C. C.; Vasquez, A., Nanoparticle characterization by PCS: The analysis of bimodal distributions. *Particulate Science and Technology* **2008**, *26* (5), 413-437.
34. Kato, H.; Nakamura, A.; Ouchi, N.; Kinugasa, S., Determination of bimodal size distribution using dynamic light scattering methods in the submicrometer size range. *Materials Express* **2016**, *6* (2), 175-182.
35. Srisopa, A.; Ali, A. M. I.; Mayes, A. G., Understanding and Preventing the Formation of Deformed Polymer Particles during Synthesis by a Seeded Polymerization Method. *Journal of Polymer Science Part A-Polymer Chemistry* **2011**, *49* (9), 2070-2080.
36. Moayed, S. H.; Fatemi, S.; Pourmahdian, S., Synthesis of a latex with bimodal particle size distribution for coating applications using acrylic monomers. *Progress in Organic Coatings* **2007**, *60* (4), 312-319.

Chapter Three

3. Polymerization of styrene and benzyl methacrylate in the presence of DPE capped poly(methyl methacrylate)

3.1. Introduction

As outlined in the overall Introduction and Chapter 2 of this Thesis, there are still many questions surrounding the use of 1,1-diphenylethylene (DPE) in free radical polymerization. In Chapter 2 DPE was used to form a precursor, referred to as stage one of the DPE method. This Chapter will build on that data to form diblock copolymers, referred to as stage two. The mechanism of such blocking and how much, if any, diblock copolymer is formed is investigated.

Raether *et al.*¹ reported that the DPE method can be used with “styrene, methacrylates, acrylates, methacrylic acid, acrylic acid and *N*-vinyl compounds in organic solvents, without solvents or in water”. There is little supporting evidence for these claims contained within their publication but subsequent research by numerous groups suggests that these workers are correct.²⁻⁵

The DPE method has been used for bulk polymerizations to prepare a PMMA-DPE precursor polymer and then extend this with St.⁶ The precursor was purified by precipitation and no additional initiator was added for the second stage polymerization. This suggests that the precursor forms polymer radicals or is driven by radicals from the self-initiation of St.⁷ Possible mechanisms for this reactivation in the presence or absence of additional radical species are shown in Figure 3.1 and Figure 3.2, respectively. The diblock PMMA-PSt copolymer was precipitated into excess cyclohexane to remove any PSt homopolymer impurity and assess the extent of blocking during the St polymerization. However, block copolymer yield is unclear, and the St monomer conversion is not stated. Analysis of the diblock copolymer by SEC indicated an increase in overall molecular weight but also an increase in dispersity owing to a low molecular weight tail.

While other precursor polymers have been investigated,⁸ many publications focus on solution polymerization forming a PMMA-DPE precursor. Shi and coworkers⁹⁻¹¹ extended a PMMA-DPE precursor formed in the bulk with AA, tBA or vinyl acetate (VAc). Only one of these publications (extension with VAc) involved addition of further initiator during the second-stage polymerization.¹¹ It is difficult to discern whether the PMMA-DPE precursor is extended or simply obscured by a second higher molecular weight species in the SEC chromatograms. However, in one case the molecular weight does appear to increase with conversion, indicating behaviour similar to that reported for RDRP techniques.¹¹ A lower molecular weight shoulder corresponding to the precursor is discernible in all these publications. This indicates that some, but not all, of the precursor may have been extended. This feature persists despite attempts to remove MMA and AA homopolymers from the final latex product in one study.⁹ To attempt

to prove the presence of diblock copolymer, methanol was added to the solution to induce self-assembly. In all cases, scanning electron microscopy (SEM) images indicated the formation of particles.

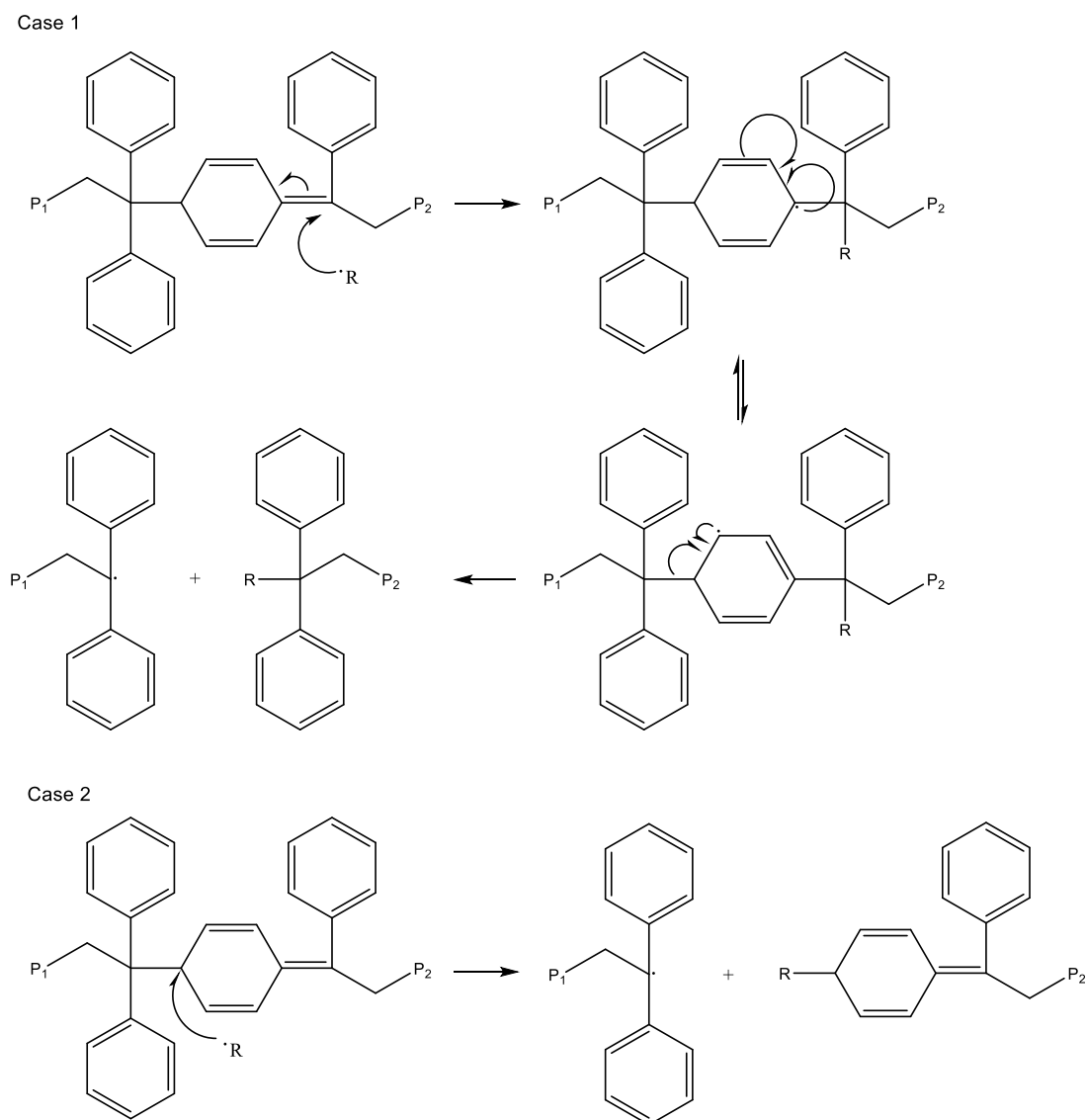


Figure 3.1. Possible mechanism during stage two of the DPE method using an influx of radical species.¹²
Reprinted (adapted) with permission from Elsevier (Licence number: 4576501059173).

There are also examples of diblock copolymer formation via miniemulsion polymerization using the DPE method.³ This process required the use of toluene and hexadecane to produce a secondary phase after the PMMA precursor was again synthesized in the bulk. The miniemulsion kinetics and products were compared to those obtained for a similar solution polymerization.

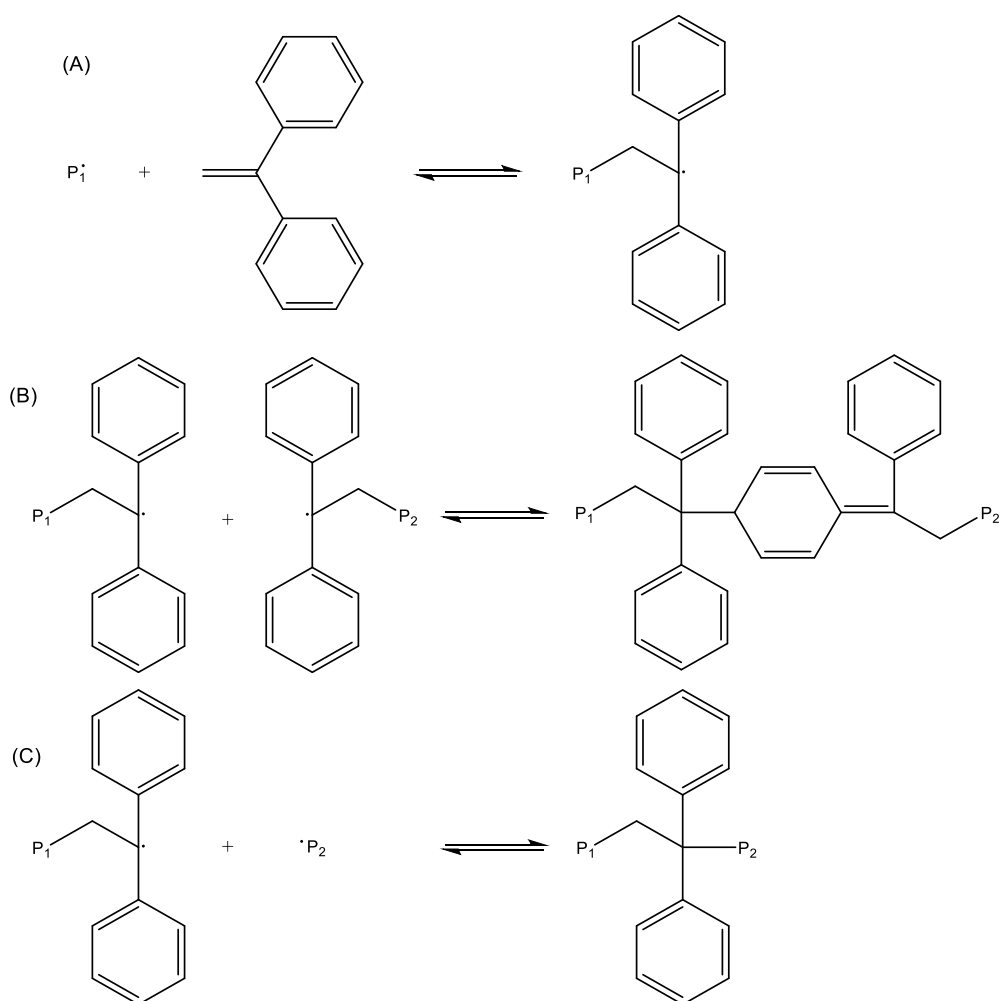


Figure 3.2. Possible mechanisms for reactivation of a DPE-capped precursor without addition of any radical species.

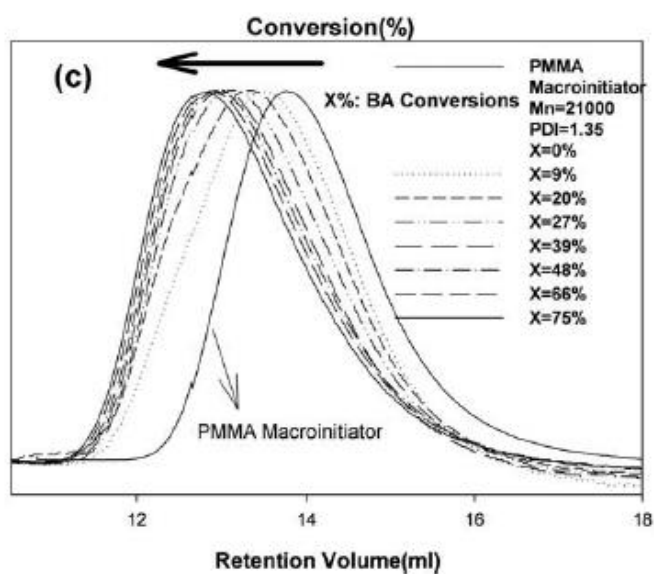


Figure 3.3. SEC data recorded during precursor (macroinitiator) extension at varying conversions. Reprinted (adapted) with permission from John Wiley and Sons (Licence number: 4561400037281).¹³

The miniemulsion polymerizations gave faster rates of polymerization and better CLRPP characteristics. However, a bimodal SEC traces were observed and the evidence for the formation of diblock copolymers is inconclusive. Further work by the same group using Pickering emulsion polymerizations produced unimodal SEC data and a reduction in retention volume with conversion (see above).¹³

There are numerous examples of the use of PMMA-DPE precursors to form diblocks via heterophase polymerization.^{14, 15} In one of these examples the precursor was extended with St.¹⁶ However, there is little evidence for block copolymer formation. No initiator was added during stage two but extension could be the result of thermal initiation of St. However, in another publication, SEC data appears to show depletion of precursor with the gradual appearance of a polymer at shorter elution times.¹⁷ This is perhaps some of the more compelling evidence of successful extension of the PMMA-DPE precursor.

PMMA-DPE precursor has been extended with nBA without additional initiator, with a blocking efficiency of over 80 % being reported.¹⁸ This precursor was not purified before use, but enough time had passed between the two polymerizations that all remaining potassium persulfate (KPS) from the initial charge should have been consumed. A secondary particle population was formed and the SEC traces of precursor and diblock overlap considerably but indicate a reaction of some kind seems to occur in this system.

The surfactant-free emulsion polymerization (SFEP) examples using DPE often involve encapsulation of a particle by the growing polymer. Zhang and coworkers^{4, 5, 19-21} encapsulated iron oxide particles with AA-MMA-DPE or St-maleic anhydride-DPE before extension with various monomers. Similarly, carbon black was encapsulated with AA-BA-DPE before extension with St. Each of these formulations contain a hydrophilic and hydrophobic monomer in order to use SFEP effectively. These studies focus on the potential application of a product and do not analyse the diblock copolymers in any detail.

The method of adding a hydrophilic monomer to a DPE-mediated SFEP has also been utilised by Viala *et al.*,²² who utilized MMA-*stat*-AA-DPE as a “controlsurf” and extended this precursor with St with and without additional initiators. [A “controlsurf” is a reactive surfactant with the ability to control radical polymerizations.] However, diblock copolymer analysis was minimal and the apparent block copolymer yield (BCY) was calculated by comparing ¹H NMR signals of the precursor and remaining St. This formulation does show that St polymerization can occur without the addition of further initiator with optimized conversions of more than 70 %. This line of enquiry was continued by Bremser *et al.*²³ with

various second monomers but diblock copolymer formation was never convincingly demonstrated.

The above examples indicate that a second stage polymerization can occur without the addition of initiator. The possible mechanism is shown in Figure 3.2. However, some literature examples include additional initiator which could lead to a large amount of homopolymer formation. While SEC data often shows the formation of a higher molecular weight polymer species, there is little direct evidence to confirm formation of a genuine diblock copolymer.

In this Chapter MMA is polymerized by SFEP in the presence and absence of DPE to form various PMMA-DPE precursors. These precursors are heated at 90 °C for 24 hours to remove any residual APS initiator. Styrene (St) or benzyl methacrylate (BzMA) is then added and the resulting polymerization and its product (if any) are analysed. Any reaction at this stage will be due to either self-initiation of the monomer or extension of the precursor via DPE chemistry. To the author's knowledge, this is the first example of genuine diblock copolymers being formed by the DPE method in SFEP conditions without an additional hydrophilic monomer. The formation of diblock copolymers is sought after in emulsion polymerizations for use in coatings, as the combination of high and low glass transition temperature (T_g) polymers can give improved film properties and avoid possible polymer separation.

3.2. Experimental

All syntheses were carried out in the BASF coatings department (Ludwigshafen, Germany). Analysis was performed at both BASF and the University of Sheffield (UK).

3.2.1. *Synthesis of precursor polymer*

A 500 mL 5-neck round-bottom flask (RBF) was fitted with anchor stirrer, stirrer guide, nitrogen inlet, condenser, stopper and septa seal for addition of reagents and sample removal. Reactions were carried out using an oil heater bath at 90 °C and an overhead stirrer. The RBF was charged with deionized water (84 g) and deoxygenated for 60 minutes. An aliquot of MMA was also deoxygenated over this period. After this time period, the RBF was lowered into the oil bath and allowed to reach the reaction temperature for 15 mins. DPE (0.32 g, 1.78 mmol) dissolved in deoxygenated MMA (14.54 g, mol) was then added and the temperature of the reaction mixture was allowed to reequilibrate for 5 minutes. Finally, APS (0.829 g, 3.63 mmol) dissolved in ammonia solution (2.5 % w/v, 4.5 g, mol) was added to start the polymerization. Samples were taken at regular time intervals and the polymerization was allowed to proceed for 6 hours. Polymerization was halted by opening the reactor to air and

removing the RBF from the oil bath. The final latex was adjusted to pH 8 with ammonia solution (2.5 % w/v).

3.2.2. Stage-two DPE method for the polymerization of styrene (St)

PMMA-DPE precursor was synthesised as described above. After 4 h, 100 % MMA conversion was reached and the pH of the polymerization was adjusted to pH 8 using ammonia solution (2.5 % w/v). At this time, distilled water (91 g) was added to the reactor and heated for 15 minutes to reach reaction temperature. Then St (15.13 g, 145 mmol) was added to the reactor. When no additional APS was added, the second-stage polymerization commenced immediately. Alternatively, the reaction mixture was allowed to equilibrate for 15 minutes before addition of APS with time points starting from this point. The amount of APS was either 0.1 (0.083 g, 3.64×10^{-4} mol) or 0.5 (0.415 g, 1.82 mmol) equivalents of the original quantity of APS used in the precursor polymerization, added as a 25 wt% aqueous APS solution. Samples were taken at regular time intervals and the polymerization was allowed to proceed for a further 4 hours. Polymerizations were quenched by opening the reactor to air and removing the RBF from the oil bath. The latex was adjusted to pH 8 with aqueous ammonia solution (2.5 % w/v).

Some syntheses of the precursor were also allowed to continue for 24 h in order to consume any residual initiator from the initial APS charge. At this point, the same method as described above was followed, with varying amounts of added APS and allowed to react for a further 24 h. Aqueous ammonia solution (2.5 % w/v) was added after the additional water charge to maintain the polymerization at pH 8, with regular adjustments being made if necessary.

3.2.3. Stage-two DPE method for the polymerization of benzyl methacrylate (BzMA)

PMMA synthesised in the presence or absence of DPE was also used for the second-stage polymerization of BzMA. This method involved heating the precursor reaction mixture for 24 h, with no further initiator being added with the BzMA charge. After 24 h, deoxygenated deionized water (148 g) was added to ensure that the total solids content did not exceed 15 wt%. Aqueous ammonia solution (2.5 % w/v) was then added to maintain the polymerization at pH 8. After 15 minutes, BzMA (25.59 g, 145 mmol) was added to the polymerization and allowed to react for a further 24 h at 90 °C.

3.2.4. Characterization

Other characterizations studies not given below were carried out at the University of Sheffield as described in Chapter 2.

3.2.4.1. *Tetrahydrofuran Size Exclusion Chromatography*

Size exclusion chromatography (SEC) analysis was conducted at the BASF site in Ludwigshafen, Germany and at the University of Sheffield, UK. The location of the analysis is indicated in the relevant figures.

Analysis was conducted at BASF on a 1260 Infinity system supplied by Agilent technologies with RI and UV detectors connected in series. Tetrahydrofuran was used as eluent at a flow rate of 1 ml/min at 40 °C, with an injection volume of 100 µL sample at 5 mg/mL concentration. Polystyrene standards (Agilent Easivials) were used to calibrate the instrument.

The characterization method of SEC data obtained at the University of Sheffield using DMF eluent is given in Chapter 2 of this Thesis.

3.2.4.2. *Hydrodynamic Chromatography*

Hydrodynamic chromatography (HDC) was carried out at the BASF site in Ludwigshafen also. This particular piece of equipment has numerous BASF-only parts and settings and as such this proprietary information cannot be disclosed in this Thesis.

3.3. Results and Discussion

In contrast to the reactions carried out in Chapter 2 of this thesis, these syntheses were carried out at the BASF site in Ludwigshafen (Germany). The results obtained in Chapter 2 were used as a starting point that could be optimised for the new reactor and slightly different reaction conditions. The main issue was the nitrogen purity at the BASF site. In view to this, it was determined that the reaction conditions referred to as D2A3 in Chapter 2 were most appropriate. Using less initiator led to a lower solids content and some residual monomer in the latex. The focus of this Chapter is to attempt to chain-extend these precursors.

3.3.1. *Effect of pH on PMMA-DPE precursor formation*

During optimization of the reaction conditions, attempts to increase the stability of the latex by increasing the pH of the reaction mixture prior to the polymerization, were undertaken. The amount of coagulation could be reduced as a result of increasing the pH of the reaction mixture from pH 2 to pH 8, yielding a final solids contents of 14.18 % at pH 8 and 13.43 % at pH 2. This indicated a more stable latex and/or higher conversion. The MWD indicated by SEC was similar, with a somewhat lower dispersity and molecular weight being observed at higher pH (Figure 3.4).

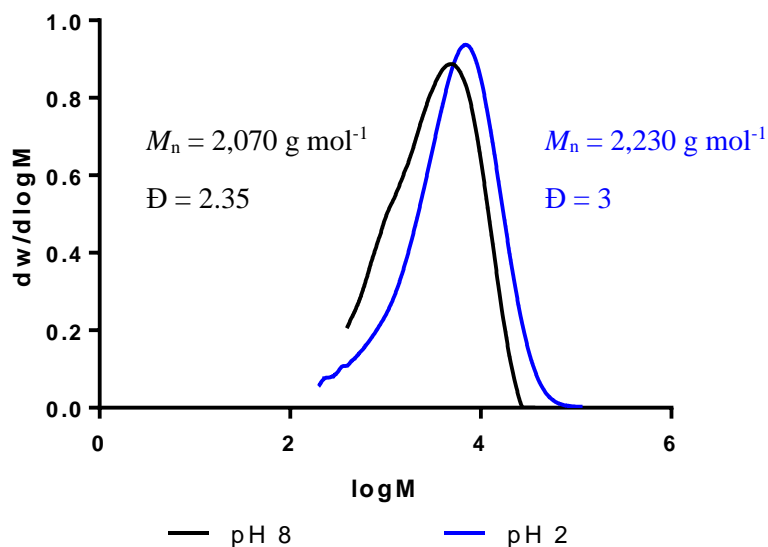


Figure 3.4. Molecular weight distributions obtained for PMMA-DPE precursors synthesized at pH 2 and 8. Molecular weight distributions were determined by SEC in DMF (0.1 % LiBr) against PMMA standards at the University of Sheffield.

When the mass spectrum of PMMA-DPE synthesised at BASF at pH 8 was compared to PMMA-DPE synthesised at the University of Sheffield at pH 2 there were no differences in the major peaks, but the peak ratios did change (Figure 3.5 and Figure 3.6). This indicates that the pH at which the reaction is carried out, as well as the polymerization scale and other factors such as nitrogen purity, do not significantly affect the SFEP DPE mechanism outlined in Chapter 2 of this Thesis (Scheme 2-1).

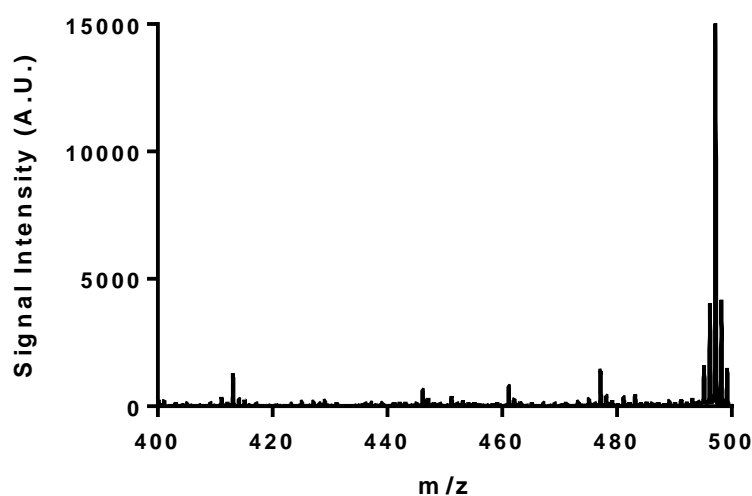


Figure 3.5. Mass spectrum of D2A3 synthesised at pH 2 between 400 and 500 m/z.

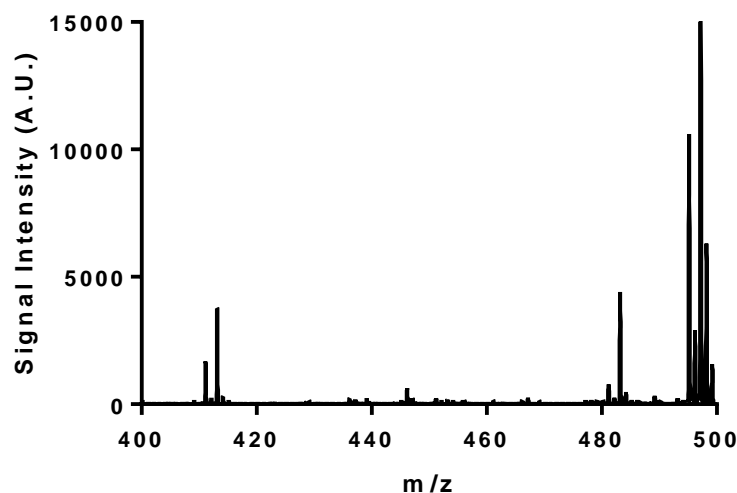


Figure 3.6. Mass spectrum of PMMA-DPE synthesised at pH 8 between 400 and 500 m/z.

When these particles were examined using TEM, it was determined that they had a different appearance to particles synthesized in Chapter 2. Reactions performed at both pH 2 and 8 yielded bimodal particle distributions but the latter latex appeared to be tackier (Figure 3.7). At pH 8, the smaller particles coalesced either onto the surface of a larger particle or together to form larger particles. If the polymer molecular weight were lower, as shown in SEC data above, this could cause the polymers to have a lower T_g . However, this difference is perhaps not large enough to cause such a change in morphology. Nevertheless, this should not affect the attempted formation of diblock copolymer using this polymer as a precursor for stage two of the DPE method. Thus, all subsequent syntheses were conducted at pH 8.

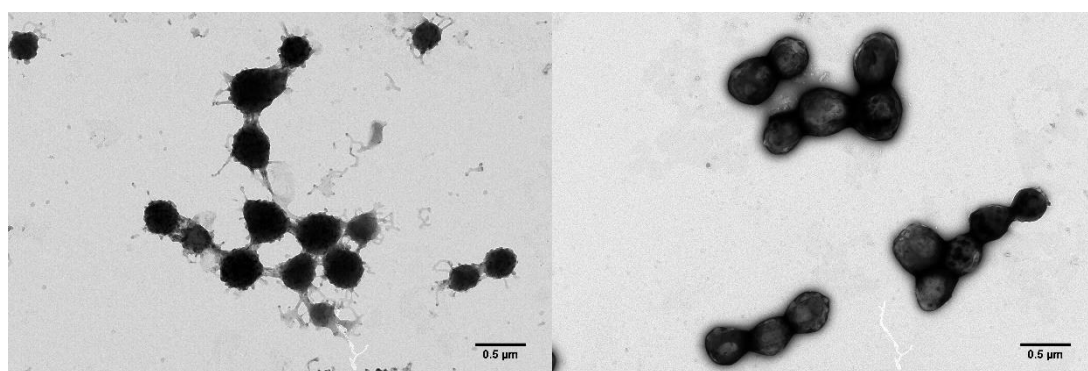


Figure 3.7. TEM images obtained for PMMA-DPE latexes synthesized at pH 8 (left) and pH 2 (right).

3.3.2. *Extension of PMMA and PMMA-DPE with varying concentrations of APS initiator*

As discussed in the Introduction to this Thesis, the DPE mechanism of formation of diblock copolymer is unknown. For extension to occur, the uncapping or breaking of the polymer

backbone containing the DPE unit is the most obvious mechanism by which chain extension could arise. Whether this extension can occur without the addition of a secondary charge of initiator has been discussed in the literature.^{18, 22}

Another explanation is the use of thermally self-initiating monomers such as St. A considerable number of studies use St as a second monomer but do not appear to take this into account.^{14, 17, 21} To attempt to determine which of these scenarios is correct and whether the use of a self-initiating monomer is essential, St will be used as the second monomer in initial experiments, and be replaced with BzMA in later experiments. For initial experiments additional initiator was added with the second monomer addition.

The reaction time required to reach full conversion, as determined by the solids content, was around 3 hours for the synthesis of PMMA-DPE precursor. Consequently, the reaction mixture was heated for 4 h, to ensure residual MMA was as low as possible. At this point, water was added to the reaction, to maintain the overall solids content of the latex below 15 wt%, and 15 minutes was allowed to re-equilibrate to reaction temperature. This protocol was then repeated for the addition of St, before addition of APS initiator. The amount of APS was varied to monitor the effect of initiator concentration on the St polymerization. The amount of additional APS was either 0.5 or 0.1 equivalents of the APS used for the synthesis of PMMA-DPE, or no initiator. These were three separate reactions using three different PMMA-DPE precursors. The molecular weight distributions determined by SEC are shown in Figure 3.8. It is clear that each polymerization still contains a significant amount of PMMA-DPE precursor. The molecular weight of the species formed in this second-stage polymerization increased as the amount of initiator was reduced, as expected for a free-radical polymerization. The St polymerization reached full conversion within 30 minutes when further APS is added, and within 1 hour with no additional APS. Given the large amount of initiator needed to form the PMMA-DPE precursor, it is likely that a significant amount of residual initiator remains at the start of the second-stage polymerization. It is possible that this excess initiator may homopolymerize the St in preference to reinitiating the PMMA-DPE precursor. Thus, it was decided to reduce the overall amount of initiator in the polymerization in order to increase the proportion of reinitiated precursor.

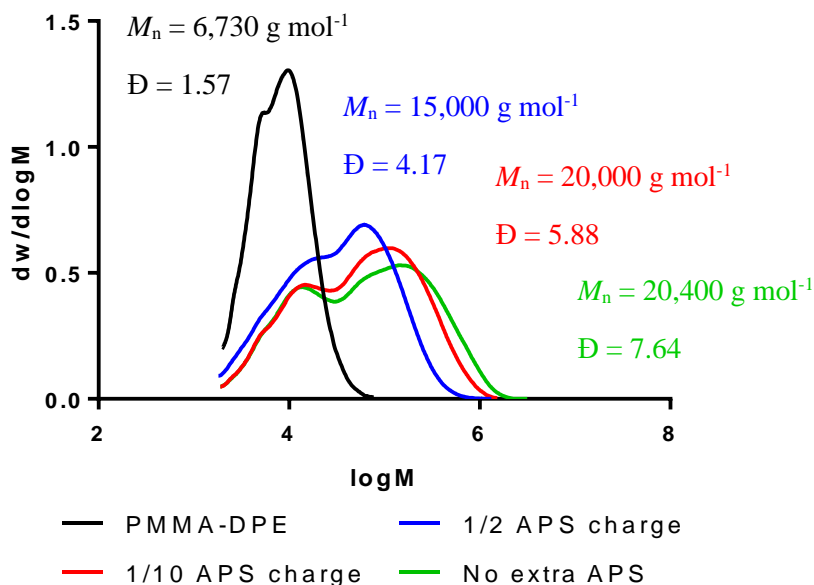


Figure 3.8. Molecular weight distributions recorded for the PMMA-DPE precursor and final PMMA-DPE-PSSt synthesized with varying amounts of APS initiator added 4 h from the start of the polymerization of PMMA-DPE. SEC data obtained using the DMF eluent system (0.1 % LiBr) against PMMA standards at the University of Sheffield.

In order to reduce the amount of excess initiator in the system, and hopefully increase the chain extension efficiency of PMMA-DPE, the PMMA-DPE reaction mixture was heated for 24 hours, from this point forward. The half-life of persulfate initiator varies with both temperature and pH but at 90 °C it should be consumed almost entirely within this time frame.²⁴ In principle, purification of the precursor could have been achieved by precipitation to remove residual monomer, DPE and initiator, but this would have destabilized the latex. Dialysis may also have removed residual APS and MMA but this purification method is too slow to be convenient.

For these polymerizations, the amount of initiator added was 0.5 and 0.1 equivalents of that used to form the PMMA-DPE precursor. Both polymerizations reached full conversion within 30 minutes, with the final MWDs shown in Figure 3.9. Again, there is a large amount of unreacted precursor, with the lower initiator concentration yielding the higher molecular weight diblock copolymer (or polystyrene homopolymer). The amount of mCTA consumed also appears not to change. It is impossible to discern from these MWDs if the precursor is being chain-extended or not. Previous publications use an extra aliquot of initiator in stage 2 bulk and solution polymerizations but did not show a clear increase in molecular weight with consumption of precursor.¹²

Addition of initiator, while needed for certain RDRP such as RAFT polymerizations, could cause considerable formation of polystyrene homopolymer. At this point, it was decided that the DPE method would be better investigated if no initiator was added for the second-stage polymerization. This would help to determine if the PMMA-DPE plays any role in the St polymerization and whether the addition of initiator is actually necessary when using a thermally self-initiating monomer.

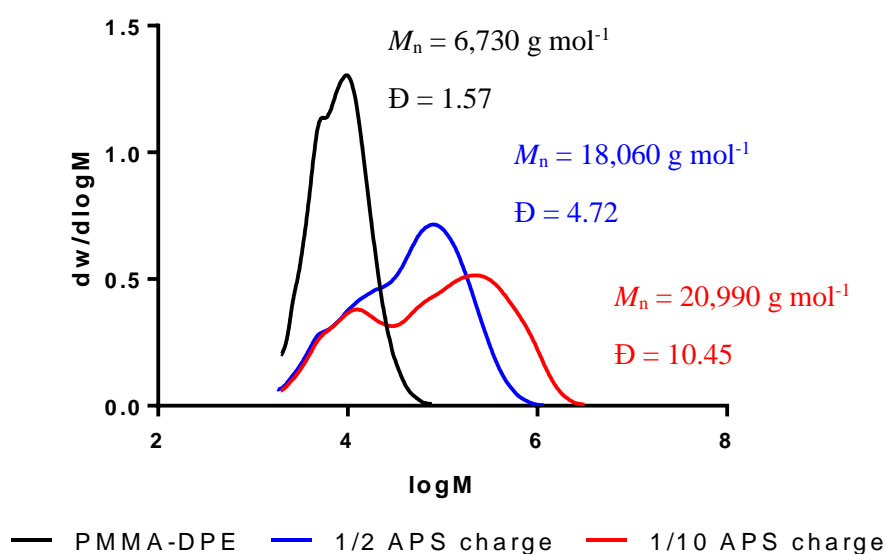


Figure 3.9. Molecular weight distributions obtained PMMA-DPE precursor and PMMA-DPE-PSt synthesized with varying amounts of APS initiator added 24 h after the synthesis of PMMA-DPE. SEC data obtained using the DMF eluent system at the University of Sheffield.

3.3.3. Extension of PMMA and PMMA-DPE with St without additional initiator

Earlier publications suggest that the formation of diblocks from a DPE-containing precursor can be achieved without additional initiator.^{18,22} However, because St thermally self-initiates, this could lead to the formation of molecular weight polystyrene homopolymer without reactivation of the PMMA-DPE precursor.

To investigate the effect of DPE in this polymerization two precursors were prepared in the presence or absence of DPE, PMMA-DPE and PMMA respectively. While the PMMA precursor has a higher molecular weight, as shown in Chapter 2 of this thesis, it is unlikely that this difference alone would affect the second-stage polymerization. These precursors were synthesized by SFEP and heated for 24 h to remove residual APS initiator, as discussed previously. Water was added to keep the solids content of the following polymerization below 15% and St was added once the latex had again reached the reaction temperature. Final products after the polymerization of St in this section are referred to as PMMA-PSt and

PMMA-DPE-PSt, using precursors formed in the absence or presence of DPE, respectively. These products are not referred to as blocks throughout this body of work because it was initially unclear whether chain extension was successful or not.

3.3.3.1. Polymerization kinetics

Samples were taken from reaction mixtures at various time points. The solids contents were obtained using thermogravimetric analysis (TGA) and converted into conversions for the second monomer (Figure 3.10). The solids contents achieved for the two precursor polymerizations were comparable (PMMA = 14.8 wt%, PMMA-DPE = 15.0 wt%) and both were thought to have reached approximately 100 % conversion. The lowest solids content was taken to be 0 % conversion for both polymerizations with 100 % conversion being 7.5 wt% for this second polymerization owing to dilution with water (15 wt% with both monomers at 100 % conversion). For the PMMA-DPE precursor, the St conversion increased steadily for 6 hours before reaching a plateau at around 8 hours. For the PMMA precursor, there was little change in conversion over the first 6 h, but after 8 h the conversion did increase slightly. The polymerization rates for reactions containing PMMA-DPE and PMMA vary significantly. The PMMA should not take part in the St polymerization in any meaningful way so these observations support the hypothesis that the PMMA-DPE is being reactivated in some way. This could lead to a faster rate of consumption of the monomer and possibly chain extension. However, Viala *et al.*¹² published results showing a decrease in polymerization rate when PMMA-DPE was added to the solution polymerization of St with additional AIBN. This could be due to the additional initiator consuming the St rather than reactivating the precursor. No other publications found on stage 2 of the DPE method showed any conversion data.

After 24 h, the St conversions of the two polymerizations are comparable. This is likely to correspond to 100 % monomer conversion, with perhaps some St escaping from the reactor (which had to remain unsealed for safety reasons). This is likely due to self-initiation of the St consuming all the monomer in the polymerization containing PMMA, but at a lower rate compared to PMMA-DPE. Any remaining DPE within the PMMA-DPE precursor system that could cap this polystyrene homopolymer being formed should reduce this rate, as seen in the formation of precursor, but the opposite effect was observed. These data suggest that the PMMA-DPE precursor generates radical species or perhaps is reactivated by St radicals, thus monomer is consumed at a faster rate.

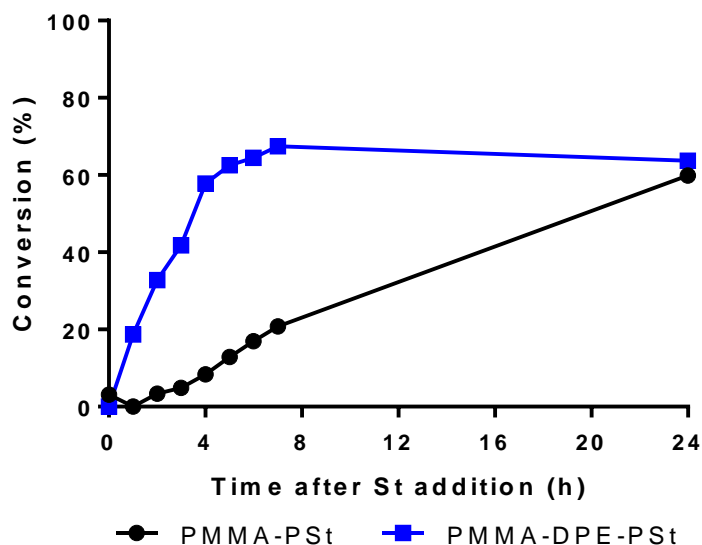


Figure 3.10. Conversion vs time plots, obtained from gravimetric analysis data, for the chain extension of PMMA and PMMA-DPE precursors with St at 90 °C.

3.3.3.2. MWDs of PMMA and PMMA-DPE precursor chain extension with St without initiator addition

When St was added to the PMMA precursor, a high molecular weight shoulder appeared on the MWD (Figure 3.11). Under these conditions, this feature is likely to be PSt homopolymer, as the PMMA “precursor” should not be able to chain-extend to form diblock copolymers. This confirms that the polymerization of St occurs even in the absence of further APS initiator. This molecular weight is higher than that of the PMMA and as a result could give the mistaken impression that chain extension has been achieved. This is problematic for the chain extension of PMMA-DPE, as the homopolymerization of St could also to occur in such polymerizations. This observation will be taken into account in the following discussion but had not been previously confirmed or referred to in literature.

The MWD recorded after the attempted chain extension of PMMA-DPE with St after heating 24 hours at 90 °C can be seen in Figure 3.12. The original molecular weight attributed to the PMMA-DPE precursor is discernible in the SEC trace recorded for the PMMA-DPE-PSt. Although, residual APS is no longer present after 24 h at 90 °C, chain extension of the precursor is not significantly improved. The molecular weights of the polymer products overlap and do not give the clean chain extension observed for other forms of RDRP, which show a linear evolution in molecular weight for all polymer chains with increasing conversion.

This was also seen in several other publications on stage 2 of the DPE method,^{3, 8, 18} this tells us that clean and 100 % extension of DPE containing precursor is not easily achievable.

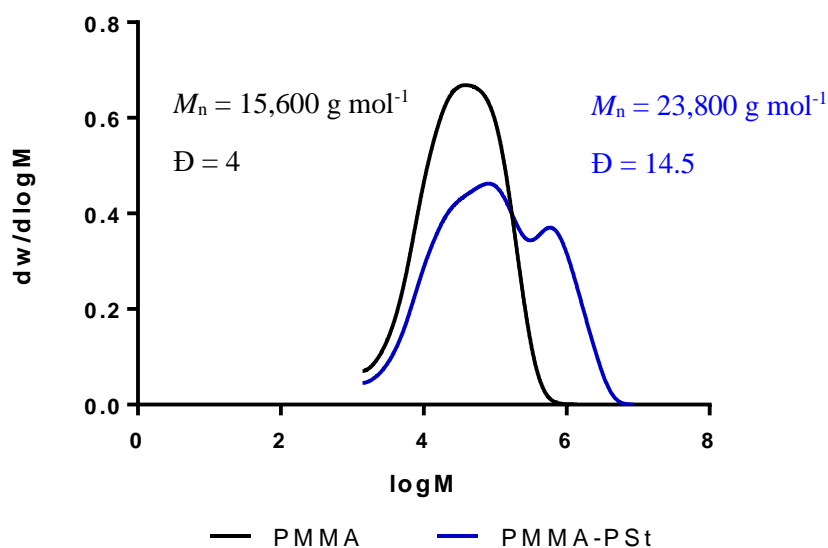


Figure 3.11. MWDs for PMMA synthesized in the absence of DPE and the resulting copolymer mixtures of PMMA and PSt (PMMA-PS t) when St is added to the polymerization after 24 hours at 90 °C. Data obtained by SEC in THF against PSt standards at BASF.

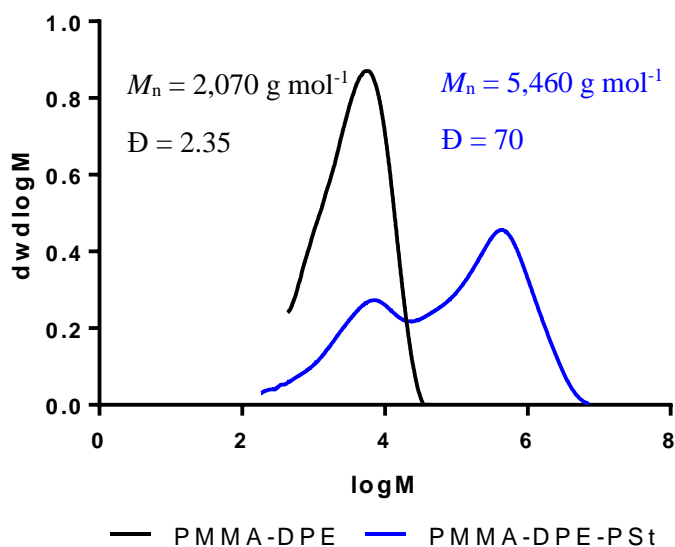


Figure 3.12. MWDs recorded for PMMA-DPE and the resulting polymeric species (PMMA-DPE-PS t) when St is added after 24 h of heating the precursor at 90 °C to destroy excess initiator. Data obtained by SEC in THF against PSt standards at BASF.

The MWD of the PMMA-DPE-PS t product obtained after 24 h at 90 °C to destroy excess initiator was monitored by SEC over the course of the reaction at various time points (Figure 3.13, a summary of M_n and Đ values are displayed in Table 3-1). The proportion of precursor

decreases relative to the amount of higher molecular weight polymer over the course of the polymerization. This does not necessarily mean that the precursor is being consumed or extended in this reaction, but the amount of higher molecular weight polymer certainly increases over time. Interestingly, the molecular weight of this second-stage polymer also increases with reaction time. This suggests chain extension, as the molecular weight of any free PSt homopolymer should not increase with monomer conversion. It is worth noting, however that any residual DPE within the reaction mixture, which was shown to be present within the latex in Chapter 2, could during cap the growing PSt chains. As DPE is consumed during the second-stage polymerization, these polymer chains would increase the overall molecular weight. While the relative precursor concentration decreases during the polymerization, it does not completely disappear. This could be simply due to insufficient reaction time (or second monomer) for the precursor to be fully consumed. An alternative explanation is that these are simply “dead chains” of PMMA that are incapable of extension.

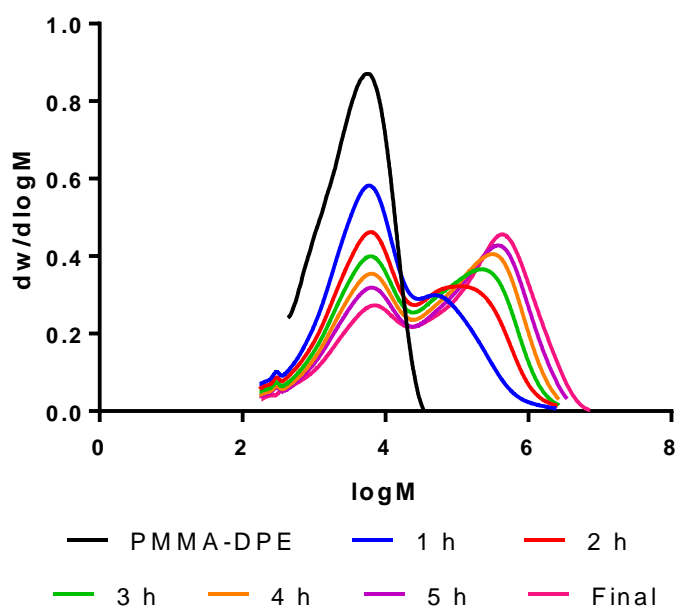


Figure 3.13. Molecular weight distributions obtained for PMMA-DPE and time points for the formation of PMMA-DPE-PSt. Determined by SEC in DMF (0.1 % LiBr) against PMMA standards at the University of Sheffield.

Table 3-1. Summary of $M_{n,SEC}$ and \bar{D} values, obtained by SEC in DMF (0.1 % LiBr) against PMMA standards at the University of Sheffield, for the MWDs shown in Figure 3.13.

Sample	$M_{n,SEC}$ (g mol ⁻¹)	\bar{D}
PMMA-DPE	2,070	2.35
1 h	2,660	20
2 h	3,200	33
3 h	3,740	40
4 h	4,270	47
5 h	4,680	58
Final	5,460	70

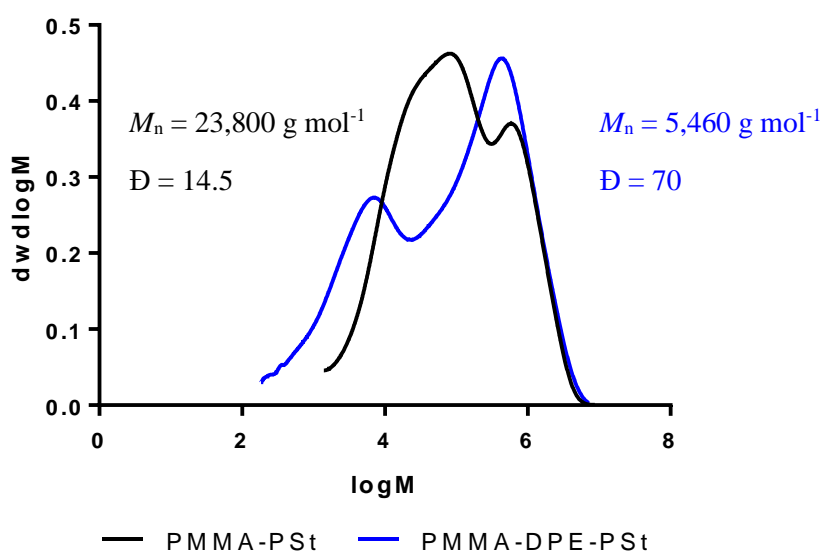


Figure 3.14. MWDs obtained for PMMA-PSt and PMMA-DPE-PSt. Data obtained by SEC in THF against PSt standards at BASF.

Figure 3.14 shows the overlaid MWDs of the final products formed in the presence and absence of DPE, PMMA-DPE-PSt and PMMA-PSt, respectively. It is worth noting that the higher molecular weight polymers formed in stage two of these polymerizations are comparable in molecular weight. This could be simply coincidental or both MWDs could be the result of PSt homopolymer formation indicating that the PMMA-DPE does not control the growth of all chains. This does not mean that chain extension is not taking place but may indicate that it is not the only type of polymerization occurring in such syntheses.

In an attempt to prove the presence of diblock copolymers for the PMMA-DPE polymerizations, the PSt homopolymer was removed from the reaction mixtures. This was achieved by dissolving the polymer product in tetrahydrofuran (THF) and precipitating it into excess hot cyclohexane. Hot cyclohexane is a solvent for PSt homopolymer but should not dissolve PMMA or PMMA-*b*-PSt. However, when the insoluble and soluble fractions were

examined by ^1H NMR spectroscopy there was little or no difference in the spectra obtained. As a result, the MWDs of the two fractions were examined by SEC.

The MWDs of the soluble and insoluble fractions and the original sample can be seen in Figure 3.15. The MWD of the soluble fraction, which is theoretically just PSt homopolymer, is very similar to that of the original sample. This indicates that the MWD is dominated by PSt homopolymer, with other products contributing less to the overall MWD by refractive index (RI) detection. Interestingly, the cyclohexane-insoluble fraction contained considerably more precursor (as expected) but also contains some of the second-stage polymer. This could be because PSt homopolymer is not efficiently removed by precipitation, or because PMMA-*b*-PSt is formed in the reaction in the absence of any DPE. There is no obvious reason why this should occur but the cyclohexane-soluble fraction appears to contain polymer that has the same molecular weight as the precursor.

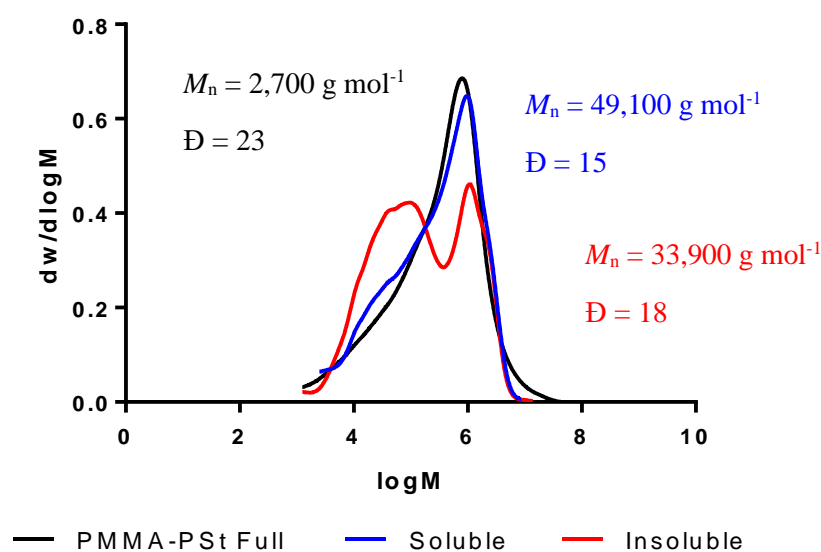


Figure 3.15. MWDs obtained for PMMA-PSt before and after its precipitation into excess hot cyclohexane. Determined by SEC in DMF (0.1 % LiBr) against PMMA standards at the University of Sheffield.

The MWDs obtained for PMMA-DPE-PSt and the two cyclohexane fractions can be seen in Figure 3.16. The cyclohexane-soluble fraction has a similar MWD to that of PMMA-PSt. Also, the relative amount of second-stage polymer is greater than that in the St polymerizations not containing DPE. The cyclohexane-insoluble fraction contains a lower molecular weight shoulder, as does the MWD of PMMA-DPE-St. This suggests that during shipping process from BASF to the University of Sheffield these samples somehow reacted. Thus, the results are ambiguous.

The same separation method was used by Viala *et al.*¹² to examine the block copolymer yield of the extension of PMMA-DPE latex with St and was determined to be > 90 %. In order for the DPE method to be competitive with other forms of RDRP for the synthesis of block copolymers in industry this is a characteristic that must be investigated further.

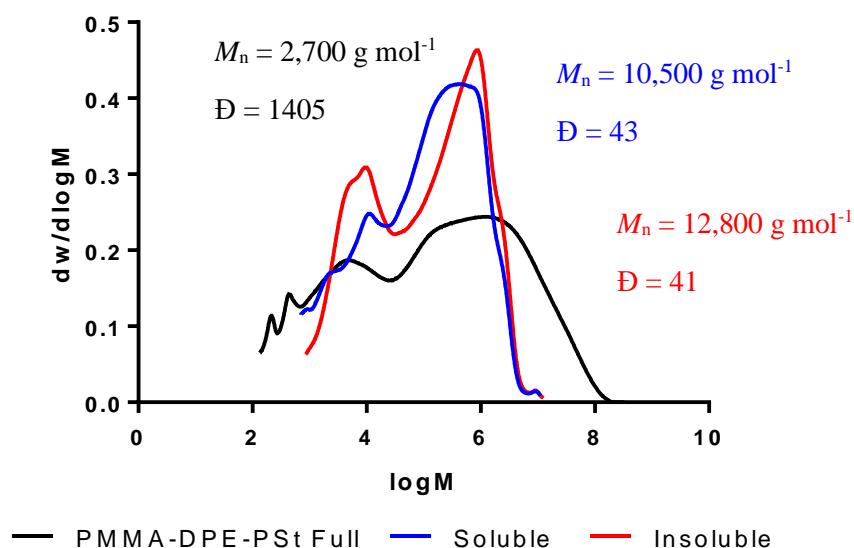


Figure 3.16. MWDs recorded for PMMA-DPE-PSt before purification by precipitation, and the soluble and insoluble fractions in hot cyclohexane. Determined by SEC in DMF (0.1 % LiBr) against PMMA standards at the University of Sheffield.

3.3.3.3. Particle size distributions and imaging of the precursor extension with St

PMMA-PSt is formed in the absence of DPE. PMMA latex was formed, with the latex being heated at 90 °C for 24 h to destroy residual initiator before St was added. Hydrodynamic chromatography (HDC) was used at BASF to examine the particle size distribution (PSD) of PMMA and PMMA-DPE latexes and the products formed when St was polymerized in their presence. However, this method, like dynamic light scattering (see Chapter 2), gave irreproducible results (Supplementary Figures 6.1, 6.2, 6.3) and so the samples were examined by transmission electron microscopy (TEM) at the University of Sheffield.

Figure 3.17 shows micrographs obtained by TEM and the corresponding size histograms determined using ImageJ for PMMA-DPE, PMMA-DPE-PSt and PMMA-PSt. As mentioned previously (Chapter 2), the micrographs for PMMA-DPE appear to show two particle populations. But the smaller particles appear to be coating the larger PSD and could have led to problems with analysing the overall PSD by DLS or HDC. When St is polymerised in the presence of this latex, the result is an increase in mean particle size and polydispersity for both populations, with smaller particles no longer attached to the outside of the larger particles.

They could also be smaller particles of PMMA-DPE that have become swollen with St prior to its polymerization, forming a PSt shell. The micrographs obtained for PMMA-PSt latexes show that, while the larger particles are still dominant, a secondary population of particles was also formed that are likely to be PSt homopolymer. This is not entirely unexpected. But, as mentioned in previous chapters, the formation of a bimodal particle distribution may not just be not problematic but also beneficial in the formulation of coatings.

It is hard to draw comparisons with literature for these PSDs as this is the first instance of surfactant-free polymerization using stage 2 of the DPE method. Other conventional emulsion polymerizations report both an increase in particle size and/or the formation of a bimodal distribution.^{17, 18} This is again likely to be caused by the formation of homo-PSt particles but as these systems were not bimodal prior to extension, unlike the ones seen in this work, these particles could not be caused by the swelling of smaller particles with St.

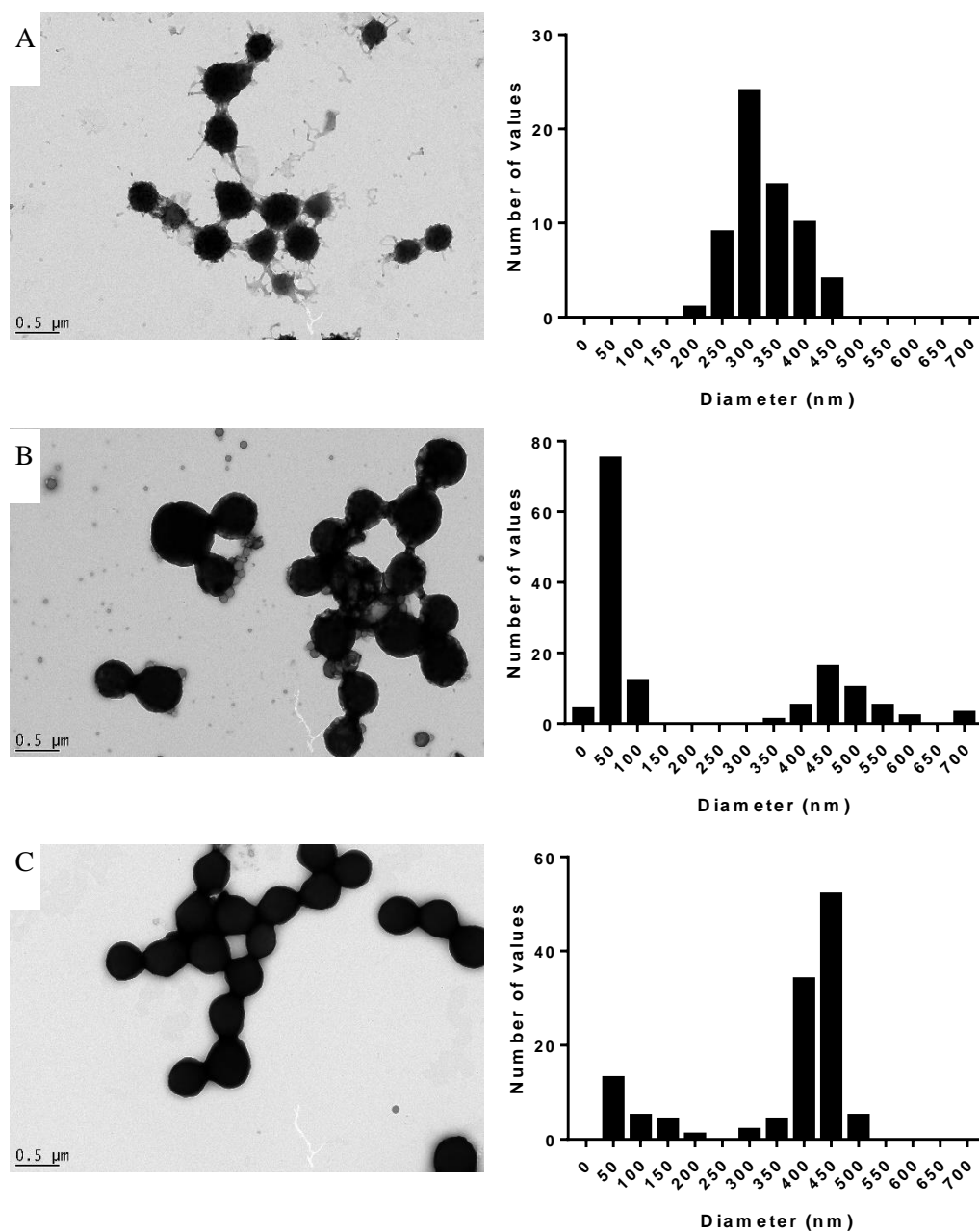


Figure 3.17. TEM micrographs and histograms of PSD of (A) PMMA-DPE, (B) PMMA-DPE-PSt, and (C) PMMA-PSt latexes.

3.3.4. Extension of PMMA-DPE with benzyl methacrylate

Extension of PMMA precursors formed in the absence and presence of DPE was also attempted with benzyl methacrylate (BzMA). In comparison to the extension using St, this monomer should not thermally self-initiate. This should minimize side-reactions not involving the precursor polymer and hence suppress homopolymer formation. However, it is considerably harder to remove any PBzMA homopolymer. Because of this problem, a control experiment using the PMMA precursor formed in the absence of DPE for the polymerization

of BzMA was also carried out. The use of benzyl methacrylate with the DPE method is only reported as an aside in a publication by Viala *et al.*¹² in reference to research undertaken as part of the author's PhD Thesis. However, no data is given in the publication, with the conclusion from that volume of work being that BzMA could not chain extend due to the inability of the monomer to self-initiate. This was not seen with St or MMA. Therefore, this work is the first instance of the use of BzMA with the DPE method that we can access.

3.3.4.1. Conversion by solids contents of the extension with BzMA

Conversion vs. time curves calculated from solids contents are shown in Figure 3.18. The lowest solids contents for the polymerizations were taken as 0 % conversion with a maximum expected increase of 7.5 wt% (half of the expected 15 wt% total) on these values indicating 100 % conversion. The conversion for the BzMA polymerization containing the PMMA-DPE precursor increased over 6 h. At this point, the conversion appears to decrease slightly at 8 h but the final conversion reaches 100 % after 48 h. This indicates a polymerization is taking place to high conversion without addition of any further initiator. When BzMA was added to the PMMA precursor formed in the absence of DPE there was very little conversion, if any, for the first 8 hours. However, there was a slight increase 24 h after BzMA addition, with the conversion reaching just 20 %. This indicates that the PMMA-DPE precursor is capable of forming radicals that enable the polymerization of BzMA. This is in direct contrast to the unreported findings of Viala *et al.*¹² discussed above. As both polymerizations were performed without additional initiator for stage two there is no clear reason why one reaction should be more successful than the other. Due to the lack of data presented in the publication it is difficult to draw further conclusions.

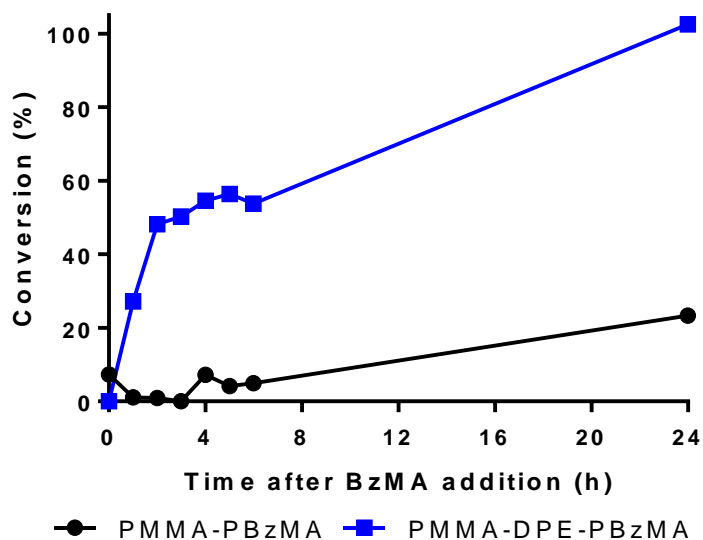


Figure 3.18. Conversion vs time, obtained by gravimetric analysis, of PMMA and PMMA-DPE precursor extension with BzMA.

3.3.4.2. SEC analysis of the stage two polymerization of BzMA

Molecular weight distributions obtained for PMMA and PMMA-PBzMA can be seen in Figure 3.19. The MWD of PMMA synthesised in the absence of DPE overlaps closely with the MWD observed for PMMA-PBzMA. Figure 3.18 shows that only 20 % of the BzMA had been polymerized, and this MWD indicates that the PBzMA homopolymer has a similar molecular weight to that of the PMMA precursor. While extension of the PMMA was not expected, this distribution indicates that no extension of the PMMA occurred. This important point was much less obvious for the polymerizations conducted with St as the second monomer.

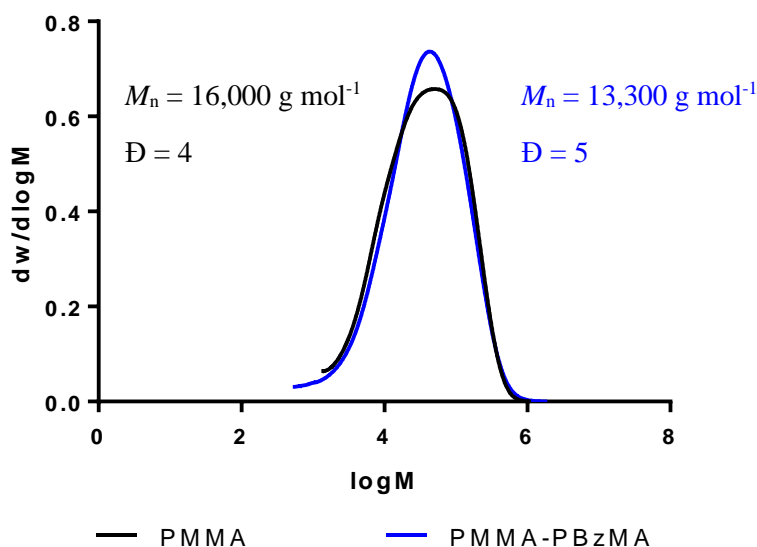


Figure 3.19. MWDs obtained for PMMA and PMMA-PBzMA synthesized in the absence of DPE. Data obtained by SEC in THF against PSt standards at BASF.

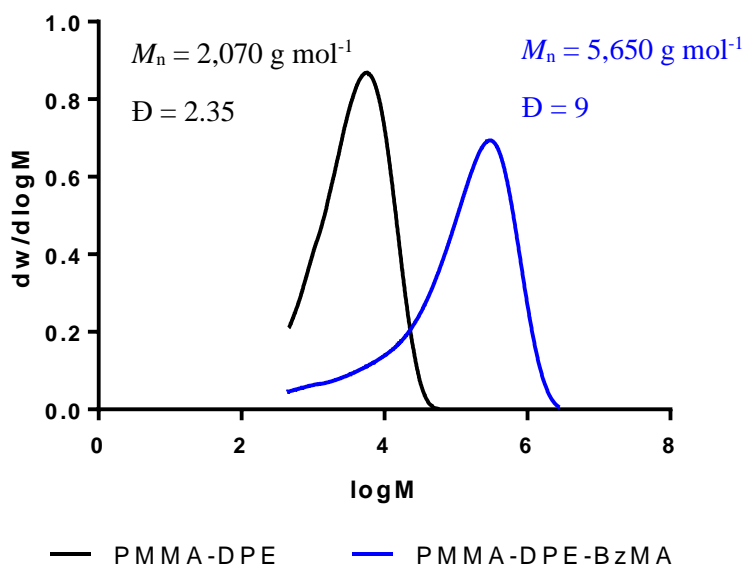


Figure 3.20. MWDs obtained for PMMA-DPE and PMMA-DPE-PBzMA analysed at BASF using a THF eluent system. Values obtained against PSt Standards.

When PMMA was synthesized in the presence of DPE, the MWD changes significantly when BzMA is added to the polymerization after 24 h (Figure 3.20). It appears that the PMMA-DPE precursor is consumed in the second-stage polymerization and is almost replaced with a higher molecular weight polymer. This suggests that the reactivation and consumption of PMMA-DPE is feasible without a second charge of initiator. Therefore, the possible mechanism of the DPE method is shown in Figure 3.2, where the DPE capping is reversible and reactivates the

polymer radical. However, it is not clear whether the DPE molecule is removed from the polymer and this was investigated further using ^1H NMR spectroscopy. NMR spectroscopy was chosen as using SEC with UV detection would be unsuitable due to the presence of the aromatic ring of BzMA, which would make detection of the DPE group impossible.

When St was added to PMMA-DPE, the molecular weight of the resulting polymer increased over time (Figure 3.13). This was not observed when BzMA was added to PMMA-DPE (Figure 3.21, M_n and \bar{D} values are given in Table 3-2). In these polymerizations, the molecular weight of the second polymer remained approximately constant but the relative size of the small and large molecular weight peaks changed during the polymerization. As mentioned previously, the molecular weight increases linearly with conversion for RAFT polymerizations. This was not observed here, which indicates that the BzMA polymerization is not a controlled polymerization.

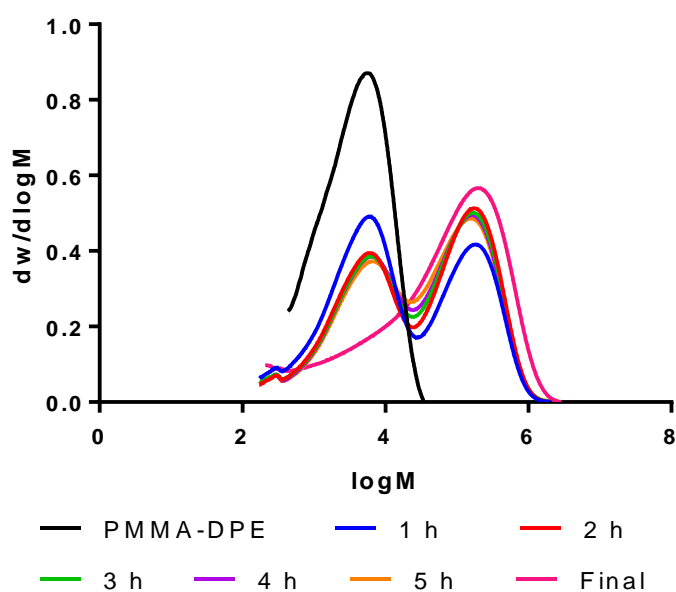


Figure 3.21. Molecular weight distributions obtained for PMMA-DPE and time gap points taken after addition of BzMA during formation of PMMA-DPE-PBzMA. Obtained using a DMF SEC system (0.1 % LiBr).

Table 3-2. $M_{n,SEC}$ and \bar{D} values for the MWDs in Figure 3.21. Obtained by SEC in DMF (0.1 % LiBr) against PMMA standards at the University of Sheffield.

Sample	$M_{n,SEC}$ (g mol^{-1})	\bar{D}
PMMA-DPE	2,070	2.35
1 h	3,070	30
2 h	3,920	29
3 h	3,880	28
4 h	4,000	27
5 h	4,060	26
Final	5,650	9

After these samples were shipped to the University of Sheffield, they were reanalysed by DMF and THF SEC (Figure 3.22). When examined by DMF SEC, another shoulder can be seen in the MWD of PMMA-DPE and the precursor is not fully consumed in the MWD of PMMA-DPE-PBzMA. In contrast, the PMMA-DPE MWD recorded by THF SEC has changed drastically after shipping, with only a small shoulder for a species that has a similar molecular weight to that of the precursor in PMMA-DPE-PBzMA. It is unclear whether these new features were formed in transit from residual active species and residual monomer, or if they are the result of the different conditions of the SEC instruments. But these changes may affect the data that follows, which was obtained after shipping the samples to the UK. This may also be problematic for the long-term storage of these polymers and their industrial use.

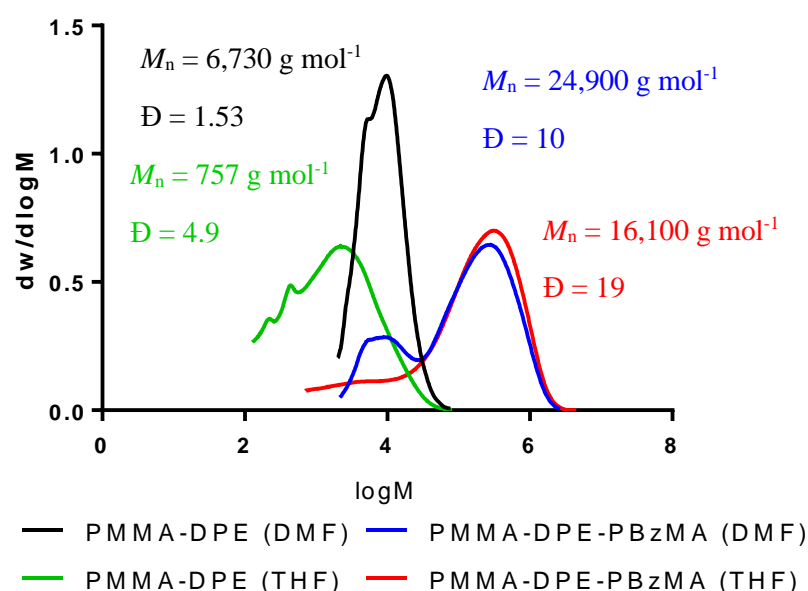


Figure 3.22. MWDs obtained for PMMA-DPE and PMMA-DPE-PBzMA after being shipped to the University of Sheffield. Samples were run on THF and DMF (0.1 % LiBr) eluent SEC systems. M_n and \bar{D} values are against PSt and PMMA standards for THF and DMF system, respectively.

3.3.4.3. ^1H and Diffusion Ordered Spectroscopy (DOSY) NMR spectroscopy analysis of the polymerization of BzMA in the presence of PMMA and PMMA-DPE

The ^1H NMR spectra of PMMA-PBzMA and PMMA-DPE-PBzMA can be seen in Figure 3.23. The spectra contain the same resonances in different ratios. As expected from the lower conversion of BzMA in PMMA-PBzMA, the residual BzMA monomer in this spectrum is considerably higher compared to that in the PMMA-DPE-PBzMA spectrum. This is clear from inspecting signals at 6.15, 5.57 and 5.2 ppm, as well as with the multiplicity of resonances at 7.2 – 7.5 ppm assigned to the aromatic ring on the BzMA residues. Unfortunately, these aromatic signals make it impossible to monitor the presence of DPE in

either polymer product. In contrast, PBzMA signals are smaller in PMMA-PBzMA prepared without DPE, as indicated by the signals at 4.97, 0.97 and 0.81 ppm.

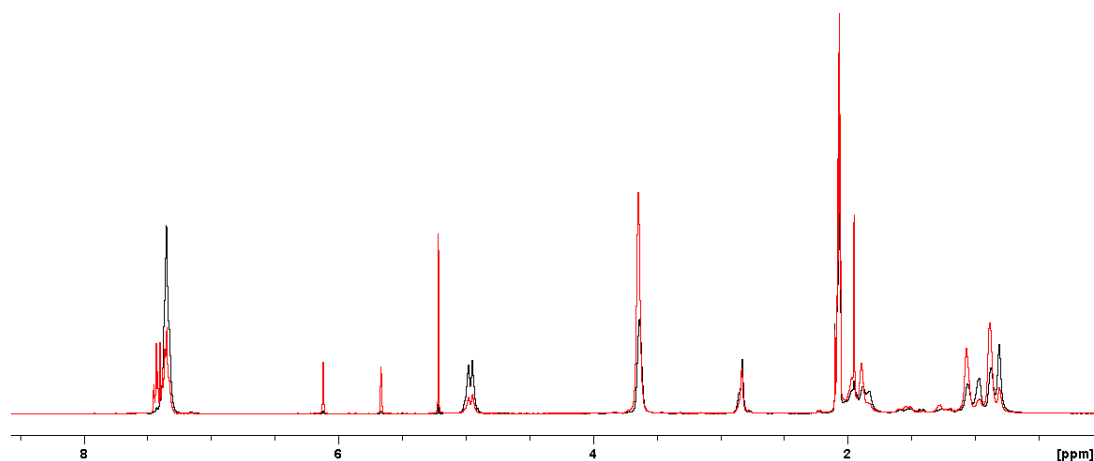


Figure 3.23. Overlaid ^1H NMR spectra for PMMA-PBzMA (red) and PMMA-DPE-PBzMA (black) recorded in deuterated acetone. Solvent signals for acetone and water are observed at 2.05 and 2.88 ppm, respectively.

Diffusion ordered spectroscopy (DOSY) NMR can be used to determine the diffusion coefficient of resonances within ^1H NMR spectra. The DOSY NMR spectrum for PMMA-PBzMA can be seen in Figure 3.24. Unfortunately, several PMMA and PBzMA signals overlap, so an average diffusion coefficient (D) is obtained for several resonances.²⁵ This increases the difficulty of obtaining accurate D values for each component of what is most likely a polymer mixture rather than diblock copolymer. Firstly, water (2.88 ppm) and acetone (2.05 ppm) signals are observed at $\log D$ values of -8.0. This is expected as these solvents should diffuse fast. The most negative D values are for resonances associated with PBzMA at 3.70 ppm and PMMA at 0.85 ppm. Again, this is expected as the polymers should diffuse more slowly. Remaining signals are assigned to BzMA resonances and overlapping PBzMA, PMMA and BzMA resonances. This produces an average value that is less than those of the other PMMA and PBzMA peaks.

The water and acetone signals also possess at lower $\log D$ values in the spectrum recorded for PMMA-DPE-PBzMA (Figure 3.25). Residual BzMA resonances are also observed in this spectrum at 5.22 ppm, with a $\log D$ value of 8.2. Again, this causes the elongation and averaging of polymer resonances that overlap with BzMA resonances at 7.4 and 3.6 ppm. Remaining signals with $\log D$ values below 8.5 can be attributed to both PMMA and PBzMA. Unfortunately, these data do not conclusively prove the formation of diblock copolymer chains but the similarities in $\log D$ values do provide supporting evidence for such species.

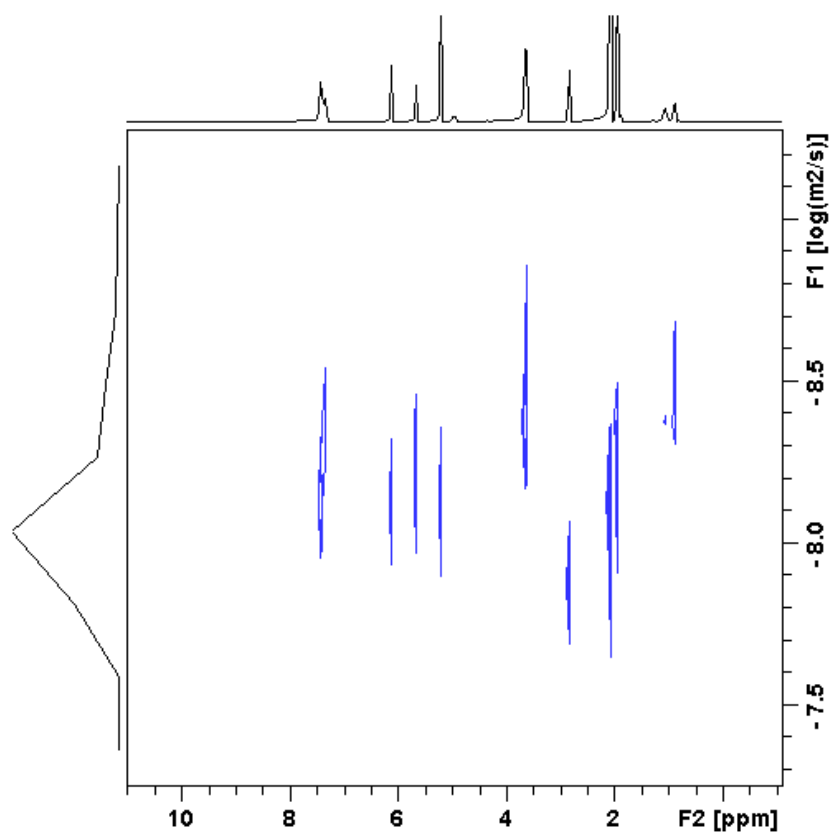


Figure 3.24. DOSY spectrum of PMMA-PBzMA in deuterated acetone.

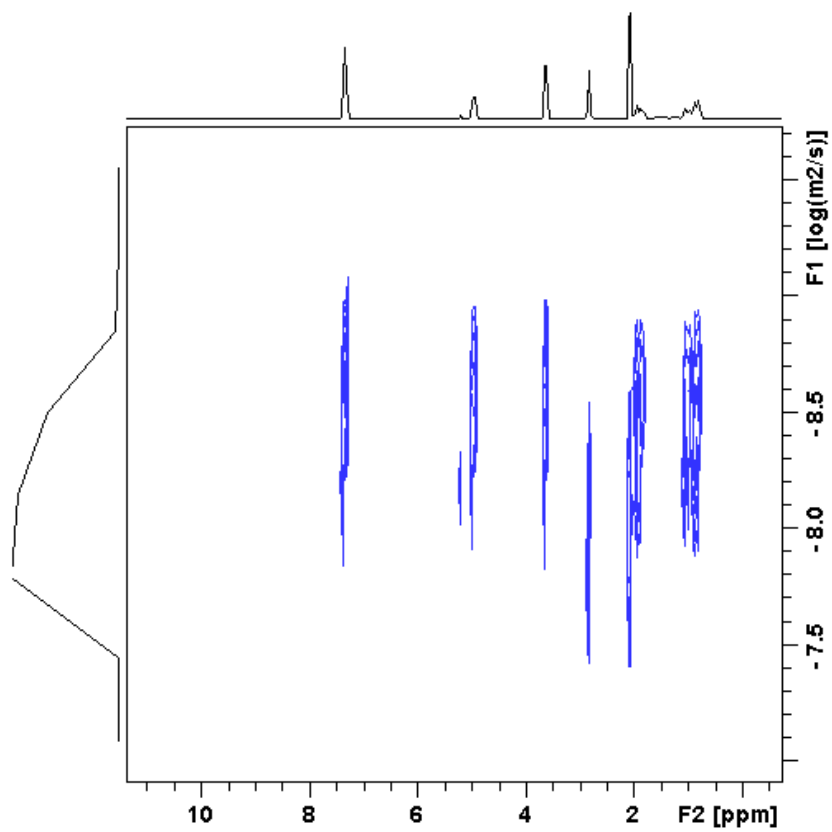


Figure 3.25. DOSY NMR spectrum of PMMA-DPE-PBzMA in deuterated acetone.

3.3.4.4. *Particle sizing and imaging after polymerization of BzMA*

Particle size distributions of PMMA and PMMA-PBzMA latexes obtained by HDC were again seen to not be reproducible (supplementary Figures 6.4, and 6.5). As a result, analysis of the resulting latexes at the University of Sheffield by TEM was used to investigate particle size distributions. TEM images of PBzMA-based latexes and the particle size histograms can be seen in Figure 3.26. PMMA-DPE is shown for comparison. After the second-stage polymerization, the particle size distribution has changed drastically. PMMA-PBzMA, like the PMMA-PSt shown previously, contains a secondary particle size distribution that most likely corresponds to PBzMA homopolymer.

Comparing PMMA-DPE to PMMA-DPE-PBzMA, the larger particles increase from 330 ± 57 nm to 493 ± 74 nm. This indicates swelling of the original latex with BzMA and its subsequent polymerization within or around these particles. In addition, a considerable number of smaller particles (45 ± 12 nm) are formed during this polymerization. This is surprising, as the chain extension indicated by SEC appears clean and does not suggest any PBzMA homopolymer formation. This could also be additional polymer formed during shipping to the University of Sheffield but these smaller particles were not detected at BASF by HDC. Overall, the PSD of these latexes is broadened and the mean particle diameter increased by this BzMA polymerization, suggesting secondary nucleation.

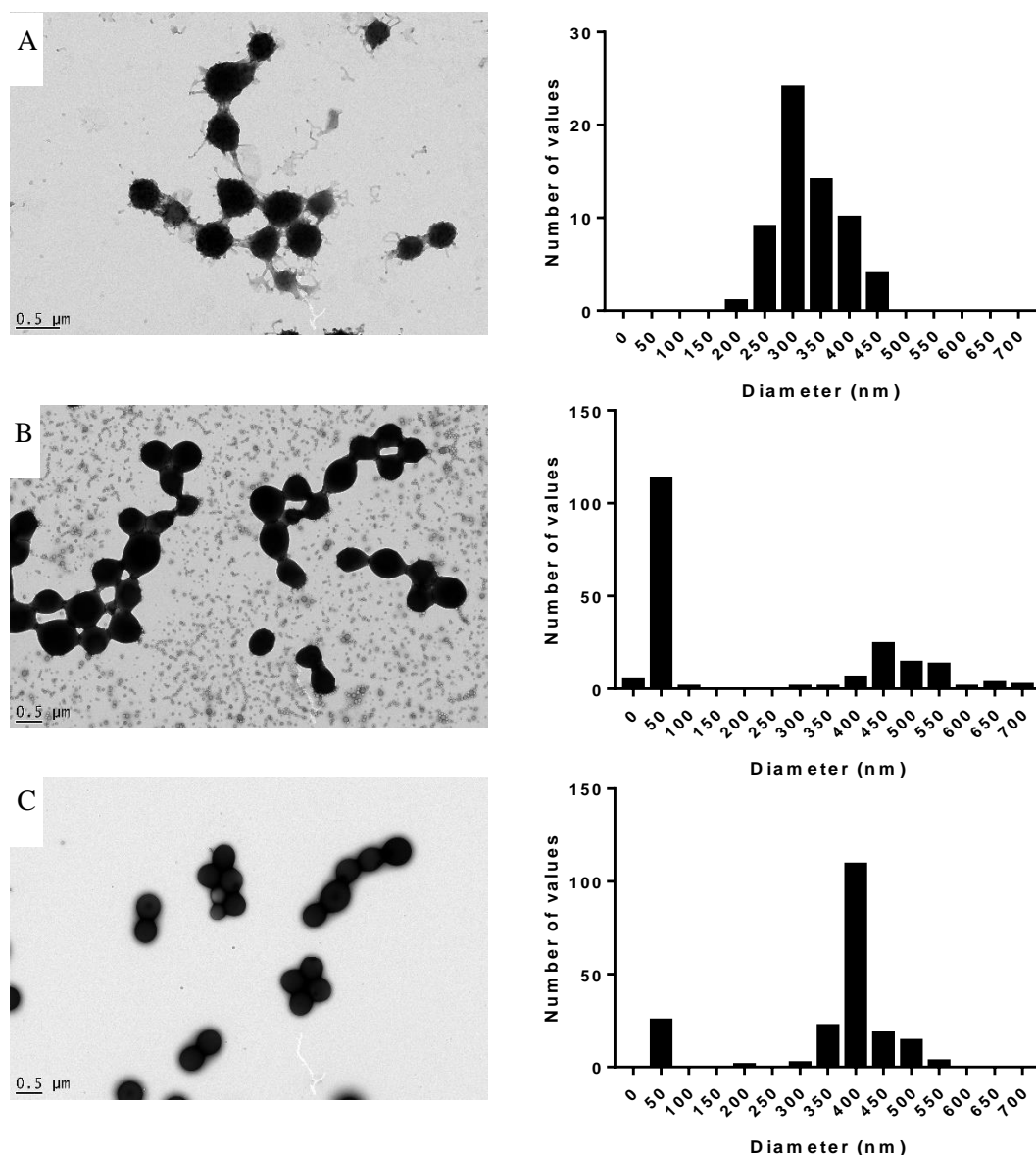


Figure 3.26. TEM images and particle size histograms for (A) PMMA-DPE, (B) PMMA-DPE-PBzMA, and (C) PMMA-PBzMA latexes.

3.4. Conclusions

Synthesis of PMMA-DPE conducted at pH 8 gave a more stable latex with less coagulum compared to syntheses performed at pH 2. The pH change did not seem to affect the DPE mechanism. Thus, all subsequent polymerizations in this Chapter were carried out at pH 8.

Chain extension of PMMA synthesised in the presence or absence of DPE was attempted by St polymerization. When APS initiator was added either after full MMA conversion (within 4 h) or after all the initial initiator charge was consumed (within 24 h), the MWD broadened significantly but there was no real evidence for chain extension to form a PMMA-PSt diblock

copolymer. To better understand the mechanism, and hopefully increase the proportion of diblock copolymer formed, polymerizations were also attempted without additional initiator. This produced MWDs a higher molecular weight component. The separation of PMMA-PSt and PMMA from PSt homopolymer was attempted using hot cyclohexane as a precipitant. However, this fractionation gave conflicting results to that expected and puzzling data. Owing to self-initiation of St, both PMMA-DPE and PMMA syntheses yielded PSt homopolymer. To determine whether PMMA-DPE could form reactive species without addition of further initiator, these reactions were also carried out using BzMA instead of St.

The protocol of heating PMMA-DPE for 24 h at 90 °C prior to addition of BzMA should mean that PMMA-DPE is the only source of radicals for the BzMA polymerization. The BzMA conversion is considerably lower when DPE is not added to the MMA polymerization for the precursor, with SEC showing very little change in MWD in the absence of DPE. In the presence of DPE, a higher molecular weight species is formed with a relative reduction in the PMMA-DPE precursor molecular weight. An increase in molecular weight for the polymer product suggests that PMMA-DPE can be used to generate PMMA radicals which can be extended to form PMMA-PBzMA diblock copolymers. In principle, this could be proven by DOSY NMR, but in practice overlapping signals meant that this technique was of rather limited utility.

This Chapter presents the first accessible data on the polymerization of BzMA in stage 1 or 2 of the DPE method. The conversion of BzMA was considerably higher in the presence of PMMA-DPE compared to that for PMMA. This indicates that the PMMA-DPE precursor could generate radicals so the BzMA polymerization could be conducted without any added initiator. SEC showed that any PBzMA formed in the presence of PMMA had the same molecular weight as that of the precursor. In contrast, PBzMA formed in the presence of PMMA-DPE had a higher molecular weight and this precursor appeared to be chain-extended. However, the polymer product did not increase in molecular weight with conversion, indicating that this second-stage polymerization was uncontrolled free radical polymerization. The polymers were examined by DOSY NMR but again the results proved inconclusive. TEM images show that the polymerization of BzMA in either system broadened the MWD and increased the mean particle diameter, with a second population of new particles being formed.

Unfortunately, the blocking efficiencies and \bar{D} values of the diblock copolymers is not comparable to those of RAFT polymerizations.²⁶ This requires further investigation but is a valid method of the production of diblock copolymers by the polymerization of BzMA in the presence of PMMA-DPE if the dispersity of the polymers is not an issue.

3.5. References

1. Raether, B.; Nuyken, O.; Wieland, P.; Bremser, W., Free-radical synthesis of block copolymers on an industrial scale. *Macromolecular Symposia* **2002**, *177*, 25-41.
2. Tasdelen, M. A.; Degirmenci, M.; Yagci, Y.; Nuyken, O., Block copolymers by using combined controlled radical and radical promoted cationic polymerization methods. *Polymer Bulletin* **2003**, *50* (3), 131-138.
3. Luo, Y. D.; Chou, I. C.; Chiu, W. Y.; Lee, C. F., Synthesis of PMMA-b-PBA Block Copolymer in Homogeneous and Miniemulsion Systems by DPE Controlled Radical Polymerization. *Journal of Polymer Science Part A-Polymer Chemistry* **2009**, *47* (17), 4435-4445.
4. Guo, F. G.; Zhang, Q. Y.; Zhang, B. L.; Zhang, H. P.; Zhang, L., Preparation and characterization of magnetic composite microspheres using a free radical polymerization system consisting of DPE. *Polymer* **2009**, *50* (8), 1887-1894.
5. Guo, F. G.; Zhang, Q. Y.; Zhang, H. P.; Zhang, B. L.; Gu, J. W., Controlled preparation of Fe₃O₄/P (St-MA) magnetic composite microspheres by DPE method. *Journal of Polymer Research* **2011**, *18* (4), 745-751.
6. Wieland, P. C.; Raether, B.; Nuyken, O., A new additive for controlled radical polymerization. *Macromolecular Rapid Communications* **2001**, *22* (9), 700-703.
7. Khuong, K. S.; Jones, W. H.; Pryor, W. A.; Houk, K. N., The mechanism of the self-initiated thermal polymerization of styrene. Theoretical solution of a classic problem. *Journal of the American Chemical Society* **2005**, *127* (4), 1265-1277.
8. Chen, D.; Fu, Z. F.; Shi, Y., Synthesis of amphiphilic diblock copolymers by DPE method. *Polymer Bulletin* **2008**, *60* (2-3), 259-269.
9. Lan, D.; Chen, D.; Fu, Z. F.; Shi, Y., Synthesis of amphiphilic diblock copolymers by direct radical polymerization of acrylic acid via DPE method. *Polymer Bulletin* **2011**, *66* (2), 175-185.
10. Chen, D.; Liu, R. X.; Fu, Z. F.; Shi, Y., Synthesis of poly(methyl methacrylate)-b-poly(acrylic acid) by DPE method. *E-Polymers* **2008**, *8*, 1-11.
11. Chen, D.; Shi, Y.; Fu, Z. F., Synthesis of Poly(vinyl acetate) Containing Diblock Copolymer by DPE Method. *Journal of Applied Polymer Science* **2009**, *111* (3), 1581-1587.
12. Viala, S.; Antonietti, M.; Tauer, K.; Bremser, W., Structural control in radical polymerization with 1,1 diphenylethylene: 2. Behavior of MMA-DPE copolymer in radical polymerization. *Polymer* **2003**, *44* (5), 1339-1351.
13. Chou, I. C.; Lee, C. F.; Chiu, W. Y., Preparation of Novel Suspensions of ZnO/Living Block Copolymer Latex Nanoparticles via Pickering Emulsion Polymerization and Their Long Term Stability. *Journal of Polymer Science Part A-Polymer Chemistry* **2011**, *49* (16), 3524-3535.
14. Wang, W. W.; Zhang, Q. Y., Synthesis of block copolymer poly (n-butyl acrylate)-b-polystyrene by DPE seeded emulsion polymerization with monodisperse latex particles and morphology of self-assembly film surface. *Journal of Colloid and Interface Science* **2012**, *374*, 54-60.
15. Wang, W. W.; Zhang, Q. Y.; Guo, F. F.; Gu, J. W.; Yin, C. J., Preparation of diblock copolymer PBA-b-PSt by DPE method in emulsion. *Journal of Polymer Research* **2011**, *18* (5), 1229-1235.
16. Zhao, M. J.; Shi, Y.; Fu, Z. F.; Yang, W. T., Preparation of PMMA-b-PSt Block Copolymer via Seeded Emulsion Polymerization in the Presence of 1,1-Diphenylethylene. *Macromolecular Reaction Engineering* **2014**, *8* (8), 555-563.
17. Wang, W. W.; Zhang, H. P.; Geng, W. C.; Gu, J. W.; Zhou, Y. Y.; Zhang, J. P.; Zhang, Q. Y., Synthesis of poly (methyl methacrylate)-b-polystyrene with high molecular weight by DPE seeded emulsion polymerization and its application in proton exchange membrane. *Journal of Colloid and Interface Science* **2013**, *406*, 154-164.

18. Wang, W. W.; Liu, M. J.; Gu, J. W.; Zhang, Q. Y.; Mays, J. W., Convenient synthesis and morphology of latex particles composed of poly (methyl methacrylate)-b-poly (n-butyl acrylate) by 1, 1-diphenylethylene (DPE) seeded emulsion polymerization. *Journal of Polymer Research* **2014**, *21* (8), 8.
19. Yuan, D.; Zhang, H., Nanosized palladium supported on diethylenetriamine modified superparamagnetic polymer composite microspheres: Synthesis, characterization and application as catalysts for the Suzuki reactions. *Applied Catalysis A-General* **2014**, *475*, 249-255.
20. Guo, F. G.; Zhang, Q. Y.; Wang, W. W.; Zhang, H. P.; Sun, J. L., Preparation of pH-responsive Fe₃O₄/Poly (acrylic acid-stat-methyl methacrylate-block-(2-dimethylamino) ethyl methacrylate) magnetic composite microspheres and its application in controlled release of drug. *Materials Science & Engineering C-Materials for Biological Applications* **2011**, *31* (5), 938-944.
21. Zhou, Y. Y.; Zhang, Q. Y.; Liu, Y. L.; Wang, W. W., Encapsulation and dispersion of carbon black by an in situ controlling radical polymerization of AA/BA/St with DPE as a control agent. *Colloid and Polymer Science* **2013**, *291* (10), 2399-2408.
22. Viala, S.; Tauer, K.; Antonietti, M.; Lacik, I.; Bremser, W., Structural control in radical polymerization with 1, 1-diphenylethylene. Part 3. Aqueous heterophase polymerization. *Polymer* **2005**, *46* (19), 7843-7854.
23. Bremser, W.; Raether, B., A method for controlled radical polymerization and for the synthesis of solvent free dispersions. *Progress in Organic Coatings* **2002**, *45* (2-3), 95-99.
24. <http://datasheets.scbt.com/sc-202946.pdf>.
25. Antalek, B.; Hewitt, J. M.; Windig, W.; Yacobucci, P. D.; Mourey, T.; Le, K., The use of PGSE NMR and DECRA for determining polymer composition. *Magnetic Resonance in Chemistry* **2002**, *40*, S60-S71.
26. Chong, Y. K.; Le, T. P. T.; Moad, G.; Rizzardo, E.; Thang, S. H., A more versatile route to block copolymers and other polymers of complex architecture by living radical polymerization: The RAFT process. *Macromolecules* **1999**, *32* (6), 2071-2074.

Chapter Four

4. The effect of RAFT agent solubility in the surfactant-free emulsion polymerization of methyl methacrylate

4.1. Introduction

Over the last 30 years controlled / living radical polymerization (CLRP) has been widely explored, with growing interest over time.¹ This has been due to the greater control over many aspects of the polymer product, such as molecular weight, dispersity and architecture.^{2,3} Novel copolymer architectures include diblock⁴ and triblock copolymers,⁵ star⁶ and comb polymers.³

CLRP has been recently reclassified as reversible-deactivation radical polymerization (RDRP). One of the major classes of RDRP is reversible addition-fragmentation chain-transfer (RAFT) polymerization. RAFT is very versatile and can be applied to a wide range of vinyl monomers under relatively mild conditions.⁷

Surfactant-free emulsion polymerization (SFEP) RAFT has been much less extensively researched than classical SFEP. Various parameters have been investigated in the search for robust SFEP formulations. These include the use of a macromolecular chain transfer agent (mCTA),⁸ seeded emulsion polymerization, a co-solvent and small molecule RAFT agents.⁹

The use of mCTAs is possibly the most popular solution to efficient surfactant-free RAFT polymerization. mCTAs can be prepared by RAFT solution polymerization in a suitable solvent before transferring into aqueous solution. An example of this was published by Ratcliffe *et al.*¹⁰, who formed a poly(glycerol monomethacrylate) mCTA in ethanol before conducting an emulsion / dispersion polymerization using a binary mixture of a water-miscible 2-hydroxyethyl methacrylate and water-immiscible 4-hydroxybutyl methacrylate.

A common method for successful emulsion polymerization is to add a small amount of a hydrophilic monomer.¹¹ However, when used with RAFT SFEP this approach did not produce a stable latex with St and sodium acrylate.¹² This problem could be avoided when these same monomers were copolymerized in the bulk to produce a mCTA first and then added to water until spontaneous phase inversion occurred. This seed could subsequently be chain-extended by the addition of a second monomer and initiator charge.

A suitable co-solvent can also be utilised for better results under aqueous conditions primarily. Thus, Gilbert *et al.*¹³ added DMF to the polymerization of methyl methacrylate to form a homogeneous phase from which the polymer precipitates, forming a latex. This is a dispersion polymerization but was conducted under surfactant-free conditions in aqueous media. Co-solvents were also used in conjunction with pre-formed seed particles formed by conventional emulsion polymerization to aid RAFT agent transport into the particles.¹⁴ However, the co-solvent must be removed before the second-stage polymerization.

This work will focus more specifically on small molecule RAFT agent use in SFEP. Many of the small molecule RAFT agents used in SFEP are themselves surfactants.^{15, 16} An example of this is the use of sur-iniferters, which act simultaneously as surfactant, initiator, transfer agent and terminator. The first instance of this was reported by Kwak *et al.*¹⁷ using 4-diethylthiocarbamoylsulfanylmethyl benzoic acid (DTBA, Figure 4.1) and UV radiation to initiate the reaction. The evolution of M_n vs monomer conversion was linear up to 60 % conversion whereupon the M_n decreased drastically. This study was later extended by Kim *et al.*¹⁸ who synthesised PMMA-*b*-PSt core-shell type particles under similar conditions.

Charleux *et al.*¹⁹ used the “surface-active RAFT agent” 2-(dodecylthiocarbonothioylthio)-2-methylpropanoic acid (TTCA, Figure 4.1). This RAFT agent contains a long hydrophobic aliphatic chain and a charged group to mimic a surfactant. However, the polymerization of St was completely inhibited due to R group radical exit from the micelle and the polymerization of n-BMA led to particle formation but was uncontrolled. When a small amount of St was added, the copolymerization was well controlled and produced a stable latex with mean particle sizes below 150 nm.

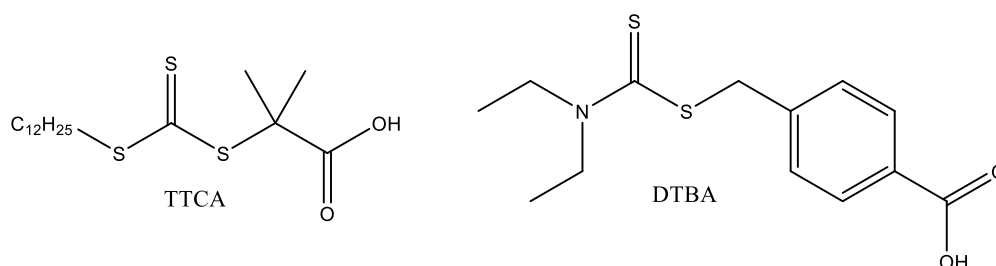


Figure 4.1. Small molecule RAFT agents.

Despite these advances, to the best of the authors knowledge small molecule RAFT agents have not been used successfully in SFEP syntheses without any of the above-mentioned adjustments.

In this research, RAFT solution polymerization of MMA was first carried out in the presence of 2-cyano-2-propyl benzodithioate (CPB), 4-cyano-4-(2-phenylethane sulfanylthiocarbonyl) sulfanylpentanoic acid (PETTC) or a morpholine-functionalised trithiocarbonate based PETTC derivative (MPETTC) (Figure 4.2). These scoping experiments confirmed that all three RAFT agents enabled good control over the polymerization of MMA. Once this was confirmed, SFEP RAFT syntheses were conducted at varying pH. The neutral RAFT agent (CPB) was shown to be ineffective under SFEP conditions, whereas PETTC and MPETTC could be used with some success provided that the solution pH was adjusted to ensure that the respective RAFT agent was charged. This caused each RAFT agent to become amphiphilic.

4.2. Experimental

4.2.1. Materials

Methyl methacrylate (MMA; 99 %, ≤ 30 ppm MEHQ), ammonium persulfate (APS, ≥ 98 %), 2-cyano-2-propyl benzodithioate (CPB; >97 %), 2,2'-azobis(2-methylpropionitrile) (AIBN; 98 %) triethanolamine ($>99\%$) and ammonium hydroxide solution (~ 25 % NH_3) were all purchased from Sigma-Aldrich (UK). MMA inhibitor was removed using an aluminium oxide basic column and AIBN was recrystallized from methanol before use. HPLC grade toluene was purchased from Fisher Scientific (UK). NMR solvents CDCl_3 (99.80 % D) and acetone- d_6 (≥ 99.9 atom % D) were purchased from VWR chemicals (UK) and Aldrich (UK), respectively. Deionized water was obtained from an Elgastat Option 3 water purifier. PETTC and MPETTC were kindly donated by the Armes group (University of Sheffield, UK).

4.2.2. RAFT Solution polymerization of MMA

A 50 mL 2-neck round bottom flask (RBF) was fitted with a condenser and rubber septum and charged with toluene (8.6 g) and a magnetic stirrer bar. This toluene and a separate aliquot of MMA were deoxygenated for 30 minutes. The reactor was then heated to 90 °C under nitrogen with stirring. Deoxygenated MMA (1.454 g, 14.5 mmol) was weighed into a vial containing CPB (0.039 g, 0.176 mmol) and slowly injected into the reaction vessel. After 5 minutes a solution of AIBN (0.0058 g, 0.0353 mmol) dissolved in toluene (0.2 mL) was added. 0.3 mL sample aliquots were taken at predetermined time points and the reaction was allowed to continue for up to 6 hours. Polymerizations were quenched by opening the flask to air and cooling to room temperature. ($M_n = 4,900$ g mol $^{-1}$, $\text{Đ} = 1.15$)

Other reactions were carried out using the same method using PETTC (0.060 g, 0.177 mmol) and MPETTC (0.080 g, 0.177 mmol) in place of CPB as well as PMMA synthesised in the absence of RAFT agent. (No RAFT agent $M_n = 27,000$ g mol $^{-1}$, $\text{Đ} = 1.98$. PETTC $M_n = 6,200$ g mol $^{-1}$, $\text{Đ} = 1.21$. MPETTC $M_n = 5,900$ g mol $^{-1}$, $\text{Đ} = 1.29$.)

4.2.3. RAFT emulsion polymerization of MMA

A 50 mL 2-neck RBF was fitted with a condenser and a rubber septum and charged with H_2O (8.6 g) and a magnetic stirrer bar. This H_2O and a separate aliquot of MMA were deoxygenated for 30 minutes. The reactor was then heated to 90 °C under nitrogen with stirring. Deoxygenated MMA (1.454 g, 14.5 mmol) was weighed into a vial containing CPB (0.039 g, 0.176 mmol) and slowly injected into the reaction vessel. After 5 minutes, a 26 % w/v APS solution (APS; 8.0 mg, 0.0351 mmol, in 0.031 g H_2O) was added. 0.3 mL aliquots were taken at predetermined time points and the reaction was allowed to continue for up to 6 hours.

Polymerizations were quenched by opening the reactor to air and cooling to room temperature. Solid samples were obtained using a Lablyo mini-lyophilizer. (Reactions were assumed to reach 100 % conversion, $M_n = 18,200 \text{ g mol}^{-1}$, $\bar{D} = 3.4$)

Polymerizations were also conducted in the absence of any RAFT agent ($M_n = 101 \text{ kg mol}^{-1}$, $\bar{D} = 4.47$). These polymerizations and CPB-containing reactions were conducted at the natural pH of the reaction mixture (pH ~ 2) and adjusted to pH 8 after the polymerization. PETTC (0.060 g, 0.177 mmol) was used in the place of CPB with reactions taking place at pH 5 and 7 (pH 5, $M_n = 740,600 \text{ g mol}^{-1}$, $\bar{D} = 2.93$; pH 7 $M_n = 7,080 \text{ g mol}^{-1}$, $\bar{D} = 1.69$). With another set of reactions using MPETTC (0.080 g, 0.177 mmol) at pH 2, 5 and 8 (pH 2, $M_n = 8,400 \text{ g mol}^{-1}$, $\bar{D} = 1.16$. pH 5 and 8 SEC data were not reproducible). Otherwise the reaction conditions were kept the same. All reactions were assumed to reach 100 % conversion.

The polymerization of MMA was also carried out in the presence and absence of MPETTC under the same conditions but with azobisisobutyronitrile AIBN (0.0353 mmol, 5.8 mg) initiator instead of APS (without RAFT agent $M_n = 38,900 \text{ g mol}^{-1}$, $\bar{D} = 12.2$. MPETTC $M_n = 7,120 \text{ g mol}^{-1}$, $\bar{D} = 1.33$).

4.2.4. Analyses

Please refer to Chapter 2 for the characterization techniques and analysis conditions. Additional analysis techniques are given below.

4.2.4.1. Tetrahydrofuran Size Exclusion Chromatography

The SEC set-up for data acquired with additional UV-Vis absorption data comprised two 5 μm mixed C columns, an Agilent Technologies Infinity series RI detector operating at a wavelength of $950 \pm 30 \text{ nm}$ wavelength and an Agilent Technologies 1260 infinity UV detector operating at a fixed wavelength of 260 nm. Measurements were conducted at 30 °C at a flow rate of 1 mL / min in THF eluent containing 0.05 % w/v butylhydroxytoluene (BHT). Column calibration of the RI detector was conducted with a series of PMMA standards (M_p range 831 to 2,200,000 Da) and a series of PSt standards for the UV detector calibration (M_p values ranging from 580 to 552,500 Da). Samples were dissolved at 2 mg mL⁻¹ in tetrahydrofuran (THF) using toluene (10 $\mu\text{L mL}^{-1}$) as a flow rate marker.

The characterization method of SEC data obtained using DMF eluent is given in Chapter 2 of this Thesis.

4.2.4.2. Zeta potential and Dynamic Light Scattering

DLS and zeta potential studies were conducted on a Malvern Instruments Nano series Zetasizer at 298 K. DLS samples (0.01 wt%) were analyzed in disposable cuvettes and scattering was detected at 173°. Results were averages of at least 3 runs. Zeta potential samples were prepared at 0.01% w/w in 1 mM potassium chloride solution and the pH was adjusted using varying concentrations of potassium hydroxide and hydrochloric acid. Dispersions were analyzed in Malvern DTS1070 disposable folded capillary cells.

4.3. Results and Discussion

4.3.1. RAFT solution polymerization

The RAFT agents used in this Chapter are shown in Figure 4.2. CDB is a dithiobenzoate and was purchased from Sigma-Aldrich. PETTC and MPETTC are trithiocarbonates and were kindly donated by the Armes group. These RAFT agents became charged at suitable pH and were chosen for this reason as it was thought that this charge would aid in both the partitioning of the RAFT agents and the stabilisation of the latex particles.

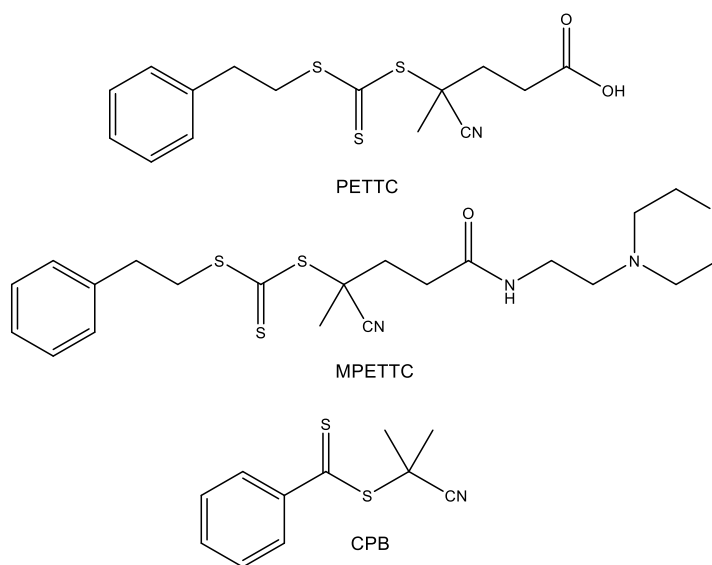


Figure 4.2. RAFT agents used in this research.

Before using these RAFT agents for heterogeneous polymerizations, it was important to confirm that they can be used successfully with the chosen monomer. Thus, RAFT solution polymerizations of MMA were carried out in toluene, at 90 °C, using AIBN initiator. These conditions mirror those of Chapter 2 of this Thesis, whereby DPE was used for the precursor polymers prior to subsequent attempts at chain extension to form diblock copolymers.

The synthesis referred to as D2A2 in Chapter 2 of this Thesis was used to inform the molar ratios of reagents for this results Chapter also. The CTA:initiator ratio of 1:1.4 in Chapter 2 was used, as well as the more common ratio of 5:1 for RAFT polymerizations.²⁰ The molecular weight distributions for both polymerizations can be seen in Figure 4.1. The ratio of 5:1 gave a lower M_n which was close to the theoretical M_n (this will be discussed later) and a significantly lower dispersity. As a result, the remaining polymerizations were performed using a CTA:initiator ratio of 5:1.

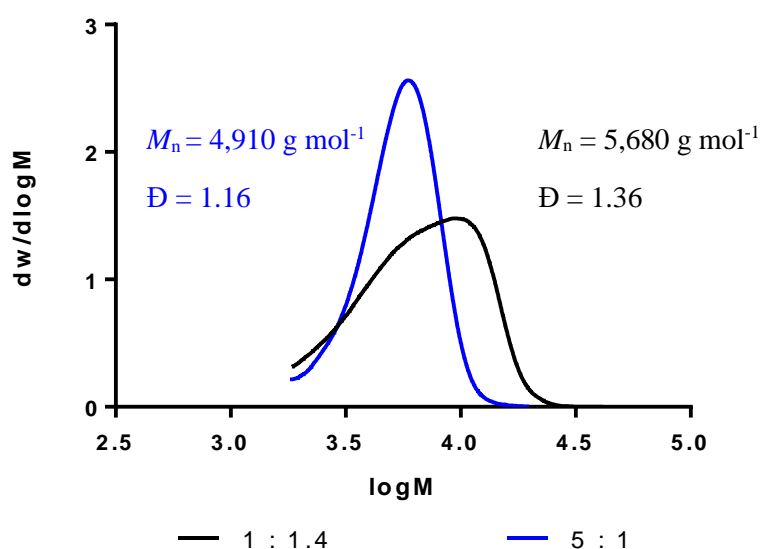


Figure 4.3. Molecular weight distributions obtained by SEC analysis of PMMA synthesised with CPB RAFT agent at two different CPB:AIBN ratios. M_n was determined by SEC in DMF (0.1 % LiBr) against PMMA standards.

In order to confirm that the chosen RAFT agents can be used to impart control over the polymerizations, a control reaction was also conducted without any chain transfer agent (CTA). This will be compared to the reactions containing each of the three chosen RAFT agents and their M_n , \mathcal{D} and particle size distributions.

^1H NMR spectroscopy was used to monitor the conversion of the MMA polymerization over time (Figure 4.4). There is relatively little difference between the kinetics of the reactions conducted in the presence or absence of CTA. If a RAFT agent is suitable for the chosen monomer and reaction conditions there should be little effect on the conversion.²¹ This is because the equilibria established by the RAFT agent should not be the rate-determining step and the RAFT agent should fragment to give the R group as an initiating radical preferentially. Overall, the conversion reaches a maximum of 60 % (for CPB). This is likely due to the amount of initiator and the rapid decomposition of AIBN at higher temperatures.²²

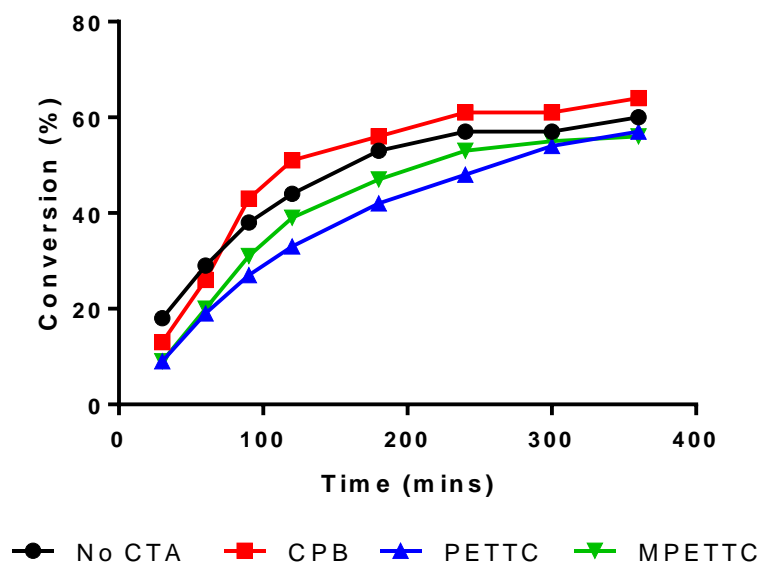


Figure 4.4. Monomer conversion, determined by ^1H NMR spectroscopy, for the polymerization of MMA [1.47 M] with and without RAFT agents [17.9 mM] at 90 °C.

Figure 4.5 (see below) shows the M_n vs conversion plots for polymerizations performed with and without CTA. Conversion and molecular weight were determined by ^1H NMR spectroscopy and SEC, respectively. As expected, the increase in molecular weight without any CTA is not linear and the molecular weight is much higher even at less than 20 % conversion. Results for CPB and MPETTC show roughly linear increases in molecular weight with conversion. This indicates good control with consistent chain growth. However, when using PETTC as the CTA the molecular weight is higher than expected at lower conversions (< 20%). This could be due to a brief uncontrolled period at the start of the reaction. Overall, these data indicate that the three chosen RAFT agents confer control over the polymerization of MMA.

The molecular weight distributions (MWDs) of PMMA synthesised with and without the various RAFT agents are shown in Figure 4.6. The \mathcal{D} values are considerably reduced when using a CTA (from $\mathcal{D} = 1.98$ with no CTA to $\mathcal{D} = 1.15$ - 1.29 when using a CTA). The molecular weight is also reduced when a CTA is used, as expected.

Chapter 4: The effect of RAFT agent solubility in the surfactant-free emulsion polymerization of methyl methacrylate

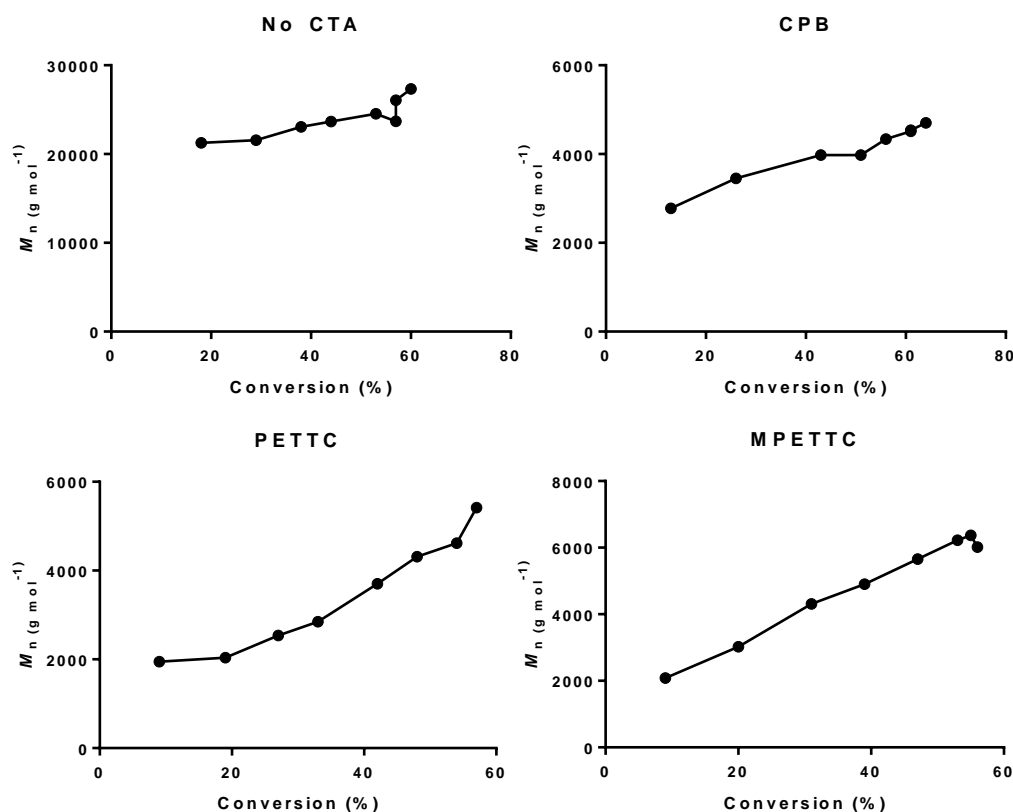


Figure 4.5. Monomer conversion vs M_n for the polymerization of MMA in the absence and presence of various RAFT agents. Monomer conversion was determined by ^1H NMR spectroscopy. M_n was determined by SEC in DMF (0.1% LiBr) against PMMA standards.

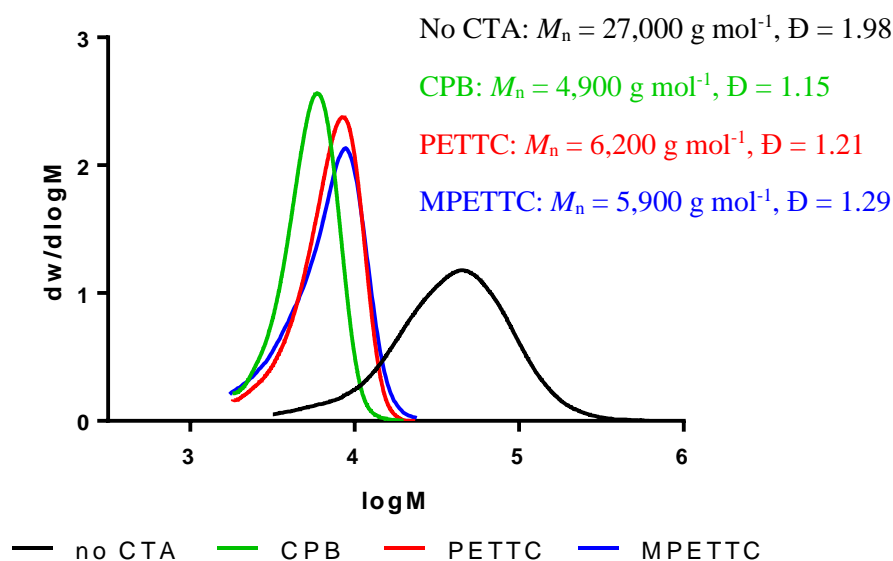


Figure 4.6. Final molecular weight distributions recorded for MMA polymerizations conducted in the presence and absence of RAFT agents. Molecular weight distributions were determined by SEC in DMF (0.1%) against PMMA standards.

Theoretical DP_n and molecular weights for CTA-containing polymerizations can be calculated using equations (1) and (2). This gave theoretical M_n values of 5,520, 5,040 and 5,050 g mol⁻¹ for CPB, PETTC, and MPETTC, respectively. These values are close to those calculated from the SEC data but are a few hundred g mol⁻¹ lower for PETTC and MPETTC, and higher for CPB.

$$DP = \frac{[MMA]}{[CTA]} \times conversion \quad (1)$$

$$Polymer\ MW = (DP \times Monomer\ MW) + CTA\ MW \quad (2)$$

In conclusion, these analyses indicate that these RAFT agents are appropriate choices for the solution polymerization of MMA. Although these reactions could be better optimised, they appear to give reasonably good control and, as a result, all three CTAs were used for the heterogeneous polymerization of MMA also.

4.3.2. Surfactant-free emulsion polymerization using RAFT polymerization

4.3.2.1. Molecular weight and dispersity control by charged RAFT agents

As mentioned previously, both PETTC and MPETTC can become charged via either ionization or protonation of their R groups. Consequently, when these RAFT agents are used in aqueous media variation in the pH of the continuous phase will drastically change their solubility and most likely affect the polymerization. As with the DPE method, these reactions were all carried out as surfactant-free emulsion polymerizations with methyl methacrylate as the monomer. The type of initiator was also changed from AIBN to APS. This is due to the relatively low insolubility of AIBN in water, which means that this initiator is not normally considered suitable for emulsion polymerizations.

The easiest way to establish whether a RAFT agent can be used to control the polymerization is to determine if the theoretical M_n ($M_{n,theo}$) is comparable to the experimental M_n ($M_{n,SEC}$) and if the \mathcal{D} is significantly lower compared to that for PMMA formed in the absence of a CTA (i.e. <1.5). Firstly, the polymerization of MMA in the absence of any RAFT agent is compared to the polymerization containing CPB (Figure 4.7). In the absence of any RAFT agent, the MWD is broad ($\mathcal{D} > 4$) and the latex is composed of high molecular weight polymer chains ($M_n > 100$ kDa). This can also be said of the reactions containing CPB. The $M_{n,theo}$ is considerably lower than that of the measured by SEC (8,420 vs 18,200 g mol⁻¹, Table 4-1) and the polymer has a $\mathcal{D} > 1.5$. However, the M_n of PMMA-CPB is lower than that of PMMA synthesised without any RAFT agent. This could be because the CPB is present at the

polymerization locus, but not in sufficiently high quantity to effectively control the polymerization. If so, this could be attributed to the hydrophobic (water-insoluble) character of the CPB.

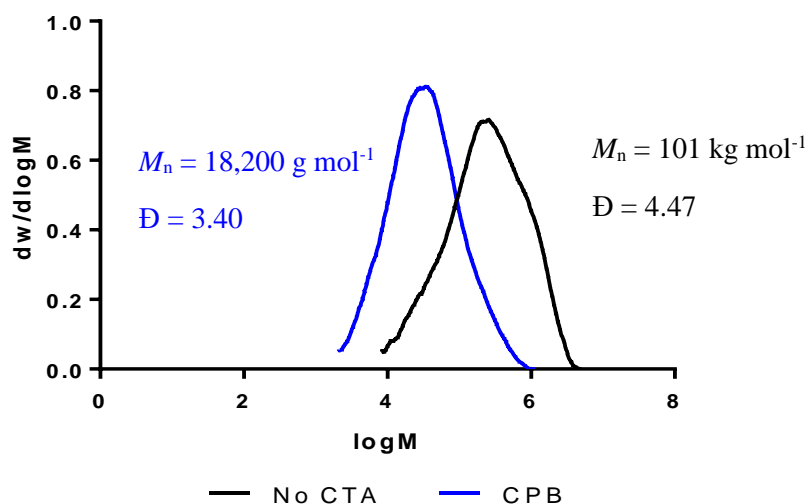


Figure 4.7. Molecular weight distributions of PMMA synthesised by SFEP in the presence of absence of CPB. MWDs were determined by SEC in DMF (0.1% LiBr) against PMMA standards.

To further probe the effect of RAFT agent solubility on the control over the MWDs, polymerizations were performed with PETTC as the RAFT agent at pH 5 and 7. The pKa of the carboxylic acid group of PETTC is 4.7,²³ and therefore much more of the RAFT agent will be able to dissolve in the continuous phase at pH 7 rather than pH 5. In Figure 4.8 (below), the molecular weight distributions of PMMA synthesised without a RAFT agent is compared to polymerizations containing PETTC performed at pH 5 or pH 7. The polymer synthesised at pH 5 has a lower molecular weight and dispersity than that synthesised without a RAFT agent. However, these values are considerably higher than the $M_{n,theo}$ ($8,540 \text{ g mol}^{-1}$) and \bar{D} exceeds 1.5. When the same polymerization is carried out at pH 7, the resulting polymer has lower molecular weight and \bar{D} than that obtained for the reaction at pH 5. The $M_{n,SEC}$ is closer to the $M_{n,theo}$ (Table 4-1) but the dispersity is still not less than 1.5, with evidence of a high molecular weight shoulder. This feature indicates a less well-controlled polymerization. At pH 5, PETTC will not be completely anionic and will thus have low solubility in the aqueous phase. Consequently, the polymerization is not well controlled because the PETTC is unable to reach the polymerization locus in sufficiently high concentration. The water solubility of PETTC significantly higher at pH 7 and, as a result, better control over the polymerization is achieved. There is still a shoulder to this MWD, which suggest an uncontrolled initial period

for the polymerization. Similar observations were also made for the solution polymerizations containing PETTC, as discussed previously.

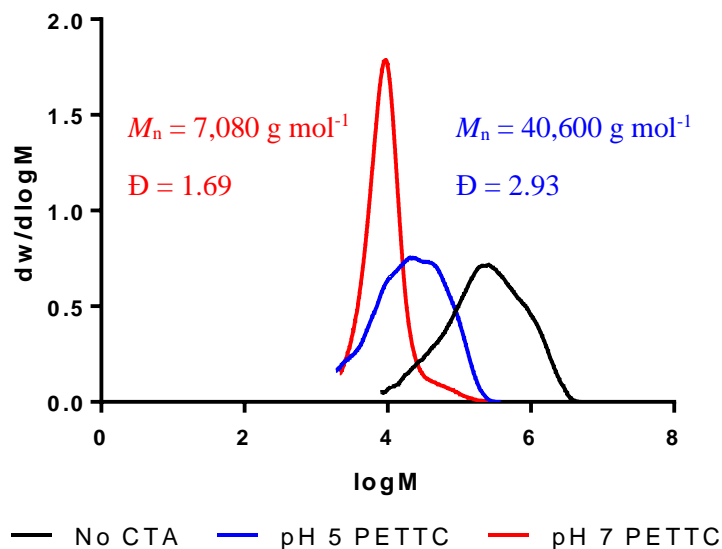


Figure 4.8. Comparison of the final molecular weight distributions for PMMA prepared using PETTC at varying pH and no RAFT agent. MWDs were determined by SEC in DMF (0.1% LiBr) against PMMA standards.

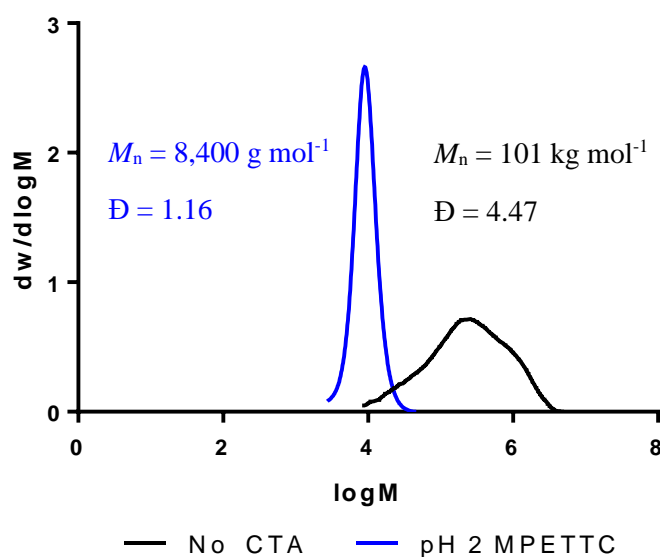


Figure 4.9. Comparison of the final molecular weight distributions for PMMA prepared using MPETTC at pH 2 and no RAFT agent. MWDs were determined by SEC in DMF (0.1% LiBr) against PMMA standards.

The MPETTC RAFT agent contains a morpholine end group which has a pK_a of 6.27.²⁴ Therefore, MMA polymerizations were carried out at pH 2, 5 and 8 to better understand the effect of water solubility on the use of this RAFT agent in SFEP. Molecular weight distributions of the PMMA products formed in the presence and absence of MPETTC at pH 2 can be seen in Figure 4.9. Reactions carried out in the presence of MPETTC at pH 2 give

lower molecular weights and lower \bar{D} (<1.2) than PMMA synthesised in the absence of RAFT agent. However, when MPETTC was added to such polymerizations at pH 5 or 8, the results were much less reproducible (Figure 4.10 and Figure 4.11). While the molecular weight is reduced compared to that of PMMA prepared in the absence of any CTA, in all cases the resulting SEC data are not reproducible. At pH 8, MPETTC should not be soluble ($pK_a = 6.27$) but the observed irreproducibility is perhaps unexpected at pH 5. This indicates that this RAFT agent must be fully ionised to effectively control the polymerization.

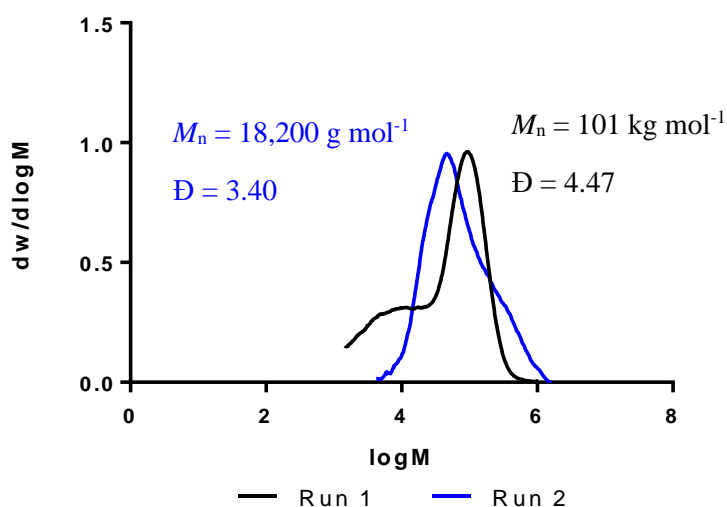


Figure 4.10. Molecular weight distributions obtained for multiple runs of the polymerization of MMA in the presence of MPETTC at pH 8. MWDs were determined by SEC in DMF (0.1% LiBr) against PMMA standards.

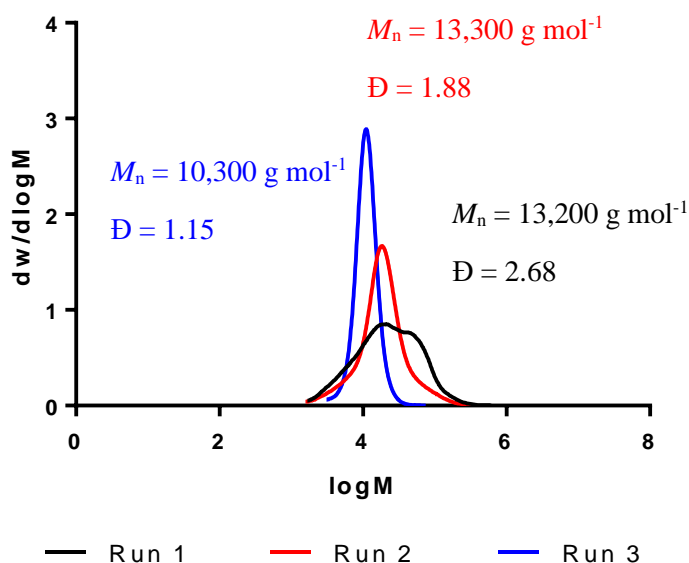


Figure 4.11. Molecular weight distributions obtained for multiple runs of the polymerization of MMA in the presence of MPETTC at pH 5. MWDs were determined by SEC in DMF (0.1% LiBr) against PMMA standards.

A comparison of M_n values from SEC data ($M_{n,SEC}$) and 1H NMR spectroscopy data ($M_{n,NMR}$) to $M_{n,theo}$ is provided in Table 4-1. $M_{n,NMR}$ values are calculated by comparing the integrated proton resonances assigned to the RAFT agent to those of the methacrylic polymer backbone to calculate the DP, and hence $M_{n,NMR}$. For such calculations (using equations (1) and (2)), the percentage conversion was assumed to be 100% for all reactions, as the coagulation of the latexes gave values lower than expected by gravimetry. Because such latexes are dried rather than purified, any free RAFT agent would lead to $M_{n,NMR}$ values being inaccurate. $M_{n,NMR}$ should therefore be the same as $M_{n,theo}$ as all the original RAFT agent should be present in the 1H NMR spectra. This is not true for MPETTC polymerizations conducted at pH 8 due to some phase separation of the water-insoluble RAFT agent, which formed an oily layer that later crystallised. This removal of MPETTC from the dried latex would therefore increase $M_{n,NMR}$ compared to $M_{n,theo}$. The value given in Table 4-1 is included only as an example of the higher $M_{n,SEC}$ values.

$M_{n,SEC}$ is closest to $M_{n,theo}$ when using MPETTC at pH 2. This indicates that the best control over M_n , and therefore the polymerization, was achieved under such conditions. The $M_{n,SEC}$ for polymerizations containing PETTC at pH 7 was lower than $M_{n,theo}$, but still closer to this value than the remaining polymerizations. Despite the lack of charge on the CPB RAFT agent, its $M_{n,SEC}$ is closer to $M_{n,theo}$ than for PETTC at pH 5. This indicates that CPB either has higher aqueous solubility or is a better choice for the polymerization of MMA compared to the other RAFT agents in their non-ionic forms. The greater control offered by CPB was also evident in the RAFT solution polymerizations discussed earlier, with $M_{n,SEC}$ closer to $M_{n,theo}$ and lower dispersity.

Table 4-1. M_n calculated using 1H NMR spectroscopy and SEC data and the theoretical M_n values for the polymerizations of MMA.

RAFT Agent	$M_{n,NMR}$ (g mol ⁻¹)	$M_{n,SEC}$ (g mol ⁻¹)	$M_{n,theo}$ (g mol ⁻¹)
CPB	7,920	18,200	8,420
PETTC pH 5	9,240	40,600	8,540
PETTC pH 7	8,690	7,080	8,540
MPETTC pH 2	8,050	8,400	8,650
MPETTC pH 8	11,250	18,200	8,650

4.3.2.2. UV Size Exclusion Chromatography

SEC was used with an in-line UV detector to examine whether the RAFT agent was present throughout the whole molecular weight distribution. All of the RAFT agents used in this body

of work contain an aromatic moiety on the Z group. If this Z group is connected to the chain-end, it should be detected as an absorbance in the UV SEC chromatogram. It is likely that, if this group is connected to the chain-end, the formation of these chains was controlled by the RAFT agent (ω -chain end). In principle, this should ensure chain extension when adding a second monomer

The SEC chromatogram obtained for PMMA synthesised in the absence of any RAFT agent can be seen in Figure 4.12. As expected, there is no response from the UV detector at 260 nm. This data is not normalised as the UV response is merely composed of background noise. This lack of response is expected as PMMA does not absorb at all in the 260 nm region.

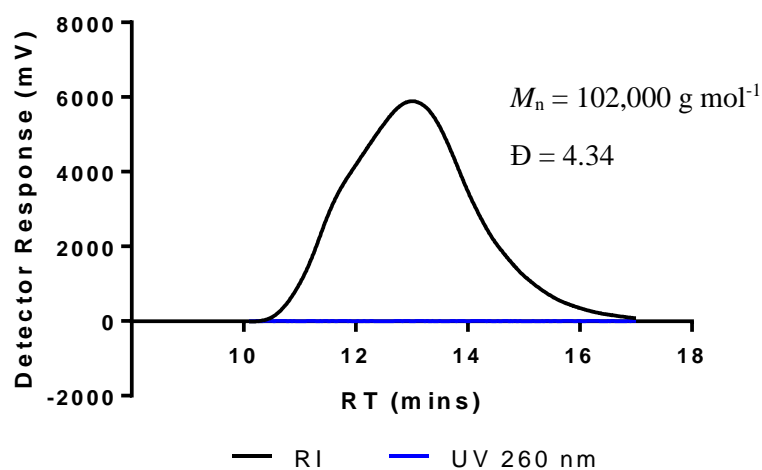


Figure 4.12. SEC chromatogram obtained for PMMA latex synthesised in the absence of RAFT agent (RI and UV detector response). MWDs were determined by SEC in THF (0.05 % w/v BHT) against PMMA standards.

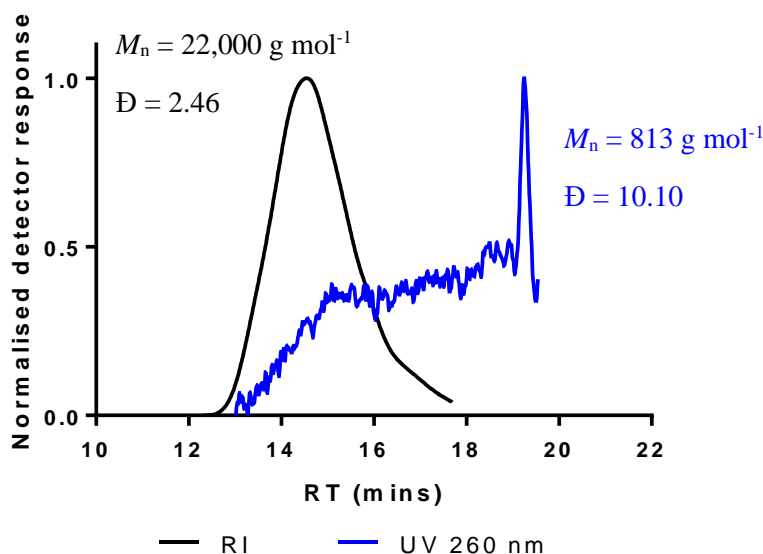


Figure 4.13. Normalised detector response from RI and UV detectors against retention time for PMMA synthesised using the CPB RAFT agent. MWDs were determined by SEC in THF (0.05 % w/v BHT) against PMMA standards for RI detection and PSt standards for UV detection.

PMMA synthesised in the presence of CPB was analysed using SEC with RI and UV detection (Figure 4.13). The normalised UV detector response shows an increase from 13 minutes which is higher compared to the PMMA latex synthesised without any RAFT agent. However, this response does not resemble the RI detector response. Thus, we can infer that the polymer chains are not all capped by the CPB RAFT agent. There is a peak at around 19 minutes in the UV response which is most likely due to free CPB. This reduces the $M_{n,SEC}$ considerably and also results in lower $M_{n,NMR}$ values for this reaction.

Polymerizations of MMA conducted in the presence of PETTC at pH 5 and 7 are shown in Figure 4.14 and Figure 4.15, respectively. The UV response for PMMA prepared using PETTC at pH 5 does not match that of the RI response, with the former having a high background noise. In contrast, when the same polymerization was conducted at pH 7, the RI and UV response overlay almost perfectly, with only a slight difference in retention time as a result of the UV detector being connected in series before the RI detector. The M_n obtained from the UV response is lower than that of the M_n obtained from the RI response. This is because polystyrene standards are required to calibrate the UV data which will not match the behaviour of PMMA in the SEC column. It is clear that the polymerization at pH 7 contains more RAFT end-groups associated with the molecular weight distribution. This is supported by the greater control over M_n and lower dispersity, indicating a well-controlled polymerization.

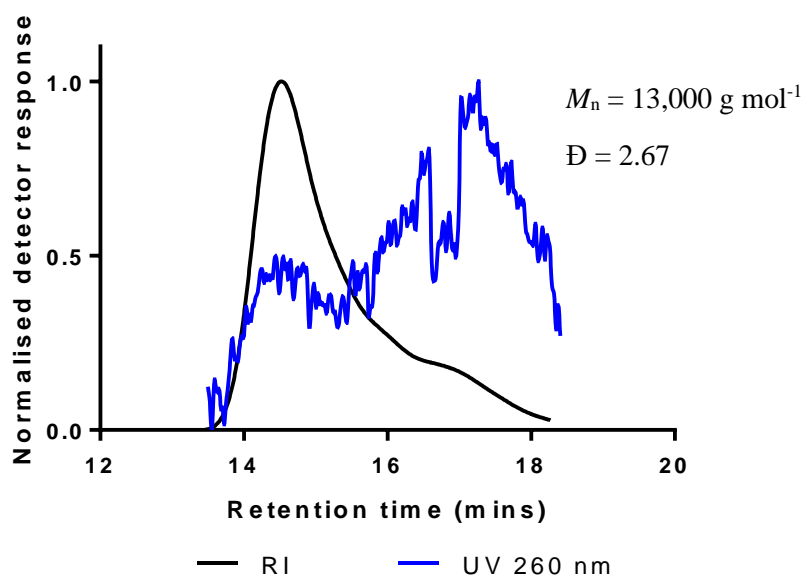


Figure 4.14. Normalised RI and UV SEC curves for PMMA synthesised with PETTC at pH 5. MWDs were determined by SEC in THF (0.05 % w/v BHT) against PMMA standards for RI detection and PSt standards for UV detection.

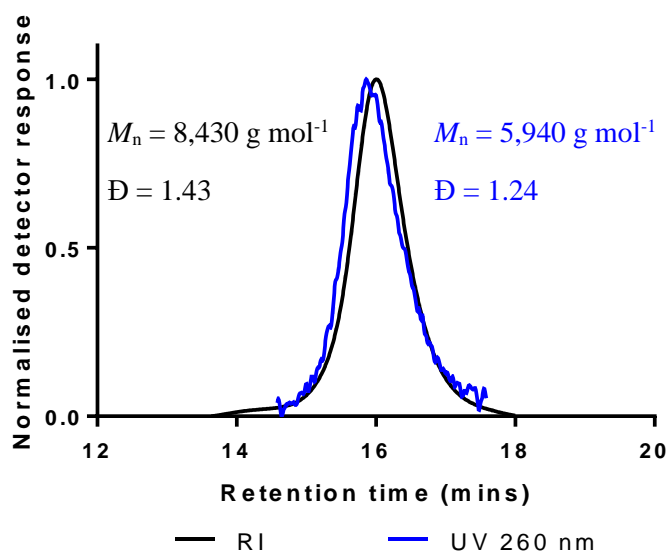


Figure 4.15. Normalised RI and UV SEC traces for PMMA synthesised with PETTC at pH 7. MWDs were determined by SEC in THF (0.05 % w/v BHT) against PMMA standards for RI detection and PSt standards for UV detection.

The UV and RI detector responses for PMMA prepared in the presence of MPETTC at pH 2 and 8 are shown in Figure 4.16 and Figure 4.17, respectively. For PMMA synthesised at pH 2, the normalized UV and RI detector responses are very similar with the former response being at an earlier retention time for reasons explained earlier. M_n is again lower for the UV response due to the polystyrene calibration standards and the dispersity of each curve is almost an exact match for syntheses performed at pH 2. From this, we can infer that the RAFT agent

is effectively reversibly deactivating the polymerization, so it is likely that the chains could be further extended. This cannot be said for the polymerization conducted at pH 8. Here, the UV and RI responses are not normalised because the former is just background noise. These results indicate that the change in pH leads to a lack of control at pH 8.

The above data are in agreement with those of the literature in that for a successful SFEP in combination with RAFT polymerization, the RAFT agent has to be suitably amphiphilic e.g. a controlsurf.^{15, 16}

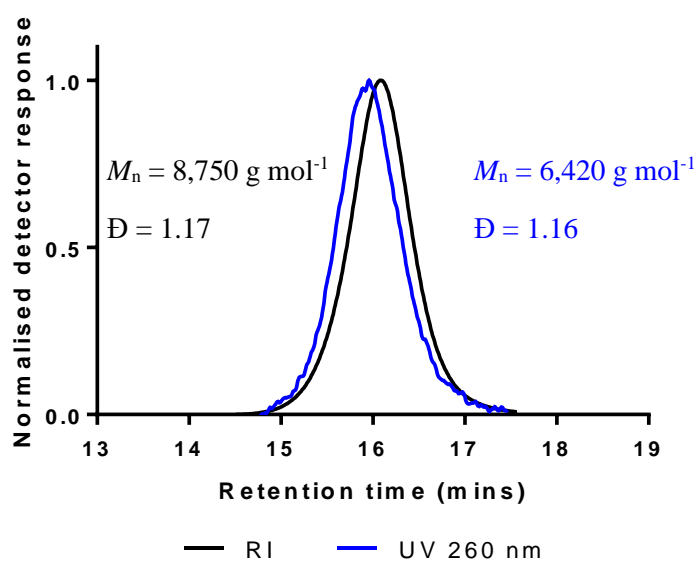


Figure 4.16. Normalised RI and UV SEC curves recorded for PMMA synthesized with MPETTC at pH 2. MWDs were determined by SEC in THF (0.05 % w/v BHT) against PMMA standards for RI detection and PST standards for UV detection.

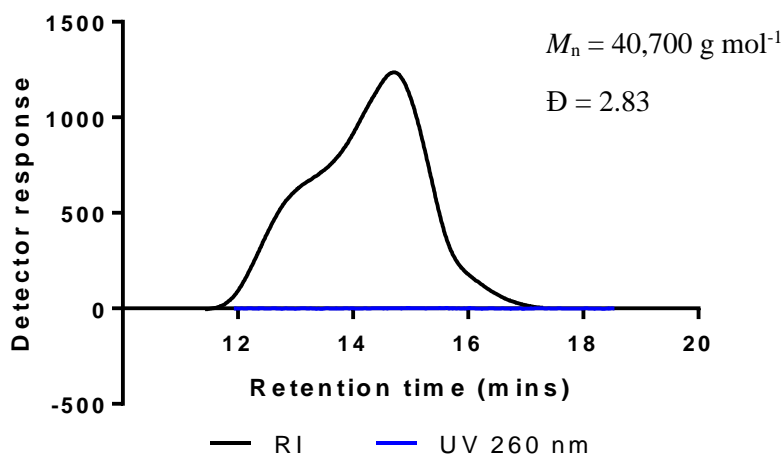


Figure 4.17. RI and UV SEC curves recorded for PMMA synthesized with MPETTC at pH 8. MWDs were determined by SEC in THF (0.05 % w/v BHT) against PMMA standards.

4.3.3. Kinetics of the emulsion polymerizations of PMMA synthesis in the presence and absence of RAFT agent

4.3.3.1. Solids content conversion analysis

Over the course of these MMA polymerizations, samples were taken at regular time intervals. These were intended to monitor the solids content over the course of the reaction and hence infer the monomer conversion. However, this is not a particularly accurate representation of the kinetics of the reaction owing to coagulation. Unfortunately, a reliable ^1H NMR spectroscopy protocol could not be established. The solids contents of these reactions over time are shown in Figure 4.18, with the theoretical 100 % MMA conversion being 14.9 wt%. From these data, it can be suggested that the reactions are complete within 60 minutes, except for the reactions involving MPETTC. All such reactions had considerably lower solids contents, which increased over the first 2 hours of the polymerization. Solids contents varied significantly and reactions often contained up to 50 % coagulum. This suggests that these reactions did reach approximately 100 % conversion (as with the other reactions), but with some retardation and the latex formed was significantly less stable. This was not expected as the cationic charge on the MPETTC at low pH should help stabilise the latex.

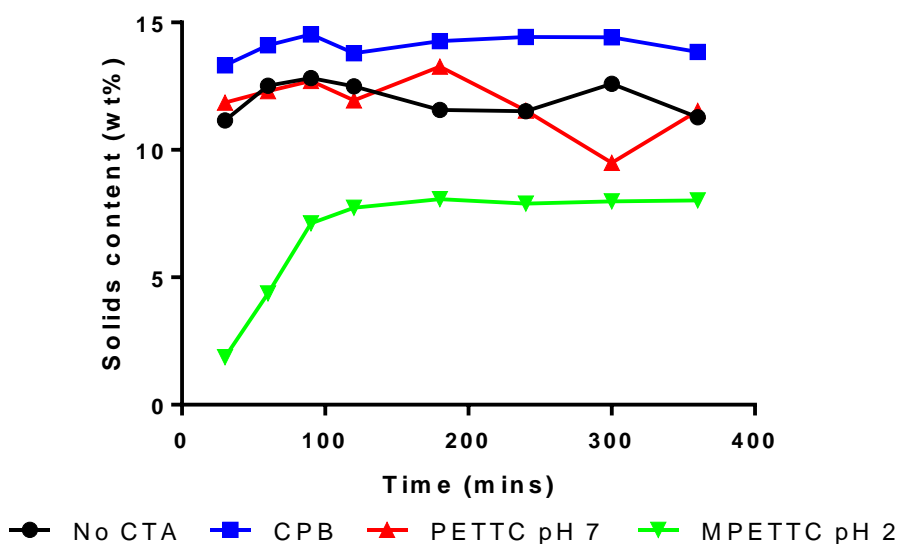


Figure 4.18. Solids content by gravimetric analysis over time for RAFT emulsion polymerizations of methyl methacrylate conducted at various pH with different RAFT agents at 90 °C. Theoretical 100 % MMA conversion solids contents is 14.9 wt%.

4.3.3.1.1. Evolution of molecular weight during the polymerization

Samples taken from the emulsion polymerizations at varying time points were analysed by SEC to determine the evolution of molecular weight during the polymerization. When the

polymerization of methyl methacrylate was carried out in the absence of RAFT agent, the SEC curve at 30 mins is very similar to that for the final latex after 360 mins (Figure 4.19). However, a lower molecular weight shoulder was formed after 360 mins, which could be a result of the reduced amount of monomer and initiator available after 60 mins. Emulsion polymerizations usually have higher polymerization rates than those in solution and are indeed faster than those RAFT syntheses carried out in toluene discussed in the first part of this Chapter. Owing to the significant level of coagulation during the polymerization, the “livingness” of the reaction cannot be examined as a molecular weight vs. conversion plot. Instead, molecular weight distributions are presented as a function of polymerization time. As mentioned earlier, the incorporation of CPB appears to have very little effect on the polymerization. The MWDs of samples taken from the polymerization at 30 and 60 mins are very similar to those of the final polymer, with some smaller molecular weight species synthesised over the polymerization (Figure 4.20).

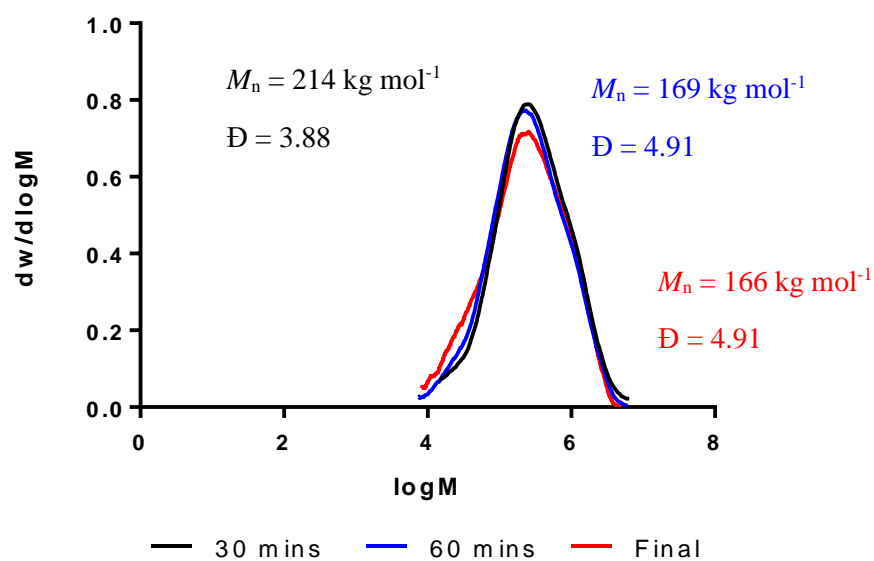


Figure 4.19. Molecular weight distributions from SEC analysis recorded using an RI detector during the emulsion polymerization of methyl methacrylate in the absence of RAFT agent. Samples were analysed by SEC in DMF (0.1% LiBr) against PMMA standards.

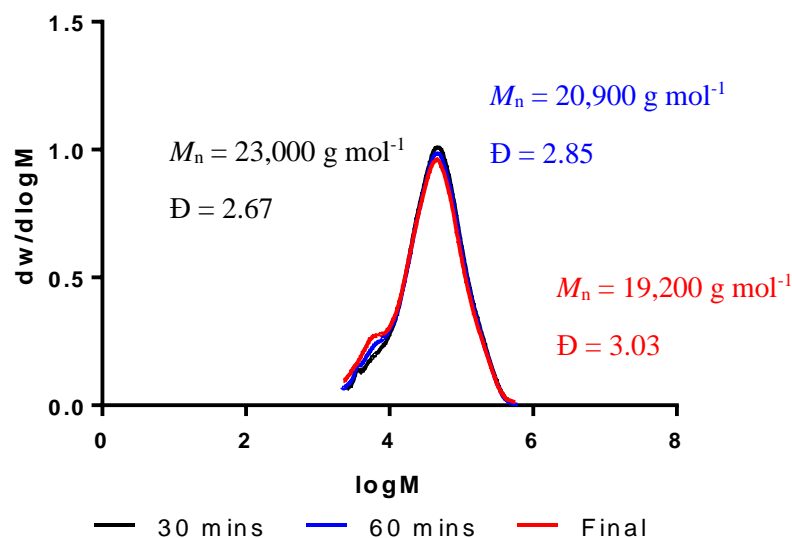


Figure 4.20. Molecular weight distributions from SEC analysis recorded using an RI detector during the emulsion polymerization of methyl methacrylate in the presence of CPB RAFT agent. Samples were analysed by SEC in DMF (0.1% LiBr) against PMMA standards.

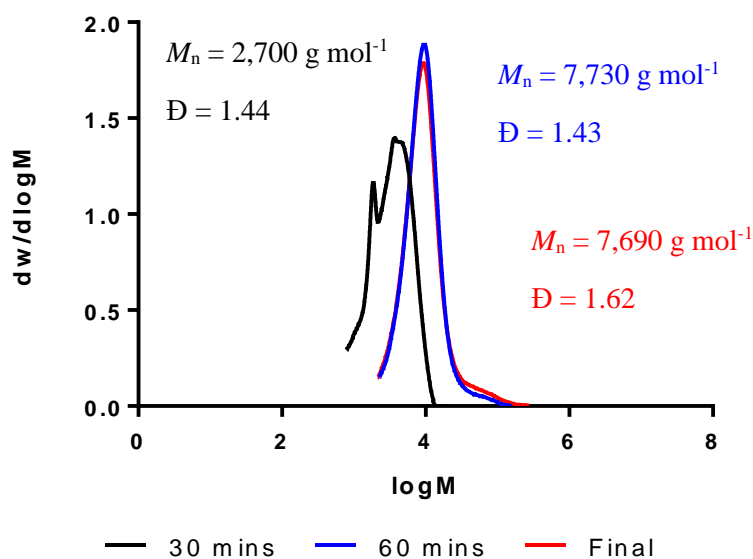


Figure 4.21. Molecular weight distributions from SEC analysis recorded using an RI detector during the emulsion polymerization of methyl methacrylate in the presence of PETTC at pH 7. Samples were analysed by SEC in DMF (0.1% LiBr) against PMMA standards.

Figure 4.21 shows the MWDs recorded during the polymerization of methyl methacrylate in the presence of PETTC carried out at pH 7. At 30 mins, the sample has a lower molecular weight than that of the sample at 60 mins. However, the only noticeable difference between 60 and 360 mins is a slight increase in the higher molecular weight shoulder. This indicates that the rate of polymerization is high as the reaction is complete within 60 minutes but the

presence of the RAFT agent does reduce this rate of polymerization compared to the polymerization carried out in the absence of RAFT agent.

In the presence of MPETTC at pH 2 the polymerization rate is reduced further (Figure 4.22). In principle, the rate of a well-controlled polymerization should not be affected as an effective reversible deactivation step should not slow the consumption of monomer²¹. In conclusion, while the presence of MPETTC RAFT agent does provide the greatest control at pH 2 it also retards the polymerization, and at pH 5 and pH 8 the polymerization is not particularly reproducible.

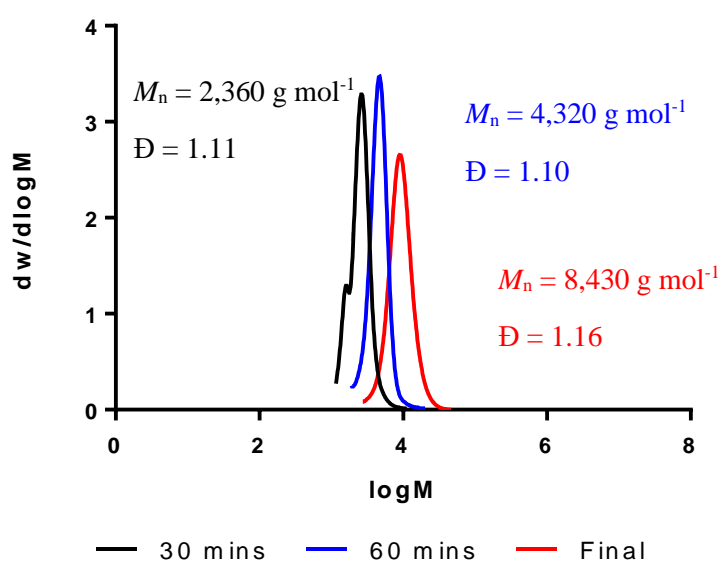


Figure 4.22. Molecular weight distributions from SEC analysis recorded using an RI detector during the polymerization of methyl methacrylate in the presence of MPETTC at pH 2. Samples were analysed by SEC in DMF (0.1% LiBr) against PMMA standards.

4.3.3.2. Particle size distributions of latexes

Particle size distributions of latexes formed with and without RAFT agent were examined by DLS and TEM. Reactions conducted without RAFT agent proved to be unimodal by DLS ($D_h = 355$ nm, polydispersity = 0.03, Figure 4.23). All diameter and polydispersity data for DLS PSDs are given in Table 4-2. This was confirmed by TEM analysis for one sample where the average particle diameter was determined to be 310 ± 20 nm using ImageJ software.

Table 4-4 contains a TEM image of the latex and the corresponding histogram determined using ImageJ. The TEM particle diameter is slightly lower than that obtained by DLS. This is because the intensity-average hydrodynamic diameter (D_h) and number-average diameter are

Chapter 4: The effect of RAFT agent solubility in the surfactant-free emulsion polymerization of methyl methacrylate

reported by DLS and TEM, respectively. Particle diameters and standard deviations of latexes synthesised in this section are given in Table 4-3.

Table 4-2. DLS diameter and polydispersity data obtained for the emulsion polymerization of MMA either in the absence or presence of a RAFT agent.

RAFT agent	Diameter(s) / nm	Polydispersity
None	355	0.03
CPB	370	0.12
PETTC pH 5	485	0.05
PETTC pH 7	470	0.06
MPETTC pH 2 (bimodal)	260 940	0.29
MPETTC pH 5 + (bimodal)	1,300 1,060	0.16 0.39
MPETTC pH 8	630	0.09

Table 4-3. TEM diameters and standard deviations obtained for the emulsion polymerization of MMA either in the absence or presence of a RAFT agent.

RAFT agent	Diameter(s) / nm	Standard deviation
None	310	20
CPB	350	29
PETTC pH 5	425	114
PETTC pH 7	415	20
MPETTC pH 2	160	70
MPETTC pH 8	545	35

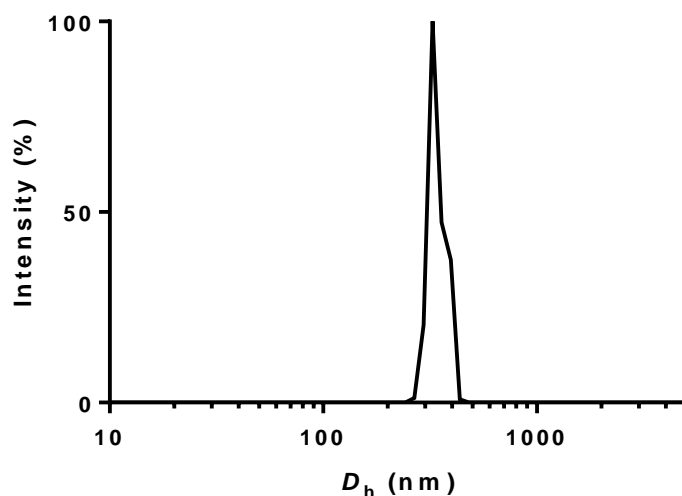


Figure 4.23. DLS size distribution of PMMA latex prepared in the absence of RAFT agent.

As previously discussed, surfactant-free emulsion polymerizations of methyl methacrylate could not be controlled with the addition of CPB RAFT agent. The mean DLS diameter of the particles was largely unaffected ($D_h = 370$ nm, polydispersity = 0.12, Figure 4.24). The TEM particle diameter were again smaller than those by DLS but had similar polydispersity (e.g. 350 ± 29 nm). These results are similar to those obtained for the polymerizations carried out in the absence of any RAFT agent, indicating that the presence of CPB has very little effect on any aspect of the SFEP.

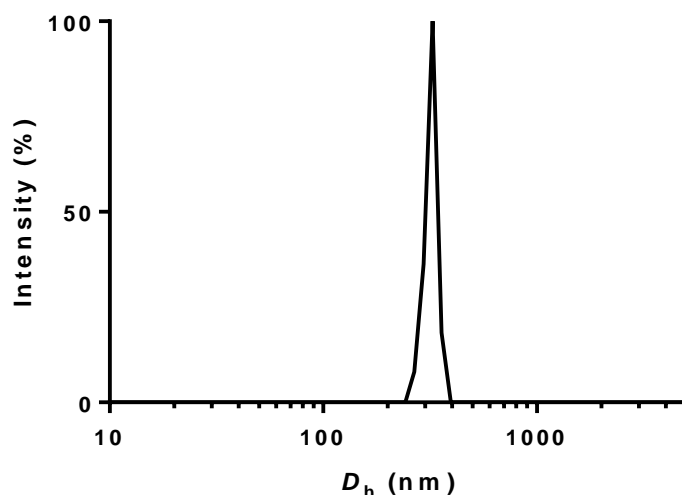


Figure 4.24. DLS size distribution for PMMA latex synthesised in the presence of CPB.

When using PETTC for the polymerization of MMA, the pH of the aqueous phase was varied from pH 5 to 7. The anionic charge on the RAFT Z-group at pH 7, should ensure colloidal

stability via charge stabilization. DLS size distributions for latexes formed at both pH values can be seen in Figure 4.25. The D_h values obtained from these data are comparable (pH 5, $D_h = 485$ nm, dispersity = 0.05; pH 7, $D_h = 470$ nm, dispersity = 0.06). Particle sizes determined by TEM were similar but considerably more disperse at pH 5 (425 ± 124 nm) than at pH 7 (415 ± 20 nm). Like the effect of adding CPB discussed above, when PETTC cannot migrate across the aqueous phase at pH 5 there is relatively little effect on the PSD, whereas the size distribution is broadened considerably at pH 7.

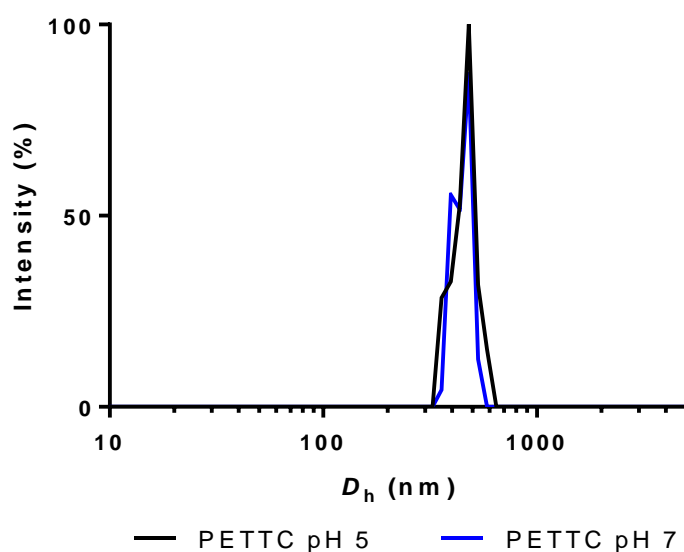


Figure 4.25. DLS size distributions recorded for PETTC-mediated emulsion polymerizations of MMA conducted at either pH 5 or pH 7.

Polymerizations with MPETTC were performed at pH 2, 5 and 8. When these samples were examined by DLS, their size distributions varied significantly (Figure 4.26). At pH 2, a bimodal size distribution was observed ($D_h = 670$ nm, dispersity = 0.29). In contrast, the same polymerization at pH 8 produced unimodal latex size distribution by DLS ($D_h = 630$ nm, dispersity = 0.09). While MPETTC-mediated polymerizations may not be reproducible by SEC, the PSDs are used as a comparison. However, this mean D_h value is considerably higher than those obtained for MMA polymerizations containing CPB or no CTA. The TEM diameters are not in agreement with the DLS values. Again, polymerizations carried out at pH 2 gave broad latex size distributions (diameter = 160 ± 70 nm). However, the bimodality was not evident (

Table 4-4). This may be due to aggregated particles giving the appearance of larger particles by DLS. The DLS diameters are intensity weighted and therefore a small number of larger particles, or possibly aggregated, may account for the difference between the DLS and TEM

data. MPETTC-mediated polymerizations conducted at pH 8 produced latexes with a similar TEM diameter (545 ± 35 nm) to the D_h values reported by DLS, with the PSDs being less broad than those for latexes synthesised at pH 2. These observations, suggest that control over the molecular weight is achieved at the expense of poor control over the PSD of the latex.

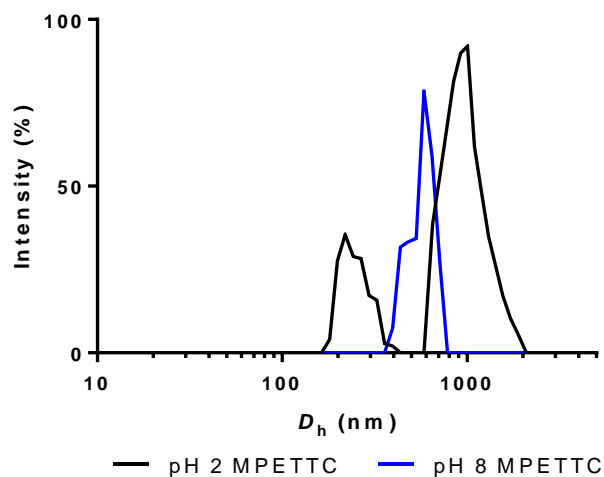


Figure 4.26. DLS size distributions recorded for MPETTC-mediated emulsion polymerizations of MMA conducted at either pH 2 or pH 8.

When polymerizations were carried out at pH 5, the DLS results were not reproducible. When the polymerization appeared to be more controlled by SEC (run 2) the DLS size distribution was bimodal (Figure 4.27). However, when the polymerization appeared uncontrolled by SEC (run 1) the DLS size distribution was unimodal, like the reactions conducted at pH 8. This suggests that control over molecular weight is achieved at the expense of PSD control.

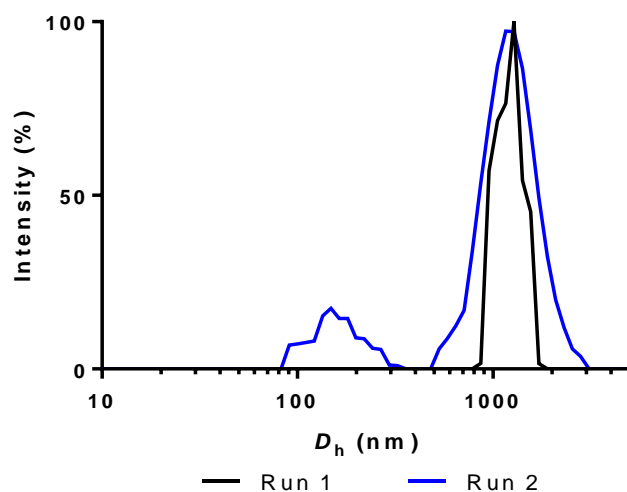
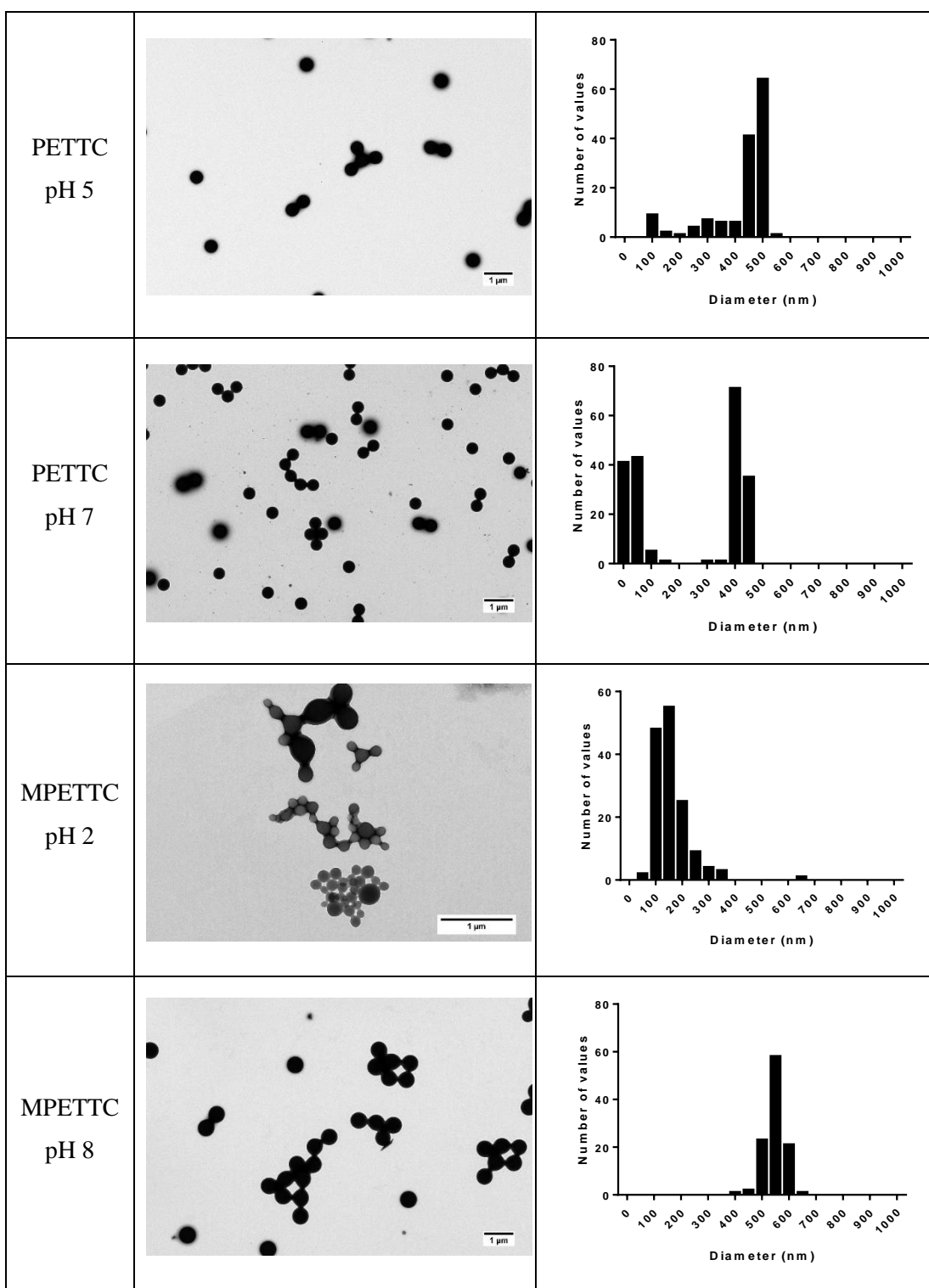


Figure 4.27. DLS size distributions recorded for two repeats of MPETTC-mediated MMA polymerizations conducted at pH 5.

Table 4-4. TEM micrographs and histograms of PSDs for all PMMA latexes synthesised in the absence and presence of various RAFT agents.

RAFT agent	TEM Micrograph	Histogram of particle diameters
No CTA		
CPB		

Chapter 4: The effect of RAFT agent solubility in the surfactant-free emulsion polymerization of methyl methacrylate



4.3.3.3. Zeta potential data with and without RAFT agent

Zeta potential measurements were carried out to determine if the addition of the charged RAFT end-group conferred colloidal stability on the latex at a suitable pH. The zeta potential and D_h data determined when varying the solution pH of the PMMA latex synthesised in the absence of RAFT agent are shown in Figure 4.28. The pH sweep was started at high pH with the addition of potassium hydroxide and reduced to low pH with the addition of hydrochloric acid. A sharp increase in the zeta potential of the latex occurs at around pH 7. This is the point at which the majority of anionic end-groups, formed as a result of the use of APS initiator, have no charge. This is unexpected as APS initiation should produce polymers with HSO_4^{2-} end-groups which should have a pKa of 2.²⁵ Another possible end-group is hydroxyl groups formed as a result of using this persulfate initiator. These end-groups should have a similar pKa to alcohols ≈ 16 and so should not affect the zeta potential in this pH range. Below pH 7, there is no surface charge to stabilise the latex. Therefore, the apparent D_h of the latex increases as the particles begin to flocculate.

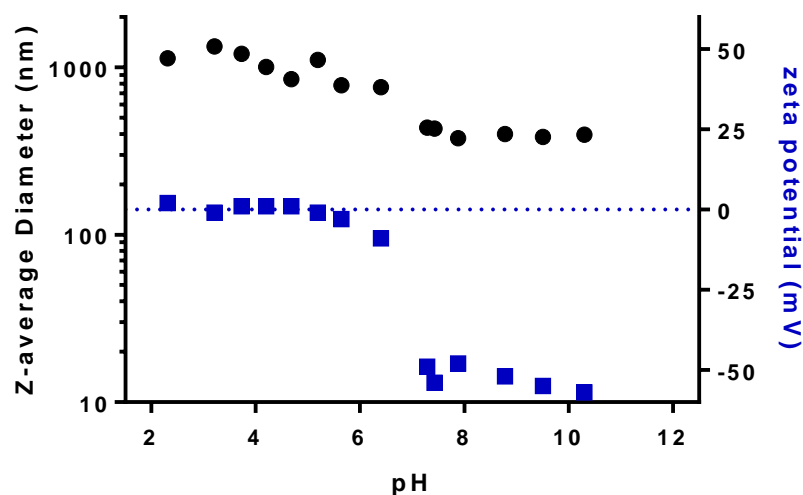


Figure 4.28. pH-dependence of zeta potential and z-average diameters for PMMA latex formed in the absence of RAFT agent.

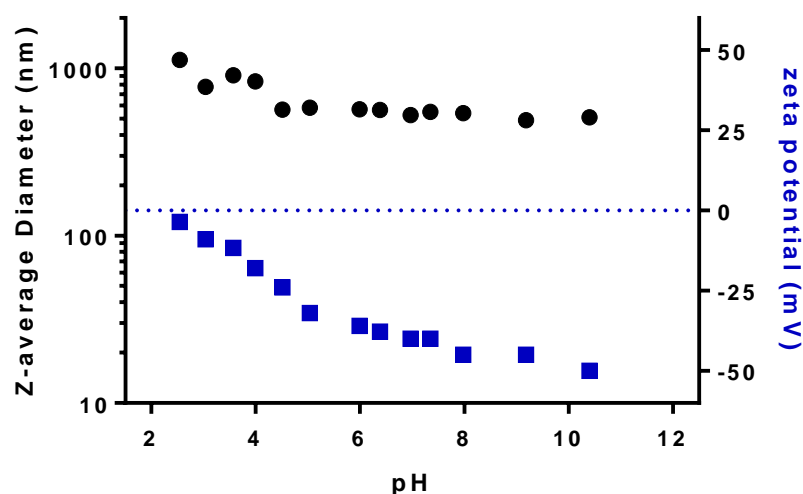


Figure 4.29. pH-dependence of zeta potential and z-average diameters of PMMA latex formed in the presence of CPB.

When CPB is added to the emulsion polymerization of MMA there is a change in the character of the PMMA latex (Figure 4.29). Again, there is a reduction in the zeta potential from negative to zero as the pH is decreased. However, this change is much more gradual. The lack of control over the dispersity and molecular weight discussed previously, as well as the lack of a UV response in the SEC chromatogram suggest that CPB is not attached to most of the polymer chains. Given the lack of charge on the R and Z groups of CPB it would be reasonable to assume that the relationship between zeta potential and pH should be similar to the latex obtained in the absence of this RAFT agent. On the other hand, it is possible that the dithiobenzoate end-group is removed by hydrolysis before the end of the MMA polymerization.²⁶ This could possibly change the zeta potential of the latex over a pH range but perhaps unlikely in the way observed in Figure 4.29. The increase in D_h is also much less for the latexes synthesised in the presence of CPB. This is expected given the modest change in zeta potential, leading to less coagulation (better colloidal stability).

This effect can also be observed in the D_h values and zeta potentials of latexes synthesised in the presence of PETTC (Figure 4.30). The use of PETTC at pH 7 appears to produce a latex similar to that formed using CPB. This is despite the fact that PETTC had a much greater effect on the MWD and the anionic carboxylic acid moiety of this RAFT agent confers anionic charge (present in the z group of PETTC) above pH 4.7.²³ The zeta potential increases gradually to pH = 6 then becomes significantly less negative. This is therefore the pH at which the latex begins to lose its surface charge but it is not clear why this behaviour differs from that of the PMMA latex synthesised in the absence of this RAFT agent.

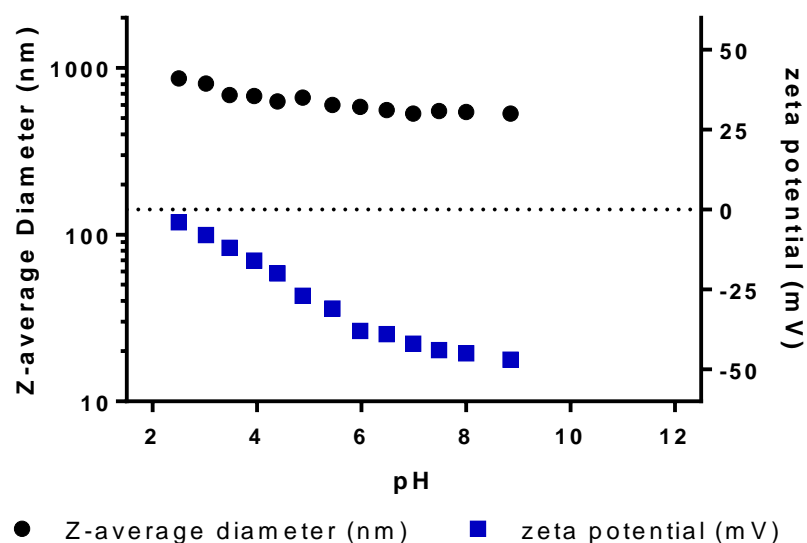


Figure 4.30. pH-dependence of the zeta potential and Z-averages for a PMMA latex formed in the presence of PETTC at pH 7.

Zeta potentials and D_h value change with varying pH for PMMA latex synthesised using MPETTC at pH 2 differs from the other latexes synthesised in this Chapter (Figure 4.31). The morpholine moiety of MPETTC is protonated at acidic pH ($pK_a = 6.27$),²⁴ at roughly the same pH at which PMMA latex synthesised without any RAFT agent has a zeta potential of zero. This should mean that the PMMA latex should be charge-stabilised under these conditions. At pH 9, the zeta potential is appreciably negative and the isoelectric point is around pH 7. At this point, the overall surface charge becomes positive. However, the zeta potential is not particularly high. This leads to an increase in D_h owing to flocculation, as the charge is not sufficient below pH 7.5 to stabilise the latex. This means that the protonated morpholine chain-ends cannot be used to stabilise the PMMA particles effectively in this system.

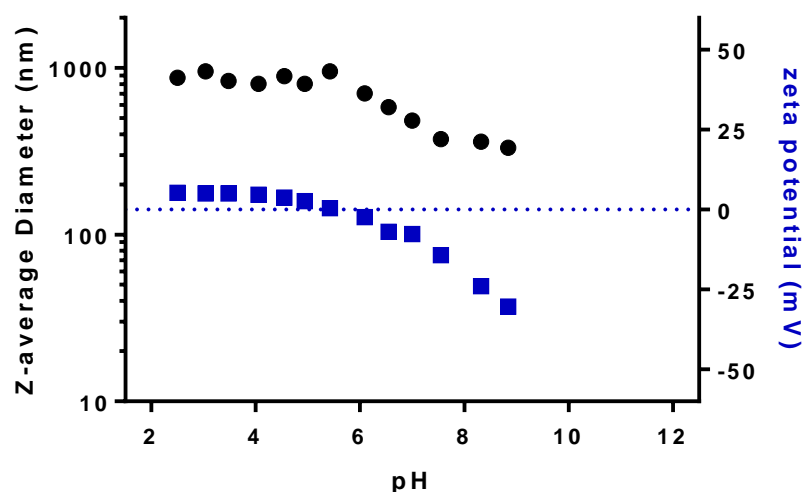


Figure 4.31. pH-dependence of zeta potential and z-average diameter for a PMMA latex formed in the presence of MPETTC at pH 2.

4.3.4. RAFT SFEP of MMA with an uncharged initiator fragment

The polymerization of MMA in the presence and absence of MPETTC RAFT agent was also carried out using azobisisobutyronitrile (AIBN) initiator. The purpose of these reactions was to determine if a latex could be formed when a non-charged initiator was used. MPETTC RAFT agent was utilised in these reactions to determine whether the cationic charge on the morpholine moiety at low pH was sufficient to stabilise the latex particles that should be formed under these conditions. MPETTC has already been shown to impart reasonable control over the polymerization at pH 2 when using an ionic initiator.

The monomer conversion was monitored by gravimetry with a maximum solids content calculated to be 14.5 % (Figure 4.32). The MMA polymerization performed in the absence of RAFT agent coagulated catastrophically almost immediately, with the solids content not reaching more than 0.37 % for any of the repeats of this reaction. The white insoluble PMMA product did not resemble a latex. When MPETTC was added to the polymerization, the solids content increased for the first 90 minutes of the reaction. At this point, however, the particles began to coagulate and the solids content did not reach higher than 12 %. Nevertheless, this is higher than the solids content achieved with APS initiator. The polymerization was allowed to proceed for 6 hours at 90 °C in order to achieve maximum conversion.

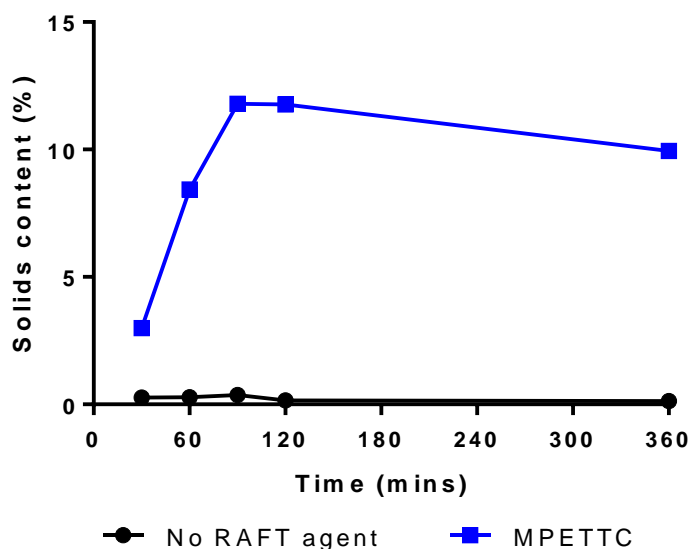


Figure 4.32. Change in solids content, obtained by gravimetric analysis, over reaction time for the SFEP of MMA with AIBN initiator in the presence or absence of MPETTC.

When the aqueous phase of the PMMA formed in the absence of RAFT agent was analysed by DLS little or no light scattering was observed. This demonstrates that, without a charged initiator such as APS, any particles that were formed coagulated immediately and could not be dispersed in the aqueous phase.

When MPETTC was added to the polymerization of MMA using AIBN as initiator a latex was formed, albeit with some coagulum. The particle size distribution (PSD) was analysed by DLS and zeta potential measurements (Figure 4.33). The pH sweep began at pH 2; the morpholine end-group derived from MPETTC should be cationic and hence stabilise the latex under these conditions. The zeta potential of the latex at pH 2 was sufficiently positive to stabilise the particles, enabling them to remain dispersed in the aqueous continuous phase. As the pH is raised, the zeta potential decreases as the morpholine group becomes deprotonated. Eventually the zeta potential reaches zero at pH 3.5 and then becomes negative at higher pH. The origin of such negative zeta potentials remains unclear. As the pH reaches pH 12 the zeta potential decreases significantly, which is likely due a background to salt effect. The z-average diameter remains high (~1000 nm) throughout the pH sweep. This suggests flocculation of the particles due to insufficient stabilization. This hypothesis requires further analysis by TEM.

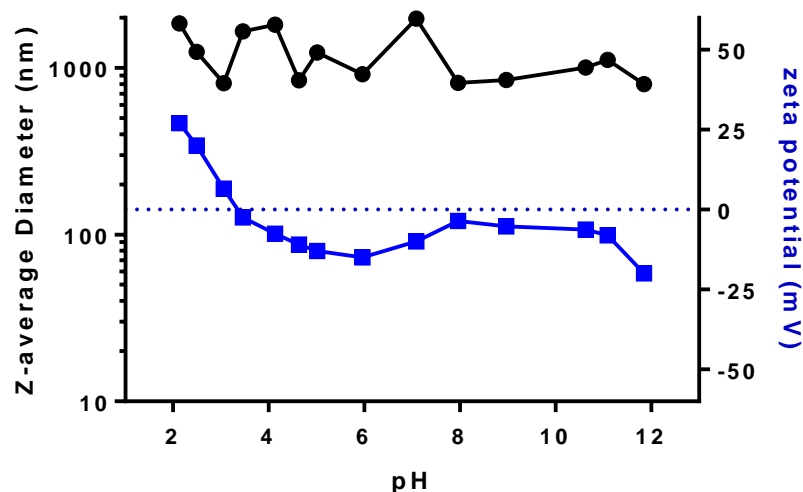


Figure 4.33. Z-average diameter vs. pH and zeta potential vs. pH curves obtained for a PMMA latex synthesised with AIBN initiator and MPETTC RAFT agent.

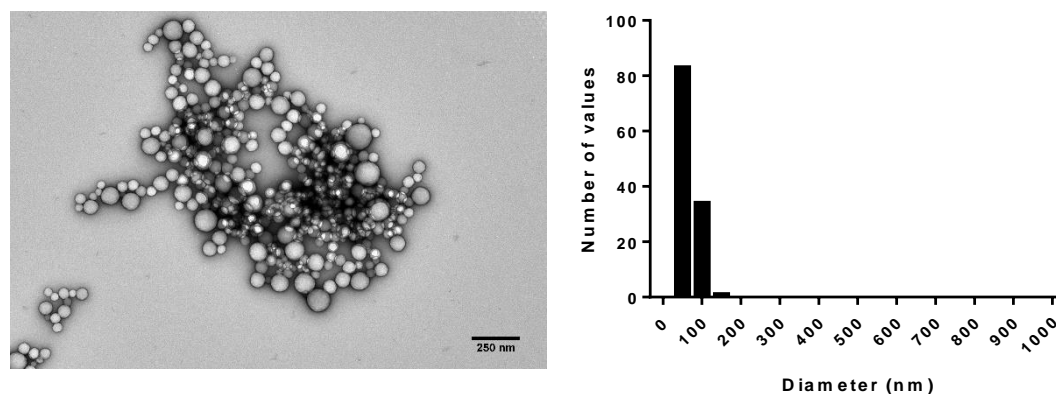


Figure 4.34. TEM images and particle size histogram for a PMMA latex synthesised with AIBN initiator in the presence of MPETTC.

A TEM image and PSD histogram of the latex formed in the presence of MPETTC are shown in Figure 4.34. The number-average particle diameter was 67 ± 20 nm. This is considerably smaller than the PMMA latex obtained using APS as an initiator (670 ± 5.5 nm). This is perhaps an unexpected finding as smaller particles require more stabiliser due to the higher specific surface area. The TEM image supports the hypothesis that the DLS diameter was artificially high owing to incipient particle flocculation.

To determine whether the inclusion of MPETTC conferred control over the molecular weight distribution, the PMMA samples were analysed by SEC. The coagulum obtained from the polymerization in the absence of RAFT agent had a very broad MWD ($\bar{D} > 12$), as expected for a conventional free radical polymerization. The polymer obtained in the presence of

MPETTC however, had a lower dispersity ($\mathcal{D} = 1.33$), and also a significantly lower M_n . The dispersity could likely be lowered further by optimization of the reaction conditions. On the other hand, AIBN initiator may be less well-suited to the MPETTC RAFT agent than APS, as this initiator was not investigated by solution polymerization in the initial scoping experiments. The $M_{n,theo}$ of this polymerization is $8,650 \text{ g mol}^{-1}$, assuming 100 % conversion. This is higher than the $M_{n,SEC}$ of $7,120 \text{ g mol}^{-1}$ suggesting imperfect RAFT efficiency for MPETTC.

Overall, these data suggest that the polymerization of MMA can be carried out in SFEP conditions, using a suitable ionic RAFT agent confer surface charge. A colloidal latex was formed that remained stable post-polymerization, but control over the MMA polymerization and the degree of dispersion of the flocculated particles could be improved.

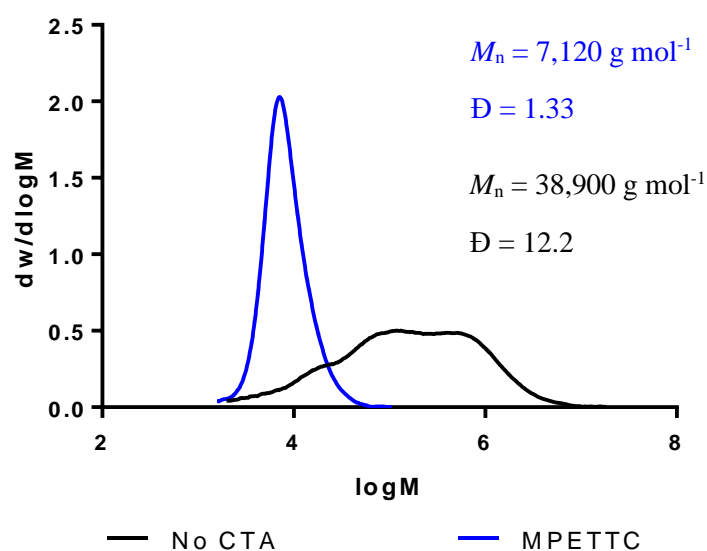


Figure 4.35. SEC curves obtained for of PMMA synthesised with AIBN initiator in the presence and absence of MPETTC. MWDs were determined by SEC in THF (0.05 % w/v BHT) against PMMA standards for RI detection and PSt standards for UV detection.

4.4. Conclusions

Solution polymerizations of MMA have been conducted in the presence and absence of three RAFT agents. These reactions were carried out to determine if these RAFT agents were suitable for controlling the polymerization of MMA. Inclusion of these RAFT agents significantly reduces the molecular weight and \mathcal{D} , and leads to a linear evolution of M_n with conversion.

These RAFT agents were then used for the surfactant-free emulsion polymerization of methyl methacrylate. This is the first instance of this reaction without the use of a suriniferter RAFT

agent. It was determined that the hydrophobic CPB RAFT agent did not produce polymers with low \bar{D} and the PMMA latex was similar to that produced without CPB. This is attributed to CPB barely taking part in the reaction due to its low water solubility. Polymerizations in the presence of PETTC and MPETTC produced varying results depending on the solution pH. PETTC produced lower \bar{D} and M_n values PMMA at pH 7 but was considerably less controlled at pH 5. MPETTC can be used at pH 2 for controlled polymerizations. However, at pH 5 and 8 poorer control was achieved and PSDs became irreproducible. These results indicate that charged CTAs are required for the best results. When a RAFT agent is amphiphilic, its aromatic group is attached to the PMMA chains, which suggests that they can be later chain-extended on addition of further monomer.

Particle size distributions were examined by DLS and TEM. MMA polymerizations in the presence of CPB afforded unimodal PSDs similar to those obtained for reactions conducted in the absence of any RAFT agent. Polymerizations containing PETTC at pH 5 and pH 7 also gave unimodal PSDs but the latex polydispersity increased at higher pH. This effect was also observed in the presence of MPETTC. When the MMA polymerization was relatively-well controlled at pH 2, the PSDs became considerably broader. Polymerizations conducted at pH 5 and 8 were poorly reproducible but reactions that provided greater control over the molecular weight afforded broad bimodal PSDs.

Overall, PETTC and MPETTC RAFT agents provided reasonable control over the MWD when used under these conditions where they were soluble as ionic species. Better control when using such amphiphilic RAFT agents has also been reported for polymerizations using added surfactant.²⁷ The disadvantages of this approach are the large amounts of coagulum due to insufficient colloidal stabilization and the production of broad PSDs. This is problematic in the potential use of these latexes in coatings as the viscosity of the of the latex decreases significantly with broadening of the PSD.²⁸ It is unlikely this would be rectified in the secondary monomer polymerization to form diblock copolymers. This would be interesting future work as the formation of diblock copolymers with amphiphilic RAFT agents has only been published once with very little examination of the product diblock.¹⁸

Other polymerizations were carried out using the uncharged AIBN initiator. When a suitable RAFT agent was not included in such polymerizations the polymer coagulated instantaneously and did not form a latex. The addition of MPETTC at pH 2 was sufficient to partially stabilise the latex and did confer some control over the polymerization. This indicates the charge of MPETTC is sufficient to stabilise the latex without the use of a charged initiator but 50 % coagulum does not lend this method to be used industrially.

4.5. References

1. Moad, G.; Rizzardo, E.; Thang, S. H., Living radical polymerization by the RAFT process. *Australian Journal of Chemistry* **2005**, *58* (6), 379-410.
2. Moad, G.; Rizzardo, E.; Thang, S. H., Living radical polymerization by the RAFT process - A first update. *Australian Journal of Chemistry* **2006**, *59* (10), 669-692.
3. Quinn, J. F.; Chaplin, R. P.; Davis, T. P., Facile synthesis of comb, star, and graft polymers via reversible addition-fragmentation chain transfer (RAFT) polymerization. *Journal of Polymer Science Part A-Polymer Chemistry* **2002**, *40* (17), 2956-2966.
4. Luo, Y. W.; Wang, X. G.; Li, B. G.; Zhu, S. P., Toward Well-Controlled ab Initio RAFT Emulsion Polymerization of Styrene Mediated by 2-(((Dodecylsulfanyl)carbonothioyl)sulfanyl)propanoic Acid. *Macromolecules* **2011**, *44* (2), 221-229.
5. Fu, X. W.; Lei, Y.; Yuan, Y.; Yan, P. Y.; Wang, J. L.; Zhou, C. L.; Lei, J. X., In situ polarity functionalization and properties of styrenic triblock copolymers synthesized via RAFT emulsion polymerization. *Journal of Applied Polymer Science* **2017**, *134* (11), 10.
6. Hu, J. M.; Qiao, R. R.; Whittaker, M. R.; Quinn, J. F.; Davis, T. P., Synthesis of Star Polymers by RAFT Polymerization as Versatile Nanoparticles for Biomedical Applications. *Australian Journal of Chemistry* **2017**, *70* (11), 1161-1170.
7. Keddie, D. J., A guide to the synthesis of block copolymers using reversible-addition fragmentation chain transfer (RAFT) polymerization. *Chemical Society Reviews* **2014**, *43* (2), 496-505.
8. Ferguson, C. J.; Hughes, R. J.; Pham, B. T. T.; Hawkett, B. S.; Gilbert, R. G.; Serelis, A. K.; Such, C. H., Effective ab initio emulsion polymerization under RAFT control. *Macromolecules* **2002**, *35* (25), 9243-9245.
9. Shim, S. E.; Shin, Y.; Jun, J. W.; Lee, K.; Jung, H.; Choe, S., Living-free-radical emulsion photopolymerization of methyl methacrylate by a surface active iniferter (suriniferter). *Macromolecules* **2003**, *36* (21), 7994-8000.
10. Ratcliffe, L. P. D.; Blanz, A.; Williams, C. N.; Brown, S. L.; Armes, S. P., RAFT polymerization of hydroxy-functional methacrylic monomers under heterogeneous conditions: effect of varying the core-forming block. *Polymer Chemistry* **2014**, *5* (11), 3643-3655.
11. Shi, P. F.; Zhou, H.; Gao, C. Q.; Wang, S.; Sun, P. C.; Zhang, W. Q., Macro-RAFT agent mediated dispersion copolymerization: a small amount of solvophilic comonomer leads to a great change. *Polymer Chemistry* **2015**, *6* (27), 4911-4920.
12. Freal-Saison, S.; Save, M.; Bui, C.; Charleux, B.; Magnet, S., Emulsifier-free controlled free-radical emulsion polymerization of styrene via RAFT using dibenzyltrithiocarbonate as a chain transfer agent and acrylic acid as an ionogenic comonomer: Batch and spontaneous phase inversion processes. *Macromolecules* **2006**, *39* (25), 8632-8638.
13. Li, Z.; Chen, W. J.; Zhang, Z. B.; Zhang, L. F.; Cheng, Z. P.; Zhu, X. L., A surfactant-free emulsion RAFT polymerization of methyl methacrylate in a continuous tubular reactor. *Polymer Chemistry* **2015**, *6* (11), 1937-1943.
14. Prescott, S. W.; Ballard, M. J.; Rizzardo, E.; Gilbert, R. G., Successful use of RAFT techniques in seeded emulsion polymerization of styrene: Living character, RAFT agent transport, and rate of polymerization. *Macromolecules* **2002**, *35* (14), 5417-5425.
15. Kim, J.; Kwak, J.; Kim, Y. C.; Kim, D., Preparation and size control of monodispersed surface charged polystyrene nanoparticles by reversible addition fragmentation transfer reaction. *Colloid and Polymer Science* **2006**, *284* (7), 771-779.
16. Shim, S. E.; Shin, Y.; Lee, H.; Jung, H. J.; Chang, Y. H.; Choe, S., Living free-radical emulsion polymerization of methyl methacrylate (MMA) using a surface active

iniferter (suriniferter): Polymerization parameters and molecular structure of the latex.

Journal of Industrial and Engineering Chemistry **2003**, *9* (6), 619-628.

17. Kwak, J.; Lacroix-Desmazes, P.; Robin, J. J.; Boutevin, B.; Torres, N., Synthesis of mono functional carboxylic acid poly(methyl methacrylate) in aqueous medium using suriniferter. Application to the synthesis of graft copolymers polyethylene-g-poly(methyl methacrylate) and the compatibilization of LDPE/PVDF blends. *Polymer* **2003**, *44* (18), 5119-5130.

18. Kim, J.; Kwak, J.; Kim, D., Particle growth Behavior of poly(methyl methacrylate) nanoparticles synthesized by the reversible addition fragmentation transfer living radical polymerization reaction. *Journal of Applied Polymer Science* **2007**, *106* (6), 3816-3822.

19. Stoffelbach, F.; Tibiletti, L.; Rieger, J.; Charleux, B., Surfactant-Free, Controlled/Living Radical Emulsion Polymerization in Batch Conditions Using a Low Molar Mass, Surface-Active Reversible Addition-Fragmentation Chain-Transfer (RAFT) Agent. *Macromolecules* **2008**, *41* (21), 7850-7856.

20. Perrier, S., 50th Anniversary Perspective: RAFT Polymerization-A User Guide. *Macromolecules* **2017**, *50* (19), 7433-7447.

21. Barner-Kowollik, C.; Buback, M.; Charleux, B.; Coote, M. L.; Drache, M.; Fukuda, T.; Goto, A.; Klumperman, B.; Lowe, A. B.; McLeary, J. B.; Moad, G.; Monteiro, M. J.; Sanderson, R. D.; Tonge, M. P.; Vana, P., Mechanism and kinetics of dithiobenzoate-mediated RAFT polymerization. I. The current situation. *Journal of Polymer Science Part A-Polymer Chemistry* **2006**, *44* (20), 5809-5831.

22. [https://www.sigmaaldrich.com/content/dam/sigma-aldrich/docs/Aldrich/General Information/thermal_initiators.pdf?utm_source=redirect&utm_medium=promotional&utm_campaign=insite_thermal_initiators](https://www.sigmaaldrich.com/content/dam/sigma-aldrich/docs/Aldrich/General%20Information/thermal_initiators.pdf?utm_source=redirect&utm_medium=promotional&utm_campaign=insite_thermal_initiators).

23. Lovett, J. R.; Warren, N. J.; Ratcliffe, L. P. D.; Kocik, M. K.; Armes, S. P., pH-Responsive Non-Ionic Diblock Copolymers: Ionization of Carboxylic Acid End-Groups Induces an Order-Order Morphological Transition. *Angewandte Chemie-International Edition* **2015**, *54* (4), 1279-1283.

24. Penfold, N. J. W.; Lovett, J. R.; Warren, N. J.; Verstraete, P.; Smets, J.; Armes, S. P., pH-Responsive non-ionic diblock copolymers: protonation of a morpholine end-group induces an order-order transition. *Polymer Chemistry* **2016**, *7* (1), 79-88.

25. Clayden, J.; Greeves, N.; Warren, S. G.; Wothers, P., *Organic Chemistry*. 1 ed.; Oxford University Press: Oxford, 2000.

26. Thomas, D. B.; Convertine, A. J.; Hester, R. D.; Lowe, A. B.; McCormick, C. L., Hydrolytic susceptibility of dithioester chain transfer agents and implications in aqueous RAFT polymerizations. *Macromolecules* **2004**, *37* (5), 1735-1741.

27. Lubnin, A.; Lenhard, S.; Lai, J., RAFT emulsions, microemulsions and dispersions. *Surface Coatings International Part B-Coatings Transactions* **2006**, *89* (4), 293-304.

28. <https://www.lubrizol.com/Coatings/Blog/2019/07/The-Effect-of-Particle-Size-on-Coating-Performance>.

Chapter 5

5. Conclusions and Outlook

5.1. Conclusions

From this Thesis we can determine the following conclusions.

In Chapter 2 it was shown that 1,1-diphenylethylene (DPE) can be used for the surfactant-free emulsion polymerization (SFEP) of methyl methacrylate (MMA), to reduce the polymerization rate, M_n and \bar{D} of the PMMA. Currently, these parameters cannot be predicted from the DPE concentration but they are each reduced as the DPE content is increased. The initiator concentration does not have a large effect but the anionic charge conferred by the APS initiator is sufficient to stabilise the latex with only minimal coagulation in the final product. DOSY NMR spectroscopy confirmed that DPE was present both in the polymer chain and as free DPE within the latex. The DPE attached to the chain is shown to be only a single capping unit by mass spectroscopy. One unexpected effect of the inclusion of DPE is the formation of a bimodal particle distribution, as determined by transmission electron microscopy (TEM). A second smaller particle distribution is formed over the first hour of the reaction, irrespective of the DPE content.

In Chapter 3 the chain extension of PMMA synthesised in the presence or absence of DPE with either styrene (St) or benzyl methacrylate (BzMA) was explored. Initially, St was used as the second monomer with an additional charge of initiator after full MMA conversion via DPE-mediated polymerization within 4 h. The polymerization of St proceeded rapidly, indicating DPE no longer retarded the rate of polymerization. However, the DPE did not reduce the polymer molecular weight. To reduce the rate of polymerization, the precursor polymers were heated for 24 h to remove any remaining initiator and monomer. More experiments using a second charge of APS did not yield significantly better results and, as a result, no additional initiator was added in subsequent polymerizations.

When St polymerized with no additional APS charge, its rate of polymerization was considerably faster in the presence of PMMA-DPE. St polymerized with the PMMA precursor prepared in the absence of any DPE produced a high molecular weight shoulder which did not indicate chain extension. The polymer formed when polymerizing styrene in the presence of PMMA-DPE has a considerably higher M_n than that of the precursor, but a similar M_n to that of polymer formed with PMMA precursor, which is likely homo-PSt. Unfortunately, attempted separation of the PSt homopolymer from the polymer product was unsuccessful. TEM images of both latexes indicated the formation of a secondary particle size distribution (PSD) in stage two of the polymerization as well as an increase in the mean diameter and standard deviation of the particles. This body of work showed that in the absence of added initiator, St monomer was polymerized to form a secondary polymer MWD in both the presence and absence of DPE.

BzMA was also used as the second monomer to investigate whether a polymerization could be carried out without a self-initiating monomer. With PMMA precursor, there was only a very low BzMA conversion over a 24 h period. With PMMA-DPE precursor, the BzMA conversion was considerably higher, indicating that the PMMA-DPE could act as a radical source by reversibly capping or by fragmentation of the precursor at another weaker point. The MWD obtained by SEC showed little change when PMMA was included in the polymerization but a higher molecular weight polymer was obtained with PMMA-DPE and the precursor appears to be consumed in the polymerization. DOSY NMR spectroscopy indicates that all polymers have similar diffusion coefficients, which indicates the formation of diblock copolymers. However, the presence of monomer complicates this analysis. As with St, a second PSD was formed during stage two of the polymerization and the mean diameter and standard deviation of the particles increased. This work showed that the precursors produced by the DPE method can be chain-extended without the addition of a second initiator charge.

In Chapter 4, reversible addition-fragmentation chain-transfer (RAFT) polymerization of MMA was investigated for SFEP formulations. Initially, RAFT solution polymerizations were conducted in order to determine the efficacy of the chosen RAFT agents for MMA polymerization, with good control over the M_n and \mathcal{D} being achieved. In SFEP, the RAFT agent with no ionic moiety (CPB) had very little effect on the molecular weight distribution (MWD) of the PMMA. Carboxylic acid or morpholine-functionalised RAFT agents conferred some control over the MMA polymerization depending on the solution pH. At pH 5, the PETTC RAFT agent had little effect on the PMMA M_n and \mathcal{D} but at pH 7, i.e. above the pKa of the carboxylic acid moiety, better control over the polymerization was achieved. This was also observed at pH 2 when the morpholine-based MPETTC RAFT agent was utilized but was not observed at pH 8 owing to deprotonation. Polymerizations performed at pH 5 and 8 with MPETTC were not reproducible. UV SEC could be used to detect the aromatic RAFT agent end-group on the PMMA chains. These end-groups were present across the entire MWD for polymerizations carried out at a solution pH where the RAFT agent was ionic. The presence of the RAFT agent at the chain-end suggests that these polymers could be chain-extended by further addition of monomer.

Unfortunately, as the degree of control over the polymerization was increased, the latex particle size distribution broadened. To stabilize the particles, a charged initiator (APS) was used and, in combination with the charged RAFT agent, charge-stabilized latex particles were obtained, as indicated by zeta potential measurements. However, coagulation was observed in all polymerizations, and increasingly so for polymerizations containing MPETTC RAFT agent. This was investigated further by conducting aqueous polymerizations of MMA using

azobisisobutyronitrile (AIBN) initiator, which does not produce a charged chain-end to stabilise the latex. PMMA prepared in the absence of any RAFT agent catastrophically coagulated, but the presence of MPETTC at pH 2 was enough to stabilise the latex with comparable amounts of coagulation as that observed with APS. This RAFT agent led to a cationic charge-stabilized latex as judged by zeta potential measurements but did not reduce the PMMA dispersity to less than 1.33.

5.2. Outlook

5.2.1. *The mechanism of the DPE method in solution and stabilized emulsion polymerizations*

While previous work has been carried using DPE to mediate the solution polymerization of MMA, the SFEP mechanism reported in this Thesis is in agreement with a solution polymerization study by Zhao *et al.*,¹ who varied the DPE and initiator content. Similar concentrations to those used in Chapter 2 gave semiquinoid structures in conventional emulsion polymerizations conducted by Viala *et al.*² This raises an important question: does the nature of the polymerization, i.e. homogeneous vs. heterogeneous, further change its mechanism? Emulsion polymerizations containing stabilizers and further solution polymerizations should be conducted under similar conditions to those of SFEP formulations in this Thesis to discover whether the reaction conditions affect the DPE mechanism. This work could help settle the debate of the mechanism of the DPE method but was deemed less important from the industrial sponsor of this research project compared to the ability of the DPE method to produce diblocks.

5.2.2. *DPE derivatives*

When using a RAFT agent to control the polymerization, it is clear that its aqueous solubility is a key factor. Although, DPE is hydrophobic, it can still reach the locus of polymerization, either by diffusing through the aqueous phase or via particle collisions. It would be interesting to purchase (or synthesise) a more hydrophilic derivative of DPE to study its use in emulsion polymerization. One possible example is (1-methoxy-4-[1-(4-methoxyphenyl)vinyl]benzene, Figure 5.1, which is available from Aldrich^{CPR}.³ Using a DPE derivative such as this should also prevent the formation of a semiquinoid structure, therefore eliminating one possible mechanism from further studies. With cost being the main driving force in many businesses this was deemed less important to the overall project, as these DPE derivatives would not be as readily available as DPE.

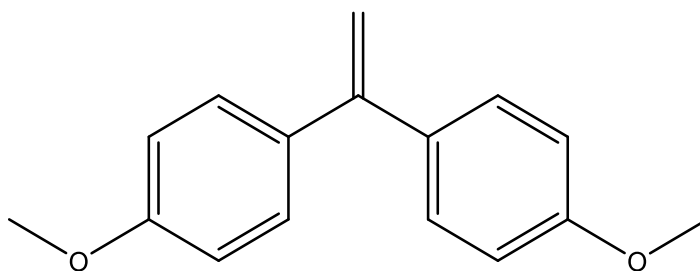


Figure 5.1. 1-methoxy-4-[1-(4-methoxyphenyl)vinyl]benzene).

5.2.3. Monomer variations

Other vinyl monomers not used in this Thesis have been reported for DPE-mediated polymerization.⁴⁻⁶ Initial experiments were attempted during the production of this Thesis. However, when MMA, St or butyl methacrylate (BMA) were used in a stage one polymerization, the results were not reproducible. Figure 5.2 shows SEC MWDs of these final polymers, with each reaction producing different results. This was attributed to insufficient stirring of the emulsion polymerization, as all reactions completed with DPE in this Thesis were conducted on a larger scale with an overhead stirrer. These alternative monomer reactions were conducted in a 50 mL round-bottom flask equipped with a magnetic stirrer bar. This additional research would add to the findings of Chapter 3 of this Thesis, in addressing whether the use of a self-initiating monomer is required for the further extension of polymers formed in the presence of DPE.

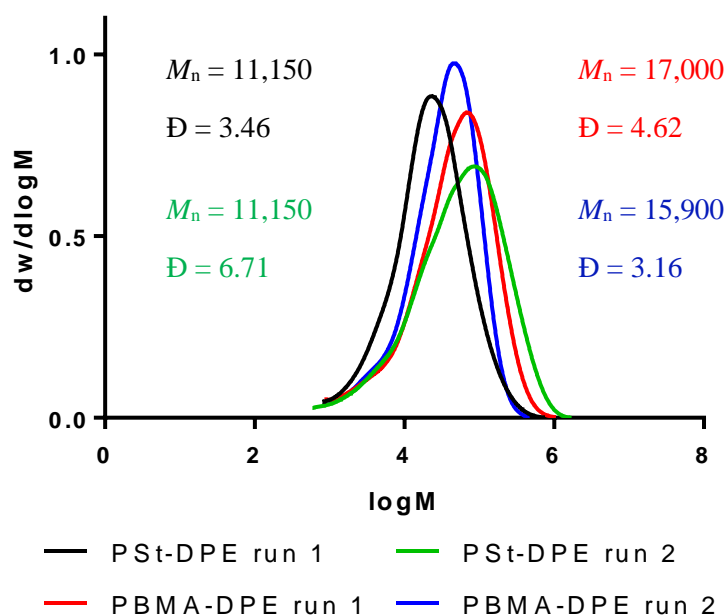


Figure 5.2. MWDs by SEC of polymerizations of BMA and St in the presence of DPE.

5.2.4. *Extension of RAFT mCTA without a second initiator charge*

The results obtained in Chapter 3 of this Thesis suggest that DPE-capped polymers can later be extended via addition of monomer by heating without further initiator. This was attributed to the DPE caper forming a relatively weak bond that can be broken at higher temperatures. It would therefore be interesting to determine if a similar reaction occurred when using a RAFT agent. This seems unlikely, as the mechanism requires an influx of free radicals but RAFT SFEP reactions with an additional initiator charge could be carried out. The use of DPE was considered the main research area of this PhD and unfortunately, due to time constraints, this work was unable to be completed.

5.3. References

1. Zhao, M. J.; Chen, D.; Shi, Y.; Yang, W. T.; Fu, Z. F., Polymerization Mechanism of MMA in the Presence of 1,1-Diphenylethylene. *Macromolecular Chemistry and Physics* **2013**, *214* (15), 1688-1698.
2. Viala, S.; Antonietti, M.; Tauer, K.; Bremser, W., Structural control in radical polymerization with 1,1 diphenylethylene: 2. Behavior of MMA-DPE copolymer in radical polymerization. *Polymer* **2003**, *44* (5), 1339-1351.
3. <https://www.sigmaaldrich.com/catalog/product/aldrich/s671711?lang=en®ion=GB>.
4. Zhang, H. P.; Zhang, Q. Y.; Zhang, B. L.; Guo, F. G., Preparation of magnetic composite microspheres by surfactant free controlled radical polymerization: Preparation and characteristics. *Journal of Magnetism and Magnetic Materials* **2009**, *321* (23), 3921-3925.
5. Zhou, Y. Y.; Zhang, Q. Y.; Liu, Y. L.; Wang, W. W., Encapsulation and dispersion of carbon black by an in situ controlling radical polymerization of AA/BA/St with DPE as a control agent. *Colloid and Polymer Science* **2013**, *291* (10), 2399-2408.
6. Guo, F. G.; Zhang, Q. Y.; Zhang, H. P.; Zhang, B. L.; Gu, J. W., Controlled preparation of Fe₃O₄/P (St-MA) magnetic composite microspheres by DPE method. *Journal of Polymer Research* **2011**, *18* (4), 745-751.

Chapter 6

6. Appendix

6.1. Appendix

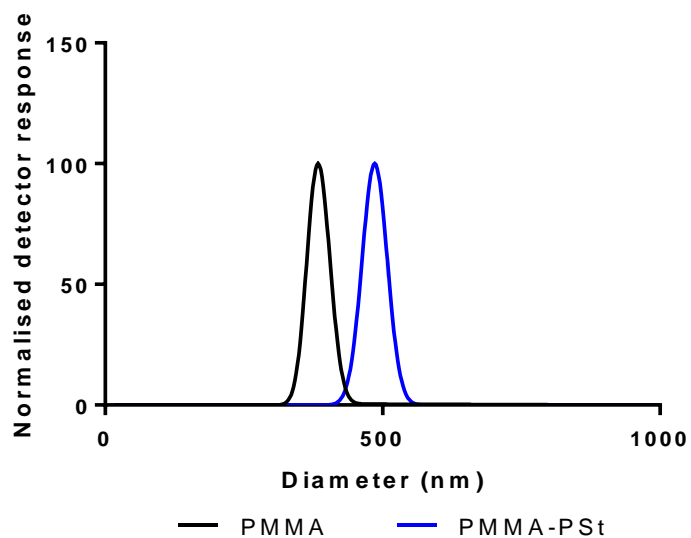


Figure 6.1. Particle size distributions of PMMA and PMMA-PSt latexes obtained by HDC.

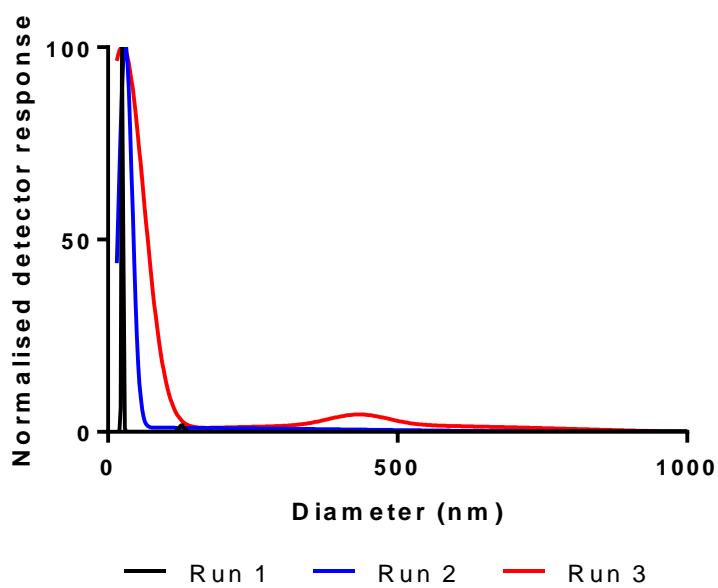


Figure 6.2. Particle size distribution data obtained by HDC for PMMA-DPE.

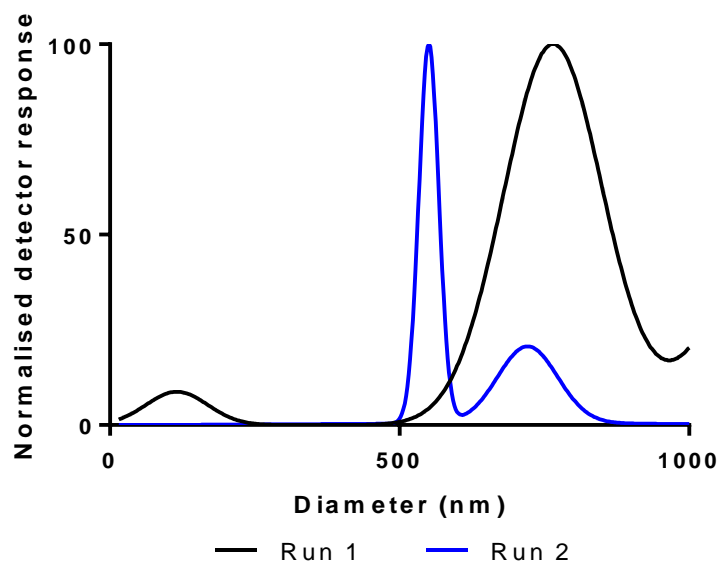


Figure 6.3. Particle size distribution data obtained by HDC for PMMA-DPE-PS.

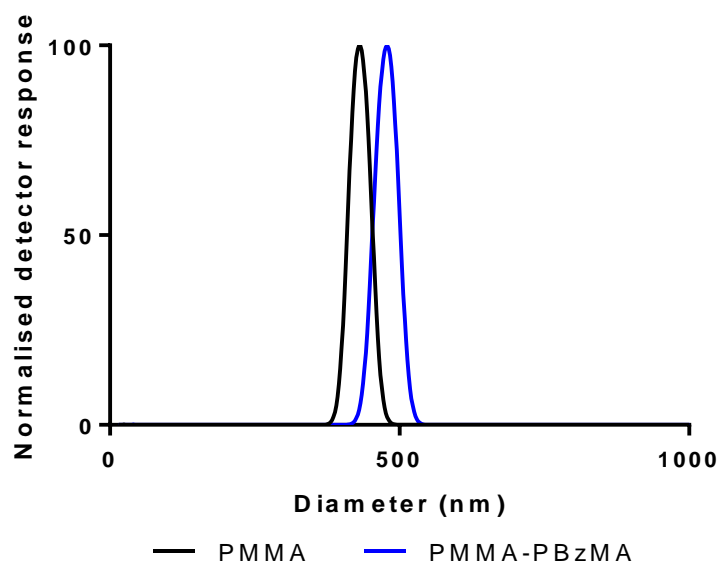


Figure 6.4. Particle size distributions of PMMA and PMMA-PBzMA latexes obtained by HDC.

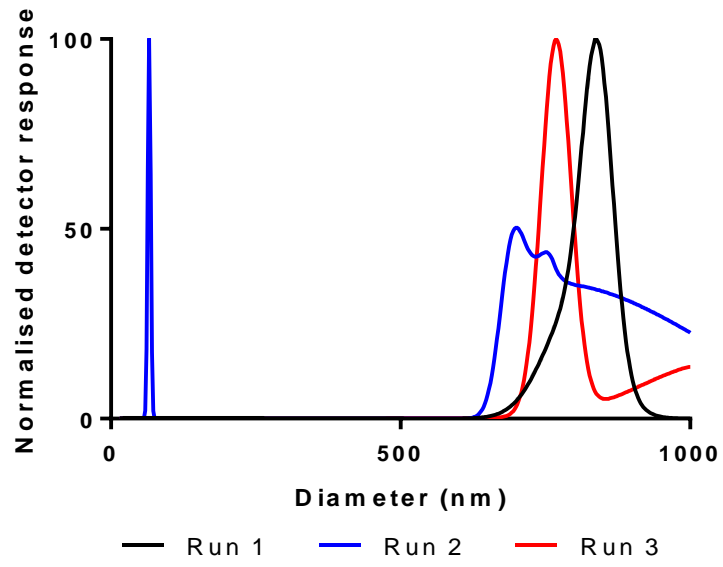


Figure 6.5. Particle size distributions obtained by HDC analysis is of PMMA-DPE-PBzMA